Production of a novel Affimer based biosensor for the detection of porcine reproductive and respiratory syndrome virus nucleocapsid protein.

Zoe Jackson

Submitted in accordance with the requirements for the degree of

Doctor of Philosophy

University of Leeds

Faculty of Biological Sciences

School of Molecular and Cellular Biology

November 2017

The candidate confirms that the work submitted is her own and that appropriate credit has been given where reference has been made to the work of others.

Acknowledgments

I would first like to thank my primary supervisor Professor Adrian Whitehouse who saw potential in a shy and nervous Masters student and encouraged me to challenge myself with the undertaking of a PhD. His encouragement, guidance and support have allowed me to progress into a confident scientist. I would also like to thank my co-supervisor Dr Darren Tomlinson for his invaluable support during the dark times of Affimer screening and for our useful brainstorming sessions featuring my excellent drawings.

A huge thank you to the Whitehouse and Hewitt group members past and present without whom I would not have managed to complete year one l*et al*one year five of this PhD. The happy working environment, the cake and the laughs have been a welcome side offering in addition to plenty of scientific advice. In particular I would like to mention Dr Sophie Schumann, Dr David Hughes and Dr Brian Jackson.

I must also take this opportunity to thank the Wellcome Trust for providing the funding for me to carry out this research and for providing a PhD scheme which allowed me to assist in the design of my project and the opportunity to experience such exciting science. I undertook a placement at BBI Solutions, Cardiff, and would like to thank them for providing me with the training and support for lateral flow development.

Finally I would like to thank my family (the one I already had and the one I gained recently) initially for their encouragement, belief and also for listening to me at times of despair. But secondly for their help in babysitting duties which have been life-saving at the end. Last but not least, I would like to say a huge thank you to my husband Brian (again) for his unwavering support and who has read this entire thesis multiple times, offering his thoughts and suggestions, as well as listening to me when I was worrying at all hours about finishing with a new baby. And so that leaves Hugo, the little boy who arrived so close to the end. Thank you for keeping me awake most nights, giving the best cuddles after a hard day's work and for being the best son anyone could wish for. Although you were not here at the start, the completion of this thesis is for you as well as me and I hope you will be proud.

Abstract

Porcine reproductive and respiratory syndrome virus (PRRSV) is an economically important infection with no current point of care (POC) diagnostic available. PRRSV causes reproductive and respiratory illness in swine with the recent emergence of highly pathogenic strains. This highlights the need for measures to control the spread of this infection to be taken more seriously in order to reduce the economic impact of this virus. Current diagnostics for PRRSV are laboratory based and inherently these tests are expensive and are not rapid enough for the adequate management of outbreaks of the virus and implementation of biosecurity measures.

This study presents a novel lateral flow device (LFD), using Affimer binding proteins to detect the nucleocapsid protein of PRRSV within a clinical sample to provide a cheap, rapid and reliable diagnostic for this infection in clinical samples. Affimer reagents were raised against the nucleocapsid proteins from two strains of PRRSV, a high pathogenic and a low pathogenic strain. Affimers that were able to distinguish between the two were taken forward for assessment in lateral flow. The Affimers were able to bind to the nitrocellulose membrane component of the device and were stable once dehydrated. The Affimers were able to migrate through the membrane via capillary action when rehydrated and can detect the viral protein at a test line within a clinical sample, swine serum.

This study provides the basis for further investigations in to the applications of Affimer reagents in lateral flow devices able to detect other viral infections as well as medically important diseases such as cancer. In addition to their use in diagnostics, this study proposes the use of Affimers raised against the nucleocapsid protein of PRRSV as molecular tools for the further investigation into the role of this protein in the viral lifecycle as well as their potential as anti-viral therapeutics to address the lack of these medicines against this virus.

Contents

List of Tables

List of Figures

Abbreviations

aa	Amino acid
AC	Alternating current
BSA	Bovine serum albumin
CBP	CREB-binding protein
DAPI	4', 6-diamidino-2-phenylindole
DMEM	Dulbecco's modified Eagles medium
DTT	Dithiothreitol
ECL	Enhanced chemiluminescence
EIS	Electrochemical impedence spectroscopy
ELISA	Enzyme-linked immunosorbent assay
EM	Electron microscopy
ER	Endoplasmic reticulum
FBS	Foetal bovine serum
Gp	Glycoprotein
GNP	Gold nanoparticle
hpi	Hours post induction
HRP	Horseradish peroxidase
IF	Immunofluorescence
IPTG	Isopropyl-β-D-thio-galactoside
LB	Luria Broth
LFD	Lateral flow device
LOC	Lab on chip
N	Nucleocapsid protein
Nsp	Non-structural protein
ORF	Open reading frame
PARP	Poly ADP-Ribose Polymerase
POC	Point of care
RTC	Replication and transcription compartment
SDS	Sodium dodecyl sulphate
TBE	Tris/borate/EDTA
TBS	Tris buffered saline
TCEP	Tris(2-carboxyethyl)phosphine
TE	Tris-EDTA buffer
TEMED	N,N,N',N'-tetramethylethane-1,2-diamine
TM	Transmembrane
UTR	Untranslated region

Chapter 1

Introduction

1 Introduction

1.1 Infectious diseases of livestock

Infectious diseases of livestock have devastating effects on global economics, animal welfare and food security. It is therefore important to conduct research into the causative agents of disease in order to improve preventative measures and investigate therapeutic agents. Outbreaks of certain infectious diseases may result in the mass culling of exposed animals. Implementation of a preventative cull of healthy animals and widespread restriction of movement are often also used to stem the spread of infection. The UK foot and mouth disease outbreaks of 2001 and 2007 are prime examples (Tildesley *et al*., 2009). Other infectious diseases, such as bovine respiratory syncytial virus (BRSV) (Snowder *et al*., 2006), classical swine fever (Boklund *et al*., 2009) and porcine reproductive and respiratory syndrome virus (PRRSV) (Nieuwenhuis *et al*., 2012) cause more subtle economic effects. These infections are often overlooked with regard to testing and control, although the losses accrued globally as a result can be hugely economically damaging and result in the preventable deaths of thousands of animals. Therefore, one of the most important factors in the control of an outbreak of an infectious disease is the ability to detect infection in a cost effective and rapid manner, in order that further control procedures may be executed. However, it is often the case that infectious diseases are difficult to detect with clinical symptoms not presenting before the disease has spread rapidly amongst a population. The implementation of a rapid, in-field or point of care (POC) biosensor is an ideal method to replace the need for lengthy, laboratory-based tests. This study aims to produce a POC diagnostic test incorporating novel non-antibody components which could be utilised in both the agricultural and healthcare settings.

1.2 Virus classification

1.2.1 Baltimore classification of viruses

All viruses are categorised under the Baltimore classification, placing them into similar groups based upon their genome and mode of replication. There are currently seven classes, table 1.1 shows this classification system (Baltimore, 1971).

Table 1.1 Classification of viruses according to the Baltimore Classification system (Baltimore, 1971).

Class	Genome	Translation of viral genome	Example viruses
Class I	dsDNA	DNA to mRNA	Herpesvirus
Class II	ss(+)DNA	ss(+)DNA to ds(+/-)DNA to mRNA	Parvovirus
Class III	dsRNA	dsRNA to mRNA	Reovirus
Class IV	ss(+)RNA	ss(+)RNA to (-)RNA to mRNA	Arterivirus
Class V	ss(-)RNA	ss(-)RNA to mRNA	Paramyxovirus
Class VI	ss(+)RNA-RT	ssRNA to (-)ssDNA to (+/-)dsDNA to mRNA	Retrovirus
Class VII	dsDNA-RT	dsDNA to mRNA	Hepadnavirus

This study focuses on the Class IV RNA virus, porcine reproductive and respiratory syndrome virus (PRRSV), a single stranded, positive sense RNA virus. The genome is translated directly with the positive sense genome serving directly as an mRNA. These viruses encode an RNA dependent RNA polymerase for genome replication, which synthesises minus RNA strands that are used as a template for positive strands of new genomic RNA (Baltimore, 1971). The molecular biology of this virus will be discussed in detail in later sections.

1.3. Nidovirales

1.3.1. Introduction to the Nidovirus order

PRRSV is an arterivirus and a member of the Nidovirlaes order. The Nidovirales are a diverse order of single stranded, positive sense RNA viruses that can be further subdivided into two categories, based upon the size of their genomes: large RNA genomes including coronaviruses (vertebrate hosts), mesoniviruses (invertebrate

hosts) and roniviruses (invertebrate hosts), whose genomes are between 20 and 32 Kb, and viruses with smaller RNA genomes including arteriviruses (vertebrate hosts), whose genomes are between 13 and 16 Kb. Nidoviruses are responsible for a number of economically important livestock infections and so there is a vested interest in research into these viruses, table 1.2 provides a summary of these infections and the associated virus family.

Table 1.2 Economically important livestock Nidoviruses

Family	Virus	Host	Reference
Arterivirus	PRRSV	Swine	(Wensvoort *et al*., 1991)
Coronavirus	Bovine respiratory coronavirus	Bovine	(Mebus *et al*., 1973; Storz *et al*., 2000)
Coronavirus	Porcine epidemic diarrhoea virus	Swine	(Wood, 1977)
Coronavirus	Porcine transmissible gastroenteritis virus	Swine	(Brian *et al*., 1980)
Coronavirus	Infectious bronchitis virus	Poultry	(Boursnell *et al*., 1987)

1.3.2. Nidovirus hosts

As previously mentioned, Nidoviruses can infect a range of hosts, primarily mammals (coronaviruses, toroviruses and arteriviruses), however, coronaviruses can also infect avian hosts, and roniviruses infect invertebrate hosts (Pasternak *et al*., 2006). Roniviruses include the Okaviruses, yellow head virus (YHV) and gill-associated virus (GAV) which primarily infect crustaceans (Wijegoonawardane *et al*., 2008). Recently a new family of viruses in the Nidovirale order has been proposed which also infect invertebrate hosts, the mesonviridae; of which there are currently two mosquito borne viruses, Nam Dinh virus and Cavally virus (Lauber *et al*., 2012). The majority of Nidoviruses are host specific, however, certain Nidoviruses possess tropism for a number of hosts. A phylogenic tree of the Nidovirus order is shown in figure 1.1 (Lauber *et al*., 2012).

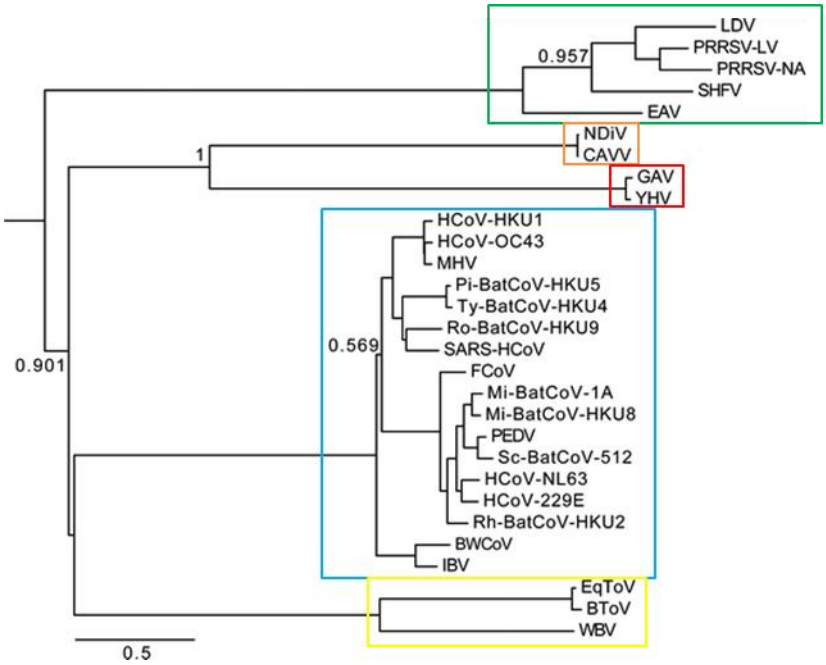

Figure 1.1 Phylogenic tree of Nidovirale order (adapted from Lauber *et al* 2012). The Nidovirus tree shows the members of the arterivirus (green), mesonivirus (orange), ronivirus (red) and coronavirus (blue) and the coronavirus subfamily torovirus (yellow) (Lauber *et al* 2012).

1.3.3. Nidovirus genome

The genomes of all Nidoviruses are flanked with a 5' cap structure and a 3' poly (A) tail (Gorbalenya *et al*., 2006). The flanking UTRs are suggested to play a role in the replication of the viral genome and the translation of viral proteins (Matthew A Kappes and Faaberg, 2015). As well as the UTR regions of the viral genome, the coding open reading frames (ORFs) are located in the intermediate region of the Nidovirus genome. A representative genome of the Nidovirale order (PRRSV) (figure 1.2) illustrates the main coding ORFs (Gorbalenya *et al*., 2006).

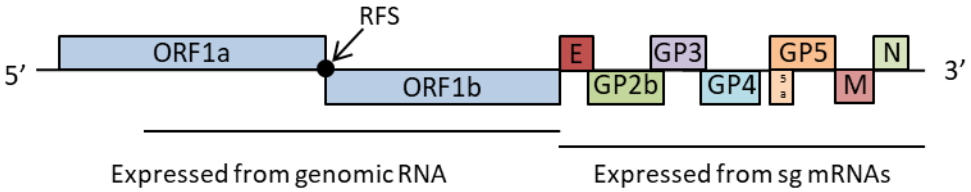

Figure 1.2 Representative Nidovirus genome (Porcine Reproductive and Respiratory Syndrome Virus). The viral genome is split into two regions, the non-structural protein genes (ORF1a and ORF1b) and the structural genes, envelope protein (E), glycoproteins (GP), membrane protein (M) and nucleocapsid protein (N). ORF1a and ORF1b are translated into polyproteins with ORF1b translated as a result of a ribosomal frame shift (RFS) and is proteolytically cleaved into the viral non-structural proteins. The structural genes are translated as a nested set of subgenomic RNAs. The genome is flanked by two non-coding regions, one at the 5' end and one at the 3' end of the genome (edited from Gorbalenya *et al* 2006).

The Nidovirales encode their own replicative machinery, including an RNA dependent RNA polymerase (RdRp) a common feature of positive sense RNA viruses. Expression of the RdRp is controlled by a ribosomal frame shift and cleavage of the subsequent polyprotein by a chymotrypsin-like protease and papain-like proteases (Koonin, 1991; Beerens *et al*., 2007). The 3'-proximal structural proteins are expressed as a nested (Latin *nidus*= nest) set of subgenomic RNAs. This genomic region also contains accessory proteins in larger Nidoviruses that allow for the adaption of host specificity (Gorbalenya *et al*., 2006). The number of structural proteins encoded in the genome and produced by the synthesis of subgenomic RNAs is virus dependent, as illustrated in figure 1.2 with arteriviruses encoding 7-9 non-structural proteins, whereas coronaviruses sometimes encode more than 9 non-structural proteins (Gorbalenya *et al*., 2006).

1.3.4. Nidovirus virion architecture

Due to the varied nature in size of Nidovirus genomes, the virion architecture varies between the different families in the order. Coronavirus virions are between 120-160 nm in diameter to encapsulate the larger genome with a fringe of projections from the surface of the virus particle with helical and extended nucleocapsids (Graham *et al*., 2013). Arteriviruses are much smaller owing to their smaller genomes, 60 nm in diameter with a 35 nm isometric or pleomorphic nucleocapsid (Snijder *et al*., 2013). Toroviruses are more pleomorphic in shape, being spherical, rod shaped or disk shaped measuring 100-140 nm in length and 35-

42 nm in width (Kroneman *et al*., 1998). All Nidovirus virions are enveloped using cellular membranes derived from the endoplasmic reticulum and golgi bodies and the envelope is studded with viral glycoproteins (Ziebuhr and Siddell, 2003).

1.3.5. Members of the Nidovirus order

1.3.5.1. Coronaviridae

Coronaviruses are able to infect a range of vertebrate hosts, although evidence of transmission of infection between species is currently limited. Severe acute respiratory syndrome coronavirus (SARS-CoV) was identified in 2003, following the transmission of respiratory illness between humans. The animal reservoirs are thought to be ferrets, Civet cats and domestic cats, although the coronavirus isolated from these animals remains distinct from the SARS-CoV, another potential reservoir is the Chinese horseshoe bat (Lau *et al*., 2005; Lo *et al*., 2006). The recently identified Middle East respiratory syndrome coronavirus (MERS-CoV) is thought to have been transmitted from the main reservoir in camels or bats to humans through close proximity living arrangements with limited human to human transmissions currently observed (Alagaili *et al*., 2014; Ithete *et al*., 2013). The tropism of these viruses is mediated by the viral proteins themselves, with the envelope proteins playing a key role in cell infectivity, specifically the spike glycoprotein (S), located on the viral envelope, is involved in binding of viral proteins to cell membranes via receptor sites and can bind to proteinaceous receptors or cellular carbohydrates (Millet and Whittaker, 2015). As shown in table 1.2, the economically important agricultural coronaviruses include bovine respiratory coronavirus, porcine epidemic diarrhoea virus, porcine transmissible gastroenteritis virus and infectious bronchitis virus.

1.3.5.2. Toroviridae

Toroviruses are a sub-family of the coronaviruses and primarily infect mammals (Snijder and Horzinek, 1993), of which there are currently four recognised virus species, human, bovine, porcine and equine toroviruses. The equine torovirus (EToV) and Berne virus (BEV) are the most thoroughly studied, although the mode

of infection and tropism of these viruses is currently poorly understood, as the virus grows poorly in cell culture conditions (Maestre *et al*., 2011).

1.3.5.3. Mesoniviridae

In 2012, a new family of viruses in the Nidovirales order was proposed. These are mosquito borne viruses isolated in the Ivory Coast and Vietnam, termed Cavally virus (CAVV) and Nam Dinh virus. Their genomes are intermediary in size between coronaviruses and arteriviruses (Lauber *et al*., 2012). CAVV was identified in the Ivory Coast in 2004 and the virion structure is similar to that of coronavirus virions. The virus has only been isolated from female mosquitos and is likely to require a vertebrate as an amplification host during its lifecycle (Zirkel *et al*., 2011). Nam Dinh virus was discovered in Vietnam in 2003 during a study into acute encephalitis syndrome (AES) associated with Japanese encephalitis virus, which causes 40% of cases of AES. It is currently unknown if Nam Dinh causes symptoms in humans (Nga *et al*., 2011).

1.3.5.4. Arteriviridae

The family of viruses focussed upon in this study are the arteriviruses in particular PRRSV. Other members of this family include lactate dehydrogenase elevating virus (LDV), simian haemorrhagic fever virus (SHFV) and equine arterivirus (EAV). They are all host specific during natural infection. Arteriviruses are thought to enter the host cell via clathrin-mediated endocytosis, however, unlike with the spike glycoprotein from coronaviruses, there is currently no convincing evidence to pin point the viral proteins involved in the tropism of arterivirus infection (Snijder *et al*., 2013). The target cells for all arteriviruses appear to be the macrophages of the respective species host (Plagemann and Moennig, 1992). The arterivirus family will be discussed extensively below.

1.3.6. Arteriviruses

Arteriviruses infect a range of mammalian hosts: mice, horses, pigs and primates. The viruses themselves are highly host specific and cause both persistent and asymptomatic infections as well as acute disease with symptoms that include haemorrhagic fever, respiratory illness and abortions (Snijder *et al*., 2013). Until

recently there were four members of the arterivirus family (section 1.3.5.4). This set of viruses were recognised as a new member in the order *Nidovirales* in the late 1990's at the Xth International Congress of Virology (Jerusalem, 1996) (Snijder and Meulenberg, 1998). In the past five years there have been a number of tentative additions to the arterivirus family including wobbly possum disease virus (WPDV), African pouched rat virus 1, and viruses distantly related to SHFV (Dunowska *et al*., 2012; Jens H Kuhn *et al*., 2016; Lauck *et al*., 2013). WPDV is the first arterivirus found to infect a non-eutherian host (Jens H. Kuhn *et al*., 2016). These tentative new additions to the family of arteriviruses have resulted in the suggested reorganisation of the family to accommodate the complexity (Jens H Kuhn *et al*., 2016).

1.3.6.1. Genome organisation

The genome of this family of viruses is small in relation to other families in the *nidovirale* order with member genomes of between 12-16 kb. The genomes of the four members of the arterivirus family are shown in figure 1.3. (adapted from Snijder *et al*., 2013).

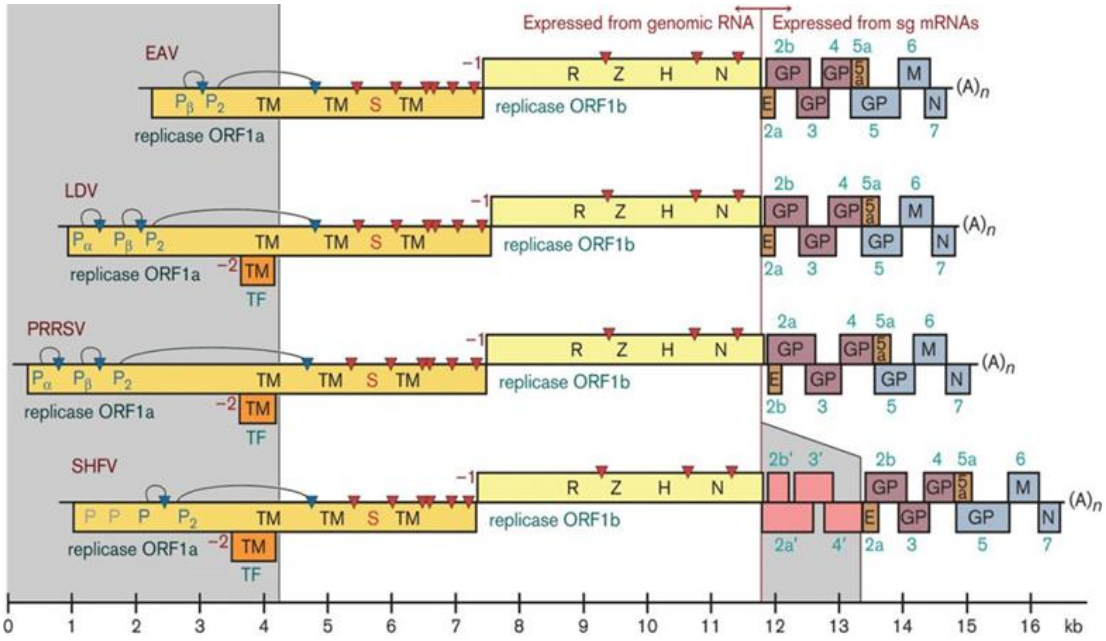

Figure 1.3 Arterivirus genomes. The genomes of arteriviruses EAV, LDV, PRRSV and SHFV are translated in two separate ways. ORF1a and ORF1b are translated from genomic RNA as polyproteins and are proteolytically cleaved by viral proteins at the locations indicated by arrows. The RNA dependent RNA polymerase (RdRp) is encoded by these ORFs. The 3' end of the viral genome contains the structural genes and these are translated from a nested set of subgenomic (sg) mRNAs. These are produced in constant but non-equimolar quantities and the genes encoded on the sgmRNAs overlap (Snijder *et al*., 2013).

The positive sense RNA genomes are polycistronic and the 10-15 ORFs are flanked by non-translated regions (NTRs) at the 3' and 5' ends. These NTRs are variable in length dependent on the virus and range from 5', 156-224 nucleotides (nt) and 3', 59-117 nt (Snijder *et al*., 2013). The 5' proximal region of the genome encodes the large replicase ORFs 1a and 1b and make up three quarters of the viral genome, the polymerase gene resembles the polymerase gene of the related coronaviruses. ORF1a and 1b overlap and are translated using a -1 ribosomal frameshift (RFS), the overlap in EAV is 19 nt (den Boon *et al*., 1991). These ORFs yield translated proteins of 1727-2502 amino acids (aa) and 3175-3959 aa respectively and upon translation are proteolytically cleaved to produce a large number of proteins (Snijder *et al*., 2013; Fang *et al*., 2012). Recently, a previously unidentified protein was discovered in PRRSV ORF1, using a programmed -2 RFS at a conserved G_GUU_UUU sequence in the central region of ORF1a. This RFS mechanisms produces a previously unidentified protein, termed nsp2TF, which comprises the N-terminal two thirds of nsp2 and 169 aa C-terminal region encoded by the newly

identified TF ORF, which is conserved in the genomes of all arteriviruses (Fang *et al*., 2012). Nsp2TF is proposed to be involved in the down-regulation of Swine Leukocyte Antigen Class 1 (SLA-1), reducing the cell-mediated immune response during infection (Cao *et al*., 2016). The replicase polyproteins of PRRSV are processed into at least 16 non-structural proteins and four proteinases (Matthew A Kappes and Faaberg, 2015).

The 3'-proximal genome region encodes the viral structural proteins. These are generally small ORFs which overlap with each other and are expressed as a nested set of subgenomic (sg)mRNAs in non-equimolar but constant amounts (Snijder *et al*., 2013). This is a characteristic of coronaviruses and arteriviruses, as each of the sgmRNAs contains a leader sequence at the 5' end (approximately 200 nt) that is identical to the 5' leader sequence of the genome (de Vries *et al*., 1990).

1.3.6.2. Arterivirus lifecycle

The tropism of arteriviruses is very narrow and this is thought to be due to the viral proteins themselves, present on the surface of the virions. The method of entry into the cell by arteriviruses has long been known to occur via clathrin-mediated endocytosis, endosome acidification and membrane fusion (Kreutz and Ackermann, 1996). The lifecycle is outlined in figure 1.4 and covers the entire infectious cycle from viral entry to release (Snijder *et al*. 2013).

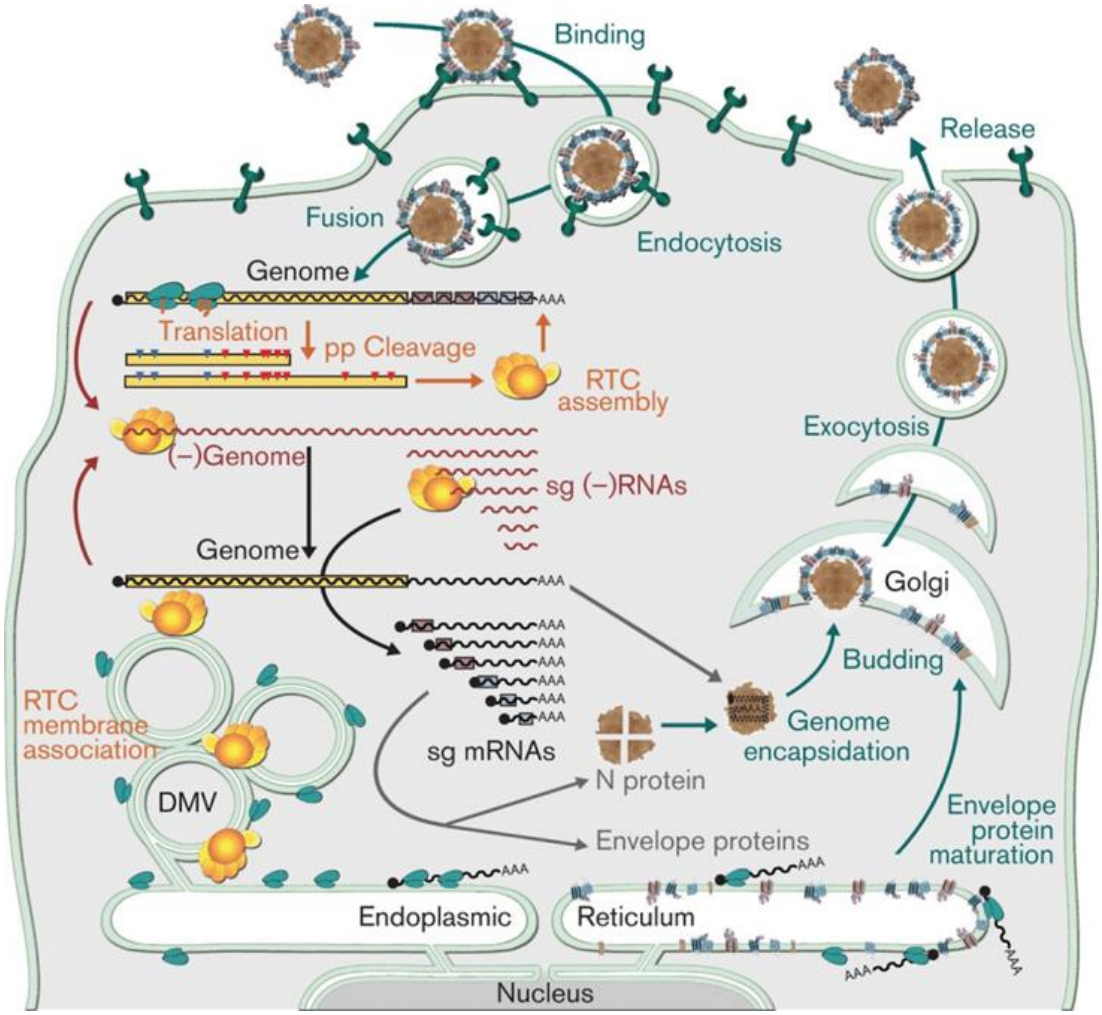

Figure 1.4 Arteriviral infection cycle. The virus enters cells via receptor-mediated endocytosis and the virus particle is disassembled in the endosome. The viral genome is released into the cytoplasm the replicase polyproteins pp1a and pp1b are translated from ORF1a and ORF1b. These polyproteins are cleaved by internal viral proteases to produce the viral proteins required to assemble the replicase complex (RdRp). The replication and transciption complex (RTC) begins minus strand RNA synthesis of the whole viral genome, including the minus strand sgmRNAs for the synthesis of the viral structural proteins. These minus strands of viral genome are then transcribed into positive strands and the complete genomes are packaged into new viral particles. The positive strand sgmRNAs are used as templates for the translation of the viral sturctural proteins which are then available for the assembly of new virions. The RTC associates with cellular membranes such as the endoplasmic reticulum (ER), where viral structural proteins mature before packaging. The newly synthesised viral genome encapsidated by the nucleocapsid (N) protein bud from smooth ER and become enveloped with the viral structural proteins and leave the infected cell via the exocytic pathway (Snijder *et al*. 2013).

The lifecycle of the virus occurs in the cytoplasm of the host cell and through the formation of replication and transcription complexes (RTCs). Upon viral genome entry into the host cytoplasm, ORFs 1a and 1b are translated to produce pp1a and pp1b that are proteolytically cleaved by viral proteinases, PCP1α, PCP1β, CP2 and 3CLSP (further discussed in section 1.3.6.4.1) to produce a number of non-

structural proteins which form the RTCs (van der Meer *et al*., 1998). It is the RTCs, associated with double membrane vesicles induced by the expression of the proteins encoded in pp1a and pp1b to provide a scaffold structure, that are the location of minus strand RNA synthesis used for the subsequent synthesis of the new positive strand RNA genome (Posthuma *et al*., 2008). RTCs are a widely used strategy in viral replication, being adopted by a number of viruses (den Boon *et al*., 2010; Romero-Brey and Bartenschlager, 2014; Paul and Bartenschlager, 2013) with the use of viral proteins as initiators of the formation of the RTCs (Ahlquist, 2006). The confinement of the replication process of viruses into compartments is favourable for optimum viral production, forming micro-environments that concentrate viral proteins and precursors and anchor the process to a location where enzymes are able to function efficiently. RTCs may also delay detection of viral replication by the host immune system (van der Hoeven *et al*., 2016; Gürtler and Bowie, 2013).

In the case of arteriviruses, the RTC produce both full length and sg length minus strands of RNA with the sg length RNA used for the synthesis of the positive sense sgmRNAs required for the synthesis of the viral structural proteins. The sgmRNAs are translated into the viral structural proteins that are involved in the production of new viral particles containing newly synthesised viral genomes (Pasternak *et al*., 2006). The viral genomes are encapsulated by the nucleocapsid (N) protein, which is then coated with a lipid envelope (55 nm bilayer) studded with further structural proteins that include the glycoproteins and membrane proteins (Snijder and Meulenberg, 1998). Viral particles appear to be assembled at the site of replication, with the nucleocapsid encapsulated genome being wrapped by the smooth endoplasmic reticulum (ER) or Golgi complex studded with the viral structural proteins. The formation of the viral particles at the ER allows them to enter into the secretory pathway and be transported to the cell membrane where they undergo exocytosis and release for infection of further host cells (Magnusson *et al*., 1970; Wood *et al*., 1970). Recently, it has been suggested that this arteriviral secretory pathway also involves plasma membrane cholesterol, at least in the case of PRRSV (Sun *et al*., 2011; Q. Yang *et al*., 2015). Cholesterol and lipid metabolism is also known to be important for the life cycles of a wide variety of viruses, where

components of the lipid synthesis pathways are hijacked for viral maturation and secretion. Other viruses that use lipid and cholesterol metabolism include hepatitis C (Popescu *et al*., 2014), canine coronavirus (Pratelli and Correspondence, 2016), HIV (Bukrinsky and Sviridov, 2006), Semliki forest virus (Marquardt *et al*., 1993), FMDV (Martín-Acebes *et al*., 2007) and Herpes Simplex Virus (Wudiri *et al*., 2014).

1.3.6.3. Arterivirus virion

The arterivirus virion is spherical and enveloped and the virus particles are between 40-60 nm in diameter consisting of an isometric core, which is approximately 80% of the virion diameter. A schematic of the virion is shown in figure 1.5. (Snijder *et al*., 2013; Spilman *et al*., 2009).

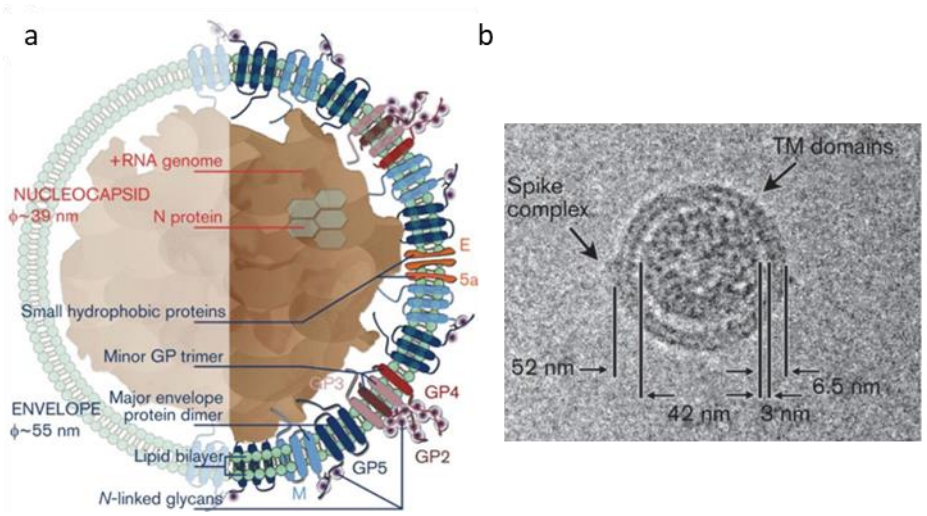

Figure 1.5 Structure of arterivirus virion. (a) Schematic diagram of the arterivirus particle. The virus particle is approximately 50-60 nm in diameter and roughly spherical. The nucleocapsid protein surrounds the viral genome which is then surrounded by the viral envelope. The envelope contains the structural glycoproteins as well as the M and E proteins as indicated. **(b)** Cryo-EM image of PRRSV virion with measurements of the viral dimensions indicted. A putative spike protein complex is also shown on the left of the virion. Edited Snijder *et al*. 2013; Spilman *et al*. 2009**.**

A breakdown of the virion size, genome size and structural proteins of the arteriviruses are listed in table 1.3.

Table 1.3 Structural proteins of arteriviruses

Virus	Diameter (nm)	Genome size (kb)	Structural protein	Gene	Size (aa)	Reference
EAV	50-60	12.7	E	2a	67	(Zhang *et al.*, 2008)
			Gp_{2b}	ORF2b	227	
			Gp3	ORF3	163	
			Gp4	ORF4	152	
			Gp5	ORF5	255	
			M	ORF6	162	
			N	ORF7	110	
LDV	55	14.2	Minor Gp	ORF2	227	(Palmer *et al.*, 1995)
				ORF3	191	
				ORF4	175	
			VP_3	ORF5	199	
			M	ORF6	172	
			N	ORF7	116	
PRRSV	45-55	15.1	Gp_2	ORF2a	255	GenBank: KC771271.2
			E	ORF2b	73	
			Gp_3	ORF3	265	
			Gp_4	ORF4	183	
			ORF5a	ORF5a	51	
			Gp5	ORF5	201	
			M	ORF6	173	
			N	ORF7	128	
SHFV	45-50	15.7	Minor Gp	ORF2a	223	(Bailey *et al.*, 2014)
			Minor Gp	ORF2b	202	
			Minor Gp	ORF3	166	
			E	ORF4a	81	
			Minor Gp	ORF4b	204	
			Minor Gp	ORF5	195	
			Minor Gp	ORF6	171	
			Hypothesised protein	ORF7a	58	
				ORF7	232	
			Large Gp	ORF8	162	
			M	ORF9	111	
			N			

The virion comprises the viral RNA encapsulated by the N protein, which forms the core structure of the virus. The core is then coated in a lipid bilayer that is studded with the viral structural proteins. As mentioned in section 1.3.6.1, these structural proteins are expressed from the sgmRNAs produced during viral transcription (Pasternak *et al*., 2006). The proportion of these proteins present within the lipid bilayer is virus dependent and some of the viral proteins are not confirmed to be expressed, for example the protein encoded by ORF7a in SHFV (Bailey *et al*., 2014).

It has been shown that the structural proteins in EAV required for virion assembly are Gp5, M and N proteins with the particles forming in the absence of E, Gp_{2b}, Gp_3 and Gp_4. These particles were seen to contain viral genomic RNA (Wieringa *et al*., 2004). In the wild type virus N, M and Gp5 are the major virion components, with E occurring at intermediate amounts and the remaining Gps as minor structural proteins (Wieringa *et al*., 2004). The interactions between the structural proteins of the arteriviruses are thought to be important in the infectivity of the viral particles. For example, heterodimerisation of Gp5 and M protein via a disulphide linker has been shown to be essential for the infectivity of the virus (Snijder *et al*., 2003).

1.3.6.4. Arteriviral proteins

The number of proteins encoded in the viral genome is virus dependent, however there are a number of conserved proteins within the arterivirus family; polyprotein1ab (pp1ab), RdRp, N protein, E protein, M protein and glycoproteins, each of which will be discussed as general groups.

1.3.6.4.1. Polyprotein1ab

As with all Nidoviruses, the arterivirus pp1ab is encoded by ORF1a and ORF1b. The proteins produced from these ORFs are subsequently cleaved into between 12 and 15 smaller functional proteins by viral encoded proteinases, shown in table 1.4. (Gorbalenya *et al*., 2000).

Table 1.4 Viral proteinases of arteriviruses (Gorbalenya *et al*., 2000).

Proteinase	Alternative names	Associated end-protein	Principle nucleophile
PCP1α		nsp1α, nsp1 in EAV	Cys (Lys in EAV)
PCP1β	PCP for EAV	nsp1β, nsp1 in EAV	Cys
CP2	CP, nsp2 proteinase	nsp2	Cys
3CLSP	nsp4, SP	nsp4	Ser

The cleavage of ORF1a and ORF1b is virus specific, with some arteriviruses encoding a higher number of functional proteins within this region of the genome than others. The cleavage of PRRSV pp1ab results in the production of at least 14 functional proteins, most of these proteins have been characterised, but there are some with as yet unknown functions. These proteins are summarised in table 1.5 along with their known or predicted functions (Fang and Snijder, 2010).

Table 1.5 PRRSV pp1ab cleavage products adapted from (Fang and Snijder, 2010).

Cleavage product	Known or predicted nsp function/properties	Reference
nsp1α	Zinc finger protein, accessory protease PCPα, regulator of sg mRNA synthesis and potential interferon (IFN) antagonist. Crystal structure solved	(Kroese *et al*., 2008)
nsp1β	Accessory protease PCPβ, potential IFN antagonist	(Kroese *et al*., 2008)
nsp2	Accessory protease CP, deubiquitinating (DUB) enzyme, potential IFN antagonist, transmembrane protein, involved in membrane modification and suppression of innate immune response	(van Kasteren *et al*., 2013)
nsp3	Transmembrane protein, involved in membrane modification	(Snijder *et al*., 2001)
nsp4	Main protease SP (3CLSP)	(van Dinten *et al*., 1999)
nsp5	Transmembrane protein, potentially involved in membrane modification	(Music and Gagnon, 2010)
nsp6	Unknown	(Music and Gagnon, 2010)
nsp7α	Unknown	(van Aken *et al*., 2006)
nsp7β	Unknown	(van Aken *et al*., 2006)
nsp8	Unknown	(Snijder and Meulenberg, 1998)
nsp9	RNA dependent RNA polymerase	(Beerens *et al*., 2007)
nsp10	NTPase, RNA helicase; contains putative zinc-binding domain	(Bautista *et al*., 2002)
nsp11	Endoribonuclease (NendoU)	(Music and Gagnon, 2010)
nsp12	Unknown	(Music and Gagnon, 2010)

1.3.6.4.2. RdRp

The replication of all Nidoviruses is dependent on cytoplasmic RNA dependent RNA synthesis carried out by the RNA dependent RNA polymerase (RdRp), encoded by all of the Nidoviruses. This protein is encoded in pp1ab and is the cleavage product of nsp9. Polymerases are enzymes that are involved in the catalysis of templated synthesis of new polynucleotide sequences in a 5'-3' direction. These proteins are encoded by all organisms and RNA viruses (Lehmann *et al*., 2016). The structure of these proteins resemble a cupped hand with finger, palm and thumb domains which are used to guide the substrates and metal ions into the catalytic domain (Ferrer-Orta *et al*., 2006). The EAV RdRp is the best characterised arteriviral RdRp

and *de novo* RNA synthesis by this protein has been extensively investigated. The EAV protein requires Mn^{2+} and Mg^{2+} (can function with one or the other but optimal function is observed with 2 mM Mn^{2+} and 4 mM Mg^{2+} in *in vitro* studies), and was shown to be catalytically active without the requirement of other viral and host proteins in a *de novo* manner, relying on poly-uridine or poly-cytidine single stranded RNAs (Beerens *et al*., 2007). This, however, is not a conserved feature of Nidoviruses RdRps, where coronaviruses RdRps have been shown to synthesise RNA with the requirement of primer sequences (Beerens *et al*., 2007; Cheng *et al*., 2005).

1.3.6.4.3. Nucleocapsid protein

The N protein of arteriviruses is encoded by the sgRNAs of ORF7. This is a crucial viral protein as it encapsulates the viral genome within the virion. The N protein and the viral genome are the main components of the arterivirus nucleocapsid core. The nucleocapsid of PRRSV and EAV are one of the more widely studied arteriviral N proteins and electron microscopic (EM) analysis has shown that the PRRSV virion is approximately 52 nm in diameter, figures 1.5a and 1.6. The core of the virion, the N protein surrounding the viral genome, is on average 39 nm with a gap of around 3 nm between this core and the viral envelope. The envelope-core interactions are weak and flexible. Transmembrane (TM) spanning density can also be seen, which is thought to be the TM regions of M and Gp5 envelope proteins (Spilman *et al*., 2009; Snijder *et al*., 2013).

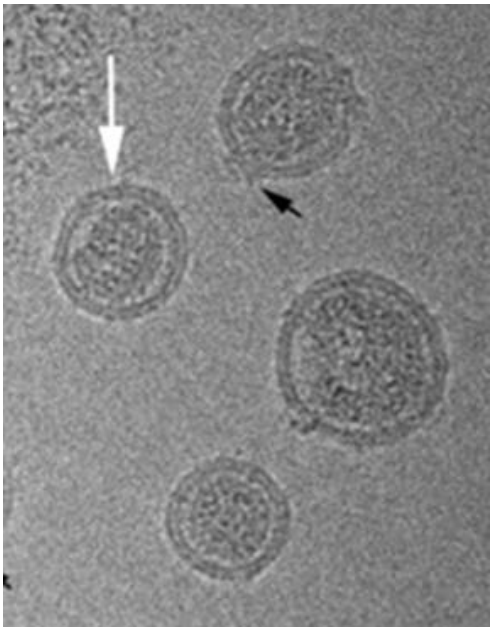

Figure 1.6 EM analysis of PRRSV viral particles. The PRRSV virion is spherical and consists of a core containing the genome surrounded by the N protein (dense region in the centre of the virion). The viral envelope can be seen as well as a spike complex indicated by the black arrow (Spilman *et al*., 2009).

It has been hypothesised that the N protein of arteriviruses forms a dimeric structure when crystallised in isolation (Doan and Dokland, 2003; Deshpande *et al*., 2007). However, recent EM analysis of the virion suggests that this is more likely to be a double layer of N protein in a linked chain with interactions between the viral RNA and the N-terminal region of the N protein, the structure of which is yet to be elucidated (figure 1.6). Moreover, the use of structure prediction software suggests that the N-terminal region of the arteriviral N protein is helical which would allow for an extended conformation that fits with the observed structure of the viral nucleocapsid core (Spilman *et al*., 2009).

The structure of the viral N proteins of PRRSV (C-terminal 65 amino acids) and EAV are shown in figure 1.7 (Deshpande *et al*., 2007; Doan and Dokland, 2003). The structure of these proteins is similar despite the sequence homology being only 16% in the N-terminal region of the protein and 35% in the C-terminal region, as well as the EAV protein being shorter by 13 amino acids (Deshpande *et al*., 2007). The RNA binding to these proteins is currently unknown, however, in PRRSV the binding of RNA is thought to occur through the lysine enriched region 34-51 aa (Wootton and Yoo, 2003), although interestingly these are absent in the EAV N

protein. Although the structure of these proteins is similar, their conformations within the context of the virus appear to be subtly different resulting in the dimer formed by the EAV N protein being a tighter structure than that of the PRRSV N protein (Deshpande *et al*., 2007).

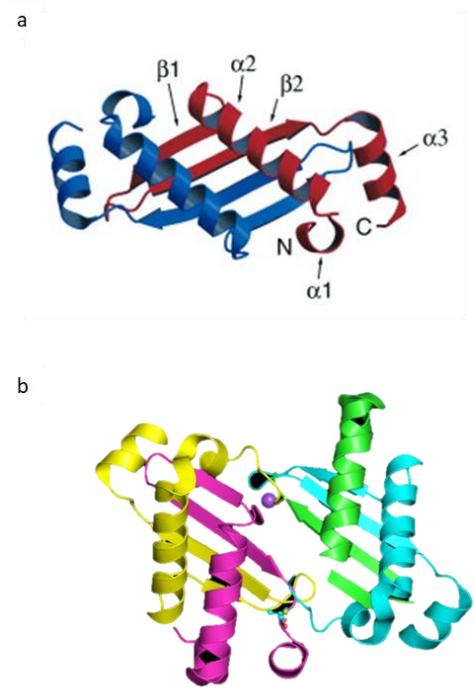

Figure 1.7 Crystal structure of PRRSV and EAV N proteins. (a) PRRSV N protein dimer, monomers shown in blue and red ribbons. The structure of this protein does not include the N terminal 57 amino acids which were removed to aid crystalisation (Doan & Dokland 2003). **(b)** EAV N protein dimer, monomers shown in pink/yellow and green/blue. The overall structural of the two dimers is similar despite sequence differences (Deshpande *et al*. 2007).

A more in depth review into the PRRSV N protein is discussed in section 1.4.3 with regards to its role in the context of PRRSV infection.

1.3.6.4.4. Glycoproteins

As with the N protein, the viral glycoproteins (Gp) are encoded by the sg RNAs of arteriviruses at the 3' end of the viral genome. The number of Gp genes varies within the arteriviral family despite the small genome size of these viruses, previously listed in table 1.3. The Gps are found within the envelope of the virion and interact with other viral structural proteins as well as host cell proteins, where they function in virus entry (Van Breedam *et al*., 2010), although the mechanisms

by which this occurs are not fully understood. It is thought that Gp5 interacts with the M protein to form a major Gp complex (figure 1.8) within the envelope and Gp2/Gp3/Gp4 interact to form the minor Gp complex as shown in figure 1.9 (Veit *et al*., 2014; Wieringa *et al*., 2003). The complex of Gp5/M interacts by a disulphide bond between the N-terminal region of the M protein (cysteine 8) and the N-terminal region of Gp5 (cysteine 27) (Snijder *et al*., 2003). Gp5 is a variable protein which can differ in length between viruses and in sequence homology between virus strains, however, the overall membrane topology is thought to be the same between arteriviruses (Veit *et al*., 2014). The membrane topology of Gp5 is predicted to result in a structure that spans the membrane three times, although this is yet to be confirmed in the context of the virus.

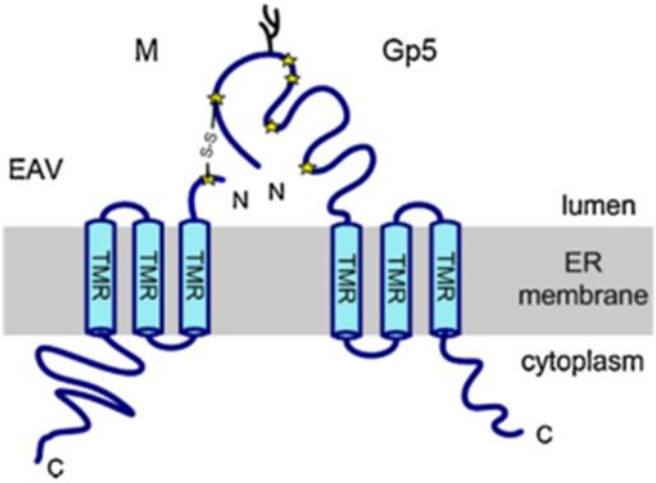

Figure 1.8 Glycoprotein 5 interaction of EAV with M protein. The N termini of the M and Gp5 proteins are joined by a disulphide bond (cystine 8 of M and cystine 27 of Gp5) with putative transmembrane domains (TMR) indicated. Dimerisation of these proteins is important for their transport from the ER to the golgi apparatus and then onto the infectious viral particle (Veit *et al*., 2014).

The complex of Gp5 and M is involved in the binding of sialoadhesin receptor in a sialic acid-dependent manner, where the sialic acids are found on Gp5, to mediate the entry of the virus into the host cell (Van Breedam *et al*., 2010). The glycoproteins of arteriviruses are N-linked glycosylated, and these proteins have been implicated in viral assembly, viral attachment to cells, virus neutralisation and protection from the immune system (Ansari *et al*., 2006; Wissink *et al*., 2004; Jiang *et al*., 2007; Fan, Liu, *et al*., 2015; Thaa *et al*., 2013; Wissink *et al*., 2005).

As well as the major Gps found in the envelope of the virion, the minor glycoproteins also play a key role in the virus lifecycle, determining viral tropism in cell culture (Tian *et al*., 2012). The structure of the complex of the minor Gps is shown in figure 1.9, the glycoproteins contain an N terminal signal domain and a single transmembrane region, in the case of Gp2 and Gp4. The branches indicate the glycosylation sites on the proteins. Gp3 also has an N terminal signalling peptide, glycosylation sites and a hydrophobic region. The number of glycosylation sites on the glycoproteins is dependent on the virus or strain of virus (Veit *et al*., 2014).

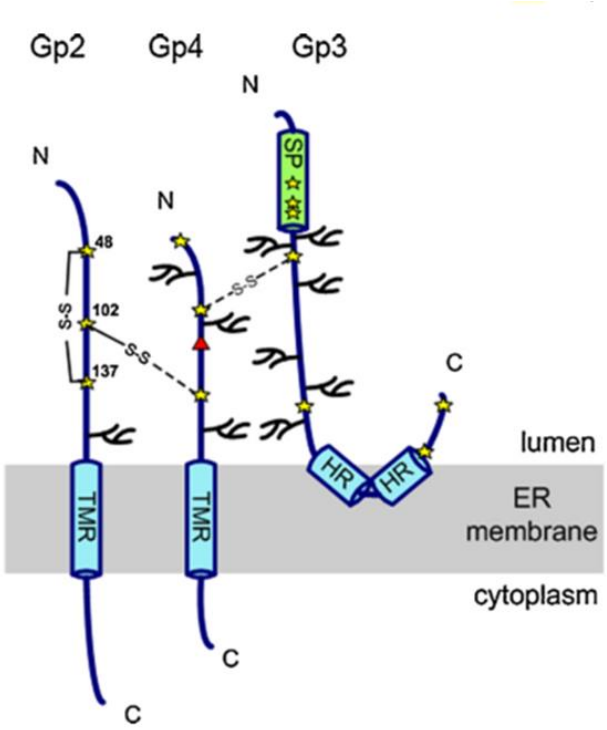

Figure 1.9 Arterivirus minor glycoproteins. A complex is formed via disulphide bonds between Gp2/3/4 as indicated -s-s- in EAV. Glycosylation is shown with the branches on the lumenal branches with expected TMR and hydrophobic regions (HR) indicated (Veit *et al*., 2014).

1.3.6.4.5. M protein

The viral M protein is encoded by ORF6 of PRRSV, EAV and LDV and ORF8 of SHFV. As previously discussed in section 1.3.6.4.4 it forms a heterodimer with Gp5 via a disulphide link (Snijder *et al*., 2003). This protein is between 18 and 19 kDa in size and the PRRSV M protein is known to have three membrane spanning domains (Music and Gagnon, 2010). The M protein also forms homodimers which may be

involved in the building of the functional Gp5/M protein complex (de Vries *et al*., 1995).

1.3.6.4.6. E protein

The E protein is encoded by ORF2 in the arteriviral genome of EAV (ORF2a) (Wieringa *et al*., 2004) and PRRSV (ORF2b) (Music and Gagnon, 2010) and ORF4 (Bailey *et al*., 2014) of SHFV, and along with the glycoproteins is found in the virion envelope. The protein itself is small (8 kDa) with three domains, although the structure is not known, it is predicted that there is a hydrophobic transmembrane domain and a hydrophilic C-terminal domain (Snijder *et al*., 1999). Two conformations have been proposed for the insertion of the E protein into the virion membrane, one with a single pass and the exposure of either the N- or C-terminus of the protein to the virus core, or a hairpin conformation with the N- and C-terminus being exposed at the same side of the membrane (Thaa *et al*., 2009). It has also been shown that the E protein is able to form homo-oligomers which function as an ion channel in the viral envelope to mediate the uncoating of the virus and release of the genome into the cytoplasm (Lee and Yoo, 2006). The E protein has been shown to be essential for the production of infectious virus but is not essential for the assembly and budding of viral particles, at least in EAV (Wieringa *et al*., 2004).

1.3.6.5. Arteriviral pathogenesis

Arteriviruses cause infections which are associated with symptoms ranging from respiratory disease, abortion or lethal haemorrhagic fever although they have been known to be implicated in the establishment of persistent infection within a population due to asymptomatic infection of animals (Snijder *et al*., 2013).

The viral proteins previously discussed in table 1.5 can be implicated in the evasion or activation of the immune response. The innate immune response to arteriviral infections have been widely explored with the investigation into individual viral proteins but not as a general viral response. Viral non-structural proteins such as nsp1α and nsp1β have been implicated in the modulation of the immune response and these will be discussed in respect of PRRSV in sections 1.4.1.1 – 1.4.1.7.

1.3.6.5.1. Arteriviral innate immune response

The response of the innate immune system to an arteriviral infection is generally poor, which is why the viruses are able to establish persistent infections. It is thought that these viruses evade the innate immune response by modulating the proteins within this system to reduce its activation and this is carried out mainly by the viral non-structural proteins (Snijder *et al*., 2013). The targets for these proteins are cytokine signalling pathways, including interferons and interleukins (Sun *et al*., 2012).

1.3.6.5.2. Humoral immune response

The antibody response to arteriviral infection is very early and high levels of antibodies are produced, they are generally raised in response to the majority of the viral proteins, however the levels of each depend on the virus species (Snijder *et al*., 2013). For example in PRRSV infection, the antibody response to the N protein is first and strongest (Darwich *et al*., 2010).

1.3.6.5.3. Cell-mediated immune response

Arteriviral cell-mediated immune responses remain poorly characterised, however, it is thought that PRRSV induces a T cell response between 2 and 8 weeks post infection, but this response is highly variable between animals with apparently no correlation with the viral load in the lymphoid tissues (Snijder *et al*., 2013; Darwich *et al*., 2010).

1.4. Porcine reproductive and respiratory syndrome virus (PRRSV)

Porcine reproductive and respiratory syndrome virus (PRRSV) is an example of an arteriviral livestock infection affecting swine. PRRSV was first identified in the late 1980's and early 1990's in Canada and North America (genotype 2) as mystery swine disease and swine infertility and reproductive syndrome and in Europe (genotype 1) as blue ear disease or PRRS (Dea *et al*., 1992; Terpstra *et al*., 1991; Wensvoort *et al*., 1991). The first description of PRRSV in Europe was in Denmark in 1990/1991 with the outbreak of mystery swine disease, which was affecting breeding sows and their litters. Sows were feverish and anorexic, with their

offspring being aborted late in gestation (day 110 of 115) or being born mummified or stillborn, with those that did survive being weak and sickly and at risk of respiratory disease (Wensvoort *et al*., 1991). The causative agent of this infection was isolated as Lelystad virus in Europe (Wensvoort *et al*., 1991; Terpstra *et al*., 1991) and VR-2332 in the US and Canada (Collins *et al*., 1992; Dea *et al*., 1992). Following the identification of this new viral agent, a positive sense, enveloped RNA virus with a genome size of 15 kb was assigned as a member of the *Arteriviridae* family in the *Nidovirale* order (Meulenberg *et al*., 1993).

25 years later, the virus is more commonly known as PRRSV and is in circulation worldwide as the most prevalent disease of swine. As a result there is the potential for the establishment of persistent, endemic infections within populations due to the lack of suitable control measures (Lunney *et al*., 2010). In 2005 the economic losses as a result of PRRSV infection were estimated to be in excess of $560 million in America alone per annum (Neumann *et al*., 2005), in 2012, this value increased to $668.58 million (Zimmerman *et al*., 2012) a value which can be vastly escalated when incorporating the losses to the worldwide agricultural industry as a whole.

A key feature of RNA viruses like PRRSV, is their rapid mutation rates, attributed to the lack of proof reading normally carried out by the RNA dependent RNA polymerase. This can result in spontaneous mutations at a rate of about one mutation per genome per replication (Drake and Holland, 1999). The virus is therefore highly prone to virulence mutations and in the last decade there have been a number of highly virulent strains of PRRSV emerging in the US and Asia with much higher morbidity and mortality rates, up to 100%, than the previously circulating strains (Li *et al*., 2007; X. Wang *et al*., 2015; Tong *et al*., 2007; Zhou *et al*., 2011; Ni *et al*., 2012; Shi *et al*., 2013). Therefore, targeting the virus with antivirals or vaccines and developing reliable diagnostics is difficult due to random mutations occurring within the numerous viral proteins.

1.4.1. PRRSV clinical presentation and pathogenicity

PRRSV, like all viruses is able to manipulate immune responses of infected hosts with evasion of the innate immune system being key to viral pathogenicity. PRRSV preferentially infects and replicates in host pulmonary alveolar macrophages

(PAMs). This infection results in the alteration of a number of cellular pathways and ultimately cellular apoptosis (Duan *et al*., 1997; Thanawongnuwech *et al*., 1997). Pathogenicity is important when considering a virus such as PRRSV. Low pathogenic strains have a low mortality and morbidity rate and the infection is generally a self-limiting respiratory illness, with only a small impact on the economics of a farm. However, a highly pathogenic (HP) strain of PRRSV can result in morbidity and mortality rates of 100% and up to 80% in infected sows and their offspring, respectively (Liu *et al*., 2017). PRRSV infection is also associated with secondary bacterial infections which may be attributed to the loss of macrophages in the lung, pulmonary intravascular macrophages (PIMs) which normally perform a bactericidal function (Thanawongnuwech *et al*., 1997). Pathogenicity and immune evasion is also important with regards to the establishment of a persistent infection lasting around four weeks post infection, where naive animals introduced into the heard become infected by the seemingly healthy animals suffering persistent infection (Wills *et al*., 1997).

1.4.1.1. Evasion of the immune response

PRRSV evades the immune system using a number of mechanisms; such as modulation of cellular signalling pathways including interferon and NF-κB, delaying detection of the virus, cytokine modulation, modulation of apoptosis, hijacking host microRNAs (miRNAs), impairment of antigen presentation, T-cell modulation and antibody dependent enhancement (ADE). These will be further discussed in the following sections.

1.4.1.2. Modulation of cellular signalling pathways

Modulation of host cell signalling pathways is a key feature of all pathogens seeking to avoid the immune response, by targeting pathways which lead to the activation of the immune system. The interferon signalling pathway is a prime example of a pathway targeted by PRRSV. This is a key signalling pathway in the innate immune response of host cells and high level production of interferons is induced in response to the detection of a pathogen by the sensing Toll-like receptors on the cell and endoplasmic surfaces. These receptors then go on to activate a number of

pathways within the cell, which in turn initiate the transcription of interferon genes (figure 1.10) (Theofilopoulos *et al*., 2004).

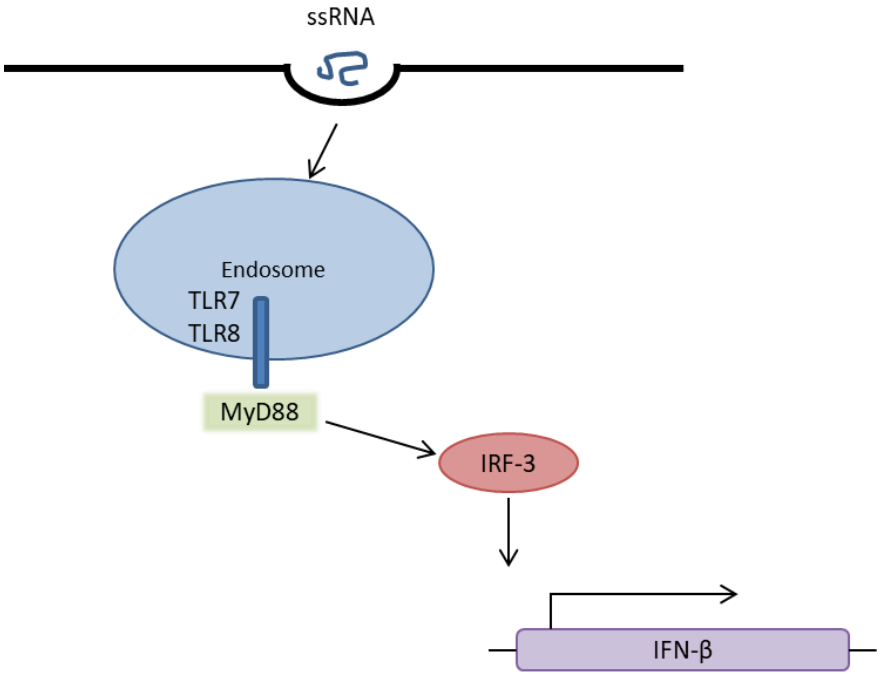

Figure 1.10 Interferon signalling pathway response to PRRSV infection. ssRNA is detected by Toll-like receptors (TLR) 7 and 8 and a signalling cascade is activated to initiate the transcription of IFN-β (Theofilopoulos *et al*., 2004).

Interferons are involved in blocking viral replication via the induction of antiviral proteins, therefore, making it a crucial pathway to be inhibited by the invading virus (Huang *et al*., 2015).

The PRRSV non-structural proteins (nsp) are directly involved in the evasion of the host immune system via modulation of the interferon signalling pathway, including nsp1, nsp2, nsp11, nsp4, as well as the structural protein N (Huang *et al*., 2015; Sun *et al*., 2012; Huang *et al*., 2014; Chen *et al*., 2014). Nsp1 is an inhibitor of IRF3 phosphorylation and nuclear translocation and inhibits NF-κB activation and suppression of IFN-β (Beura *et al*., 2010; Song *et al*., 2010). Nsp2 also contributes to the inhibition of interferon regulatory factor 3 (IRF3) with nsp1 (Li *et al*., 2010). A highly pathogenic strain of PRRSV has recently been shown to inhibit the induction and signalling of IFN-α and β in porcine alveolar macrophages. Here nsp4 blocks the IRF3 signalling pathway, in addition it also disrupts RIG-I signalling (Huang *et al*., 2016; Huang *et al*., 2014). Nsp11 is able to inhibit NF-κB signalling

due to its deubiquitination activity of IκBα and the subsequent attenuation of NF-κB target genes, due to reduced proteosomal degradation and inhibition of NF-κB nuclear translocation (D. Wang *et al*., 2015). Nsp11 and the protease 3CLSP also function to degrade IPS-1, a mitochondrial antiviral-signalling protein resulting in the inhibition of IFNβ expression (Sun *et al*. 2012; Chen *et al*. 2015). A summary illustration of the inhibition of cellular pathways by PRRSV nsp is shown in figure 1.11 adapted from (Wang and Zhang, 2014).

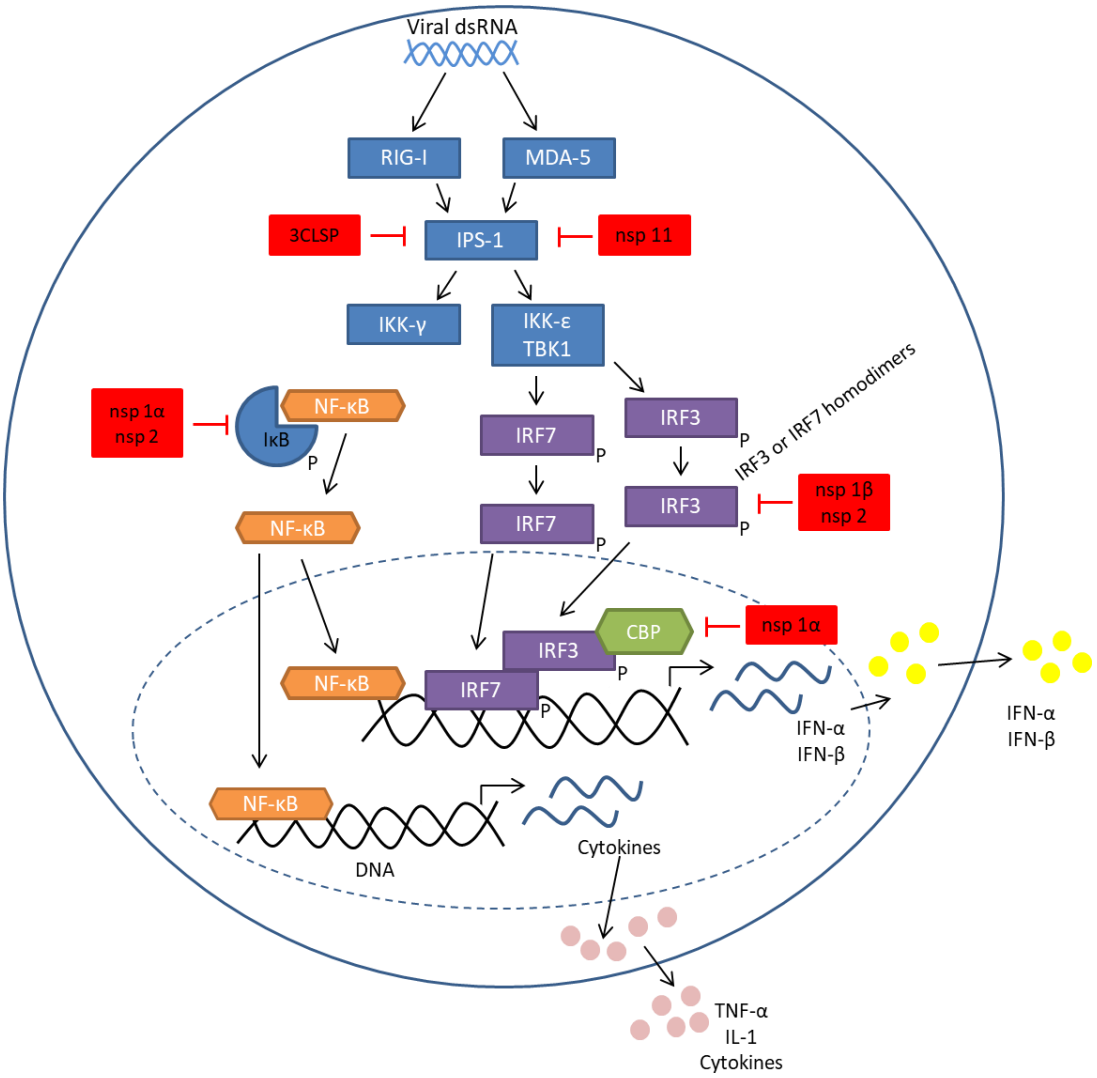

Figure 1.11 Inhibition of interferon pathways by PRRSV. Viral dsRNA is formed during PRRSV replication. The proteins in red are PRRSV proteins known to inhibit these pathways. Nsp11 inhibits IRF-3 phosphorylation and nuclear translocation by degrading IPS-1 mRNA, nsp1α inhibits IRF-3 association with CREB-binding protein (CBP) and enhances its degradation. It also interferes with IκB degradation. Nsp1β and nsp2 inhibit IRF-3 phosphorylation and nuclear translocation. Nsp2 interferes with IκB polyubiquitination and prevents its degradation. 3CLSP also degrades IPS-1 (Wang and Zhang, 2014).

Whilst they will be discussed separately, it is important to consider that the modulation of host cell signalling pathways by the virus is intimately linked to the following methods of immune evasion.

1.4.1.3. Modulation of other host cytokines

PRRSV proteins also modulate other host cytokines, including interleukin-10 (IL-10) and tumor necrosis factor-α (TNFα). Nsp1 and GP5 have been implicated in the upregulation of IL-10 expression which in turn causes a reduction in the expression of interferon-γ (IFNγ) *in vitro* and *in vivo* (Zhou *et al*., 2012; Wongyanin *et al*., 2012). The expression of TNFα from macrophages and activated T cells is attributed to the induction of an antiviral response in nearby uninfected cells and so the down regulation of TNFα by viral infections is paramount in the evasion of the host immune system (Smith *et al*., 1994). Interestingly, it has recently been shown that there is differential expression of TNFα, dependent on the PRRSV strain, with highly pathogenic strains of the virus inducing a lower TNFα response in porcine alveolar macrophages (PAMs). These are therefore better at suppressing its production via extracellular signal regulated kinase (ERK) signalling, than the low pathogenic counterparts (He *et al*., 2015; Hou *et al*., 2012).

1.4.1.4. Hijacking of host miRNAs

Host micro RNAs (miRNAs) are also important mediators of cellular antiviral responses (Lecellier *et al*., 2005; Harris *et al*., 2013) and PRRSV has been shown to manipulate the function of host miRNAs to its advantage. Although the downregulation of the NF-κB signalling pathway has previously been discussed (section 1.4.1.2) with regards to PRRSV, the role of this pathway in PRRSV infection is disputed. There is recent data suggesting that the activation of this pathway during PRRSV infection results in the upregulation of host cell miRNA, miR-30c. miR-30c is in turn involved in the inhibition of the interferon-I (IFN-I) signalling pathway via JAK1 targeting (figure 1.12) which enhances PRRSV infection *in vitro* and *in vivo* (Zhang *et al*. 2016). ssc-miR-30d-R_1 has also been shown to be decreased in the lungs of animals infected with PRRSV. This miRNA is ordinarily involved in the negative regulation of NF-κB signalling via TLR4, reducing PRRSV

replication. However, upon infection the virus downregulates this miRNA resulting in the activation of the NF-κB pathway (C. Wang *et al*., 2016). The differential data presented regarding the NF-κB pathway may be due to the changing requirements of the virus during its lifecycle.

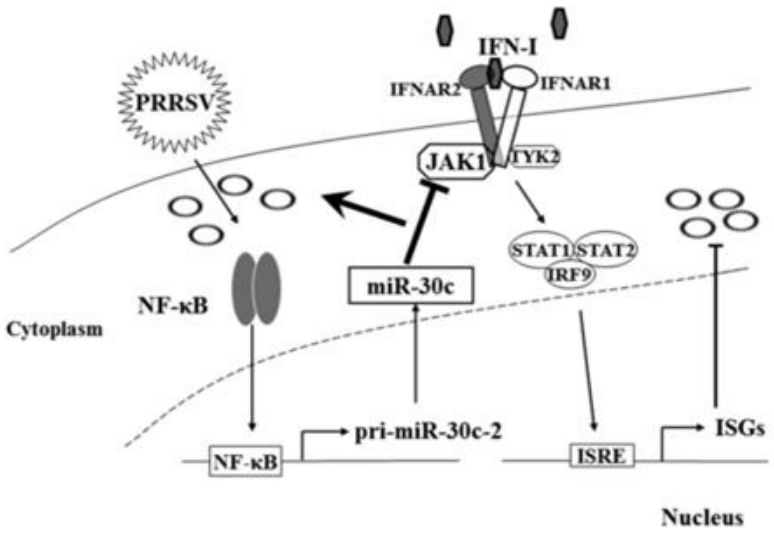

Figure 1.12 PRRSV and host miRNAs. PRRSV upregulates miR-30c to enhance viral replication by evading IFN-I–initiated innate immunity. During PRRSV infection, miR-30c is upregulated dependent on the NF-κB pathway. miR-30c interferes with IFN-I signalling by repressing JAK1 expression, leading to viral escape from the host innate-immunity response (Zhang *et al*. 2016).

miRNAs have also been shown to be involved in PRRSV-mediated modulation of argonaute protein-2 (Ago-2), by nsp1α and nsp11 in conjunction with short hairpin RNAs and double stranded RNAs to disrupt RNA silencing processes (Chen *et al*. 2015). The microRNAome has been characterised in pulmonary alveolar macrophages during PRRSV infection with a number of miRNAs found to be either up or downregulated. However, the downstream effects of these miRNA alterations is yet to be further investigated with regards to PRRSV replication (Hicks *et al*., 2013).

1.4.1.5. Modulation of T-cell response

Highly pathogenic strains of PRRSV have been shown to suppress T-helper 17 (Th17) cells in infected piglets, when compared to piglets infected with a viral strain of lower pathogenicity, which can predispose the piglets to secondary bacterial infections (Zhang *et al*. 2016). Further PRRSV-mediated modulation of the immune system via T-cells has been shown *in vivo* with the infection of piglets with two

strains of the virus resulting in the atrophy of thymus, the location of T-cell maturation, and the increase in the number of cells expressing TNFα and interleukin-10 (IL-10) (Amarilla *et al*., 2016). Modulation of T-cells by PRRSV has also been shown *in vitro* to occur by the expression of the N protein, where N protein expression in porcine monocyte-derived dendritic cells results in the significant increase in T-reg lymphocytes and IL-10 expression (Wongyanin *et al*., 2012). Regulatory T-cells are also targeted by PRRSV as they are immunosuppressive, they are responsible for the regulation of the immune response to viral infection (Huang *et al*., 2015). The ability of the virus to control T-reg cells appears to be strain specific with EU strains showing no effect on the induction of T-reg cells, compared to American PRRSV strains (Silva-Campa *et al*., 2010).

1.4.1.6. Delayed detection of virus

Recently, it has been suggested that a physical evasion of the immune system may also occur during PRRSV infection. Here the virus uses a nanotube network to facilitate intercellular infection without the release of infectious virus particles from the cell, preventing a neutralising antibody response mediated by the humoral immune system (Guo *et al*., 2016). This is highly advantageous to the virus, resulting in the rapid spread of viral particles throughout a tissue, uninterrupted by the host extracellular immune response. As well as intracellular transport of viral particles, PRRSV also uses replication vesicles, which provide a region within the infected cells for RNA replication as previously discussed (section 1.3.6.2).

1.4.1.7. Antibody dependent enhancement

Antibody-dependent enhancement (ADE) of viral infection is a mechanism employed by a number of viruses which capitalises on the presence of antiviral antibodies to facilitate the efficient entry of viral particles into host cells. This is utilised by flaviviruses (Peiris and Porterfield, 1979), HIV (Robinson *et al*., 1988), ebola virus (Takada *et al*., 2003), respiratory syncytial virus (Ponnuraj *et al*., 2003), rabies virus (King *et al*., 1984) and PRRSV (Yoon *et al*., 1997), among others. It is hypothesised that this phenomenon occurs when a viral particle of one serotype is

bound by antibodies against another serotype. Ordinarily this would be known as a neutralising effect of the antibody and the virus would fail to bind to the surface receptor of the host cell (Takada and Kawaoka, 2003). However, in the case of ADE, antibodies binding to the virus particle also bind to the F-region antibody receptor (FcyR), on the surface of the host cell (Halstead *et al*., 1977). PRRSV has been shown to infect macrophages via the ADE mechanism, resulting in the down regulation of a number of cellular signalling pathways leading to the disruption of the antiviral response as previously discussed with regards to IRF, TNFα and NF-κB (sections 1.4.1.2 – 1.4.1.3) (Bao *et al*., 2013).

1.4.1.8. Clinical manifestation of PRRSV

The mechanisms by which PRRSV modulates the immune system are important when considering the clinical manifestation of the infection. As discussed in section 1.4.1 the pathogenicity of the viral strain is important for mortality and morbidity rates of infection, with these intimately linked to the type and scale of the immune response induced. The scale of the immune response mounted by the infected animal is also linked to the ability of the animal to clear the virus and the establishment of a persistent infection (figure 1.13) (Chand *et al*., 2012).

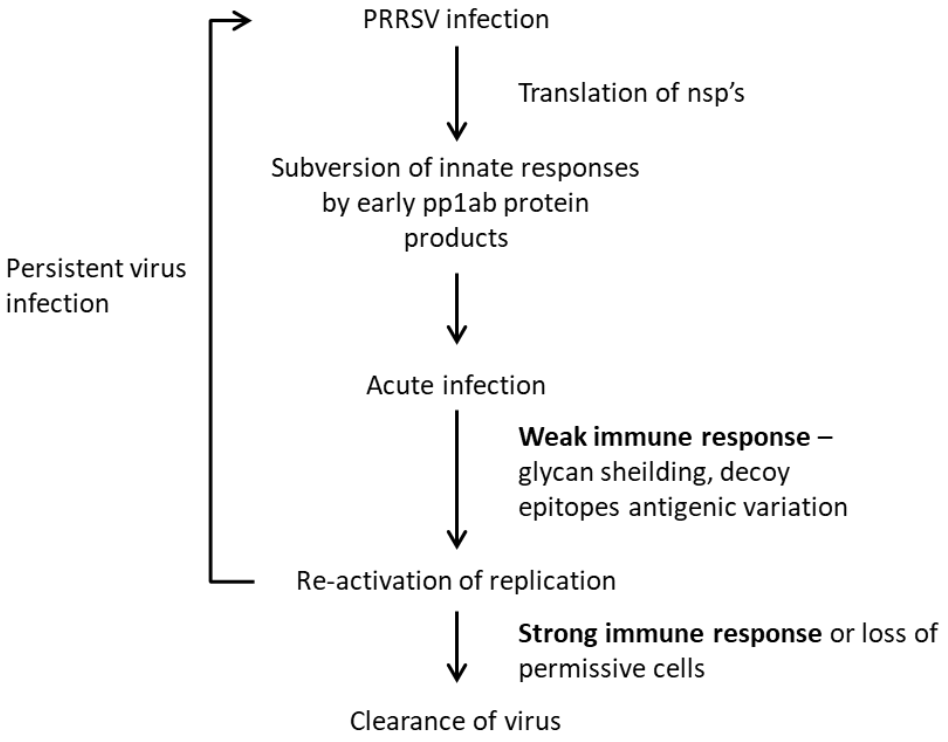

Figure 1.13 Establishment of persistent infection in an animal. Persistent infection is established when the infected animal fails to fully clear the infection from its system. This may be due to the animal having a weakened immune system due to age or as a result of other illnesses. The virus is able to continue replicating within this animal and shed infectious virus to other naive animals in the herd and allowing the establishment of persistent infection (Chand *et al* 2012).

The most evident symptom of PRRSV infection is foetal death, as respiratory illness in both adult and young animals can be difficult to diagnose and is generally a self-limiting symptom of this virus. Nevertheless, there is a risk of secondary complications such as bacterial infection and loss of daily live weight gain that can result in significant losses for the agricultural industry. Although the pathogenesis of foetal death is not yet understood, it has been hypothesised that histopathological lesions on the maternal/foetal interface is a contributing factor, as well as the viral load (Novakovic *et al*., 2016; Karniychuk and Nauwynck, 2013). As shown in figure 1.14 it is proposed that infection of monocytes adhered to the endothelial cells of the endometrium and subsequent viral replication causes apoptosis of infected cells and subsequent infection of cells within the endometrium. This allows the virus to cross the uterine epithelium and trophoblast and reach the foetal organs via the umbilical circulation. The infection of cells within the placenta can result in the detachment of the trophoblast from

the uterine epithelium which causes degeneration of the placenta and foetal death (Karniychuk and Nauwynck, 2013). The degeneration of the placental tissue post infection is also proposed as a contributing factor in the birth of weak and sickly piglets in particular. If infection occurs in the very late stages of gestation, the lesions that appear at the maternal/foetal interface may not be sufficient to cause foetal death but may cause pre-term labour and the subsequent birth of sick piglets.

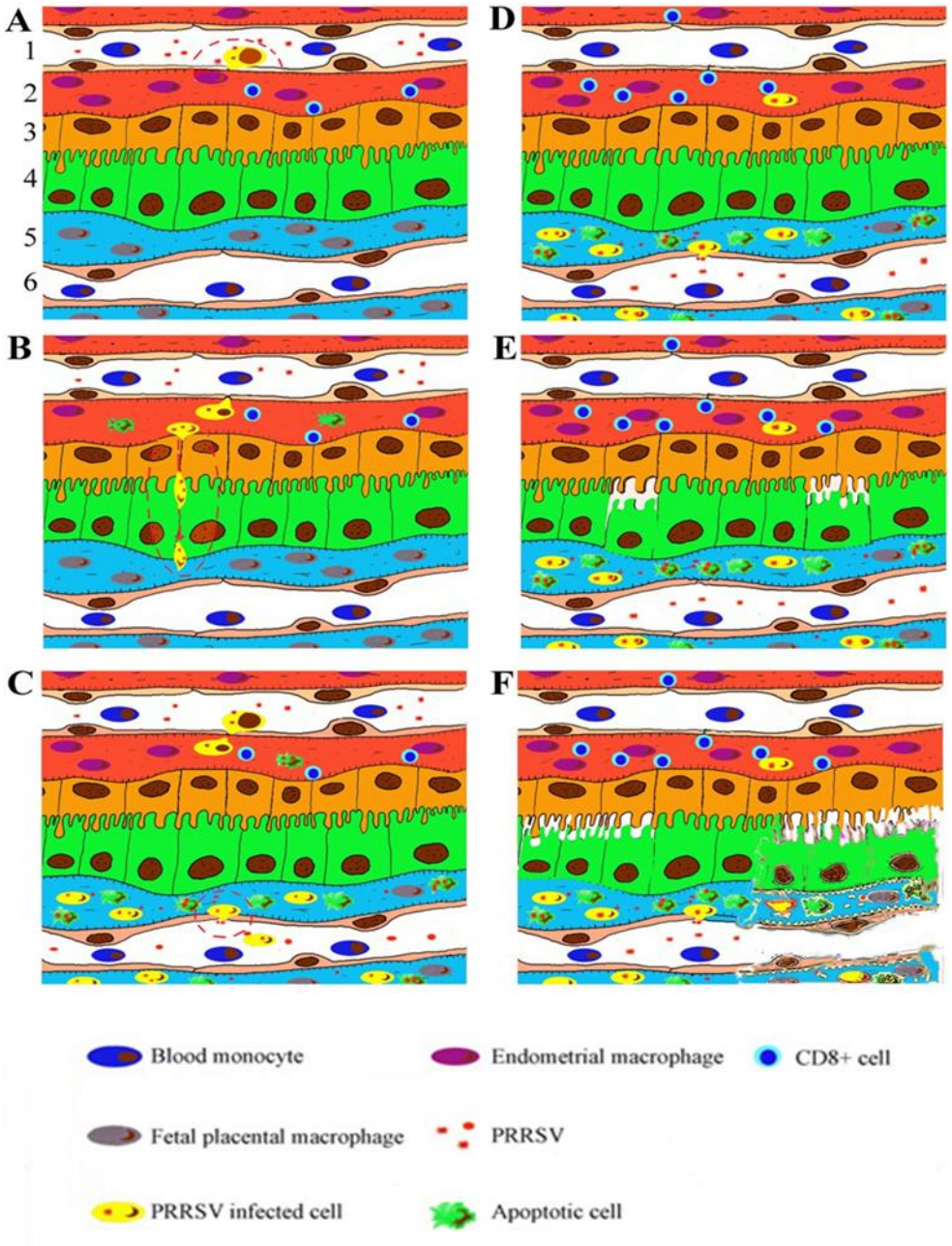

Figure 1.14 Infection of the maternal-foetal interface during PRRSV infection. 1. Maternal blood vessel. 2. Endometrial connective tissue. 3. Uterine epithelium. 4. Trophoblast. 5. Foetal placental mesenchyme. 6. Foetal blood vessel. **(A)** During viremia PRRSV attaches, enters and replicates in susceptible monocytes adhering to the endothelial cells of the endometrial vessels. Infected monocytes enter the endometrium from the maternal blood. **(B)** PRRSV replicates in the endometrial macrophages causing apoptosis in infected and surrounding cells during replication. PRRSV crosses the uterine epithelium and trophoblast, likely in association with maternal macrophages. **(C)** Focal, highly efficient PRRSV replication occurs in the foetal placental macrophages. PRRSV reaches foetal internal organs through the umbilical circulation. PRRSV causes apoptosis in infected and surrounding cells during replication in the placenta. **(D)** Maternal immunity (most probably $CD8^+$ endometrial NK cells) suppresses PRRSV replication within the endometrium, however there is highly efficient PRRSV replication in the placenta. **(E)** Focal detachment of the trophoblast from the uterine epithelium and focal degeneration of the placenta, at the places of virus replication and in the adjacent sites. **(F)** Multifocal degeneration and full degeneration of the placenta, at the places of virus replication, and in the adjacent sites (Karniychuk and Nauwynck, 2013).

The pathogenicity of PRRSV can also result in different clinical manifestations during infection. Initially, the majority of PRRSV strains in worldwide circulation were of low pathogenicity, causing significant but not life threatening losses to the infected animals. However, in the early 2000's, the emergence of highly pathogenic (HP) PRRSV strains in both America and China resulted in a huge increase in the mortality rates seen within infected herds, thereby increasing the losses felt by the industry in monetary terms. The most recent economic evaluations into the cost of PRRSV infection put the losses in Denmark between €59 and €379 per sow per 18 week period outbreak, with the cost post outbreak between €3 and €160 per sow, depending on the methods used to tackle the disease (Nieuwenhuis *et al*., 2012). Although this does not sound significant when discussed in € per/animal, it can be devastating during an outbreak which may affect hundreds of animals over many farms. It is difficult to assess the cost of the infection in Asia as the agricultural industries here are less well-regulated and infections are likely to be vastly under-reported. There are many reports of outbreaks of HP strains of PRRSV in the literature, resulting in high mortality rates. For example, images of gross pathological findings in pigs suffering from PRRSV infection can be seen in figure 1.15 (Snijder *et al*. 2013).

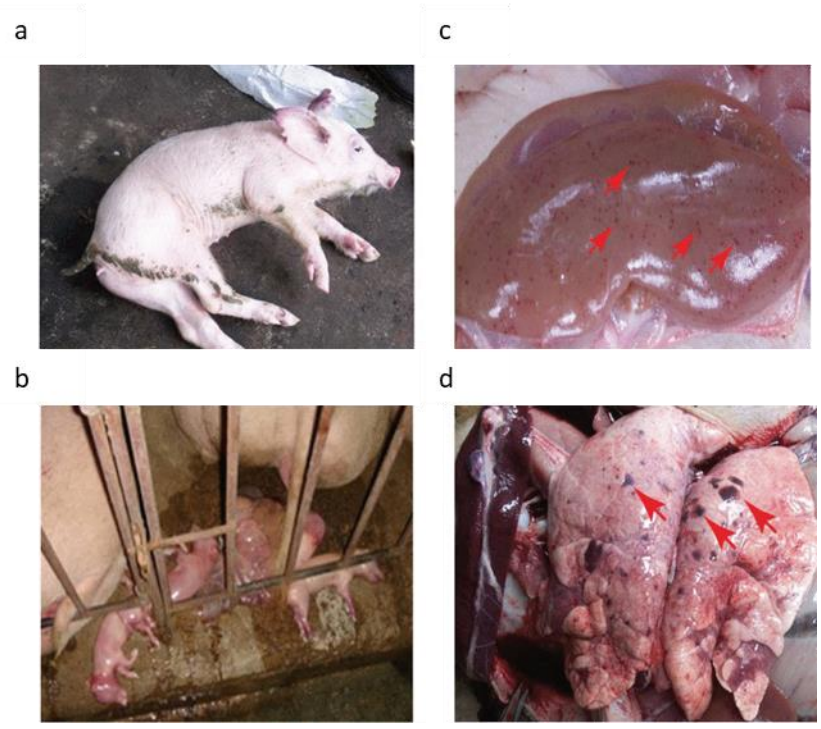

Figure 1.15 Clinical symptoms of PRRSV infected pigs. (a) Infected piglet with high fever. **(b)** Aborted foetuses. **(c)** Severe lesions on the kidney of an infected pig indicated by red arrows. **(d)** Severe lesions on the lungs of an infected pig which is unique to highly pathogenic PRRSV infection (Snijder *et al*. 2013).

Recently, HP-PRRSV has been shown to induce cellular apoptosis in the bone marrow of infected piglets as well as the thymus, both key features of the immune system, increasing the risk of secondary infections and leading to the increased mortality rates associated with this viral strain (Tong *et al*. 2016; Wang *et al*. 2015). This was previously discussed in section 1.4.1.

1.4.2. PRRSV genome

The PRRSV genome is broadly similar to that of other Nidovirus/arterivirus genomes that have previously been discussed in section 1.3.3 and so the in depth details of the genome of PRRSV will not be discussed in further detail here. The length of the PRRSV genome varies dependent on the viral strain but is generally between 14.9 kb to 15.5 kb, the discrepancies are as a result of additions or deletions in the ORFs encoding the structural and non-structural proteins. As well as the ORFs there are two non-coding untranslated regions in the genome, the 5'UTR and 3'UTR. The genome and expression profiles of the ORFs are shown in figure 1.16 (Kappes & Faaberg 2015).

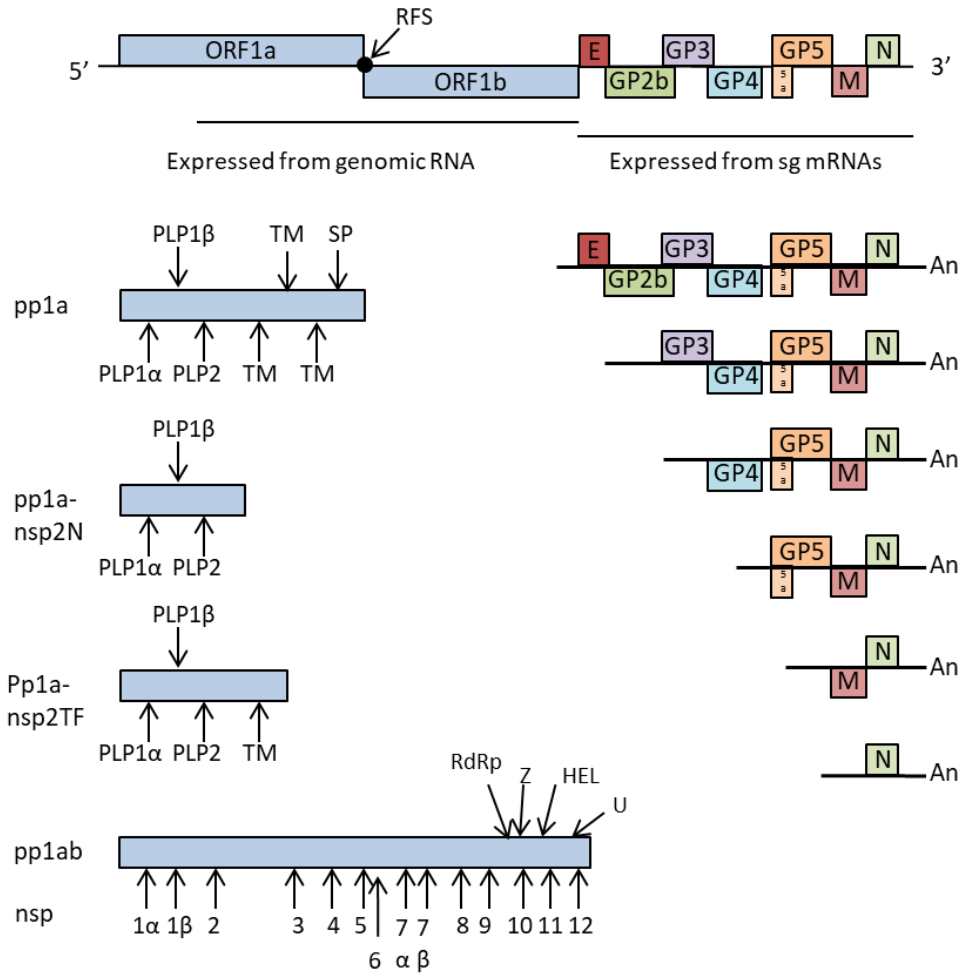

Figure 1.16 PRRSV genome transcription and translation. The first regions of the genome to be translated are polyproteins from the 5' end of the genome. The 4 polyproteins produced are pp1a, pp1a-nsp2N, pp1ansp2TF and pp1ab. Pp1a-nsp2N and pp1a-nsp2TF are translated by ribosomal frame shifts. These 4 polyproteins encode the non-structural proteins which are produced by the cleveage of the polyprotein by viral encoded proteinases (PLP1α, PLP1β, PLP2 and SP which are encoded where indicated on each polyprotein). Other viral proteins encoded in these polyproteins are the RdRp, a zinc finger domain (Z), a helicase domain and a Nidovirus uridylate specific endoribonuclease (U). The sgRNAs which are produced for the translation of the viral structural proteins are produced by a co-terminal discontinuous transcription strategy using a negative strand intermediate. The genes encoded by each sgRNA are indicated. The proteins appear to be encoded in the genome in the order in relative to the quantity required in the completed genome, with the N protein being required in large amounts, therefore, encoded in all of the sgRNAs (Kappes & Faaberg 2015).

An important feature regarding the PRRSV genome is the method of translation that occurs via the direct translation of ORF1a and ORF1b to produce the non-structural proteins, as well as the transcription and translation of the sgRNAs which encode the viral structural proteins at the 3' end of the genome (van Marle *et al*., 1999). The nested set of sgRNAs are produced in a discontinuous transcription

strategy and each sgRNA encodes a number of the structural proteins (polycistronic), apart from sgRNA7. As shown in figure 1.15 this allows the virus to produce more transcripts encoding the most vital structural proteins, such as the M and N proteins, which are encoded for by five out of six and six out of six sgRNAs respectively.

1.4.3. Nucleocapsid protein

The nucleocapsid protein will be the main focus of this study. This is a key structural protein of many viruses as it protects the viral genome. In PRRSV, the protein itself is approximately 15 kDa in size and comprises approximately 40% of the virion, making it a very good target for research purposes due to its large quantities and immunogenic potential (Meulenberg *et al*., 1995). Although the structure of the complete N protein of PRRSV is not known, a C-terminal clone of the protein was expressed in *E.coli* and a crystal structure successfully obtained (Doan and Dokland, 2003) as previously mentioned in section 1.3.6.4.3, along with the organisation of the N protein in the virion. Importantly, the role of the PRRSV N protein is not restricted to just the structural integrity of the virus, it is also involved in the activation of NF-κB (Luo *et al*., 2011; Chen *et al*., 2017), and it may be involved in the regulation of viral RNA production by recruiting host cell proteins (Liu *et al*., 2016) and enhancement of IL-10 expression (Fan, Li, *et al*., 2015; Yu *et al*., 2017). The PRRSV N protein is also known to traffic in and out of the nucleus of infected cells and contains a number of nuclear localisation signal (NLS) sequences as shown in figure 1.17 (Rowland and Yoo, 2003).

In vitro studies using over-expressed PRRSV N protein have shown it can localise to the nucleus and the nucleolus in the absence of other viral proteins or RNA, presumably by trafficking through the nuclear pore complex. The movement of the N protein is seen to be faster when imported into the nucleus compared to the export of the protein. However, trafficking is dynamic and the protein does not appear to be sequestered in the nucleus or nucleolus and is constantly exchanged between the two and the nucleus and cytoplasm (You *et al*., 2008). This trafficking appears to be vital for the lifecycle of the virus, as removal of the N protein nuclear localisation signals has a negative impact on viral replication, with viral titres 100-

fold lower and a shorter duration of viremia than wild type virus when studied *in vivo*. The importance of this process in viral replication and infectivity was also observed by the reversion of the mutant virus to produce functional nuclear localisation signals in the N protein during infection (Lee *et al*., 2006; Pei *et al*., 2008).

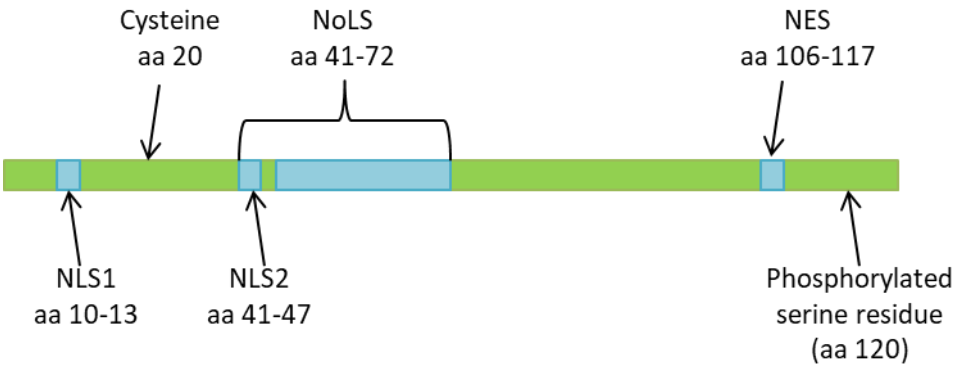

Figure 1.17 Nuclear localisation signals of the PRRSV nucleocapsid protein. The N protein contains a number of putative nuclear localisation signal (NLS) regions and has been shown to traffic to the nucleus and nucleolus of infected cells. There are NLS at amino acids 10-13 and 41-47 and nucleolar localisation signals (NoLS) at amino acids 41-72. There is also a nuclear export signal (NES) at aa 106-117. Cysteine 20 is involved in the formation of N protein dimers via covalent disulphide bonds (Rowland and Yoo, 2003).

Stable isotope labelling with amino acids in cell culture (SILAC) analysis of PRRSV N protein interactions with cellular proteins has identified over 50 potential cellular interaction partners of the N protein, with binding partners having functions in RNA binding, translation, mRNA stability, nuclear ribonucleoproteins, splicing and RNA helicases (Jourdan *et al*., 2012). It is possible that the N protein is involved in the recruitment of cellular proteins, particularly via its shuttling through the nucleus/nucleolus, that are vital for viral replication, however this has not been thoroughly investigated.

Recently it has been shown that the PRRSV N protein interacts with viral nsp9 and the cellular protein DHX9 in order to regulate viral RNA synthesis. DHX9 was previously identified in the SILAC analysis carried out by Jourdan *et al* 2012. It is thought that the recruitment of this cellular protein by the two viral proteins aids in the production of both sgRNAs, vital for structural protein production, as well as

the synthesis of new genomic RNA (Liu *et al*., 2016). Another cellular protein that interacts with PRRSV N protein is PARP-1, in the context of the virus it has been shown that inhibiting this cellular protein using a small molecule inhibitor resulted in a decrease in the production of viral genomic and subgenomic RNAs, as well as an overall decrease in viral titre (Liu *et al*., 2015).

The PRRSV N protein is a major immunogenic protein within the virion and so it was chosen for this study, as it is likely to be present in high quantities in the blood of infected animals, making it an ideal candidate for direct detection of viral infection (Dea *et al*., 2000). As well as being highly immunogenic, the N protein sequence is also highly conserved between viral strains. The two strains of the virus used in this study are examples of a low (strain NVSL 97-7895) and a high pathogenic (strain SD16) strain from genotype 2 PRRSV and the amino acid sequences are shown in alignment in figure 1.18. The sequences are broadly conserved with a number of single mutations throughout the sequence, in total there are eight amino acid differences highlighted in red. The conserved nature of the protein makes it an ideal candidate for the identification of detection reagents, as it is likely that they will function to identify multiple strains at once without the need for complex devices.

```
Low     MPNNNGKQQKKKRGNGQPVNQLCQMLGKIIAQQNQSRGKGPGKKIKNKNPEKPHFPLATE 60
High    MPNNNGKQQKKKKGNGQPVNQLCQMLGKIIAQQNQSRGKGPGKKNRKKNPEKPHFPLATE 60
        ************:******************************* ::************

Low     DDVRHHFTPSERQLCLSSIQTAFNQGAGTCTLSDSGRISYTVEFSLPTHHTVRLIRVTAP 120
High    DDVRHHFTPSERQLCLSSIQTAFNQGAGTCALSDSGRISYTVEFSLPTQHTVRLIRATAS 120
        ******************************:*****************:*******.**.

Low     SSA 123
High    PSA 123
        .**
```

Figure 1.18 Sequence alignment of PRRSV N proteins. The conserved nature of the proteins between PRRSV strains can be seen with mutations within the protein highlighted in red. The mutations between high and low pathogenic strains are distributed throughout the genome.

The two genotypes of PRRSV are European (Type 1) and North American (Type 2) with a predicted divergence of between a decade to a century prior to clinical identification and therefore with a period of independent evolution on the two continents(Kappes and Faaberg, 2015). The two strains used in this study are

members of genotype 2 which is also prevalent in China and Asia and has been shown to mutate into highly pathogenic strains as illustrated by strain SD16 in this study. Therefore as well as identifying between a high and low pathogenic strain of PRRSV, the diagnostic proposed in this study may also be able to distinguish between the two genotypes which could be further investigated as a result of this study.

1.4.4. Entry of PRRSV into permissive cells

As previously discussed in section 1.3.6, arteriviruses are very host specific and PRRSV is known only to infect porcine cells *in vivo*. However, it is able to replicate in MARC-145 cells (derived from African green monkey cells) (Kim *et al*., 1993), primary porcine alveolar macrophages (Wensvoort *et al*., 1991) and differentiated porcine monocytes (Delputte *et al*., 2007) in cell culture. It is widely accepted that the entry of the virus into these cells occurs via receptor-mediated endocytosis via clathrin coated vesicles (Pensaert *et al*., 1999), which is facilitated by siloadhesins on the surface of these permissive cells (Vanderheijden *et al*., 2003). This receptor had previously been identified on the surface of macrophage cells isolated from the lungs, thymus, tonsils, spleen and lymph nodes of infected pigs (Duan *et al*., 1998).

1.4.5. Control and current diagnostics

The current controls and diagnostic approaches for PRRSV infection within a population are limited and often poorly implemented, allowing for the rapid spread of infection. The economic burden of this infection is hard to analyse because the losses are not always clear, particularly in endemically infected herds and so it is difficult to evaluate the efficient use of biosecurity and diagnostic measures (Nathues *et al*., 2017). This is partly due to the lack of point of care diagnostics and the reliance on laboratory testing of clinical samples and partly due to the lack of suitable vaccinations and biosecurity measures employed as a result of animal movements.

1.4.5.1. Vaccination

There are a number of commercially available vaccines against PRRSV, however, as highlighted so far in this study, RNA viruses are highly mutagenic meaning that the

vaccines can quickly become redundant during an infection. One such vaccine is manufactured against PRRSV strain DV, a European isolate, under the name Porcillis PRRS by MSD Animal Health. Ingelvac PRRS®MLV, Inglevac PRRS®ATP and ReproCyc® PRRS EU, all manufactured by Boehringer Ingleheim, provide cross protection against a number of strains of PRRSV including the European Lelystad strain. Inglevac PRRS®MLV is known to provide delayed protection, with antibodies normally detectable 3-4 weeks post vaccination, this is not ideal for the vaccination of herds as movement is likely to be required at shorter time frames. This vaccine has however been shown to reduce viremia and virus shedding, as well as improving growth performance if administered during an outbreak or to endemically infected animals (Charerntantanakul, 2012). The Boehringer Ingleheim vaccines have also been combined with other vaccines, for example ReproCyc® PRRS-PLE, which protects against heterologous PRRSV, *Parvo Leptospiria* and *Erysipelothrix*. These vaccines contain a modified live PRRSV component against various strains of the virus and claim to provide duration of immunity (DOI) of at least 4 months post vaccination. Although they cannot be used on PRRSV naive herds but are safe for sows and gilts. There is also an inactivated vaccine available, PROGRESSIS®, manufactured by Merial.

Research carried out into the efficacy of these vaccines, shows that they do not provide complete protection against PRRSV infection, even when the vaccines are administered to animals challenged with the correct strain. Notably, the vaccines are unable to elicit a sufficient and rapid enough antibody response to prevent the infection and instead serve to reduce the severity of the infection. In addition, a number of these vaccines must be administered regularly in order to retain any immunity, which is vital for example in breeding animals (Delrue *et al*., 2009; Ko *et al*., 2016). Vaccines have been trialled against highly pathogenic strains of PRRSV, however, as observed with the low pathogenic strains of the virus targeted by the previously mentioned commercially available vaccines, the efficacy of the vaccines is not ideal and the reduction in severity of the disease was the primary outcome of the vaccinations (Iseki *et al*., 2017).

A great deal of investment is now being made into the research of improved vaccines against PRRSV, which can protect against multiple strains of the virus. Most approaches focus on using highly conserved regions of viral proteins or combining multiple viral proteins into the vaccine, circumventing any mutations which may occur in the circulating strains. Virus-like particles (VLPs) are also attractive candidates for replacement of attenuated or inactivated vaccines, as they mimic the viral particle in terms of dimensions and protein content. However, they lack the essential viral genome and so are effectively disabled and have a major advantage over live attenuated vaccines due to no possibility of reversion to wild type (Noad and Roy, 2003). The proteins which are incorporated into the VLP, as well as being similar in sequence between viral strains, have to be able to promote a sufficient immune response from the host cell in order to function as a vaccine. Efficacy of this approach has been previously shown with the successful human papillomavirus vaccine (Campo and Roden, 2010). A number of PRRSV vaccines based on VLPs have been produced, although currently no available vaccines of this kind are in clinical use (Binjawadagi *et al*., 2016; Garcia Duran *et al*., 2016; Van Noort *et al*., 2017; Uribe-Campero *et al*., 2015; Murthy *et al*., 2015).

1.4.5.2. Biosecurity

Biosecurity within the agricultural setting is a vastly underutilised method of control of any infection and is not limited to PRRSV. In the UK, animals placed into quarantine before and after movement in order to monitor disease status is exploited with regards to economically devastating diseases, such as FMDV (Delgado *et al*., 2016). These methods would be equally successful in the prevention of infections, such as PRRSV. Vaccination of animals and the correct quarantine procedures, as well as cleanliness within the herd, can be successfully implemented to reduce the spread of PRRSV especially when faced with a novel strain of the virus (Arruda *et al*., 2016). At present however, this is not routinely carried out with regards to most infection risks, particularly in developing countries, primarily due to a lack of knowledge surrounding biosecurity and availability of resources to perform adequate quarantines and vaccination schedules.

1.4.5.3. Genetic modification of animals

As well as the prophylactic response to viral infection using vaccines, a study has produced genetically modified PRRSV resistant animals using CRISPR-Cas9 gene editing approaches removing CD163. This protein has been proposed as a host cellular receptor required for the entry of the virus into host cells. The animals were followed for 35 days post infection and none showed any clinical signs of infection (fever or respiratory), viremia or antibody response although the reproductive response was not investigated (Whitworth *et al*., 2015; Burkard *et al*., 2017). The production of a gene-edited animal is highly controversial and is currently not an economically or ethically viable method of controlling a viral infection, such as PRRSV. Although the genetic modification of animals for human consumption cannot currently be carried out using gene editing, selective breeding based on molecular markers of resistance may be an underutilised route for the breeding of animals with a higher disease resistance to PRRSV and other livestock infections (Prajapati *et al*., 2017).

1.4.5.4. Current diagnostics for PRRSV

The current diagnostic methods for PRRSV infected animals are based upon visual assessment to identify the clinical symptoms outlined in section 1.4.1.8 or the direct diagnosis of infection, by taking a clinical sample and subsequent analysis in a laboratory setting. The World Organisation of Animal Health outlines laboratory procedures which can be performed on serum, whole blood, tissue samples including lungs, spleen, lymph nodes, and tonsils of infected animals with specimens used for direct virus isolation (Zeman *et al*., 1993), RT-PCR (Spear and Faaberg, 2015; S. Xiao *et al*., 2014; Drigo *et al*., 2014; Suarez *et al*., 1994) and serological tests for antibody detection (Y. Wang *et al*., 2016; Y.H. Xiao *et al*., 2014). These are routinely used by veterinary surgeons although they are time consuming and costly. For example, an ELISA test to detect the presence of antibodies within a clinical sample is required to be transported to a laboratory, undergo processing to remove contaminants and subsequent incubation with the ELISA plate and the detection reagent. A recently devised ELISA test to detect antibodies against the viral Gp5 protein was required to be performed for 30 minutes for incubation of

serum sample and additional 10 minutes incubation with the detection reagent (Y. Wang *et al*., 2016). The commercial cost for an ELISA diagnosis of EAV is £15 per test and a commercial diagnosis of PRRSV using PCR is £25 per sample or £27 for a pool of 5 samples. (BioBest UK).

1.5. Biosensors

'Biosensor' is a vague term for devices that are used for the detection of biological molecules and other compounds in samples, using biological reagents such as antibodies, nucleic acids and enzymes (Higgins and Lowe, 1987). They normally work based on electrochemical (Hammond *et al*., 2016), optical (Borisov and Wolfbeis, 2008), thermal (Ramanathan and Danielsson, 2001), magnetic (Rocha-Santos, 2014) and piezoelectric (Skládal, 2016) transducers or are immunochromatographic for example lateral flow devices (LFDs) (Posthuma-Trumpie *et al*., 2009), in order to give a read out of the presence of a target within a sample. Biosensors can be incorporated into LFDs and microfluidic lab-on-a-chip (LOC) devices (Temiz *et al*., 2015), including DNA chips (Nestorova *et al*., 2016) and are used in a wide variety of circumstances for example, medical care (Patel *et al*., 2016), food production (Thakur and Ragavan, 2013), animal management (Neethirajan *et al*., 2017), environmental monitoring (Pol *et al*., 2017) and security and defence (Matatagui *et al*., 2014).

Point of care (POC) biosensor diagnostics are vital to the health and veterinary care settings not only for diagnosis but also for monitoring disease progression, for example detection of hallmarks of cancer and so they are required to be cheap, portable reliable, rapid and easy to use (Syedmoradi *et al*., 2017).

1.5.1. Lateral flow devices

POC diagnostics are attractive alternatives to laboratory testing of samples in veterinary care. The most user friendly POC diagnostic is the lateral flow device (LFD). The most widely known of these is the human pregnancy test, first filed for patency in 1977 in its earliest form (Patent number US 4123509 A). Ideally POC devices need to avoid the preparation of a sample so that the clinical sample can be applied directly to the device. There are a number of modifications that can be

made to devices in order to process a clinical sample within the test itself and these include the addition of filter components to remove undesirable constituents in the test sample (Songjaroen *et al*., 2012). LFDs are very simple to design and produce and have the same basic set up as shown in figure 1.19a, adapted from Biagini *et al*. 2006. The main component of the device is the nitrocellulose membrane which is striped with two antibodies, a test antibody against the protein of interest, and a control antibody against the conjugate antibody (this antibody is conjugated to a gold nanoparticle). The conjugate antibody is contained within the conjugate pad, which is layered on top of the nitrocellulose membrane below the test line. A sample pad is then placed on top of the conjugate pad. At the other end of the nitrocellulose membrane, an absorbance pad is placed to collect excess sample. This device is then encased in a plastic housing with a hole where the sample is loaded as well as windows for viewing the test result (figure 1.19b). Test A shows an unperformed test, test B shows a negative result (only a control line appears) and test C shows a positive result (test and control lines are visible).

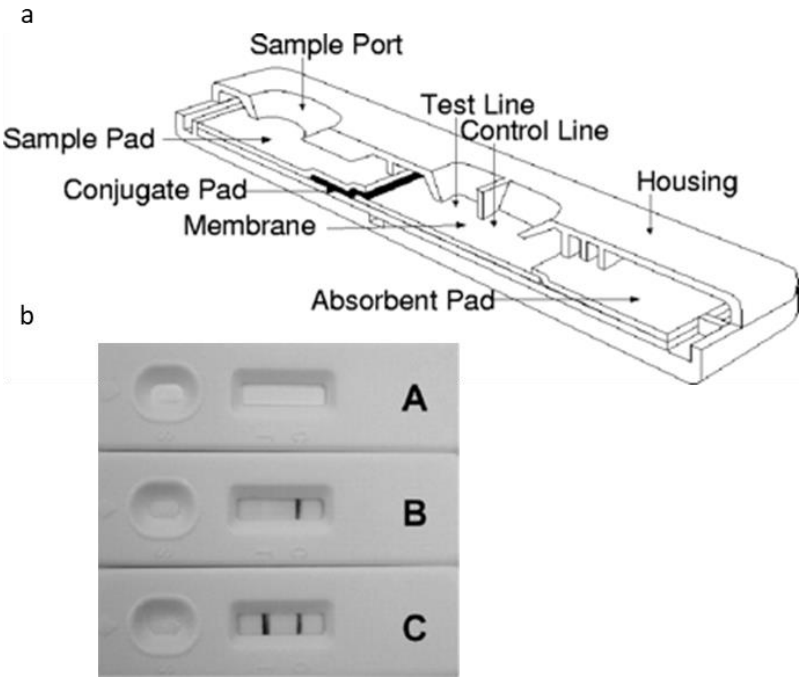

Figure 1.19 Diagram of lateral flow device. (a) The Lateral flow device is based upon a nitrocellulose membrane which contains 2 lines, a control line and a test line. The conjugate pad is a second membrane which contains the detection reagent conjugated to gold nanoparticles placed directly under the sample pad. The absorbent pad at the end of the membrane absorbs any excess sample. This assembles test strip is then placed in a plastic housing to prevent damage. **(b)** An example of a lateral flow device (A) a device before sample is added. (B) A negative test device where the control line has appeared to confirm the test was successfully performed. (C) A positive test device with the control and test lines visible (Biagini *et al*. 2006).

The finer details of the LFD are shown in figure 1.20, for descriptive purposes a pregnancy test will be described with the detection of human chorionic gonadotrophin (hCG). The sample is loaded onto the sample pad and if hCG is present in the sample it will bind to the anti-hCG antibody in the conjugate pad. This complex will migrate down the nitrocellulose membrane by capillary action until the sample reaches the test line. Here the antibody recognises the hCG at a different epitope on the protein to the conjugate antibody. The complex is captured by this antibody and a positive test line appears on the nitrocellulose membrane by changes in surface plasmon resonance as a result of GNP aggregation (Zhao *et al*., 2008). The sample continues to migrate down the nitrocellulose membrane to the control line where the excess conjugate antibody is captured by an antibody against the species in which the conjugate antibody was raised.

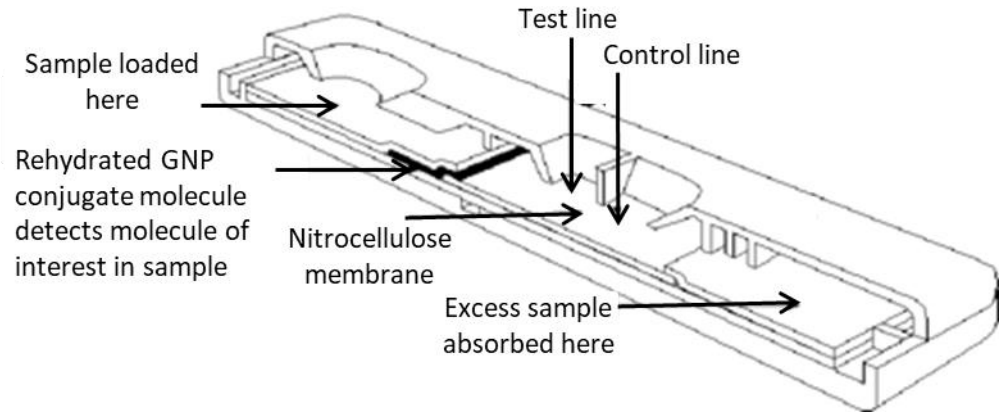

Figure 1.20 Mechanism of lateral flow device. The sample is loaded onto the sample pad, directly above the conjugate pad containing a reagent conjugated to GNP which can detect the molecule of interest in the sample. The sample moves up the device by capillary action and reaches the test line on the membrane where the molecule of interest in the sample is detected. Presence of the molecule of interest in the sample results in the formation of a complex between the conjugate molecule-molecule of interest-test line molecule and the appearance of a positive test line. The excess sample migrates further up the sample to the control line where excess conjugate molecule is detected and the appearance of a control line indicates the test was successful (adapted from Biagini *et al*. 2006).

The GNP conjugation to the antibody is commonly used because of the colour change observed upon binding to the test and control line antibodies, however,

alternatives are available including carbon (Qiu *et al*., 2015), selenium (Wang *et al*., 2014) and fluorescent molecules (Lee *et al*., 2013; Xu *et al*., 2014). These alternative reagents can be used to increase sensitivity of the device (carbon) or to reduce costs or allow for quantification of the result by using fluorescence and computer analysis of the strip. GNPs are also easy to modify for the addition of reagents and so are often used in LFDs.

1.5.2. Microfluidic lab-on-chip (LOC) devices

Microfluidic lab-on-chip (LOC) devices are more complex than the LFDs as they analyse the sample using other means than a visible colour change at a test and control line, as well as including another layer of complexity regarding the introduction of microfluidics. These devices can be used to analyse very small volumes of sample material due to the design of the device. Using microfluidics, there is a reduced time taken to transport the sample to the analysis elements as well as reduced distances over which this occurs. This allows for single drops of blood or indeed single cells to be analysed using microfluidic LOC devices (Lafleur *et al*., 2016). There are a number of methods by which the signal can be detected in an enzyme based LOC device, such as electrochemical, affinity based, fluorescence and magnetic detection. A basic schematic of a microfluidic LOC device is shown in figure 1.21 (Conde *et al*., 2016).

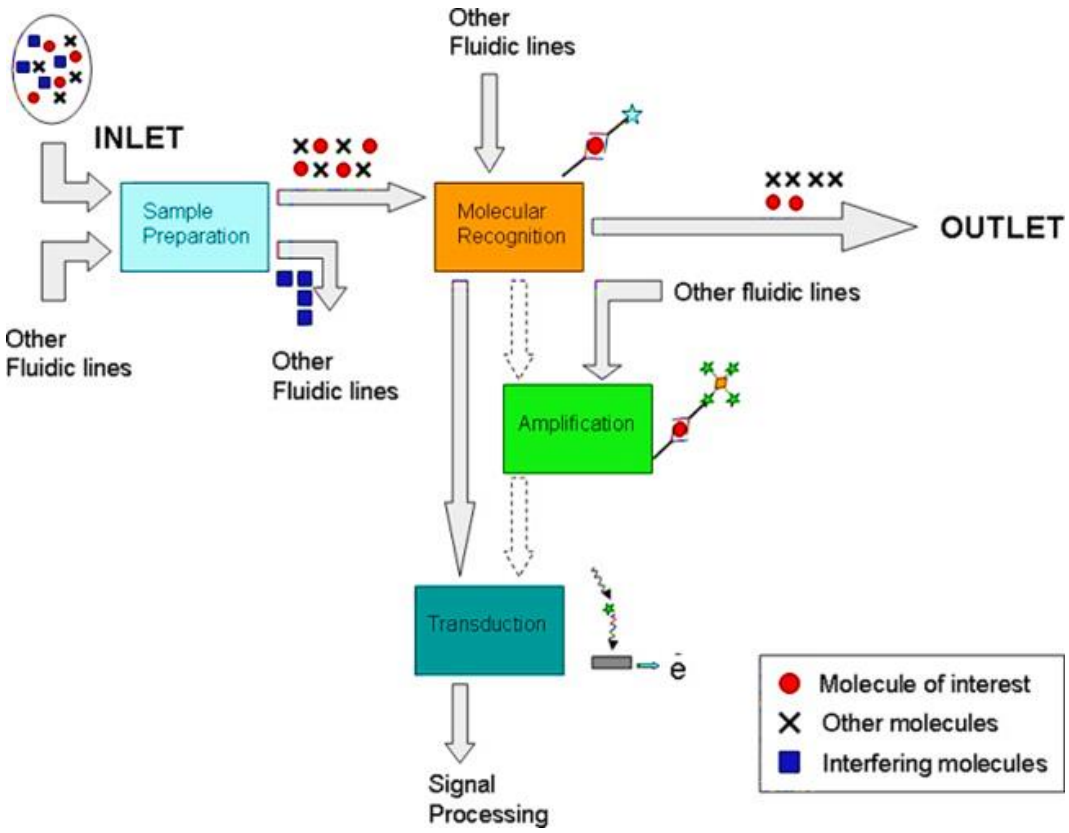

Figure 1.21 Lab on Chip - A simple schematic of a fully integrated LOC device. The sample is loaded at the inl*et al*ong with any fluidics required for sample preparation (buffers). The target in the prepared sample is recognised by the probe at the molecular recognition site and binding occurs. Excess target and sample flows to the outlet. The signal from the molecular recognition events can be amplified to give a larger signal for detection and therefore improve sensitivity of the sensor and can include the use of enzymes, fluorophores or nanoparticles. The signal passes through a transducer to convert the recognition event into a measurable signal; electrical, optical, magnetic, colourimetric (Conde *et al*., 2016).

1.5.2.1. Electrochemical LOC

Electrochemical impedance spectroscopy is increasingly used in biosensors and can detect variations of resistance and capacitance seen upon binding events (Hammond *et al*., 2016). Amperometric biosensors transduce the biological recognition events caused by an electroactive species at the sensing surface, into a current signal, to quantify an analyte present in a sample and are a simple design that can be used in low cost, portable devices. The main example of a LOC device is the home glucose monitor used by diabetics (Newman and Turner, 2005). Impedimetric biosensors use electrochemical impedence spectroscopy (EIS) where impedance is measured over a range of alternating current (AC) frequencies (100 kHz – 1 mHz) and this has been incorporated into sensors to detect cancer (Han *et*

al., 2016) and other disease markers (Sharma *et al*., 2016), bacteria (Bekir *et al*., 2015) and viruses (Hushegyi *et al*., 2016). Carbon-nanotube-based electrochemical biosensors have also been used to increase the sensitivity of biosensors and have been incorporated into biosensors to detect for glucose (Guiseppi-Elie *et al*., 2002) and cholesterol (Carrara *et al*., 2008).

1.5.2.2. Enzyme LOC

Enzymes can be integrated into LOC devices to catalyse chemical reactions with the electroactive species produced or consumed being detected by current changes (Lafleur *et al*., 2016). Glucose detection has used this approach, as well as devices able to detect Epstein-Barr virus (EBV) (Horak *et al*., 2014) and cholesterol (Ali *et al*., 2013).

1.5.2.3. Fluorescence LOC

Fluorescence based biosensors are a popular microfluidic biosensor because they offer high selectivity, low detection limits and are easy to use (Lafleur *et al*., 2016). They have been used in sensors able to detect *E.coli* (Chung *et al*., 2015), cancer biomarkers (Kim and Kim, 2014) and cholera toxin (Bunyakul *et al*., 2015).

1.5.2.4. Affinity based LOC

Affinity based biosensors use electrochemical signalling from a binding event to detect an analyte in a sample, however it is common for sample preparation to be required to make the analyte available to the sensor or remove other interfering molecules within a sample (Bunyakul and Baeumner, 2014). Real samples from milk to detect antibiotics (Daprà *et al*., 2013), stool (Bunyakul *et al*., 2015) and blood (Ferguson *et al*., 2013) have been analysed using affinity biosensors.

1.5.2.5. Magnetic LOC

Magnetic transduction is used to detect magnetic microbeads and work by detecting the change in magnetic field of the sensor and detecting the change in voltage produced by the sensor components (Lafleur *et al*., 2016). These have been used to detect hepatitis B virus (Zhi *et al*., 2014) and bacteria (Fernandes *et al*., 2014).

1.5.3. Biosensors and non-antibody binding protein detection reagents

The common theme of the majority of biosensors is the inclusion of an antibody detection mechanism which is raised against the protein or molecule of interest. The use of antibodies has recently been challenged by a number of alternative binding proteins which show potential as substitute reagents in the previously mentioned biosensor devices. Antibodies have long been vital tools for research, however they has been long standing concern over their lack of validation and renewability (Bordeaux *et al*., 2010; Bradbury and Plückthun, 2015). In a 2008 study, less than 50% of 6000 commercially available antibodies recognised their specific targets or performed poorly in certain applications (Berglund *et al*., 2008). These new non-antibody reagents aim to address these issues whilst also improving sensitivity and reaction time in molecular research applications. These alternatives will be discussed in detail below.

As previously discussed (section 1.5.1) LFDs ordinarily use antibody components as the detection reagents for proteins in the clinical samples. However, due to the ethical issues and economics of antibody production, there has been an increased interest in the development of alternative reagents that can replace antibodies. Replacement of antibodies has been demonstrated with the use of peptide aptamers in enzyme-linked immunosorbent assays (ELISAs) (Chen and Yang, 2015b), chemical or nucleic acid ligand replacement in LFDs (Chen and Yang, 2015a), peptide aptamers used in immunochemical assays; immunoprecipitation, Western blotting, cytofluorimetry (Skerra, 2007) and Affimers used in microscopy (Tiede *et al*., 2017) to name a few. This project focusses on the use of non-antibody binding proteins as antibody replacements and the scope for production of these reagents is vast.

1.5.3.1. Nanobodies

Nanobodies are a single domain protein, derived from camelid antibodies, with a molecular mass of around 15 kDa, around 10 times smaller than a conventional antibody and they can be cloned into bacterial expression systems. Nanobodies are highly diverse research tools and are able to perform comparably to antibodies

whilst being adaptable with regards to modification and easily produced at high quantities (Beghein and Gettemans, 2017). However, the production methods for nanobodies still requires the initial immunisation of camelids for the harvest of peripheral blood mononuclear cells (PBMC) to isolate the mRNA which can be entered into phage display (Dmitriev *et al*., 2016). They therefore suffer the same ethical issues as traditional antibody production.

Nanobodies can be chemically and genetically modified and can be reliably expressed in mg/L of culture at reproducible properties. They have also been shown to bind to their target proteins with nanomolar affinity (Dmitriev *et al*., 2016; Skottrup *et al*., 2011; De Genst *et al*., 2006). Nanobodies are also highly soluble due to their water exposed hydrophilic regions on the FRs (Beghein and Gettemans, 2017). They have been used in a number of molecular biology applications including: immunolabelling and antigen manipulation in live cells to investigate their potential for use in immunotherapy (Herce *et al*., 2017), primary detection reagents in fluorescent microscopy, fluorescence-activated cell sorting (FACS), magnetic-activated cell sorting (MACS) and immunohistochemistry (de Bruin *et al*., 2016), super-resolution microscopy (Ries *et al*., 2012; Platonova *et al*., 2015). They can also be used in mass spectrometry to investigate macromolecular assemblies (Shi *et al*., 2015). Nanobodies can be expressed intracellularly as an alternative to RNAi to knockout protein functions (Newnham *et al*., 2015; Bertier *et al*., 2017). Nanobodies are also useful tools for X-ray crystallography, where they can be used as chaperones to stabilise the structure of proteins which are otherwise difficult to crystallise (Rasmussen *et al*., 2011; Staus *et al*., 2016).

Nanobodies are based upon the heavy chain-only antibodies produced by camelids which can be produced recombinantly, these domains are antigen-recognising (Hamers-Casterman *et al*., 1993). These heavy chain-only antibodies were originally termed nanobodies but are also known as variable domains (VHHs) or single domain antibodies, the region of the camelid antibody which derives the nanobody is shown in figure 1.22 (Dmitriev *et al*., 2016).

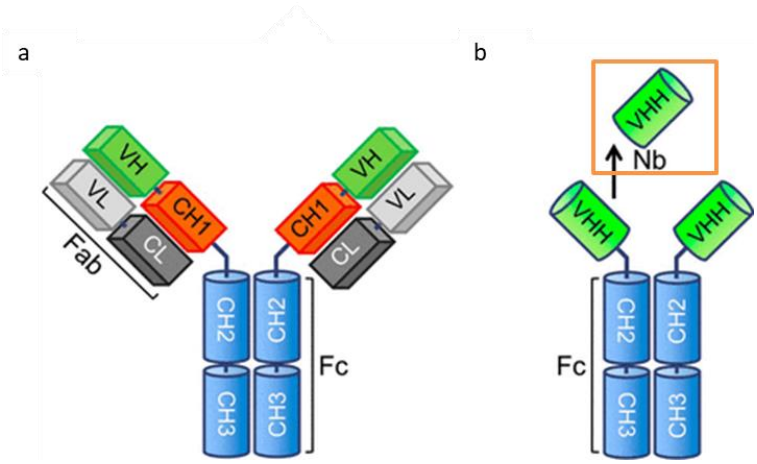

Figure 1.22 Comparison between an IgG antibody (a) and a heavy chain only camelid antibody (b). **(a)** Antibodies consist of two heavy chains (VH/CH1) and two light chains (CL/VL) and antibody binding is determined by the complementarity determining regions in these domains. The Fc region of the antibody is involved in cell surface interactions. **(b)** The heavy chain only antibody of camelids lack the light chains whilst retaining binding and specificity to antigens. As highlighted by the box, these antibodies can be further truncated to retain only the variable antigen binding domains (VHH) which are termed nanobodies (Dmitriev *et al.*, 2016).

Nanobody structure includes three complementarity-determining regions (CDRs), organised into three loops which are structured by a framework region (FR), the loop regions are generally quite ridged which favours high antigen binding affinities (figure 1.23) (Beghein and Gettemans, 2017).

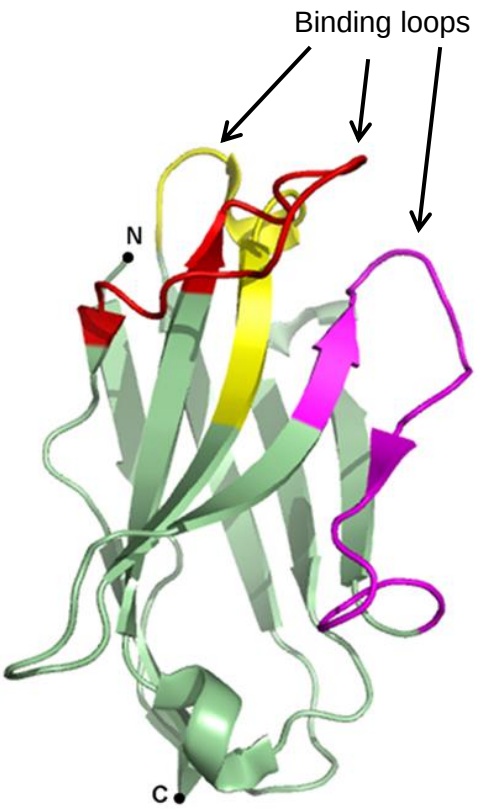

Figure 1.23 Crystal structure of a Nanobody. The nanobody has 3 CDR regions and four framework regions (FRs) the CDR regions are shown in yellow, pink and red. This nanobody recognises gelsolin, an actin binding protein (PDB ID 2X1O). The FR regions contain hydrophilic residues to aid solubility of the nanobodies (Beghein and Gettemans, 2017).

1.5.3.2. AdNectins™

Originally termed Monobodies, AdNectins™, are approximately 10 kDa proteins based on the 10th fibronectin type III domain which bind to therapeutically relevant targets with high affinity and can be produced to a high yield in bacterial expression systems, the structure of these proteins are shown in figure 1.24 (Lipovsek, 2011; Koide and Koide, 2007).

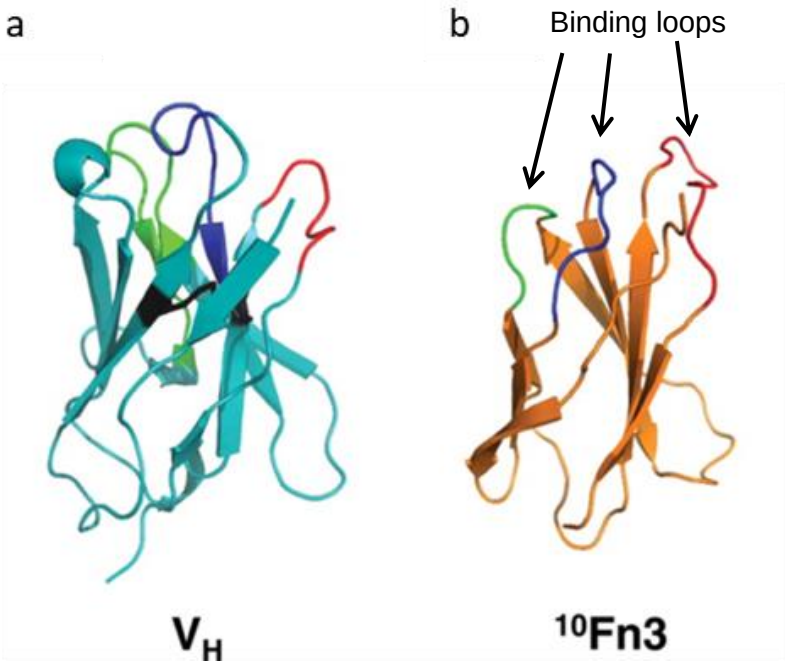

Figure 1.24 Crystal structure of AdNectins™. The V_H domain (a) provides a comparison of the antibody antigen recognition site compared to the basic AdNectin™ structure. (b) The antibody vairable domains of ^{10}Fn3 are two anti-parallel beta sheets with solvent-accessible loops inbetween. Unlike V_H regions of antibodies, ^{10}Fn3 have no di-sulphide bonds or free cysteine residues which allows the protein to retain high thermostability (Lipovsek, 2011).

AdNectins™ have been shown to have therapeutic potential as anti-tumour properties in mice (Mamluk *et al*., 2010) and a number have now reached the clinical trial stage. AdNectin™ CT-322 is a VEGFR-2 inhibitor and was successfully administered to patients with solid tumours resulting in an anti-tumour effect in phase I trials (Tolcher *et al*., 2011). An ongoing American trial investigating AdNectin™ BMS-986089 is studying the safety and tolerability of this treatment for Duchenne Muscular Dystrophy and is expected to be completed in 2020 by Bristol-Myers Squibb. AdNectins™ have not been used in molecular biology techniques. These proteins have also been suggested to show improved tissue penetration and decreased immunogenicity compared to antibodies as well as being well suited for multi-functionality due to the ability to oligomerise (Weidle *et al*., 2013).

As well as therapeutic functions, AdNectins™ have been shown to function as crystalisation chaperones and due to their high affinity and isoform specificity they have been proposed as tools for the investigation into cellular functions of their targets, for example human small ubiquitin-related modifier (SUMO) proteins

(Gilbreth *et al*., 2011). They have also been used in the *in vitro* and *in vivo* imaging of tumours expressing cancer biomarker hEphA2 (Kim *et al*., 2017). AdNectins™ are also tools for the investigation of ion channel function (Chavan *et al*., 2017) and modification of enzyme specificity (Tanaka *et al*., 2015).

1.5.3.3. Designed Ankyrin repeat protein

Designed Ankyrin repeat protein (DARPin) libraries have been designed to produce high affinity binders to target proteins. A library was designed in 2004 containing DARPins of differing repeat numbers (either two or three repeats) which were expressed using ribosome display, the theoretical library size was 5.2 $x10^{15}$, library with two repeats and 3.8 $x10^{23}$, library with three repeats (Binz *et al*., 2004). This library was screened against *E.coli* maltose binding protein (MBP) and validated DARPins which could be purified up to 200 mg/l in *E.coli* culture, with high affinity (nanomolar) they were shown to function in competition ELISA assays and were successfully co-crystallised with their target protein. A representation of the structure of the DARPins is shown in figure 1.25 (Binz *et al*., 2004).

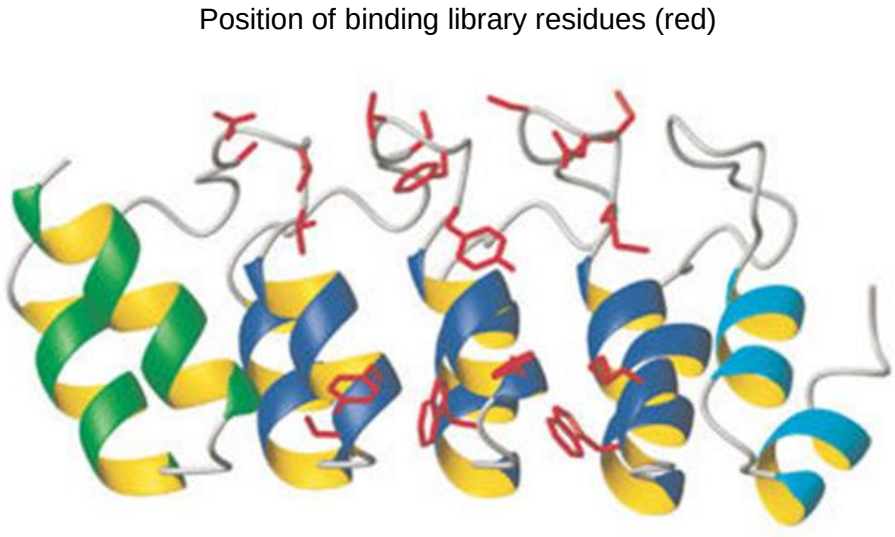

Figure 1.25 Crystal structure of maltose binding protein (MBP) DARPin (off7). The potential interaction sites are shown in red (stick mode). The AR module is 26 residues with 6 randomised potential interaction residues of any aa except cysteine, glycine or proline with randomised framework residues (asparagine, histidine or tyrosine) (Binz *et al*., 2004).

DARPins have since been designed to function as molecular biology tools for example, fluorogen-activating designed AR proteins (FADAs), which have been used

to image proteins on the cell surface or cytosol (Schütz *et al*., 2016), study of biological processes such as the conformational changes of p-ERK in mouse embryo fibroblasts (Kummer *et al*., 2013) or apoptosis (Schilling *et al*., 2014). They have also been shown to be successful chaperones for crystalisation of target proteins (Bukowska and Grütter, 2013; Schilling *et al*., 2014), and can be applied in diagnostics for immunohistochemistry (Theurillat *et al*., 2010) and *in vivo* imaging of tumours (Kramer *et al*., 2017). Recently they have been proposed as tools for affinity purification as a direct replacement for antibodies (Hay *et al*., 2015).

1.5.3.4. Anticalin

Anticalins, also known as lipocalins, are a diverse family of extracellular proteins of between 150-190 amino acids, larger than other antibody alternatives, in a single polypeptide chain which has a common 6 or 8 stranded β-barrel as shown in figure 1.26 (Richter *et al*., 2014; Grzyb *et al*., 2006).

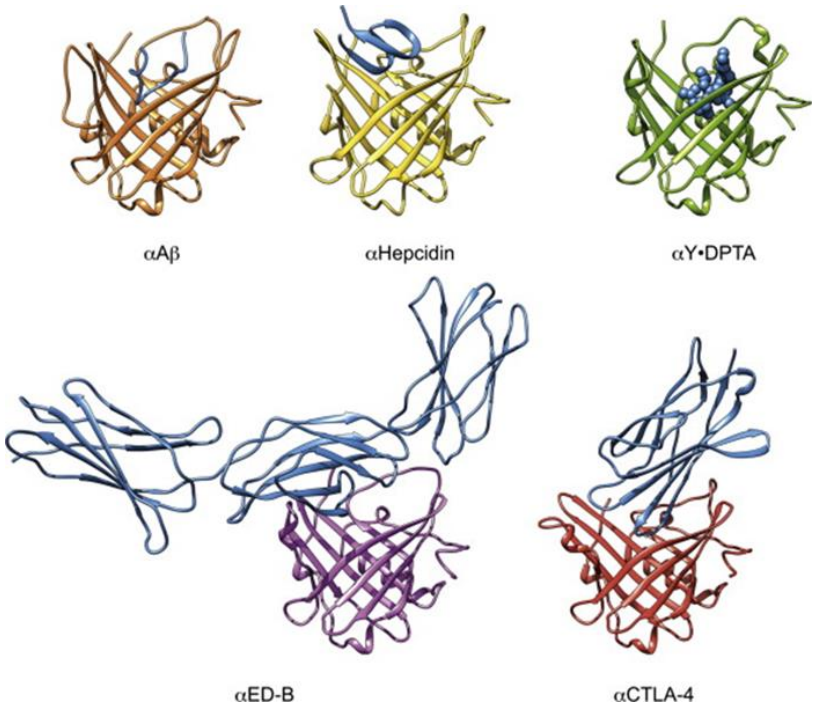

Figure 1.26 Crystal structure of five Anticalins based on the human Lcn2 scaffold. Anticalins are depicted in complex with the peptide ligands (Blue). αAβ40 (orange; to be published) and hepcidin (yellow; to be published), the small hapten-like molecule Y^{III}·DTPA (green; PDB code 4IAX) and with the two protein targets ED-B (magenta; PDB code 4GH7) and CTLA-4 (red; PDB code 3BX7). The anticalins share the conserved beta-barrel structure (Richter *et al*., 2014; Grzyb *et al*., 2006).

Rather than being used as molecular biology reagents, these proteins are proposed as replacements for therapeutic antibodies and have been raised against a number of biologically relevant proteins, such as cytotoxic T lymphocyte-associated antigen 4 (CTLA-4) (Mocellin and Nitti, 2013), vascular endothelial growth factor A (VEGF-A) (Mross *et al*., 2014) and hepatocyte growth factor receptor (HGFR) (Olwill *et al*., 2013).

1.5.3.5. Affibody

Affibodies are derived from the B domain of the immunoglobulin binding region of staphylococcal protein A which is a cysteine free, 6.5 kDa, 58 amino acid peptide folded into a three-helical structure (Löfblom *et al*., 2010; Myers and Oas, 2001). The three helical structure of an affibody is shown in figure 1.27 (Ståhl *et al*., 2017).

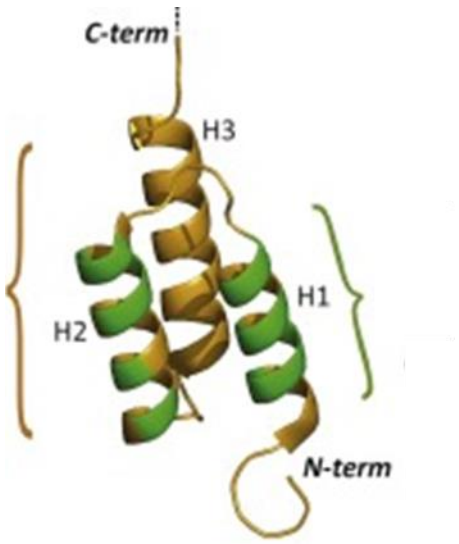

Figure 1.27 Crystal structure of affibody. Large 'naïve' libraries of affibody molecules are constructed via combinatorial protein engineering of typically 13 positions (green) in helices one and two (H1/H2) of the 58-residue cysteine-free three-helix bundle Z-domain scaffold (brown). Modifications can be made at the N and C termini (indicated) to add functional groups such as fluorophores (Ståhl *et al*., 2017).

Affibodies have been proposed as tools in both therapeutics and molecular biology, they can be used in *in vivo* imaging (Sörensen *et al*., 2014; Choi *et al*., 2016; Sörensen *et al*., 2016), therapeutic delivery by liposomes (Beuttler *et al*., 2009; Alavizadeh *et al*., 2016), targeted drug delivery to tumours (Alexis *et al*., 2008;

Orlova *et al*., 2010), microscopy (Moon *et al*., 2016), flow cytometry (Wang *et al*., 2015).

1.5.3.6. Affilin

Affilins are binding proteins based on the β-sheet of human γ-β-crystallin where a universal binding site was created through the randomisation of eight solvent exposed amino acid residues, the structure of Affilin SPC-1-G3 (PDB accession code 2JDG) is shown in figure 1.28 (Ebersbach *et al*., 2007).

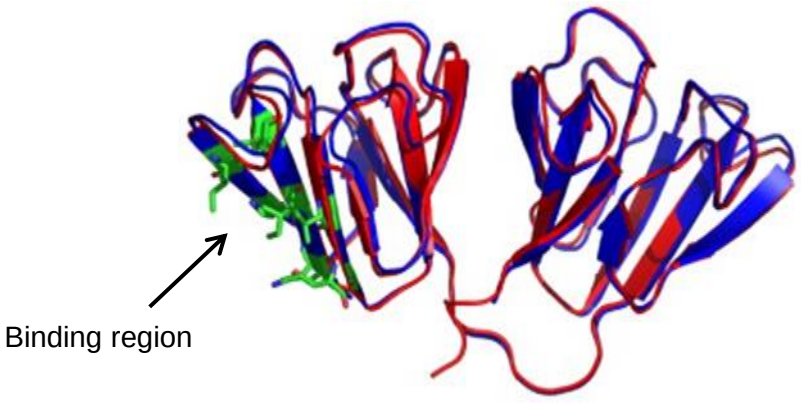

Figure 1.28 Crystal structure of Afillin. In red is the wild-type γ-B-crystallin and in blue is the IgG-Fc binding Affilin (SPC-1-G3). The different in amino acid sequence at 8 residues in the N terminal region does not alter the overall structure (Ebersbach *et al*., 2007).

Affilins have also been used as tumour targeting molecules like affibodies, DARPins and AdNectins™ (Lorey *et al*., 2014) and have also been raised against human papillomavirus E7 protein and shown to inhibit cellular proliferation when expressed intracellularly. These molecules have not been used as molecular biology tools but have been taken forward as potential therapeutics by Scil Proteins GmbH.

1.5.3.7. Avimer

Avimers are based on the A-domains of proteins of cell surface receptors which are each approximately 35 amino acids (4 kDa) separated by linkers of approximately 5 amino acids, avimers exploit the multiple binding sites resulting from these A-domains to produce high affinity and specificity in binding (Silverman *et al*., 2005).

The structure of the avimer is shown in figure 1.29 (Vazquez-Lombardi *et al*., 2015; Silverman *et al*., 2005).

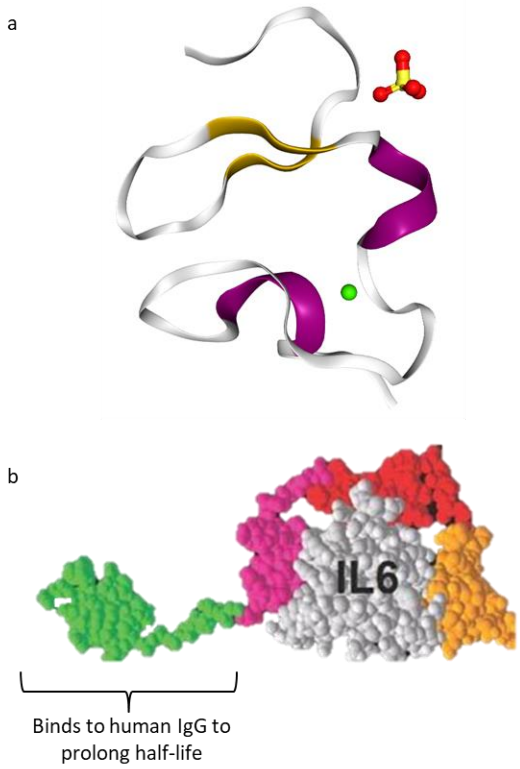

Figure 1.29 Structure of an Avimer. **(a)** (Ca^{2+} ion green, SO_4 ion red/yellow). The ribbon illustration of an Avimer against IL-6. **(b)** The first region binds to IgG and the remaining structure binds to different epitopes of IL-6 (Vazquez-Lombardi *et al*., 2015; Silverman *et al*., 2005).

Avimer AMG-220, which targets IL-6 had been entered into clinical trials for evaluation in patients suffering from Crohn's disease, however, the trial was halted and subsequent data was not made available (Vazquez-Lombardi *et al*., 2015).

1.5.3.8. OBodies

The oligonucleotide/oligosaccharide (OB) fold is a 5 stranded beta-barrel domain with a concave binding face for ligand binding and are found in diverse organisms with little sequence conservation (Murzin, 1993; Steemson *et al*., 2014). The barrel structure can be seen in the naïve protein structure and the evolved structure where the OBody is bound to hen egg-white lysozyme (HEL) as shown in figure 1.30 (Steemson *et al*. 2014).

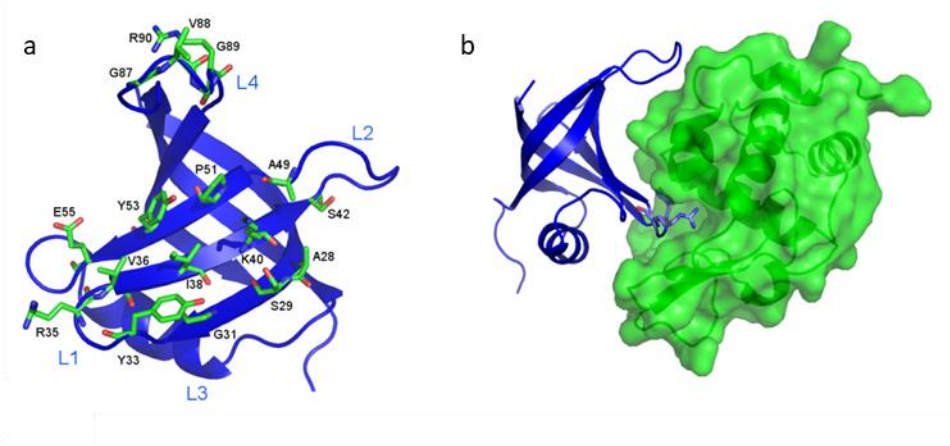

Figure 1.30 Obody bound to hen egg white lysozyme. (a) A model of *Pyrobaculum aerophilium* aspartyl tRNA synthetase (AspRS) wild type protein on which the design for the library was based. **(b)** Model of the structure of the newly designed Obody NL8 in complex with HEL. The beta barrel structure is conserved and the binding is occuring on the concave face as expected (Steemson *et al*. 2014).

OBodies have been trialled in the bioengineering of bacteria for affinity purification like DARPins and nanobodies (Hay *et al*., 2015). They have the potential to be used as molecular biology reagents as well as point of care diagnostics, however there is currently no published work to demonstrate their efficacy.

1.5.4. Affimers

The reagent used in this study is a non-antibody binding protein called an Affimer, previously referred to as an Adhiron (figure 1.31) (Tiede *et al*., 2014). Affimers are small proteins based on the phytocystatin consensus sequence. They have high thermostability, *T*m up to 101°C and are produced using phage display and *E.coli* expression and are highly stable and expressed at high concentrations (Tiede *et al*., 2014). First published in 2014, there have now been over 350 successful screens performed by the Bioscreening Technology Group (BSTG) at the University of Leeds, producing reagents for a number of applications within molecular biology (Tiede *et al*., 2017).

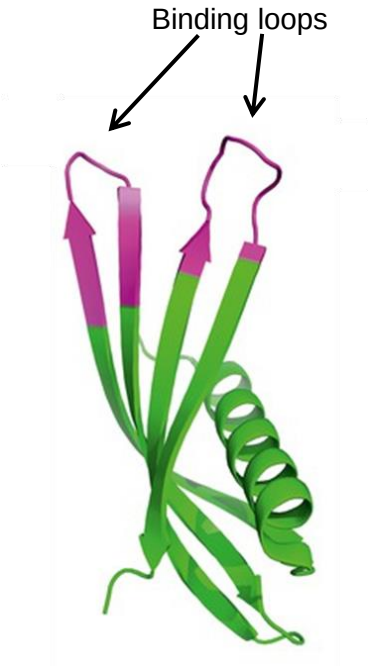

Figure 1.31 Crystal structure of an Affimer. The structure is based upon an alpha helix and 4 anti-parallel beta sheets with two loop regions which are the locations of the variable regions of the protein (Tiede *et al*., 2017).

The Affimer library is diverse, with a library size of approximately $1.3x10^{10}$. The sequence does not contain any cysteines, allowing for the insertion of a single cysteine at the C-terminus of the protein that is available for post purification modification. The Affimers were constructed using a consensus phytocystatin sequence (derived from 57 sequences from *Orysa sativa*, *Zea mays* and *Helianthus annuus*) which possessed a number of ideal attributes required for antibody alternatives; small (approximately 100 aa), highly soluble and stable, absence of disulphide bonds so no structural modification was needed, and they are monomeric (Tiede *et al*., 2014). The variable loop regions were inserted into the Val Val Ala Gly and Pro Trp Glu loops of the consensus sequence and these new loops each contained a randomised nine amino acid sequence as well as being truncated. The modified sequence was then cloned into a phagemid vector developed by the BSTG that allows the Affimer to be fused on a truncated pIII protein of the M13 phage when expressed in ER2738 *E.coli* in the presence of helper phage. The Affimer expressing phage are entered into phage display

screening against target proteins and more specific and higher affinity binders are identified through repeated screening rounds (Tiede *et al*., 2014).

1.5.4.1. Affimer diversity

The Affimer scaffold has been shown to successfully function as a molecular tool in a number of techniques ranging from dissection of cellular pathways to microscopy techniques. The broad range of target proteins already entered into Affimer screening and the success of these, as previously mentioned (section 1.5.4), holds the Affimer scaffold as a viable direct replacement for antibodies with the correct modification of current methods. A number of these have been reported in a recent eLife publication utilising Affimers (Tiede *et al*., 2017).

1.5.4.2. Affimer dissection of intracellular signalling pathways

Affimers were raised against 5 growth factor receptor bound protein 2 proteins (Grb SH2 domain), using Affimers for this purpose allows for the inhibition of individual SH2 domains which is not possible with the use of siRNA knockdown, this removes the function of entire proteins containing multiple SH2 domains. Therefore, by inhibiting individual domains whilst maintaining the overall function of a protein, it allows the dissection of the signalling mechanism of these proteins at a more detailed molecular level. The Affimers were raised to the SH2 domains using domains engineered with N terminal biotin acceptor proteins which could be used to capture the proteins from cell lysate and used in the phage display screening. Results comparing cross reactivity between Affimers raised against Grb2 SH2 domain and other Grb protein SH2 domains (Grb 7, 10, 14), showed that Affimers have specificity to Grb2 SH2 domains with very little cross-reactivity (figure 1.32) (Tiede *et al*., 2017).

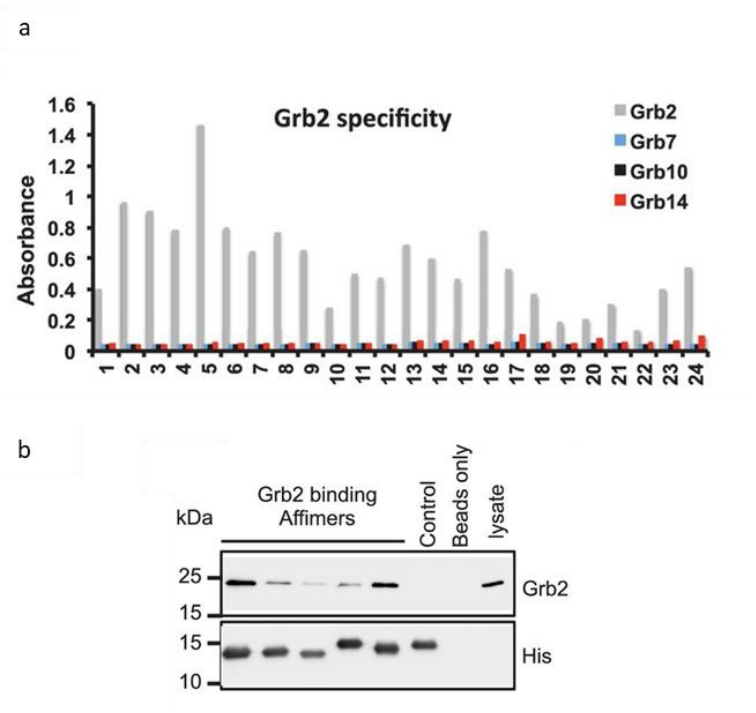

Figure 1.32 Grb2 Affimer specificity. (a) The 24 monoclonal Affimers raised against Grb2 SH2 domains were tested for specificity against other Grb SH2 domains and show specificity to Grb2 SH2 domains and no cross reactivity to other SH2 domains. **(b)** The Affimers are able to pull down endogenous Grb2 when bound to cobalt magnetic beads and incubated with cell lysate (Tiede *et al*., 2017).

1.5.4.3. Affimer inhibition of extracellular receptor function

Inhibition of cell receptor functioning using Affimers against vascular endothelial growth factor receptors (VEGFRs) has also been investigated. VEGFRs are important in angiogenesis, lymphangiogenesis and arteriogenesis and can be therapeutic targets in diseases such as cancer. Affimers were raised against VEGFR2 and their binding was shown in immunohistochemistry staining (in comparison to VEGFR2 antibody staining), as well as inhibition seen when incubated with cells in tissue culture, as demonstrated by a decrease in VEGFR-dependent tubule length in a tubulogenesis assay (figure 1.33) (Tiede *et al*., 2017).

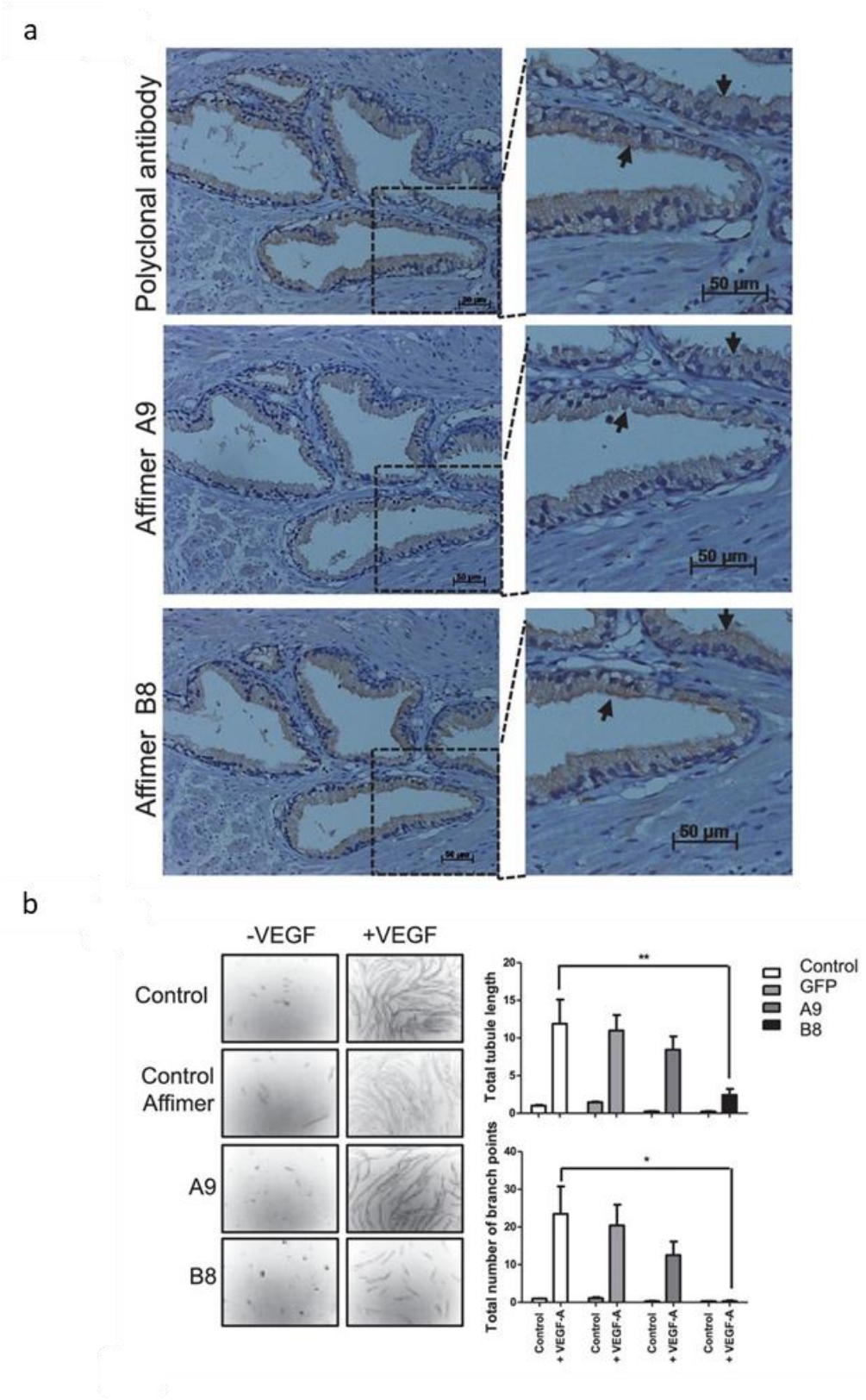

Figure 1.33 Affimer inhibition of extracellular receptor function. (a) Affimer binding in immunohistochemistry staining. When compared to the staining obtained by antibody binding to VEGFR2 the staining is identical when using the two Affimer proteins (A9 and B8). Darker staining can be seen at cell membranes as expected as highlighted by the arrows. **(b)** The tubulogenesis assay shows a significantly reduced tubular length in cells incubated with Affimer B8 compared to the control Affimer (Tiede *et al*., 2017).

The use of Affimers in immunohistochemistry and microscopy techniques (section 1.5.4.5) may also allow for greater sensitivity of these techniques when compared to antibodies due to increase number of binding events, resulting from the reduced size of the Affimer verses the antibody.

1.5.4.4. Affimers to modulate ion channel function

Ion channel modulation has been shown using Affimers raised against Transient Receptor Potential Vanilloid 1 (TRPV1) channels. Thirteen Affimers were identified against a peptide derived from an outer pore domain of TRPV1, as the purification of entire, functional and structurally intact membrane proteins is difficult. One Affimer (Affimer 2) of the thirteen previously identified was able to stain full length TRPV1 expressing U2-OS cells, shown in comparison to TRPV1 antibody staining where colocalisation of the two reagents was observed (figure 1.34a). The modulation of the channel by the Affimers was also observed by measuring intracellular calcium levels post Affimer treatment and capsaicin activation, resulting in significantly enhanced channel activation (figure 1.34b) (Tiede *et al*., 2017).

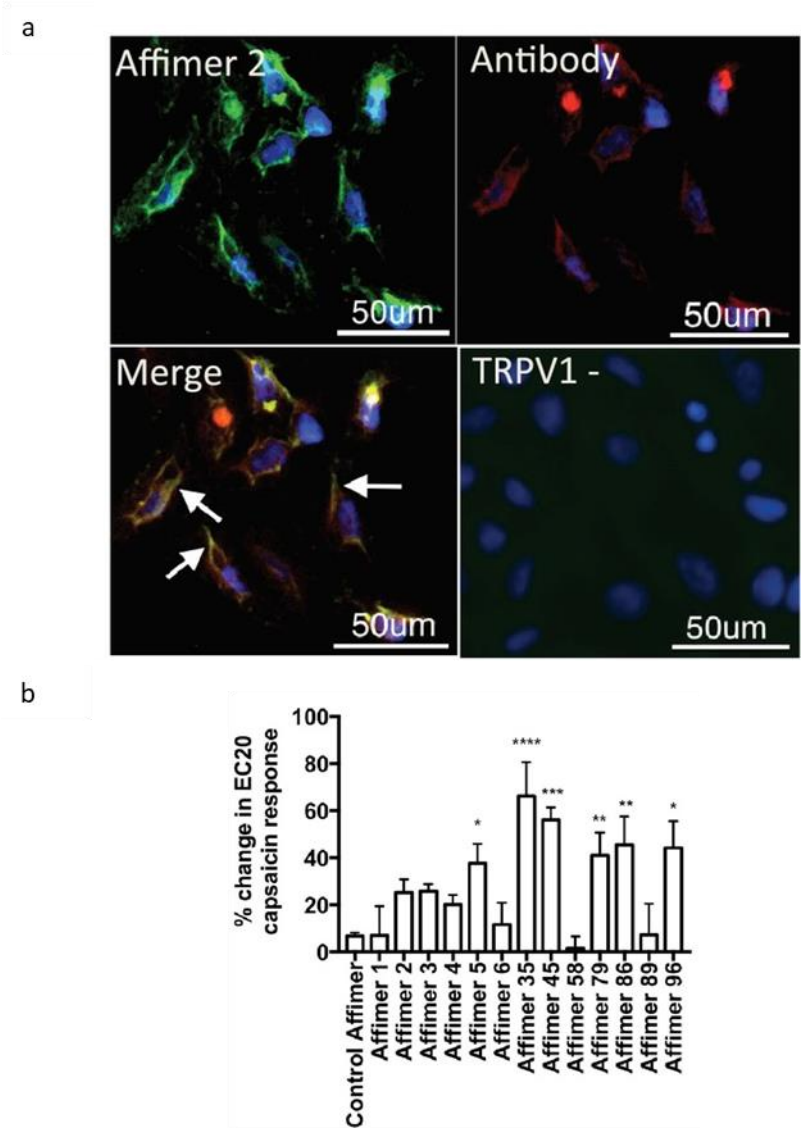

Figure 1.34 Affimers in the modulation of ion channels. (a) Affimers (green) are able to colocalise with Antibody (red) staining of TRPV1 channels in fluorescence binding assays. The sensitivity of the Affimer appears to be greater than the antibody counterpart in this assay. **(b)** The treatment of cells with Affimers 5, 35, 45, 79, 86 and 96 showed a significant increase in the activation of TRPV1 upon capsaicin activation compared to capsaicin treatment alone (Tiede *et al*., 2017).

1.5.4.5. Affimers in imaging techniques

As previously mentioned with regards to immunohistochemistry (section 1.5.4.3), the small size of Affimers compared to their antibody counterparts may allow them to be employed to increase the sensitivity of imaging techniques. This is due to the potential increase in binding events resulting from decreased stearic hindrance.

In vivo imaging techniques were successful using an Affimer against tenascin C (TNC), which is associated with cancer progression. Affimers were injected

intravenously and tissue sections from sacrificed animals probed for Affimer binding (figure 1.35). As well as showing potential as *in vivo* imaging reagents, it is thought that the clearance of the Affimers from the body would be much quicker than antibody counterparts, providing a lower background reading from unbound reagent (Tiede *et al*., 2017).

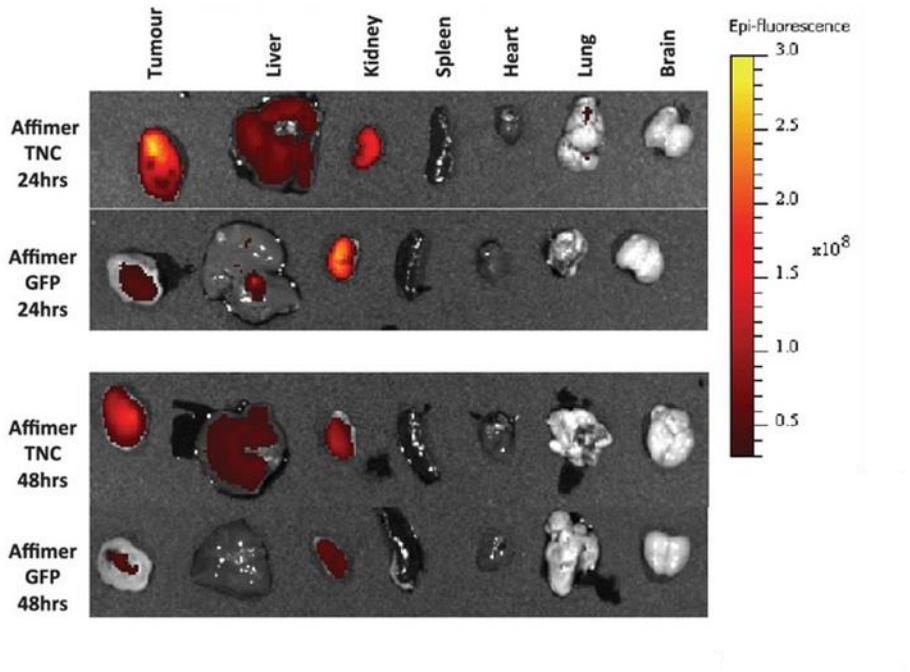

Figure 1.35 In vivo imaging using Affimer reagents. Rhodamine labelled Affimers against TNC were injected intravenously and tissue samples evaluated for Affimer binding 24 and 48 hours later. Affimer binding was seen in the tumour as well as the liver and kidney, suggesting metastasis of the cancerous cells (Tiede *et al*., 2017).

Affimers can also be used in microscopy techniques as direct replacements for antibodies using fixed cells. They have been shown to function successfully in fixed cell staining with fluorescence detection of Herpes Virus of Turkeys (HVT) infected cells when compared to antibody detection (figure 1.36a). In this case, Affimers were able to distinguish between infected and vaccinated animals. Moreover, they have been shown as potential reagents for single particle tracking in super resolution microscopy due to their small size in comparison to their antibody counterparts. Here, Affimer binding to human epidermal growth factor 4 receptor (HER4) are shown in figure 1.36b compared to antibody staining in both wide field and dSTORM images. Figure 1.36c shows an Affimer binding to polymerised

microtubules in dSTORM image compared to the antibody counterpart where the staining pattern is similar (Tiede *et al*., 2017).

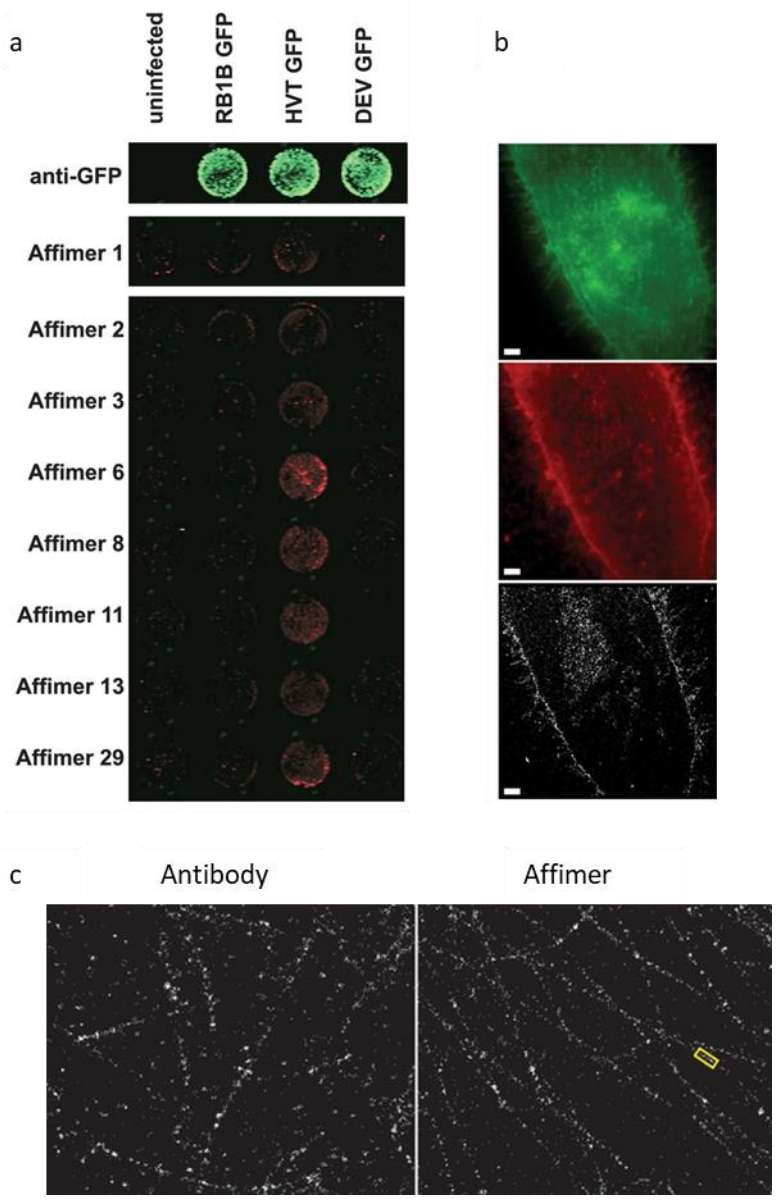

Figure 1.36 Affimers is microscopy techniques (a) Affimer staining of fixed cells using GFP and streptavidin-800. Affimers were raised against HVT and Affimers incubated with viral infected cells and Affimer 6 inparticular showed the same distribution within the cells infected with HVT as shown when the virus was detected using an antibody. There was no cross reaction with other related viruses. **(b)** Super resolution microscopy of HER4 using Affimers, (top) antibody staining in wide field view, (middle) Affimer staining with wide field view, (bottom) dSTORM image if Affimer staining **(c)** 3D STORM imaging of antibody and Affimer stained tubulin (Alexa Fluor-647) (Tiede *et al*., 2017).

1.5.4.6. Other examples of Affimer applications

As well as biologically relevant proteins, Affimers have also been raised against small organic compounds, in this case 2,4,6-trinitrotoluene (TNT). Using a TNT analogue, Affimers were able to distinguish between TNT and also two analogues of DNT (Tiede *et al*., 2017).

Affimers can also be used to investigate the binding motifs of proteins for example HIF-1α/p300. In this case an Affimer was raised to probe the interaction between HIF-1α and p300. This will help to better inform decisions regarding inhibition of this interaction when designing small molecule inhibitors (Kyle *et al*., 2015). They have also been used in the manipulation of nanoparticle synthesis to produce cubic nanoparticles rather than the conventional spherical shapes (Rawlings *et al*., 2015). Affimers can also function as peptide anchors, allowing for the study of proteins which may not have a stable structure (Stadler *et al*., 2014) and could also be implemented as co-crystalisation partners for proteins which do not crystalise easily due to structural integrity or solubility issues. Affimers have also been used in the development of electrochemical biosensors (Raina *et al*., 2015; Sharma *et al*., 2016). Recently Affimers have been shown to function in an Affimer-antibody combined diagnostic kit for the biomarker for hepatocellular carcinoma, glypican-3 (Xie *et al*., 2017).

1.5.4.7. Why use Affimers?

As discussed with other non-antibody scaffolds, excluding nanobodies as these rely on initial camelid involvement, there is a complete removal of the requirement for animal use in the production of Affimers, as they can be produced recombinantly from the first stage of the process. This makes them a desirable reagent for the direct replacement of antibodies within the molecular biology setting and as previously discussed they have been shown to function in a wide ranging number of techniques. The Affimers can be purified to a concentration between 50-100 mg/l of culture and the purification success rate is greater than 95% (Tiede *et al*., 2014). When compared to the purification of antibodies this is an improvement to the complicated precipitation and chromatography steps needed to obtain antibodies of similar purities and concentrations (Fisher, 2011). Unlike most

antibodies, Affimers can be produced 'in house' once identified using techniques and equipment available in most laboratory settings.

1.5.5. Aims of the project- Advantages and limitations and why they need improving

PRRSV is a highly contagious livestock infection which can cause significant losses to the agricultural industry and so it is vital that it can be rapidly detected on site with a relevant POC diagnostic. The aim of this project was to produce a novel Affimer-based LFD which was able to directly detect the presence of the PRRSV N protein within a sample.

The project involved the cloning and expression of two PRRSV N proteins from a low pathogenic and a high pathogenic strain of the virus in order to investigate if an Affimer-based sensor could be produced to detect the presence of viral proteins and to distinguish between viral strains.

A library of Affimer reagents was screened using phage display technology using the two N proteins as target proteins to obtain a pool of specifically binding Affimers. These Affimers were characterised for their binding against both of the target N proteins to further assess their binding specificity with the intention of reducing the original pool of reagents to those which could bind one or the other N protein and a smaller pool which could bind both N proteins.

The final pool of Affimer reagents were incorporated into a simple LFD as direct replacements for the antibody reagents ordinarily used in these devices to determine if they were suitable alternatives for this application. The use of Affimer reagents in this application will have wide reaching implications and pave the way for their use in POC diagnostics for a number of clinically relevant diseases in both human and animal healthcare.

Chapter 2

Materials and Methods

2 Materials and methods

2.1. Growth and maintenance of bacteria

2.1.1. Bacterial strains

A number of bacterial strains of *E.coli* (table 2.1) were used in this study to exploit their specific functions, for example transformation and replication of plasmid DNA, or protein expression.

Table 2.1 Genotypes of Competent bacteria used in this study. All bacteria were grown at 30 °C unless otherwise stated

E.coli strain	Genotype	Source
DH5α	F⁻Φ80*lac*ZΔM15Δ(*lac*ZYA-arg*F*)U169 *rec*A1 *end*A1 *hsd*R17(rK,mK+) *pho*A *sup*E44λ⁻ *thi*-1 *gyr*A96 *rel*A1	ThermoFisher Scientific
BL21(DE3)	F⁻ ompT hsdSB(r_B^-, m_B^-) gal dcm (DE3)	New England Biolabs®Inc
BL21(DE3)pLysS	F⁻ *omp*T *hsd*SB(rB–, mB–) *gal dcm* (DE3) pLysS (CamR)	Promega
BL21-Gold(DE3)	F⁻ ompT hsdS(r_B^- m_B^-) dcm^+ Tetr gal λ(DE3) endA The	Agilent Technologies
BL21-CodonPlus-RIL	F⁻ ompT hsdS(r_B^-, m_B^-) dcm^+ Tetr gal λ(DE3) endA Hte [argU ileY leuW Camr]	Agilent Technologies
BL21-CodonPlus-RP	F⁻ompT hsdS(r_B^-, m_B^-) dcm^+ Tetr gal endA Hte [argU proL Camr]	Agilent Technologies
ER2738	(F'proA⁺B⁺,lacIq,Δ(lacZ)M15,zzf::Tn10(TetR)/fhuA2 glnV Δ(lac-proAB) thi-1 Δ(hsdS-mcrB)5)	Lucigen

Cultures were grown in Luria broth (LB) [1 % (w/v) tryptone, 0.5 % (w/v) NaCl, 0.5 % (w/v) yeast extract] with shaking at 30 °C or colonies grown on Luria broth agar (LBA) [LB with 1.5 % agar] at 37 °C.

2.1.2. Preparation of rubidium chloride chemically competent bacteria

A glycerol stock of the relevant bacterial strain was streaked onto LBA (containing selection antibiotic if necessary) and grown overnight at 37 °C. A single colony was picked and used to inoculate 5 ml of LB media (selective if necessary) which was incubated overnight at 37 °C, 230 rpm. 0.5 ml of this culture was used to inoculate 50 ml LB media (selective if necessary) and the culture incubated at 37 °C, 230 rpm until an OD_{600} of 0.4-0.6 was reached. Cells were pelleted by centrifugation at 3545

xg for 5 minutes at 4°C. The pellet was resuspended in 40 ml filter sterilised, ice cold Transformation buffer 1 (TBF1) [30 mM KOAc, 10 mM $CaCl_2$, 50 mM $MnCl_2$, 100 mM RbCl, 15% (v/v) glycerol, adjusted to pH 5.8 with acetic acid] and incubated on ice for 5 minutes. The cells were pelleted at 3545 *xg* for 5 minutes at 4 °C, resuspended in 2 ml filter sterilised, ice cold TFB2 buffer [10 mM MOPS, 75 mM $CaCl_2$, 10 mM RbCl, 15 % (v/v) glycerol adjusted to pH 6.5 with KOH] and incubated on ice for 15-60 minutes. The cells were aliquoted into 150 µl samples and stored at -80 °C.

2.2. DNA protocols

2.2.1. Bacterial expression plasmids

A number of expression plasmids were used in this study for the expression of target recombinant proteins and Affimers, these plasmids are listed in table 2.2, along with a brief description of their key features.

Table 2.2 Native and recombinant plasmids used in this study

Plasmid	Description	Source
pTriEx™ 1.1	An expression vector, containing C-terminal HSV tag™ and His_8 tag™, which enables gene expression in mammalian (CMVie promoter), bacterial (T7*lac* promoter) and baculovirus infected insect cells (p10 promoter)	Novagen®
pET28a	An expression vector, containing a N-terminal His_6-tag (plus an optional C-terminal His_6-tag) and T7 promoter for bacterial protein expression	Novagen®
pET28aSUMO	A pET28a derived plasmid with a N-terminal His-SUMO tag (plus an optional C-terminal His_6-tag) and T7 promoter for bacterial protein expression.	Modified from Novagen® (Ariza *et al*., 2013)
pCR®-Blunt II-TOPO®	A vector used for the cloning of blunt ended DNA products containing the M13 primer sites for sequencing or PCR screening.	ThermoFisher Scientific
pET11a	A bacterial expression vector with a *Bam*HI cloning site and T7 promoter	Novagen®
pGEX-6P-1	A bacterial expression vector for the expression of GST-tagged recombinant proteins via a tac promoter. Thrombin recognition site for cleaving of the desired protein from the GST-tag.	GE Healthcare
pBSTG1	A phagemid cloning vector based derived from pHEN1 vector. Sequences cloned into this vector create a fusion sequence for expression of Affimers in bacteriophage M13.	(Tiede *et al*., 2014; Hoogenboom *et al*., 1991)

2.2.2. Polymerase chain reaction (PCR)

PCRs were performed in 0.2 µl PCR tubes (Axygen), using a TC-412 thermal cycler (Techne™). Reactions were set up as follows using Platinum® *Pfx* DNA polymerase: 1x Reaction Buffer, 1 mM $MgSO_4$, 10-50 ng DNA template, 0.3 µM each dNTP, 0.3 µM forward primer, 0.3 µM reverse primer, 1 U Platinum® Pfx DNA polymerase and nuclease free dH_2O added up to 50 µl. The conditions of PCR reactions are shown in table 2.3.

Table 2.3 Thermal cycling programs for PCR

Step	Process	Condition
1	Initial denaturation	95 °C for two minutes
2	Denaturation	95 °C for 15 seconds
3	Annealing	55 °C for 30 seconds
4	Extension	68 °C for 1 minute per kb
5		30 cycles of steps 2-4
6	Maintenance	4 °C

2.2.3. Agarose gel electrophoresis

DNA samples were mixed with an appropriate volume of 10x DNA loading buffer [30 % (v/v) glycerol, 0.25 % (w/v) Orange G] and 5 µl of each sample was loaded onto a 0.7 % (w/v) agarose gel in TBE [2 mM EDTA, 80 mM boric acid, 90 mM Tris-base] containing 5 µg/ml ethidium bromide (ThermoFisher Scientific) together with a 1 kb plus DNA ladder (ThermoFisher Scientific). Electrophoresis was performed in Mini-Sub Cell GT apparatus (Bio-Rad) in TBE buffer at 120 V and bands were visualised under UV using the GeneGenius bio-imaging system (Syngene).

2.2.4. Purification of DNA from agarose gels

Agarose gels were visualised on a transilluminator and DNA fragments were excised from the gel using a scalpel. To maintain DNA integrity, UV exposure was kept to a minimum. Extraction of the DNA was performed using the QIAquick gel extraction kit (QIAGEN), following the manufacturer's instructions. DNA was eluted in 50 µl dH_2O and stored at -20 °C.

2.2.5. Plasmid purification from *E.coli*

Single colonies grown on LBA plates were used to inoculate an appropriate volume of LB containing selective antibiotic(s) and grown overnight at 37 °C, 230 rpm. Plasmid purification was performed using QIAprep Spin Miniprep and QIAGEN Plasmid Maxiprep kits (QIAGEN) according to manufacturers' instructions. DNA was eluted in the appropriate volume of nuclease free H_2O and stored at -20 °C.

2.2.6. DNA sequencing

Purified DNA was diluted to 100 ng/µl and sequencing performed by GATC biotech using universal primers as shown in figure 2.4.

Table 2.4 Sequencing primers

Plasmid	Forward primer	Reverse primer
pTriEx™ 1.1	T7 promoter	T7 terminator
pET28a	T7 promoter	T7 terminator
pET28aSUMO	T7 promoter	T7 terminator
pCR®-Blunt II-TOPO®	M-13 forward	M-13 reverse
pET11a	T7 promoter	T7 terminator
pGEX-6P-1	pGex fwd	pGex rev
pBSTG1	M-13 forward	M-13 reverse

2.3. Molecular cloning

2.3.1. pCR®-Blunt II-TOPO®

Zero Blunt® TOPO® PCR cloning kit (Life Technologies) was used for the highly efficient cloning of blunt ended DNA products in this study.

All genes cloned into pCR®-Blunt II TOPO® were done so in accordance with the manufactures' protocol; 2 µl of PCR product was added to 1 µl of salt solution with 1 µl of the linearised TOPO® cloning vector in a total volume of 6 µl. The reaction was incubated for 30 minutes at room temperature. The reaction was added to 50 µl of DH5α cells and transformed as described in section 2.4.1.

2.3.2. Cloning into expression vectors

Bacterial expression vectors pTriEx™ 1.1, pET28a, pET28aSUMO, pET11a and pGEX-6P-1 were used in this study and the appropriate genes were cloned into these vectors from pCR®-Blunt II TOPO® as indicated in table 2.5.

Table 2.5 List of primers, enzymes and parent vectors used in the construction of the Target expression constructs used in this study (restriction sites highlighted in red)

Recombinant vector	Parent Vector	Intermediate vector	Forward Primer Sequence (5'-3')	Primer sequence (5'-3')	Restriction Enzyme
pET28aSumo-NLP	pTriEx 1.1	pCR®-Blunt II TOPO®	GGATCCATGCC AAATAACAACG	AACGCCGGCGTTA CGCTGATGATGG	*Bam*HI/*Not*I
pET28aSumo-NHP	TArget Clone	pCR®-Blunt II TOPO®	CCCGGATCCATG CCAAATAACAAC GGCAAGCAG	AAAGCGGCCGCA TCATGCTGAGGGT GATGCTGTGGC	*Bam*HI/*Not*I
pET11a (with cysteine)	pBSTG1	pCR®-Blunt II TOPO®	ATGGCTAGCAA CTCCCTGGAAAT CGAAG	TTACTAATGCGGC CGCACAAGCGTCA CCAACCGGTTTG	*Nhe*I/*Not*I
pET11a (without cysteine)	pBSTG1	pCR®-Blunt II TOPO®	ATGGCTAGCAA CTCCCTGGAAAT C GAAG	TACCCTAGTGGTG ATGATGGTGATGC	*Nhe*I/*Not*I
pGEX-6P-1-NHP	TArget Clone	pCR®-Blunt II TOPO®	CCCGGATCCATG CCAAATAACAAC GGCAAGCAG	AAAGCGGCCGCA TCATGCTGAGGGT GATGCTGTGGC	*Bam*HI/*Not*I
pTriEx 1.1-NHP	TArget Clone	pCR®-Blunt II TOPO®	CCGGATCCCATG CCAAATAACAAC GGCAAG	AATAGCGGCCGCT GCTGAGGGTGAT GCTGTGGC	*Bam*HI/*Not*I
pET28a-NHP	TArget Clone	pCR®-Blunt II TOPO®	CCCGGATCCATG CCAAATAACAAC GGCAAGCAG	AAAGCGGCCGCA TCATGCTGAGGGT GATGCTGTGGC	*Bam*HI/*Not*I

2.3.3. Restriction enzyme digest

Restriction digests were performed according to the manufacturer's instructions (New England Biolabs) in a total volume of 50 µl: 1 U restriction enzyme(s), 1 µg DNA, 1x NEBuffer, nuclease free dH_2O added to 50 µl. Reactions were incubated for two hours at 37 °C and double digests were performed where possible in a compatible buffer. The restriction enzymes used are shown in table 2.5. The resulting DNA fragments (vector and insert) were analysed on 0.7 % (w/v) agarose gels and then excised and purified from the gel (section 2.2.4.).

2.3.4. DNA ligation

The insert and vector were then used in ligation reactions, performed according to manufacturer's instructions in a total volume of 10µl containing 1x Ligase buffer (NEB), 50-100 ng linearised vector DNA and varying molar ratios of insert DNA fragments (generally this was a 1:3 ratio). Reactions were performed for a minimum of 1 hour at 16 °C using a TC-412 thermal cycler (Techne™). 5 µl of the ligation reaction was added to 50 µl DH5α and a transformation performed (section 2.4.1.).

2.4. Protein over-expression and purification

2.4.1. Transformation of chemically competent bacteria

50 µl aliquots of chemically competent bacteria (per transformation) were thawed on ice, 50ng of plasmid DNA was added to the aliquot and incubated on ice for 5 minutes. The cells were heat shocked at 42 °C for 30 seconds and returned to ice for 5 minutes. 200 µl of antibiotic free LB was added to each transformation reaction and these were incubated at 37 °C for 1 hour 230 rpm. The bacteria were then plated onto LB agar plates containing the appropriate antibiotic(s) (kanamycin or ampicillin at 50 µg/ml, chloramphenicol at 34 µg/ml) and incubated at 37 °C overnight.

2.4.2. Expression of recombinant proteins

Expression of recombinant proteins was performed in the appropriate *E.coli* strain (table 2.1). Plasmids were transformed into chemically competent cells (section 2.4.1.), single colonies were used to inoculate 10 ml selective LB media and cultures grown overnight at 37 °C, 230 rpm. The following day, overnight cultures were used to inoculate a larger culture volume at a 1/100 dilution. Cultures were grown to an OD_{600} 0.4 - 0.6 at 30 ^{o}C, 230 rpm and induced with a final concentration of 0.1 mM IPTG and cultured overnight at 30 °C, 230 rpm. The induced bacteria were then harvested by centrifugation at 3545 *xg* at 4 °C for 10 minutes in an Eppendorf 5804R centrifuge. Bacterial cell pellets were stored at -20 °C or lysed directly after harvesting.

2.4.3. Protein purification

Cell pellets were resuspended in lysis buffer [For recombinant His_6-tagged viral proteins: PBS, 150 mM NaCl, 50 mM imidazole, 0.1 % (v/v) Triton X-100, 5 U DNase, 5 U RNase, 100µg/ml lysozyme, for Affimers: 50 mM NaH_2PO_4, 300 mM NaCl, 20 mM imidazole, 5 U DNase, 5 U RNase, 100µg/ml lysozyme, for GST-tagged recombinant viral proteins: PBS, 150 mM NaCl, 0.1 % (v/v) Triton X-100, 5 U DNase, 5 U RNase, 100µg/ml lysozyme]. Cells were lysed by sonication (Sanyo Soniprep 150) on ice by the following cycle: 6x (10 seconds on, 20 seconds off) sample rested on ice for five minutes and the sonication repeated.

The lysate was transferred to micro-centrifuge tubes (removing a sample for SDS-PAGE analysis) and centrifuged at 13,000 *xg* for 30 minutes at 4 °C (Eppendorf 5418R). The supernatant was removed and filtered using a 0.45 µm Amicon syringe filter. A sample of the pellet and the supernatant was taken for SDS-PAGE analysis.

2.4.3.1. Nickel ion affinity chromatography-Sepharose His-Trap HP columns for purification of recombinant viral proteins

For purification of His-tagged proteins from large volumes, a 5 ml Ni^{2+} sepharose HisTrap HP column (GE Healthcare) was used. Purification was performed at 4 ^{o}C with the column attached to a peristaltic pump, maximum flow rate 1 ml/minute.

Columns were prepared by washing with five column volumes of dH_2O and equilibrated with 5 column volumes of lysis buffer [PBS, 150 mM NaCl, 50 mM imidazole, 0.1 % (v/v) Triton X-100]. The filtered bacterial cell lysate (section 2.4.3.) was loaded onto the column and the flow through collected. The column was then washed with five column volumes of wash buffer [PBS, 150 mM NaCl, 50 mM imidazole] wash fractions were collected. To elute the bound recombinant proteins, three column volumes of each buffer was added to the column and fractions collected, each buffer contains an increasing concentration of imidazole, [PBS, 150 mM NaCl and 80/160/240/320/400 mM imidazole]. The previously indicated elution fractions as well as whole cell, soluble, insoluble and wash fractions were mixed with an equal volume of 2x Laemmli buffer and analysed by

SDS-PAGE (section 2.4.4.1) followed by Coomassie blue staining (section 2.4.4.2) and western blotting (section 2.4.4.3.).

The used columns were stripped using 3 column volumes of 1x stripping buffer (4x strip buffer: 2 M NaCl, 80 mM Tris-HCl pH 7.9, 4 M imidazole) and stored in 20% ethanol in dH_2O at 4 °C.

2.4.3.2. Nickel ion affinity chromatography- Batch method for purification of Affimers

For purification of His_6-tagged Affimers from small volumes the Ni-NTA batch method was used. An appropriate volume of Ni^{2+}-NTA (QIAGEN) beads were prepared at 4 °C by centrifuging the beads at 800 *xg* (Eppendorf 5804R) for five minutes and removing the supernatant. The beads were washed three times in lysis buffer [50 mM NaH_2PO_4, 300 mM NaCl, 20 mM imidazole, pH 7.4] with centrifuging at 800 *xg* (Eppendorf 5804R) for three minutes between washes and removing the supernatant. The filtered bacterial cell lysate was loaded onto the beads and incubated for two hours at 4 °C. The lysate containing the beads was added to a 1 ml polypropylene column (QIAGEN) and allowed to flow through under gravity, collecting the flow through. The column was then washed with three column volumes of wash buffer [50 mM NaH_2PO_4, 500 mM NaCl, 20 mM imidazole, pH 7.4] collecting wash samples. The protein was eluted four times in 2 ml elution buffer [50 mM NaH_2PO_4, 500 mM NaCl, 300 mM imidazole, pH 7.4]. Fractions of the purification were analysed on SDS-PAGE (section 2.4.4.1) followed by Coomassie blue staining (section 2.4.4.2).

2.4.3.3. GST purification of recombinant viral proteins

For purification of GST-tagged recombinant viral proteins a batch method using glutathione sepharose 4B beads was used. The appropriate volume of glutathione sepharose 4B was prepared at 4 °C by centrifugation at 800 *xg* using an Eppendorf 5804R centrifuge removing the supernatant and washing three times with lysis buffer [PBS, 150 mM NaCl, 0.1 % (v/v) Triton X-100]. The filtered bacterial cell lysate was loaded onto the beads and incubated for two hours at 4 °C. The lysate containing the beads was added to a 1 ml polypropylene column (QIAGEN) and

allowed to flow through under gravity, collecting the flow through. The column was washed with three column volumes of wash buffer [PBS, 500 mM NaCl, pH 7.4] collecting wash samples. The protein was eluted four times in 2 ml elution buffer [PBS, 500 mM NaCl, 10 mM reduced glutathione, pH 7.4]. Fractions of the purification were analysed on SDS-PAGE (section 2.4.4.1) followed by Coomassie blue staining (section 2.4.4.2).

2.4.4. Protein analysis techniques

2.4.4.1. SDS-PAGE analysis

All gels used contained 15 % polyacrylamide made as described by Green *et al*., 2012 and consisted of a stacking gel overlaying a resolving gel. Protein samples were boiled for five minutes in 2x Laemmli buffer [4% SDS, 20% glycerol, 10% 2-mercaptoethanol, 0.004% bromophenol blue and 0.125 M Tris HCl, pH approx. 6.8] and loaded onto the gel in addition to Precision Plus Protein™ Dual Colour Standard protein ladder (BioRad). Electrophoresis was carried out in BioRad Mini-Protean Tetra System tanks containing 1x tris-glycine running buffer [10x stock: 0.1 % (w/v) SDS, 250 mM Tris-base, 192 mM glycine] at 180 V for approximately 45 minutes.

2.4.4.2. Coomassie blue staining of SDS-PAGE gels

Gels were stained with Coomassie blue [50% (v/v) methanol, 10 % (v/v) acetic acid, 0.05 % (w/v) Brilliant Blue R-250] for one hour before destaining [50 % (v/v) methanol, 10 % (v/v) acetic acid] for one hour.

2.4.4.3. Western blotting of SDS-PAGE gels

Proteins were transferred from SDS-PAGE polyacrylamide gels onto Protran 0.45 nitrocellulose membrane (GE Healthcare) using Bio-Rad Mini-Protean 3 cell tanks according to the manufacturer's instructions. The nitrocellulose membrane and polyacrylamide gel were sandwiched between Whatman 3mm filter paper (GE Healthcare) soaked in transfer buffer [20% (v/v) methanol, 25 mM Tris-base, 190 mM glycine] and placed in the tank. Transfer was carried out at 100V, for one hour in transfer buffer. The transferred membrane was incubated in 5% (w/v) milk powder in TBS-T [500 mM NaCl, 20 mM Tris-base, 0.1 % (v/v) Tween-20] for one

hour. The membrane was incubated in primary antibody diluted in TBS-T for a minimum of one hour and washed for three five minute intervals. The membrane was incubated in secondary antibody diluted in TBS-T for a minimum of one hour before being washed for three five minute intervals. The blots were covered with EZ-ECLA and EZ-ECLB mixed 1:1 and incubated for two minutes before visualisation with Hyperfilm ECL™ (GE Healthcare) in a Konica SRX-101A developer.

2.4.4.4. Protein concentrations

The concentrations of purified proteins were determined using a Bradford Assay (BioRad) according to manufacturer's instructions.

2.4.5. Labelling of expressed recombinant proteins

2.4.5.1. Biotinylation of recombinant proteins

2.4.5.1.1. Method 1: EZ-Link® NHS-SS-biotin to label amine containing proteins

EZ-Link® NHS-SS-Biotin (ThermoFisher Scientific) was warmed to room temperature and immediately before use, a 5 mg/ml solution prepared in DMSO. An appropriate volume of NHS-SS-biotin was added to a 1 mg/ml protein solution in a total volume of 100 µl PBS (PBST for hydrophobic proteins), amount of linker required was altered according to molecular weight, and incubated at room temperature for one hour. Any excess biotin was removed using a Zeba™ Spin Desalting Column, 7K MWCO (ThermoFisher Scientific) according to the manufacturer's instructions. The sample was then mixed with an equal volume of 80 % (v/v) glycerol and stored at -20 °C.

2.4.5.1.2. Method 2: Peptide disulphide bonds reduced with TCEP disulphide reducing gel and labelling of available sulfhydryl groups

An appropriate volume of TCEP (tris(2-carboxyethyl)phosphine) Disulphide Reducing Gel (ThermoFisher Scientific) was centrifuged at 1000 *xg* for 1 minute and the supernatant discarded. The gel was washed 3 times with PBS containing 1 mM EDTA with centrifuging at 1000 *xg* for 1 minute between washes. PBS with 50 mM EDTA was added to the gel with an appropriate volume of a 1 mg/ml solution of

peptide. The sample was incubated at room temperature for one hour with rotation to keep the gel in suspension. To recover the supernatant containing the reduced peptide, the sample was centrifuged for one minute 1000 *xg* immediately before labelling with biotin.

A 5 mg/ml maleimide-Biotin (ThermoFisher Scientific) stock solution was prepared in DMSO. An appropriate volume of stock solution was added to an appropriate volume of reduced peptide and the reaction incubated at room temperature for two hours or overnight at 4 °C. Excess label was removed using Zeba™ Spin Desalting Columns 7K MWCO according to manufacturer's instructions. The sample was mixed with an equal volume of 80 % (v/v) glycerol and stored at -20 °C.

2.4.5.1.3. EZ-Link™ maleimide activated horseradish peroxidase labelling of single cysteine containing Affimers

The single cysteine residues of the Affimers were reduced using the TCEP method (section 2.4.5.1.2) and the activated maleimide-HRP conjugated to the Affimer according to the manufacturer's instructions (ThermoFisher Scientific) where the reduced protein was incubated with maleimide-HRP overnight at room temperature.

2.4.5.1.4. Alexa Fluor® C5 maleimide labelling of single cysteine containing Affimers

The single cysteine residues of the Affimers were reduced using the TCEP method (section 2.4.5.1.2) and the activated Alexa Fluor®C5 maleimide conjugated to the Affimer according to the manufacturer's instructions (ThermoFisher Scientific) where the reduced protein was incubated with Alexa Fluor®C5 maleimide overnight at room temperature. Excess label was removed using Zeba™ Spin Desalting Columns 7K MWCO according to manufacturer's instructions.

2.4.6. ELISA to check labelling of proteins

2.4.6.1. Biotinylated proteins

1, 0.1, 0.01 µl of biotinylated targets were added to Nunc-Immuno™ MaxiSorp™ Strips (ThermoFisher Scientific) containing 50 µl PBS and incubated overnight at 4 °C. The wells were washed three times with PBST on a plate washer and blocked

with 250 µl 10x blocking buffer (Sigma-Aldrich-Aldrich) and incubated for three hours at 37 °C. The wells were washed three times with PBST on a plate washer. The wells were then incubated with High Sensitivity Streptavidin-HRP diluted 1:1000 in 2x blocking buffer (10x blocking buffer diluted in PBST) for 1 hour at room temperature on a vibrating platform. The wells were washed 6 times with PBST on a plate washer and incubated with Seramum Blau® fast TMB/substrate solution (Seramum) and allowed to develop for three minutes at room temperature. The absorbance was measured at 620nm using a Multiskan Ascent 96/384 Plate Reader (MTX Lab Systems Inc).

2.4.6.2. HRP labelled proteins

1, 0.1, 0.01 µl of HRP labelled targets were added to Nunc-Immuno™ MaxiSorp™ Strips (ThermoFisher Scientific) containing 50 µl PBS and incubated overnight at 4 °C. The wells were washed three times with PBST on a plate washer. The wells were incubated with Seramum Blau® fast TMB/substrate solution (Seramum) and allowed to develop for three minutes at room temperature. The absorbance was measured at 620nm using a Multiskan Ascent 96/384 Plate Reader (MTX Lab Systems Inc).

2.4.6.3. Fluorescence labelled proteins

1, 0.1, 0.01 µl of Alexa Fluor® labelled targets were added to Nunc-Immuno™ MaxiSorp™ Strips (ThermoFisher Scientific) containing 50 µl PBS and incubated overnight at 4 ^{o}C. The wells were washed three times with PBST on a plate washer. The fluorescence was measured using a plate reader (PolarStar Optima).

2.5. Phage display techniques

All reactions for phage display were carried out in Eppendorf Protein LoBind Tubes unless otherwise stated. The protocol for phage display is outlined in figure 2.1.

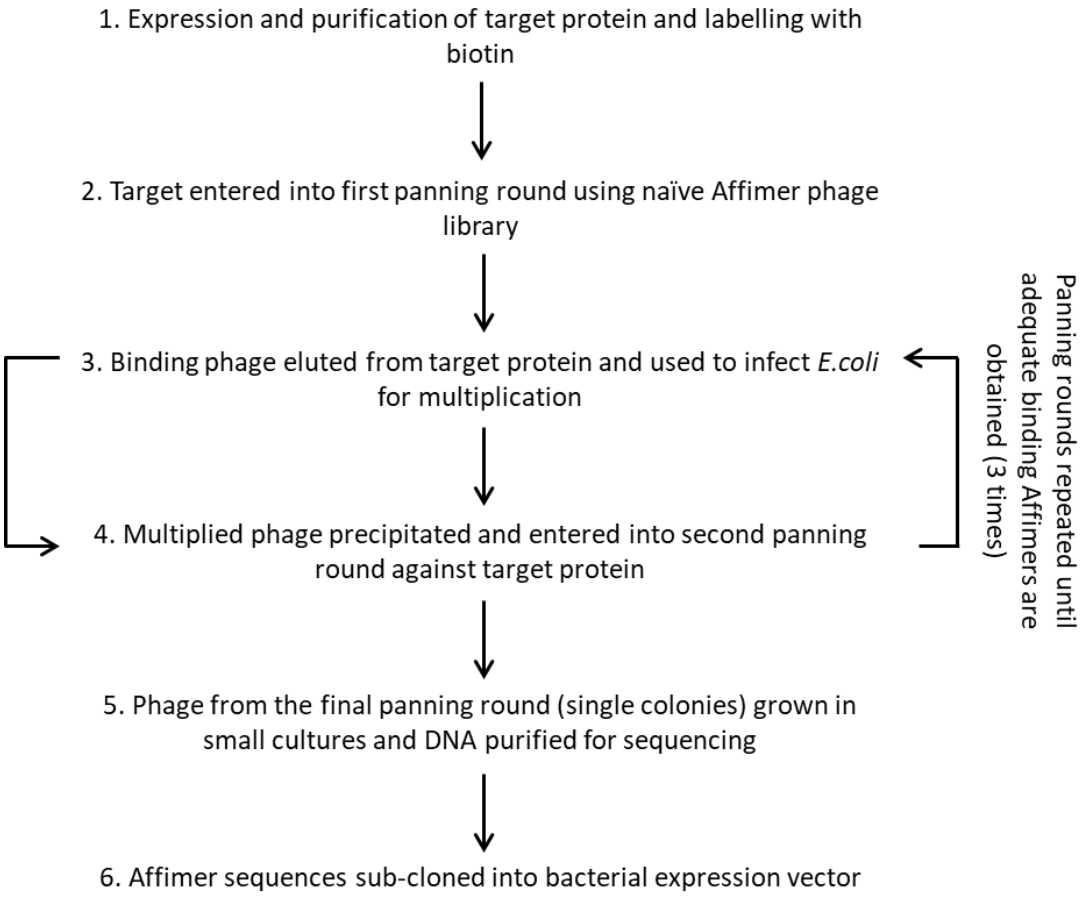

Figure 2.1 Phage display protocol for screening of Affimers. Target proteins were screened using the Affimer phage library for a total of three panning rounds, with the Affimers from the final panning round taken forward for sequencing to identify unique loop region sequences.

2.5.1. First panning round

ER2738 cells were grown overnight on selective LBA (12 µg/ml tetracycline) at 37 °C. A single colony was used to inoculate 5 ml 2TY media (10 % (w/v) yeast extract, 16 % (w/v) tryptone, 0.5 % (w/v) NaCl) with 12 µg/ml tetracycline overnight in an orbital incubator 230 rpm at 37 °C. Streptavidin coated (HBC) 8-well strips (ThermoFisher Scientific) were blocked using 2x blocking buffer overnight at 37 °C, a total of four wells for each target. The wells were washed once with PBST on a plate washer and fresh 2x blocking buffer added to the wells. The phage library was pre-panned three times against the streptavidin coated plates: the phage library was added to the first pre-pan well and incubated at room temperature for one hour on a vibrating platform shaker. The blocking buffer was removed from the second pre-panning well and the phage containing supernatant from the first

well removed to the second and incubated for one hour at room temperature shaking. This was repeated a third time. During the pre-panning steps, the biotinylated target, diluted 1:200 in 2x blocking buffer, was bound to the panning well for two hours at room temperature on a vibrating platform shaker. The wells containing the biotinylated target were washed six times with PBST and the pre-panned phage transferred from the appropriate pre-panning well into the well containing the target and incubated at room temperature for two hours shaking. One hour before elution of phage from panning wells, a dilution of the overnight ER2738 cells was set up to give an 8 ml culture per target at A_{600} of 0.6 at time of infection.

2.5.1.1. Elution of phage and infection of ER2738 cells

The final panning wells were washed six times with PBST on a plate washer and the phage eluted and used to infect ER2738 cells. The phage was eluted in 0.2 M glycine, pH 2.2 for ten minutes at room temperature followed by neutralisation with 1 M Tris-HCl, pH 9.1 before addition to the aliquot of ER2738 cells. The remaining phage was eluted in triethylamine for six minutes at room temperature and neutralisation with 1 M Tris-HCl, pH 7 before addition to the aliquot of ER2738 cells. The infected cells were incubated at 37 °C for one hour with no shaking and were mixed at least once during the incubation.

2.5.1.2. Plating out ER2738 cells and preparation of phage

1µl of phage infected ER2738 cells were plated onto LB agar carbenicillin plates (100 µg/ml carbenicillin). The remaining cells were centrifuged for five minutes at 3,000 *xg* and resuspended in a smaller volume and plated onto LB agar carbenicillin plates as 'remaining' sample. The plates were incubated at 37 °C overnight.

The following day, the number of colonies on the plate with the 1 µl inoculation were counted and this number multiplied by 8000 to determine the number of cells on the remaining cells plate. The ER2738 cells were then scraped from the plates containing the 'remaining' samples using 2TY media with carbenicillin (100 µg/ml). The absorbance of a 1:10 dilution was measured and used to calculate the dilution required for a fresh 8 ml culture with an A_{600} of 0.2. The cells were then

diluted in 2TY media with carbenicillin (100 µg/ml) and incubated at 37 °C for one hour 230 rpm. 0.32 µl of M13K07 helper phage (titre ca. 10^{14}/ml) was added and the cells incubated for 30 minutes at 37 °C, 90 rpm before the addition of 400 µg kanamycin and incubation overnight at 25 °C, 170 rpm.

The following day the phage infected cultures were centrifuged at 3,500 *xg* for ten minutes and the phage containing supernatant transferred to fresh falcon tubes. The required volume of phage containing supernatant was removed for use in the second panning round. PEG-NaCl [20% (w/v) PEG 8000, 2.5 M NaCl] was added to the remaining phage containing supernatant to precipitate the phage and the reaction incubated overnight at 4 °C. The phage was pelleted by centrifugation at 4,816 *xg* for 30 minutes and the supernatant removed. The pellet was resuspended in TE [10 mM Tris, 1 mM EDTA pH 8] and transferred to microcentrifuge tubes and centrifuged at 16,000 *xg* for ten minutes. The supernatant was removed and diluted with 40-50 % glycerol and stored at -80 °C.

2.5.2. Second panning round

ER2738 cells were grown in 2TY media with 12 µg/ml tetracycline overnight, at 37 °C, 230 rpm. 20 µl beads per target, (Dynabeads® MyOne™ Streptavidin T1, 10 mg/ml), were blocked with 100 µl 2x blocking buffer and incubated overnight at room temperature, 20 rpm (Stuart SB2 fixed speed rotator). The appropriate number of wells were blocked in the plates for the KingFisher Flex, panning wells were blocked with 1 ml 2x blocking buffer in a deep 96 well plate (ThermoFisher Scientific) and elution wells were blocked with 300 µl 2x blocking buffer in two KingFisher (200µl) 96 well plates (ThermoFisher Scientific), the plates were incubated overnight at 37 °C. Sufficient wells were prepared in 4x deep 96 well plates with 950 µl 2x blocking buffer directly before use.

Pre-panning of the phage was carried out using pre-blocked streptavidin coated beads. The pre-blocked streptavidin beads were centrifuged at 800 *xg* for one minute and immobilised on a magnet before removing the 2x blocking buffer. The 2x blocking buffer was replaced and the beads resuspended, 100 µl per 20 µl beads. 125 µl of phage containing supernatant from pan one was mixed with 125 µl 2x blocking buffer (or 5 µl purified phage with 245 µl 2x blocking buffer) and 25

µl pre-blocked streptavidin beads and incubated for one hour at room temperature on the rotator. The beads were centrifuged at 800 *xg* for one minute and placed on a magnet. The supernatant containing the phage was added to a fresh tube and another 25 µl pre-blocked streptavidin beads were added and again incubated for one hour at room temperature on the rotator. In parallel, the biotinylated target protein was incubated with 50µl pre-blocked streptavidin beads and incubated for two hours at room temperature on the rotator.

Immediately before use, the 2x blocking buffer was removed from the deep 96-well plate used for panning and the two (200 µl) 96-well plates used for elution. 100 µl glycine [0.2 M, pH 2.2] was aliquoted per target into the pre-blocked wells of one elution plate and 100 µl triethylamine aliquoted per target into the pre-blocked wells of the second elution plate.

The tubes containing the streptavidin beads with the biotinylated target bound were centrifuged at 800 *xg* for one minute and immobilised on a magnet and washed with 2x blocking buffer, repeating three times. The tubes containing the pre-panned phage were centrifuged at 800 *xg* for one minute and immobilised on a magnet with the supernatant removed into the appropriate tube containing the target protein bound to streptavidin beads. The beads were resuspended and transferred to the pre-blocked wells of the deep 96-well plate.

2.5.2.1. Standard panning

The KingFisher Flex protocol 'Phage_display_pH_elution' was selected (table 2.6) and the plates placed into the machine in the appropriate order. Approximately one hour before elution of phage a fresh culture of ER2738 cells was setup using the overnight culture as previously described (section 2.4.2) and incubated at 37 °C, 230 rpm. Phage were eluted and used to infect a day culture of ER2738 cells as previously described (section 2.5.1.1).

Table 2.6 KingFisher Flex 'Phage_display_pH_elution' protocol

Protocol Step	Plate	Volume (ul)	Settings
Tipcomb	96 DW tip comb		
Pick-Up: Tipcomb	KingFisher 96 KF plate		
Collect Beads	Plate: Binding Microtiter DW 96 plate		Collect count 1 Collect time (s) 1
Binding	Plate: Binding Microtiter DW 96 plate	300	**Beginning of Step** Release beads [hh:mm:ss]: 00:00:00 **Mixing/Heating Parameters** Mix time [hh:mm:ss]: 00:00:10 Speed: fast Mix time [hh:mm:ss]: 00:01:00 Speed: slow **End of step** Collect beads, count: 5 Collect time (s): 30
Wash 1	Plate: Wash 1 Microtiter DW 96 plate	950	**Beginning of Step** Release beads [hh:mm:ss]: 00:00:00 **Mixing/Heating Parameters** Mix time [hh:mm:ss]: 00:01:00 Speed: slow **End of step** Collect beads, count: 5 Collect time (s): 30
Wash 2	Plate: Wash 2 Microtiter DW 96 plate	950	**Beginning of Step** Release beads [hh:mm:ss]: 00:00:00 **Mixing/Heating Parameters** Mix time [hh:mm:ss]: 00:01:00 Speed: slow **End of step** Collect beads, count: 5 Collect time (s): 30
Wash 3	Plate: Wash 3 Microtiter DW 96 plate	950	**Beginning of Step** Release beads [hh:mm:ss]: 00:00:00 **Mixing/Heating Parameters** Mix time [hh:mm:ss]: 00:01:00 Speed: slow **End of step** Collect beads, count: 5 Collect time (s): 30
Wash 4	Plate: Wash 4 Microtiter DW 96 plate	950	**Beginning of Step** Release beads [hh:mm:ss]: 00:00:00 **Mixing/Heating Parameters** Mix time [hh:mm:ss]: 00:01:00 Speed: slow **End of step** Collect beads, count: 5 Collect time (s): 30
pH Elution	Plate: pH elution KingFisher 96 KF plate	100	**Beginning of Step** Release beads [hh:mm:ss]: 00:00:00 **Mixing/Heating Parameters** Mix time [hh:mm:ss]: 00:07:30 Speed: slow

			Postmix[hh:mm:ss]: 00:00:05 Speed: Bottom mix **End of step** Collect beads, count: 5 Collect time (s): 30
Triethylamine Elution	Plate: Triethylamine KingFisher 96 KF plate	100	**Beginning of Step** Release beads [hh:mm:ss]: 00:00:00 **Mixing/Heating Parameters** Mix time [hh:mm:ss]: 00:03:30 Speed: slow Postmix[hh:mm:ss]: 00:00:05 Speed: Bottom mix **End of step** Collect beads, count: 5 Collect time (s): 30
Leave: Tipcomb	96 DW tip comb		

2.5.3. Third panning round

The third panning round was performed as described in the first panning round (section 2.5.1) with the Streptavidin coated (HBC) 8-well strips replaced with NeutrAvidin Coated (HBC) 8-well strips and 200 µl phage containing supernatant (or 8 µl purified phage) from second panning round used.

When preparing plates following elution of phage, a range of volumes were plated, eg; 100, 10, 1, 0.1 µl and incubated overnight at 37 °C.

2.5.4. Phage ELISA

2.5.4.1. Preparation of Streptavidin coated ELISA plates

Streptavidin coated ELISA plates were prepared in advance of performing phage ELISA's as follows and stored at 4 ^{o}C for up to one week or -80 ^{o}C for longer periods. 50 µl of a 5 µg/ml Streptavidin in PBS was aliquoted per well of a 96-well F96 Maxisorp Nunc-Immuno Plate and incubated for at least four hours at room temperature or 4 ^{o}C overnight.

2.5.4.2. Preparation of phage from individual binders

200 µl 2TY containing 100 µg/ml carbenicillin was aliquoted into the appropriate number of wells in a 96-well V-bottom plate (Greiner). Individual colonies from the final panning round were used to inoculate the wells and incubated overnight at 37

°C, 1050 rpm in an incubating microplate shaker (Heidolf Incubator 1000 and Titramax 1000). The following day, 200 µl 2TY media with 100 µg/ml carbenicillin was aliquoted into a new 96-well V-bottom deep well plate and 25 µl of the overnight culture transferred into the corresponding well and incubated for one hour at 37 °C, 1050 rpm. M13K07 helper phage (titre ca.10^{14}/ml) was diluted 1/1000 in 2TY with 100 µg/ml carbenicillin and 10 µl added per well and incubated for 30 minutes at room temperature, 450 rpm. A kanamycin stock (25 mg/ml) was diluted 1/20 in 2TY media with 100 µg/ml carbenicillin and 10 µl added per well and incubated overnight at room temperature, 750 rpm. The following morning the phage infected culture plate was centrifuged at 3,500 *xg* for ten minutes and phage containing supernatant transferred directly to the previously prepared ELISA plate (section 2.5.4.1) for binding to the target protein.

20 µl of the original overnight culture was used to inoculate 5 ml 2TY media containing 100 µg/ml carbenicillin and grown at 37 °C overnight. The following day plasmid DNA was recovered using a Miniprep kit (section 2.2.5).

2.5.4.3. Performing phage ELISA

Prior to use, 200 µl 2x blocking buffer was added per well of the pre-prepared streptavidin plates (section 2.5.4.1) and the plates incubated overnight at 37 °C. The following day the wells were washed once with PBST on a plate washer (TECAN Hydrospeed). The biotinylated target protein was diluted to an appropriate dilution factor (1/1000-1/100) in 2x blocking buffer and 50 µl added per well. Control wells were left without bound target or with the appropriate biotinylated negative screen target protein at the same concentration. The plates were incubated at room temperature for one hour on a vibrating platform shaker. Wells were washed once with PBST on a plate washer and 10µl 10x blocking buffer aliquoted per well. 40 µl of previously prepared phage containing supernatant (section 2.5.1.2) was added per target containing well and corresponding control well and incubated at room temperature for one hour on a vibrating platform shaker. Each well was washed once with PBST on a plate washer and 50 µl of a 1/1000 dilution of anti-Fd-Bacteriophage-HRP antibody (Seramun Diagnostica GmbH) aliquoted per well before incubation for a further hour at room

temperature on a vibrating platform shaker. Each well was washed ten times with PBST on a plate washer and 50 µl TMB (SeramunBlau® fast TMB/substrate solution, Seramun) aliquoted per well and allowed to develop for three minutes. Absorbance per well was measured at 620 nm using a Multiskan Ascent 96/384 Plate Reader (MTX Lab Systems Inc).

2.5.5. Subcloning Affimer sequences from phagemid vector into bacterial expression vector

Affimers were subcloned from the parent phagemid vector, pBSTG1-Adh, into a bacterial expression vector, pET11a, using the primer sequences, forward shorter and pDHisIID-final-rev or pDHis-C-rev, when cloning with an added cysteine. Sequences are shown in table 2.4. Cloning was carried out as described in section 2.3.

2.6. Identification of pairs of Affimers

Affimers cloned with the C-terminal cysteine were expressed in 100 ml cultures using BL21 DE3(plysS) cells for purification using the batch method as described in section 2.4.3.2. They were labelled via the C-terminal cysteine with biotin, HRP or fluorescence labels (section 2.4.5).

2.6.1. Phage sandwich ELISA

Streptavidin plates were prepared as described in section 2.5.4.1 and blocked overnight in 200 µl 2x blocking buffer at 37 °C. The following day the plate was washed once with PBST in a plate washer and 50 µl of 2x blocking buffer aliquoted into each well. 1 µl of the biotinylated Affimer was bound to the streptavidin plate for one hour at room temperature on a vibrating shaker. The plate was washed once with PBST on a plate washer and 40 µl of 2x blocking buffer and 10 µl 0.5 M biotin added to each well and incubated overnight 4 °C.

The following day the plate was washed once with PBST on a plate washer. Non-biotinylated target protein was diluted 1:200 in 2x blocking buffer and 50 µl added to each well for one hour at room temperature. 10 µl of the phage containing supernatant was added to the corresponding wells and incubated for two hours at room temperature. The plate was washed once with PBST on a plate washer and

50 µl of a 1:1000 dilution of anti-Fd-bacteriophage-HRP antibody (Seramun) added to each well and incubated at room temperature for one hour on a vibrating platform. Phage binding was visualised with TMB as previously described (section 2.5.4.3).

2.6.2. Labelled recombinant protein sandwich ELISA

Streptavidin plates were prepared as described in section 2.5.4.1 and blocked overnight in 200 µl 2x blocking buffer at 37 °C. The following day the plate was washed once with PBST in a plate washer and 50 µl of 2x blocking buffer aliquoted into each well. 1 µl of the biotinylated Affimer was bound to the streptavidin plate for one hour at room temperature on a vibrating shaker. The plate was washed once with PBST on a plate washer and 40 µl of 2x blocking buffer and incubated overnight 4 °C.

The plate was washed once with PBST on a plate washer. Non-biotinylated target protein was diluted 1:200 in 2x blocking buffer and 50 µl added to each well for one hour at room temperature. 1 µl of HRP labelled Affimer or Alexa Fluor® labelled Affimer was added to the corresponding wells and incubated for two hours at room temperature. HRP labelled Affimer binding was visualised with TMB as previously described (section 2.6.4.2), Alexa Fluor® labelled Affimer binding was analysed by measurement on a plate reader (PolarStar Optima by BMG Labtech) Alexa Fluor® 488 was excited at 490nm and Alexa Fluor® 546 was excited at 532 nm.

2.6.3. Gold nanoparticle pairs assay

2.6.3.1. Magnetic bead pulldowns

20 µl streptavidin MyOne T1 beads (ThermoFisher Scientific) per reaction were incubated overnight in 2x blocking buffer (at room temperature with rotation). The magnetic beads were immobilised on a magnet and the blocking buffer removed and replaced with 100 µl fresh 2x blocking buffer per 20 µl of beads. The beads were then incubated with the biotinylated Affimers (section 2.4.5.1) at 5 µl of 1mg/ml Affimer per 20 µl of beads for 30 minutes at room temperature with rotation. Excess Affimer was removed with three washes in PBST with suspension

on the magnetic rack. The Affimers bound to the magnetic beads were incubated with the target protein diluted to 0.5 mg/ml in pig serum (serum was diluted 1:1 with PBST) for 30 minutes at room temperature with rotation. The magnetic beads were washed three times in PBST to remove excess target with immobilisation of the beads on the magnet. Binding of the target protein to the Affimer was confirmed by SDS-PAGE and western blot analysis (sections 2.4.4.1, 2.4.4.3).

2.6.3.2. Binding of Affimers to gold nanoparticles

Streptavidin functionalised gold nanoparticles (GNPs) (Innova Biosciences) were diluted to OD 0.1 in PBST and incubated with 5 µl of 1 mg/ml biotinylated Affimer for 30 minutes at room temperature with rotation. The GNPs were washed three times with PBST to remove any excess Affimer with centrifugation at 9000 *xg* for 6 minutes.

2.6.3.3. ELISA using Affimers bound to gold nanoparticles

Binding of the Affimers to the GNPs and ability to detect the target protein was determined using an ELISA method. GNPs coated with Affimers were incubated with or without 1 µl of 1mg/ml target protein for 30 minutes with rotation. The GNPs were washed three times with PBST by centrifugation, five minutes at 9000 *xg.* The GNPs were then incubated with 50 µl anti-his-HRP (1:10,000) for 30 minutes before washing three times in PBST. The binding of anti-his-HRP was visualised by adding 50 µl TMB and measuring the A600 using a Multiskan Ascent 96/384 Plate Reader (MTX Lab Systems Inc).

2.6.3.4. Gold nanoparticle/magnetic beads pairs assay

The Affimer coated magnetic beads, following incubation with the target protein were washed three times in PBST, after the final wash, the magnetic beads were resuspended in 50 µl of the Affimer labelled gnp. The beads were incubated at room temperature for 30 minutes with rotation. To identify any Affimers which may function as pairs the magnetic beads were immobilised on a magnet and the supernatant removed into a 96 well plate. The absorbance spectra of the sample was measured from 400-900 nm using a Clariostar plate reader (BMG Lab Tech).

2.7. Lateral flow based biosensor development

2.7.1. Striping of Affimers/antibodies onto nitrocellulose membrane

1 mg/ml solution of Affimer or antibody was prepared and, using a sequencing tip, striped in a line across the Hi-Flow Plus HF135 nitrocellulose membrane cards (Merck Millipore). Any regions of thick deposition were marked so as not to be used and the cards dried at 37 °C overnight.

2.7.2. Detection of Affimers on nitrocellulose membrane

Biotinylated Affimers were adsorbed onto nitrocellulose membrane before drying the membrane overnight at 37 °C (section 2.7.1). The Affimers were detected using anti His-HRP (1:1000) (Invitrogen™) for 30 minutes at room temperature before the membrane was washed three times and exposed in accordance to the western blot procedure (section 2.4.4.3).

2.7.3. Affimers working as pairs in a lateral flow device

Affimers and anti-his6 antibody were immobilised onto the nitrocellulose membrane cards as described in section 2.7.1. 10 µl of OD1 Affimer coated GNPs were incubated with 1 µl of 1mg/ml target protein and washed as described in section 2.6.3.3. The GNPs were resuspended to OD1 and transferred to a 96 well plate. Nitrocellulose membrane cards were cut into strips which were incubated with the resuspended GNPs for 30 minutes.

2.8. Bioinformatics analysis

Online software Clustal Omega Multiple Sequence Alignment (EMBL-EBI) was used for confirmation of DNA sequences following cloning and for the alignment of protein sequences. Sequence data was obtained National Centre for Biotechnology Information (NCBI) (www.ncbi.nlm.nih.gov) for alignment with cloning data. Numerical data was analysed in Microsoft® Excel.

Chapter 3

Production of novel Affimer reagents targeted to the PRRSV N protein

3. Production of novel Affimer reagents targeted to the PRRSV N protein

3.1. Introduction

The PRRSV nucleocapsid (N) protein is an RNA binding protein which associates with the viral RNA genome (Daginakatte and Kapil, 2001). The N protein is the major immunogenic protein of PRRSV comprising 40% of the virion (Meulenberg *et al*., 1995), as such it makes the N protein a desirable target for detection in a diagnostic test for virus infection.

The proposed diagnostic test uses novel non-antibody binding proteins, termed Affimers, as the binding reagents in a lateral flow-based device (LFD) (Chen and Yang, 2015b). Affimers are 91 amino acid scaffold proteins which contain two variable loop regions, each of which are nine amino acids in length, giving a current library size of $1x10^{10}$ clones (Tiede *et al*., 2014). The production of a biosensor which can detect the PRRSV N protein in clinical samples will serve as a proof of principle for the use of these reagents in LFDs.

LFDs are a rapid and simple method of detecting numerous targets in a non-laboratory setting in a semi-quantitative manner, as such the applications are wide reaching (Sajid *et al*., 2014). Detection targets can include pathogens, hormones, drugs and metabolites, as long as a suitable antibody can be raised against the target (Posthuma-Trumpie *et al*., 2009; Corstjens *et al*., 2012; Morales-Narváez *et al*., 2015; Song *et al*., 2014). It is possible to extend the use of LFDs by multiplexing, allowing the detection of multiple pathogens on one device, or multiple strains of a single pathogen (Zhao *et al*., 2016; Chen *et al*., 2016; Yang *et al*., 2015a). Whilst antibodies are fantastic reagents for use in a wide variety of molecular biology techniques, they do have limitations, most importantly, the use of animals in their production. Substantial numbers/species of animals are required to produce antibody reagents dependent on the amounts of reagent required, the intended use and phylogenic relationship between the antigen and the animal species (Leenaars and Hendriksen, 2005). The replacement of antibodies in LFDs with Affimers will allow for the reduction in production time for reagents as well as the complete elimination of animals from the production process.

The most familiar LFD is the pregnancy test, detecting the human chorionic gonadotrophin hormone (hCG) in urine (Leuvering *et al*., 1980). This is a widely used diagnostic test performed in a home setting without prior sample preparation. Other examples of LFDs in a clinical setting using the direct detection of antigens were early developed glucose detection (Free *et al*., 1957) and more recently for the detection of cryptococcal antigen in HIV patients (Tang *et al*., 2015; Workman *et al*., 2009). A number of Food and Drug Administration (FDA) approved assays are available from Chembio Diagnostic Systems Inc for the detection of HIV and associated infections, as well as a United States Department of Agriculture (USDA) approved test for TB; DDPP® HIV 1/2 Assay, DPP® HIV-Syphilis Assay, Chagas STAT-PAK® Assay, DPP® VetTB Assay. Although this is not an exhaustive list, it outlines the variety of clinical uses for LFDs in both a human and agricultural clinical setting.

The use of LFDs in agricultural settings is already widespread. They are used routinely in the dairy industry for the monitoring of reproductive cycles, to produce an efficient reproductive regime within a herd and to maximise the returns within the business (Nebel *et al*., 1987). For example, the LFDs are used for the detection of progesterone levels in cow's milk, allowing for the monitoring of the oestrus status and to detect early non-pregnant animals. Along with the human pregnancy test, this also demonstrates the use of a clinical sample, in this case milk, requiring no preliminary sample preparation (Samsonova *et al*., 2015). Most LFDs for use outside of laboratories use antibodies which recognise different epitopes on a target protein for its detection with a colourimetric change. The colourimetric change is provided by the surface plasmon resonance of the gold colloid which is conjugated to one of the antibodies (Verma *et al*., 2015) as detailed in section 1.5.1.

Currently, the use of LFDs for the detection of viruses is mainly focussed upon the detection of antibodies raised against the virus during infection. This provides a result which does not necessarily confirm current infection, rather a level of immunity to the virus and, therefore, the detection of viral proteins directly is a

more advantageous method to employ in a LFD, particularly for the detection of economically relevant infectious diseases (Corstjens *et al*., 2012).

The use of Affimers as alternative reagents to antibodies in the LFD proposed in this study is a novel application of these non-antibody binding proteins. Affimers are a relatively new advancement in the area of non-antibody binding proteins and so their documented uses are limited but promising in areas such as label free biosensing, cellular imaging techniques and detection of small organic compounds (Raina *et al*., 2015; Bedford *et al*., 2017; Arrata *et al*., 2017; Wang *et al*., 2017; Koutsoumpeli *et al*., 2017). They are extremely small in comparison to their antibody counterparts, approximately 12 kDa versus 150 kDa, and have so far been adopted in a number of wide ranging studies including, additive reagents for nanomaterial fabrication and inhibition of protein-protein interactions (Rawlings *et al*., 2015; Kyle *et al*., 2015). Work is also ongoing to investigate the use of these reagents for the detection of pathogens directly, as well as the detection of a number of medically important proteins, a number of these are discussed in a recent paper published in eLife as well as the use of Affimers to investigate intracellular signalling, inhibition of extracellular receptor function, modulation of ion channels and *in vivo* and fixed cell imaging, including super resolution imaging (Tiede *et al*., 2017).

The requirement for non-antibody binding proteins is centred on the improvement upon the currently available antibody alternatives, the main requirement being the limitation of the use of animals in the production of these antibody reagents. Non-antibody binding proteins can be produced at similar concentrations seen for conventional *in vitro* antibody production, 100 mg/L antibody can be achieved using cell culture technology (Kunert and Reinhart, 2016), using recombinant protein expression systems, Affimers can be expressed and purified to greater than 95% purity with a yield of 83.3 mg/L on average (Tiede *et al*., 2017). The production of any protein in a bacterial expression system is more economical than mammalian expression systems based on comparable reagent and consumable costs (Verma *et al*., 1998). The removal of the use of animals in the process of

antibody production through the use of recombinant expression systems is also a more ethical approach to reagent manufacture.

The primary method for producing Affimers is the use of phage display techniques before cloning the relevant protein sequences into bacterial protein expression vectors enabling expression of the reagents as required. This reduces manufacturing costs and times relative to antibody production (Skerra, 2007). The main functional improvements made when considering the design of non-antibody binding proteins is to reduce or eliminate the number of cysteine residues, this simplifies the basic structure of the Affimer and ensures there are no homodimer formations. Furthermore, it also increases the binding affinity to the target molecule as well as decreasing the size of the binding protein, reducing the redundancy seen in many antibodies. This is because only a small region is involved in the binding with the target protein relative to the size of the antibody (Justino *et al*., 2015; Löfblom *et al*., 2010). The reduction in size of the binding protein also lends the reagents to be used in different molecular biology applications where conventional antibody size poses a direct challenge, for example as detection reagents in super resolution microscopy. This has been explored with the use of nanobodies labelled with organic dyes targeting GFP tagged proteins (Ries *et al*., 2012). The production of a non-antibody reagent for the use in LFDs should result in an improvement in time-to-result as well as sensitivity of the test, as a direct result of the reagent being able to move through the device components at a faster flow rate.

This chapter discusses the production of target PRRSV N proteins and subsequently Affimer reagents raised against them to be used in the development of a LFD capable of detecting the viral N protein in clinical samples. First, recombinant PRRSV N proteins were produced using bacterial expression vectors and purified using chromatography techniques. Second, Affimers specific for the PRRSV target protein were identified using phage display techniques. This approach was used for two distinct N proteins, from a highly pathogenic and a low pathogenic strain of PRRSV, with a view to producing a LFD which could distinguish between the two viral strains.

3.2. Expression of his_8-tagged recombinant low pathogenic PRRSV N protein

Initially, a low pathogenic strain of the PRRSV N protein (NLP) was used to perform Affimer screening. This protein was expressed from a pTriEx 1.1 vector kindly provided by Prof Julian Hiscox (University of Liverpool). The his_8-tagged recombinant N protein was expressed in BL21(DE3)pLysS cells for four hours using IPTG induction at 37 °C. Samples were taken hourly to monitor protein expression by SDS-PAGE and Coomassie blue staining (figure 3.1). The viral protein was expressed well over a four hour period and so the four hour time point was chosen for future expression experiments. The recombinant protein was purified from the bacterial cell lysate using nickel ion affinity chromatography with fractions analysed by SDS-PAGE and Coomassie blue staining (figure 3.2). Analysis of each elution showed that the protein from the 240 mM imidazole elution contained the fewest bacterial contaminants and was therefore taken forward for the Affimer screening without further purification steps.

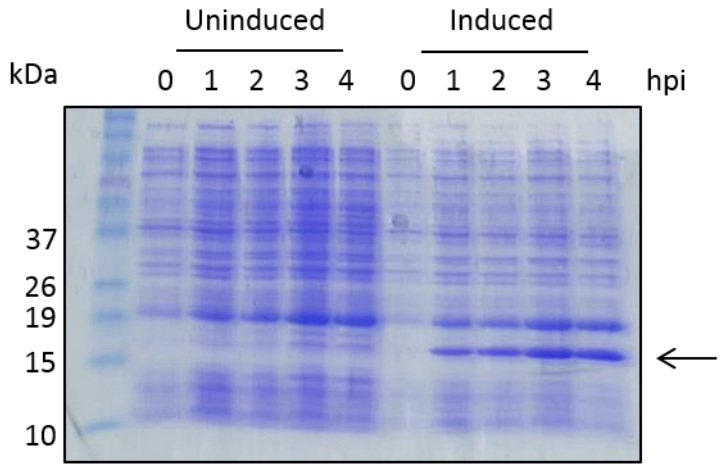

Figure 3.1 Analysis of bacterially expressed NLP-his_8. A four hour time course of induction was performed to determine the optimum time of expression of the target protein in BL21(DE3)pLysS cells. Bacteria were induced with IPTG after reaching OD 0.4 (as well as an uninduced control) and samples taken hourly for four hours (hpi: hours post induction). Samples were analysed by SDS-PAGE and Coomassie blue staining. NLP-his_8 is expressed well over four hours as indicated by the arrow at 15 kDa. The protein was not expressed in the uninduced sample.

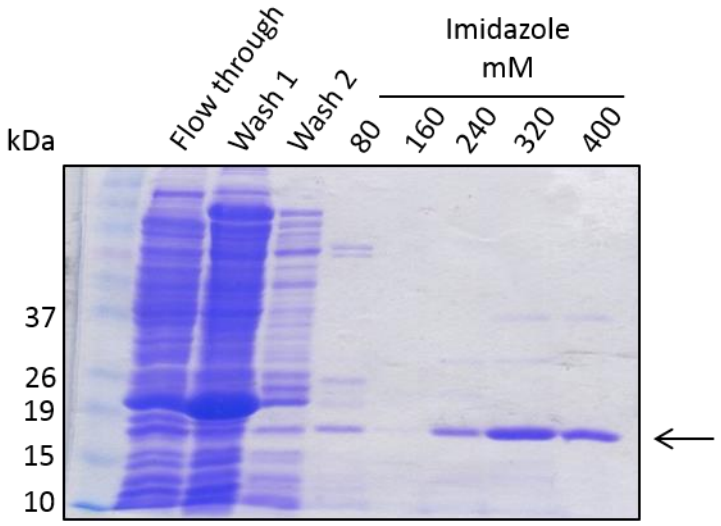

Figure 3.2 Purification of NLP-his$_8$ from bacterial lysate. The PRRSV N protein was solubilised and purified from bacterial cell lysate using nickel ion affinity chromatography. The N protein was eluted using an increasing concentration of imidazole, 80-400 mM. The N protein was eluted in the 240, 320 and 400 mM elution fractions as indicated by the arrow with the 240 mM elution fraction being taken forward for use in further experiments.

3.3. Affimer screening against his$_8$-tagged recombinant low pathogenic PRRSV N protein

Affimer screening was performed using biotinylated NLP-his$_8$ protein to identify specific binding Affimers to be taken forward as reagents for the LFD. Following three rounds of phage display panning using the phage library (data not shown), 24 potential binders were further characterised to investigate their binding to the target protein. Firstly, they were tested for their ability to bind to the target protein immobilised onto a streptavidin coated plate in a phage ELISA. Each target Affimer was expressed on the pIII minor coat protein of bacteriophage M13, as in the screening rounds and incubated with the target protein or an empty well of the plate in order to identify any non-specific binders. Detection of bound phage was performed using an HRP conjugated anti-fd bacteriophage antibody and TMB visualisation, resulting in a characteristic blue colour change when phage is present (figure 3.3a). The visualisation of the ELISA plate (figure 3.3a) shows that the 24 binders identified in this screen bind to NLP-his$_8$ and not to the streptavidin plate. This was confirmed when the A600 absorbance readings for the plate were also measured (figure 3.3b).

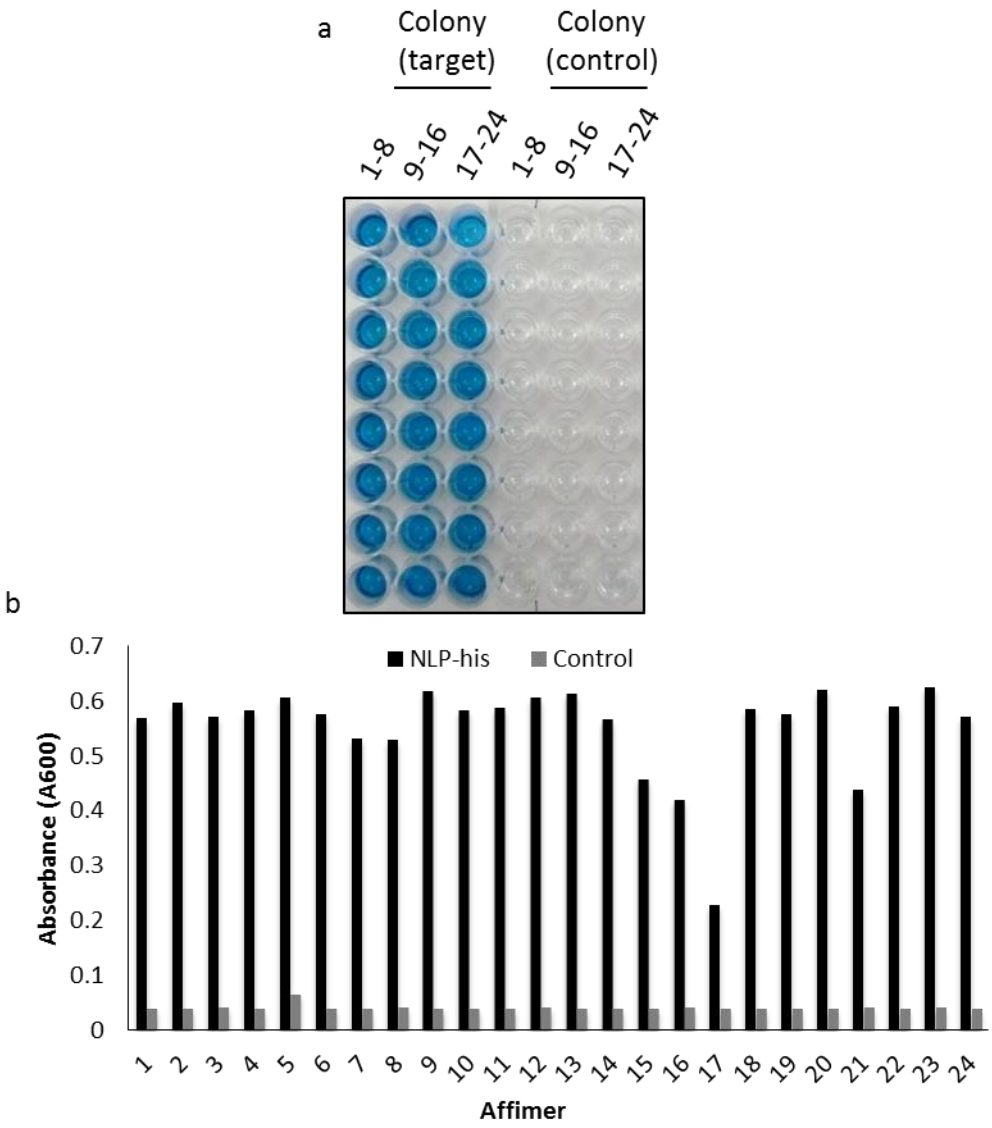

Figure 3.3 Affimer Screen against NLP-his$_8$ using phage display. (a) Following three phage display panning rounds, 24 colonies were picked and a phage ELISA performed. Each colony represented one Affimer and these were screened against the target or against an empty control well. Phage binding was probed using anti-Fd bacteriophage-HRP antibody and visualisation with TMB. All colonies picked for phage ELISA showed binding to the target protein in preference to the control wells. **(b)** Absorbance measurements were taken of the wells and show the phage binding to the target protein in preference to the blank control wells.

Upon sequencing of these 24 binders, five unique binders were identified, where the two variable loop regions contained the unique sequences for each Affimer (table 3.1).

Table 3.1 Loop sequences of unique binders to NLP-his$_8$

Affimer	Loop 1	Loop 2	Number of appearances
1	V Q L V D L T W L	N H L L E N P F D	19
15	W E P L E Q Q H R	L T V I N Y N I L	1
16	W I A E E P G V V	R Y L M G H W M W	2
17	H Y Y G Q F L Y H	R K N L L Q E F K	1
23	H D P F E M P V Q	L F I Y G R H M L	1

The Affimers that were found to contain unique loop sequences were 1, 15, 16, 17 and 23 and the number of times they were identified are shown in table 3.1. Affimer 1 was identified a total of 19 times within the pool of 24 Affimers sequenced in this case, suggesting that this was a highly specific binder with a strong binding capability. The three remaining Affimers appear in the sequencing data once and Affimer 16 appears twice which may suggest lower binding capability for each of these Affimers, although this is not investigated in this study.

3.4. Cloning of N protein from a high pathogenic strain of the virus into bacterial expression vectors

A TArget Clone vector encoding the gene for the N protein from a high pathogenic strain (NHP) of PRRSV was obtained from Dr Cheng-bao Wang (Northwest A&F University, China). Cloning into a variety of bacterial expression vectors was performed in order to improve upon the protein expression levels seen with the expression of NLP from the pTriEx 1.1 vector, used in the previously discussed experiments (section 3.2). PCR primers designed to incorporate *Bam*HI and *Not*I restriction sites were used in the amplification of the NHP gene from the TArget Clone vector. The PCR product is shown in figure 3.4, with a product of 372 bp, as expected.

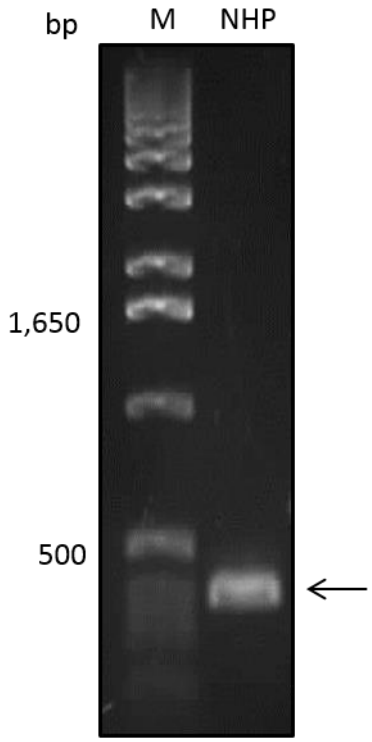

Figure 3.4 PCR amplification of NHP gene. The gene encoding the N protein from a highly pathogenic strain of PRRSV was PCR amplified from a TArget Clone vector kindly provided by Dr Cheng-bao Wang. The PCR product was analysed by agarose gel electrophoresis a product of approximately 400 bp produced as indicated by the arrow (gene size: 372 bp).

The vectors chosen for these expression trials were pTriEx 1.1 (initially used for expression of NLP), pGEX6p1, pET28a and pET28a-SUMO in order to utilise a number of different epitope tagging methods and promoters. The successful cloning of this gene into these expression vectors is shown in figure 3.5 by diagnostic digests. Successful clones were confirmed by sequencing analysis (GATC Biotech AG, data not shown).

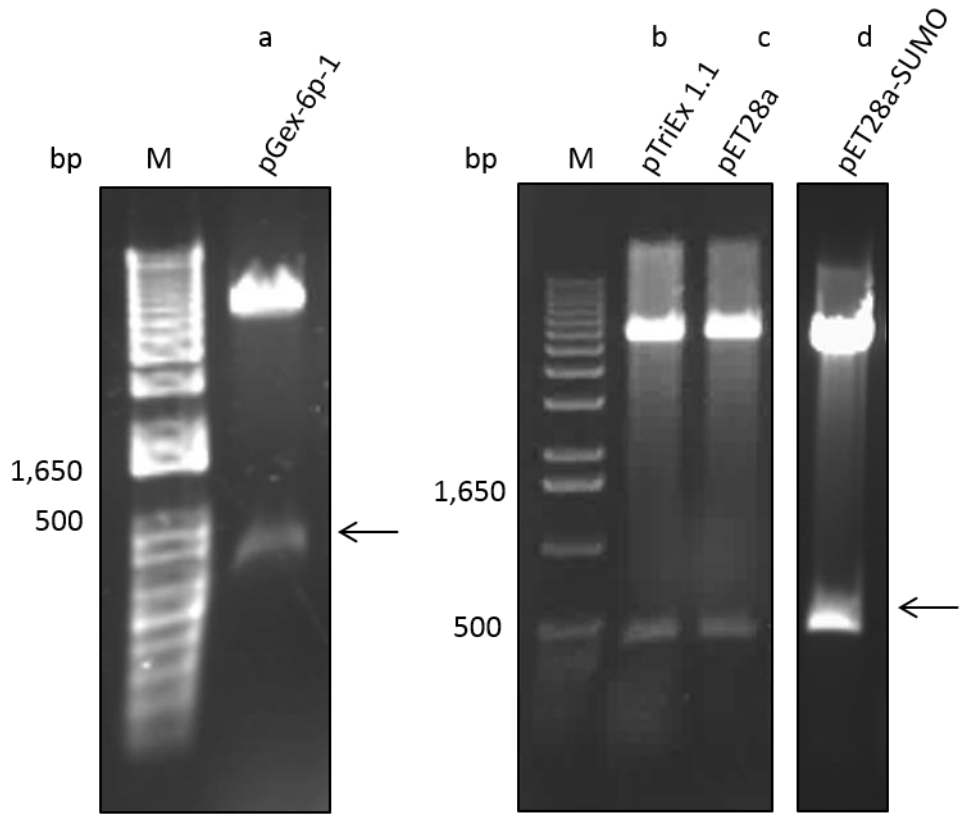

Figure 3.5 Cloning NHP gene into bacterial expression vectors. The gene encoding NHP was cloned into **(a)** pGEX-6p-1 **(b)** pTriEx 1.1, **(c)** pET28a and **(d)** pET28a-SUMO bacterial expression vectors using restriction enzymes *Bam*HI and *Not*I. Digests were performed using these enzymes to confirm the presence of the DNA insert of the correct size as indicated by the arrows (372 bp) before sequencing was performed to confirm the correct sequence.

3.5. Expression of NHP-his from bacterial expression vectors

Expression trials using the different expression vectors for this protein were undertaken in parallel. The pTriEx 1.1 vector was chosen as it had previously resulted in the successful expression of NLP. However, when expression was carried out using the same conditions, four hour induction and expression with IPTG, there was no detectable expression of NHP-his_8 as shown in figure 3.6.

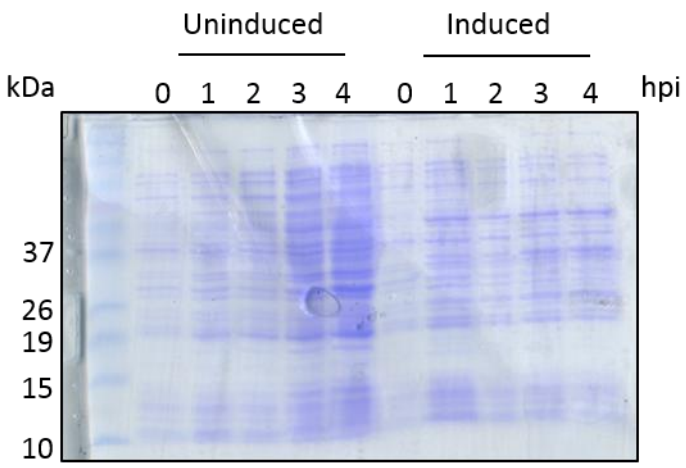

Figure 3.6 Expression of NHP-his$_8$ from pTriEx 1.1 vector. A four hour time course of induction was performed to determine the optimum time of expression of the NHP in BL21(DE3)pLysS cells. Bacteria was induced with IPTG after reaching OD 0.4 (as well as an uninduced control) and samples taken hourly for four hours. Samples were analysed by SDS-PAGE and Coomassie blue staining. The protein was not expressed in the induced time course with the bacterial lysate showing comparable banding patterns to the uninduced control. There is no increase in protein expression of a protein at the expected molecular weight, 15 kDa. (hpi: hours post induction).

pGEX-6p-1 was chosen in an attempt to provide an epitope tag that would aid solubility of the expressed protein. It was hypothesised that expressing the viral protein as a fusion with a highly soluble protein would result in a higher level of expression as a result of the increased transcription and translation of the N terminal GST-tag. The expression trials were carried out for four hours with IPTG induction at 37 °C and expression was analysed by SDS-PAGE and Coomassie blue staining (figure 3.7). With the use of this vector, GST-NHP was seen to express well over the four hour time course, with four hours providing sufficient protein expression for Affimer screening.

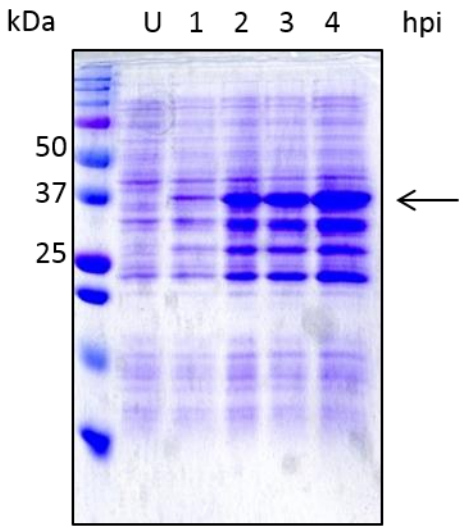

Figure 3.7 Expression of GST-NHP from pGEX-6p-1 vector. A four hour time course of induction was performed to determine the optimum time of expression of GST-NHP in BL21(DE3)pLysS cells. Bacteria were induced with IPTG after reaching OD 0.4 and samples taken hourly over four hours. Samples were analysed by SDS-PAGE and Coomassie blue staining. The GST-NHP protein was expressed in the induced time course, as indicated by the arrow, at the expected molecular weight, 39 kDa, well over the four hours (hpi: hours post induction).

Following the four hour time course, the protein was purified from the bacterial cell lysate using glutathione-based affinity purification shown in figure 3.8. The samples taken over the purification steps include the soluble and insoluble fractions, as well as 5 elution fractions. The GST-NHP protein was found to be contained within the insoluble protein fraction and therefore upon purification, there was no soluble protein eluted (figure 3.8a). This was compared to the purification of GST alone, which although was expressed at a low level in this experiment, was seen to be expressed in the soluble fraction of the bacteria and subsequently eluted across the 5 elution fractions (figure 3.8a). Additional optimisation of this protein expression was carried out with expression at 30^{o}C overnight followed by purification (figure 3.8b), however, although more protein appeared to be expressed, this remained insoluble and therefore was not purified in the glutathione elutions.

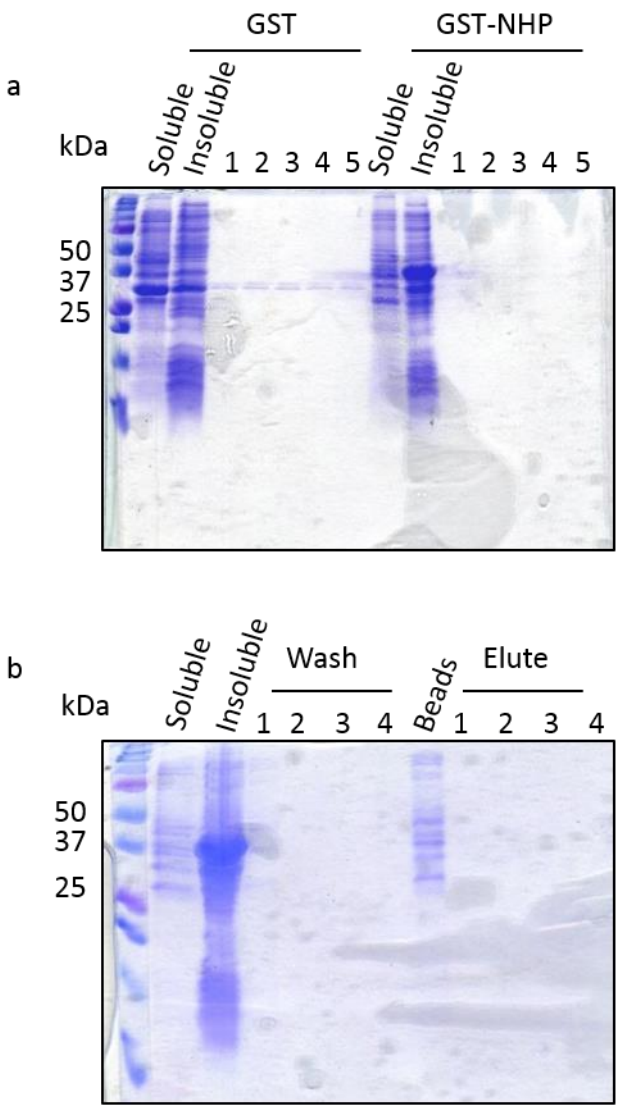

Figure 3.8 Expression trials of GST and GST labelled NHP and analysis by SDS-PAGE and Coomassie blue staining. (a) Recombinant GST and GST-NHP were expressed for 4 hours at 37^{o}C in BL21(DE3)pLysS cells and purified using Glutathione Sepharose™ beads. GST was expressed and eluted at 26 kDa. Recombinant GST-NHP was expressed at 39 kDa, however, it appears that the protein is insoluble and was therefore not purified. **(b)** Recombinant GST-NHP was then expressed overnight at 30^{o}C in BL21(DE3)pLysS cells and again purified using Glutathione Sepharose™ beads, however, again GST-NHP was expressed in the insoluble fraction.

Optimisation of protein expression was next undertaken in order to improve the solubility of GST-NHP. This was carried out using a number of different bacterial expression strains in parallel (figure 3.9). BL21-Gold(DE3), BL21-CodonPlus-RIL and BL21-CodonPlus-RP cells were chosen in the first instance. BL21-Gold(DE3) were chosen to try to increase protein expression levels to see if this would increase the amount of protein found in the soluble fraction, however, across the four hour expression time course, protein expression was seen to be lower than that of the

BL21(DE3)pLysS cells previously used. BL21-CodonPlus-RIL cells were used to increase protein expression due to the encoding of additional tRNAs and to try to increase soluble protein levels as a result of this increased protein expression. Unlike BL21-Gold(DE3) cells, BL21-CodonPlus-RIL cells showed an increase in protein expression levels across the four hour time course, however this was still at reduced levels compared with the BL21-pLysS cells. BL21-CodonPlus-RP cells showed good expression of GST-NHP with the highest expression being seen two hours post IPTG induction.

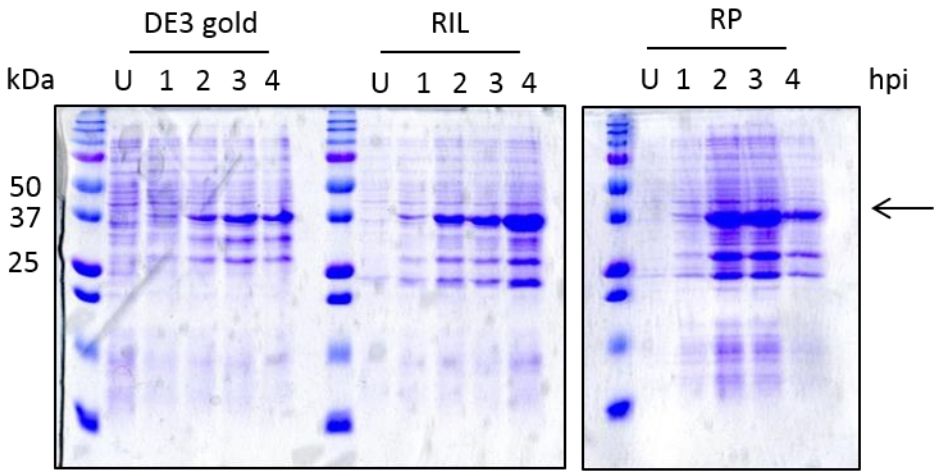

Figure 3.9 Optimising protein solubility using different E.coli strains. GST-NHP was expressed in different strains of *E.coli* in order to determine the ideal strain for the expression of soluble protein (as indicated by the arrows). BL21-Gold(DE3) cells showed poor expression of the recombinant GST-NHP protein across the four hour time course. BL21-CodonPlus-RIL cells showed an improved expression of the recombinant protein over the four hour time course compared to the BL21-Gold(DE3) cells. BL21-CodonPlus-RP cells showed the best expression two hours post induction of the recombinant protein. (hpi: hours post induction).

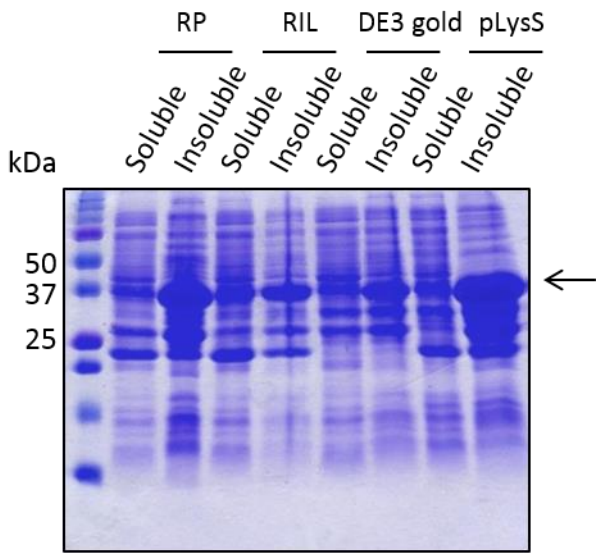

Figure 3.10 Analysis of soluble and insoluble fractions of bacterial lysate expressing GST-NHP in various cell types. Following lysis and sonication of the *E.coli* expressing GST-NHP, the soluble and insoluble fractions were taken and analysed for protein content using SDS-PAGE and Coomassie blue staining. For all of the cell types the majority of the recombinant protein is present in the insoluble fractions as indicated by the arrow.

Following the four hour expression time courses, the bacteria were harvested and lysed before the insoluble and soluble fractions were sampled and analysed by SDS-PAGE and Coomassie blue staining as shown in figure 3.10.

GST-NHP was present predominantly in the insoluble fraction of all of the cell lines used in this experiment and could therefore not be purified directly at sufficient concentrations. BL21(DE3)pLysS cells contained the most insoluble protein, with BL21-CodonPlus-RIL cells contained soluble and insoluble GST-NHP. The subsequent purification of GST-NHP from this expression system resulted in negligible protein concentration (data not shown) and this was not considered a viable expression system for this protein.

To further investigate the solubility problems with this protein, pET28a was chosen to provide expression under the control of a T7 promoter with a his_6-epitope tag. A three hour time course was taken at 37 °C to determine the optimal time for maximum protein expression within this system. As shown in figure 3.11, samples were taken hourly before and after induction and analysed by SDS-PAGE and Coomassie blue staining. An increase in expression of NHP-his_6 over the three hour time course was observed although not to the same extent as seen with a GST-tag.

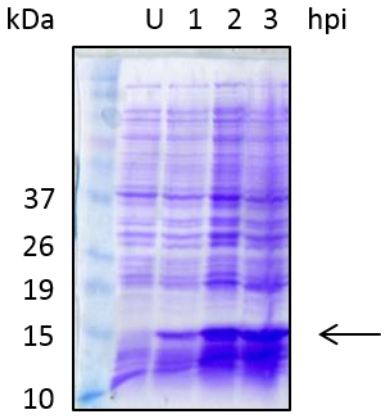

Figure 3.11 Expression of NHP-his$_6$ from pET28a. A three hour time course of induction was performed to determine the optimum time of expression of NHP-his$_6$ in BL21(DE3)pLysS cells. Bacteria was induced with IPTG after reaching OD 0.4 and samples taken hourly for three hours. Samples were analysed by SDS-PAGE and Coomassie blue staining. The NHP-his$_6$ protein was expressed in the induced time course at the expected molecular weight, 15 kDa, over the three hours as indicated by the arrow. (hpi: hours post induction).

The three hour time point was chosen for maximum expression for this protein and the bacteria were lysed and the his$_6$-tagged NHP protein purified using nickel ion affinity chromatography. Samples were taken at a number of purification stages to determine the location of the recombinant protein. Upon analysis with SDS-PAGE and Coomassie blue staining (figure 3.12), similar to GST-NHP, it was found primarily in the insoluble protein fraction. It was therefore not possible to purify sufficient protein, although protein was shown to elute in the 240-400 mM imidazole elution fractions.

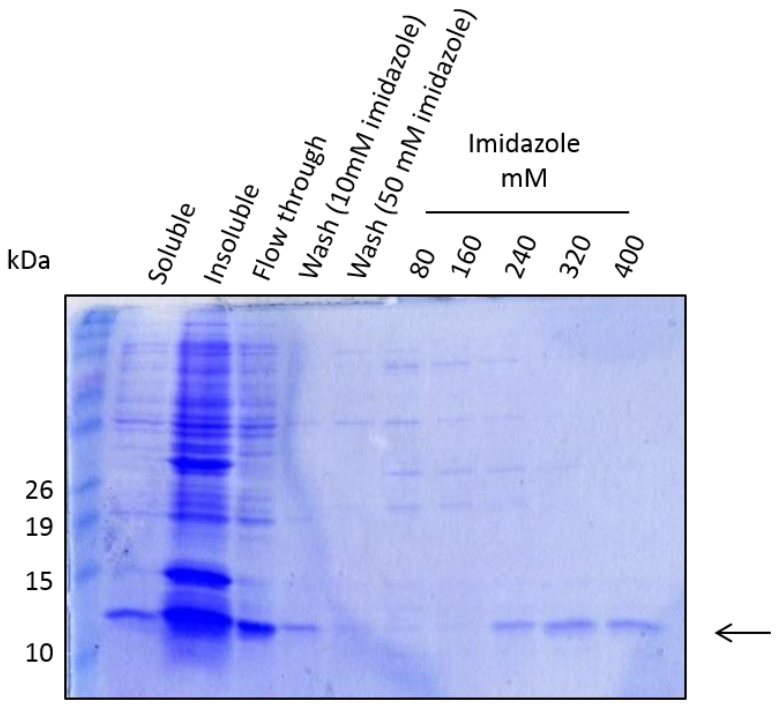

Figure 3.12 Purification of NHP-his$_6$ from pET28a vector. NHP-his$_6$ was solubilised and purified from bacterial cell lysate using nickel ion affinity chromatography. NHP-his$_6$ was eluted using an increasing concentration of imidazole, 80-400 mM. The protein was eluted in the 240, 320 and 400 mM elution fractions as indicated by the arrow.

The final vector investigated in the optimisation of NHP expression was pET28a-SUMO. Like pGEX-6p-1, pET28a-SUMO was chosen to provide an N terminal his-SUMO-tag which should improve protein solubility, a consistant challenge with the expression of this protein. The same time course of four hours was undertaken to express the protein from pET28a-SUMO in BL21(DE3)pLysS cells at 37 °C. The recombinant fusion protein was shown to be expressed over the time course at around 25 kDa, as expected, when compared to the uninduced control expression (figure 3.13).

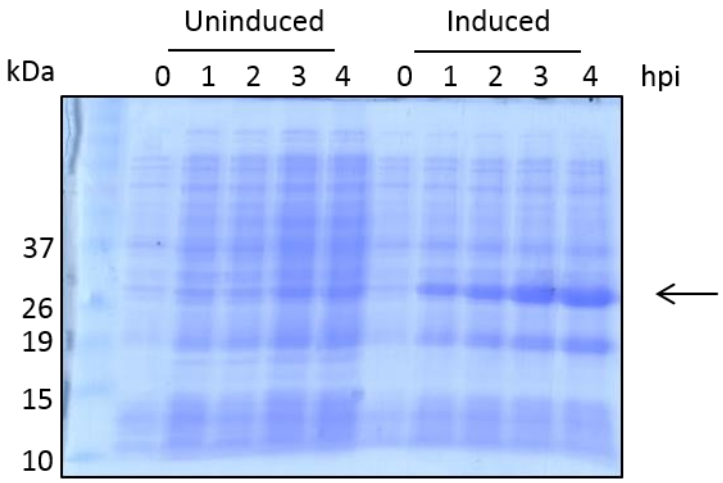

Figure 3.13 Expression of SUMO-NHP from pET28a-SUMO. A four hour time course of induction was performed to determine the optimum time of expression of SUMO-NHP in BL21(DE3)pLysS cells. Bacteria was induced with IPTG after reaching OD 0.4 and samples taken hourly for four hours (as well as an uninduced control). Samples were analysed by SDS-PAGE and Coomassie blue staining. The protein was expressed in the induced time course at the expected molecular weight, 25 kDa, over the four hours as indicated by the arrow. (hpi: hours post induction).

Expression levels were lower than those seen during the expression of GST-NHP, however, the SUMO-tagged protein was expressed in the soluble fraction of the bacteria and therefore allowed SUMO-NHP to be easily purified using nickel affinity chromatography using the C terminal his_6-tag (figure 3.14). The eluted protein was found in the 240, 320 and 400 mM imidazole elutions, with the 320 and 400 mM elutions providing the purest and highest concentration elutions. Further expression trials were carried out (data not shown) resulting in a higher level of protein expression if SUMO-NHP was expressed at 30 °C overnight and so this condition was used for future expression and purification experiments.

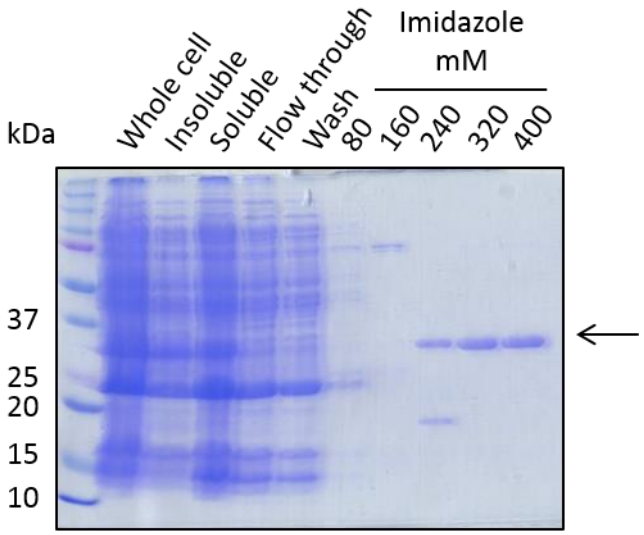

Figure 3.14 Purification of SUMO-NHP from pET28a-SUMO vector. The protein was purified from bacterial cell lysate using nickel ion affinity chromatography and analysed by SDS-PAGE and Coomassie blue staining. The protein was eluted using increasing concentrations of imidazole, 80-400 mM and was eluted in the 240, 320 and 400 mM elution fractions as indicated by the arrow. The 300 and 400 mM fractions were taken forward for further experiments.

3.6. Cloning of N protein from the PRRSV low pathogenic strain into pET28a-SUMO expression vector

Following the successful expression and purification of SUMO-NHP, it was decided to enter a similarly tagged NLP protein into expression trials in order to increase the number of Affimer reagents raised against this target protein. Following subsequent sequence analysis, a large translated amino acid excess (approximately 87 bp) from the pTriEx 1.1 plasmid was shown to be present in the NLP-his_8 protein. This originated from the use of an upstream start codon resulting in the addition of the 29 amino acids at the N terminus of the PRRSV N protein. As such, it was not known if the Affimers already raised (section 3.3) were binding to the target protein or the excess amino acids. The use of a SUMO-tagged protein allowed for the identification of those Affimers which only bound to the target protein with the use of a negative SUMO screen to eliminate any SUMO binders. Therefore, NLP was PCR amplified, using primers designed to contain *Bam*HI and *Not*I restriction sites, producing a product of approximately 370 bp, from the pTriEx 1.1 vector (figure 3.15a), and cloned into pET28a-SUMO. Insertion of the gene was confirmed using restriction enzyme digestion with *Bam*HI and *Not*I (figure 3.15b)

and by sequencing to confirm the correct gene sequence (GATC Biotech AG, data not shown).

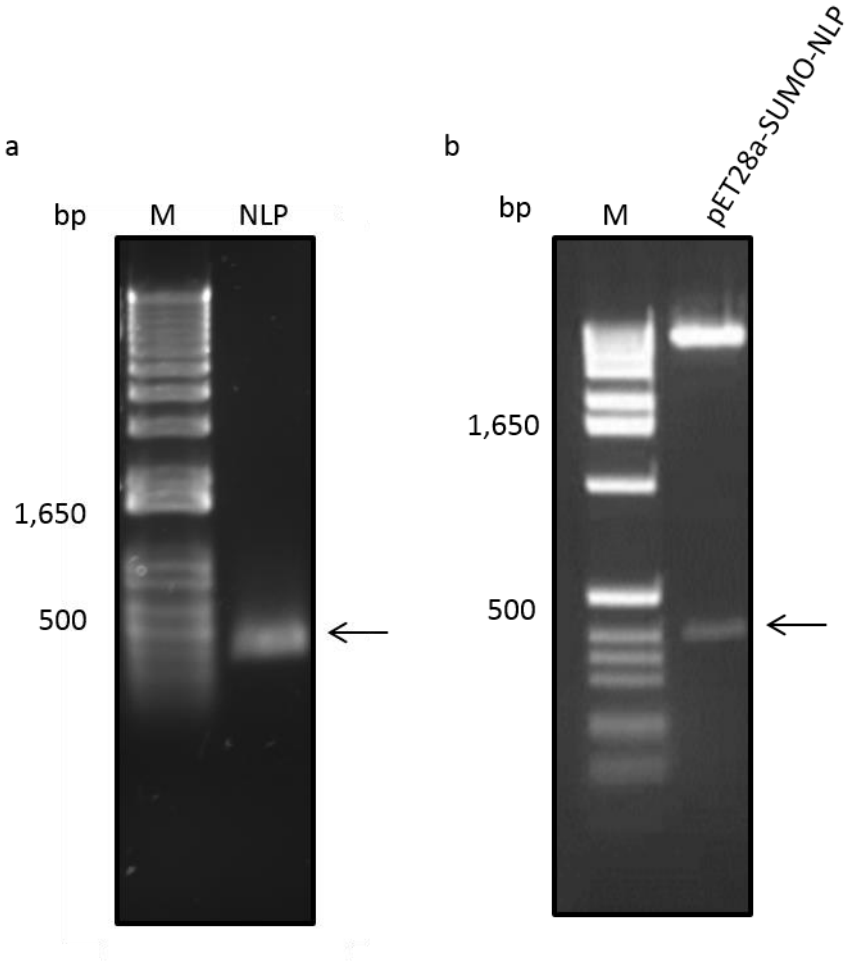

Figure 3.15 PCR amplification of NLP from pTriEx 1.1 vector and diagnostic digest confirming presence of target gene in expression plasmid. (a) The gene encoding the N protein from the low pathogenic strain of PRRSV was PCR amplified from the pTriEx 1.1 plasmid previously used in this study (kindly provided by Prof Hiscox). The PCR product was analysed by agarose gel electrophoresis resulting in an approximately 400 bp product as indicated by the arrow. **(b)** Following ligation into pET28a-SUMO, successful gene insertion was confirmed by restriction digest using *Bam*HI and *Not*I, an insert of the correct size was observed as indicated by the arrow. Sequencing was performed to ensure there were no mutations in the viral gene DNA using a T7 promoter primer.

The pET28a-SUMO-NLP vector was transformed into *E.coli* strain BL21(DE3)pLysS. Protein expression was induced overnight with IPTG at 30 °C to maximise expressed protein levels, as shown with SUMO-NHP. During the subsequent purification process, samples were taken at all points and analysed by SDS-PAGE and Coomassie blue staining (figure 3.16). SUMO-NLP was shown to express well overnight and the nickel ion affinity purification protocol allowed elution in

increasing concentrations of imidazole. SUMO-NLP was shown to elute in imidazole concentrations of 240 and 320 mM, similar conditions to the SUMO-NHP fusion protein. The 240 mM fraction was used for further experiments as this produced the cleanest fraction with the absence of breakdown products and contaminants which were present in a number of the other elution fractions. No further purification steps were undertaken.

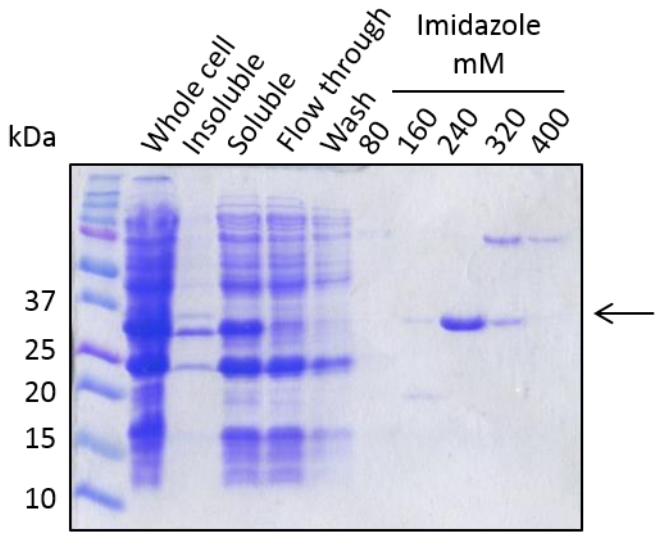

Figure 3.16 Purification of SUMO-NLP. SUMO-NLP was expressed overnight at 30 ^{o}C in BL21(DE3)pLysS cells using IPTG induction. The protein was solubilised and purified using nickel ion affinity chromatography and fractions were analysed using SDS-PAGE and Coomassie blue staining. Elutions were performed with increasing concentrations of imidazole, 80-400 mM as indicated by the arrow. SUMO-NLP was eluted in elutions 3 and 4 with elution 3 used for further experiments.

3.7. Affimer screening against recombinant PRRSV N proteins

Both purified recombinant fusion proteins, SUMO-NHP and SUMO-NLP, were then entered into Affimer screening to identify Affimers that were able to recognise the viral proteins. In order for the screening to eliminate the possibility of the Affimers binding to the SUMO-tag, the screens were performed in the presence of recombinantly expressed SUMO, known as a negative screen.

Screening of target proteins with the Affimer library was carried out in collaboration with the Bioscreening Technology Group at the University of Leeds using phage display techniques.

Biotinylation of the target recombinant proteins was required for the immobilisation of these proteins throughout the screening process. Biotinylation was carried out using EZ-Link-NHS-SS-Biotin to biotinylate amines within the target protein. Successful biotinylation of target proteins was investigated by both SDS-PAGE followed by western blotting and by ELISA. Both of these assays showed biotinylation was successful for SUMO-NHP, SUMO-NLP and SUMO (figure 3.17).

The screening of both target recombinant fusion PRRSV N proteins was carried out in the presence of excess SUMO protein which acted as a negative screen and removed the Affimers which were specific to the SUMO-tag and not for the target protein. This negative screen was carried out at all stages and all subsequent experiments were performed with a SUMO control to further confirm that the Affimers were specific for the target PRRSV proteins and not the SUMO-tag.

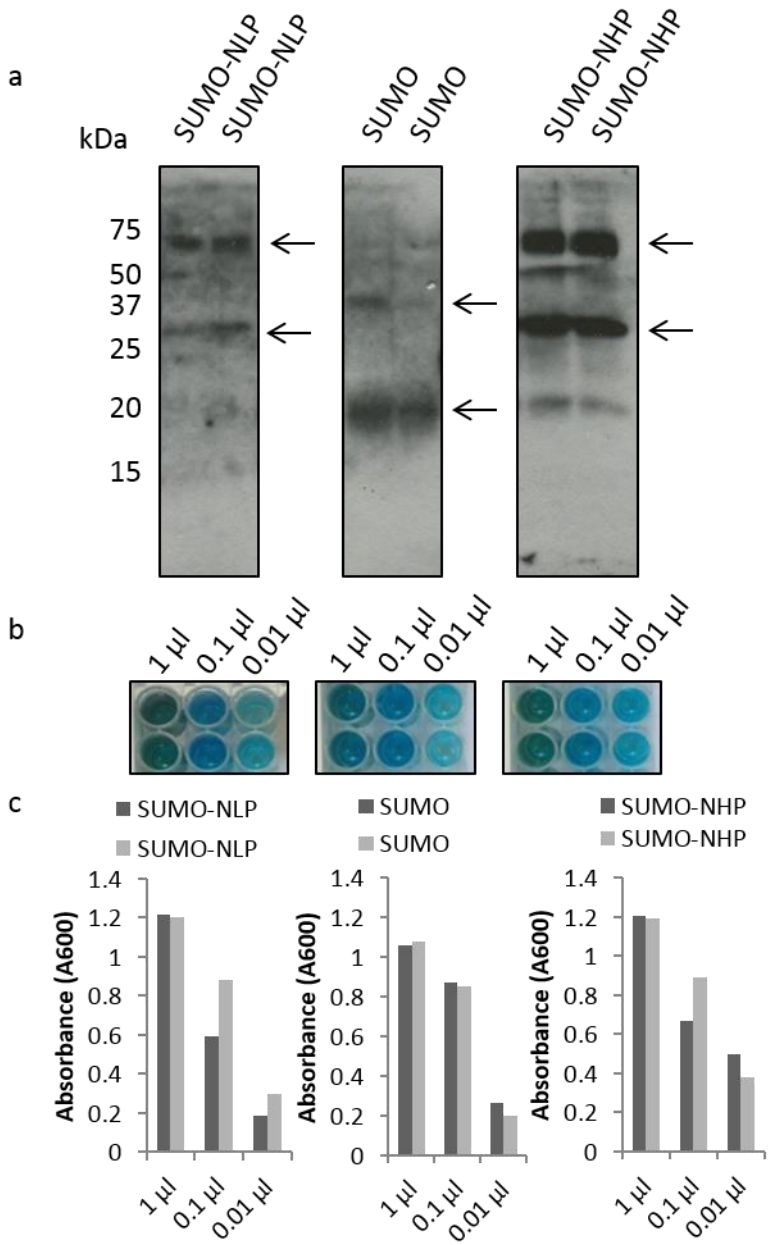

Figure 3.17 Biotinylation of target proteins for Affimer screening. Target proteins were biotinylated using EZ-Link-NHS-SS-Biotin and successful labelling was determined using western blotting **(a)** Biotinylated protein can be seen for SUMO-NLP, SUMO and SUMO-NHP as indicated by the arrows (the higher molecular weight bands indicated are protein dimers). This was further confirmed using ELISA **(b-c)** where a dilution series was performed and the biotinylated proteins detected using streptavidin-HRP. The absorbance readings show a suitable level of biotinylation of all target proteins.

3.8. Affimer screening against SUMO-NHP

Following three screening rounds against SUMO-NHP, a selection of binders were taken forward for further analysis to confirm specificity and binding to the target protein. In this case 48 binders, and sequence identification was performed as previously described (section 3.3 NLP-his_8 screen). The phage ELISA (figure 3.18a) was performed in either the presence of target protein or SUMO immobilised to the plate and any Affimers which reacted in both plates could be discounted from further investigation due to binding to the SUMO-tag. Of the 48 binders chosen from this screen, four Affimers were shown to bind to the SUMO-tag and a number of Affimers were unable to bind to the target. This was confirmed by analysing A600 measurements of the wells (figure 3.18b).

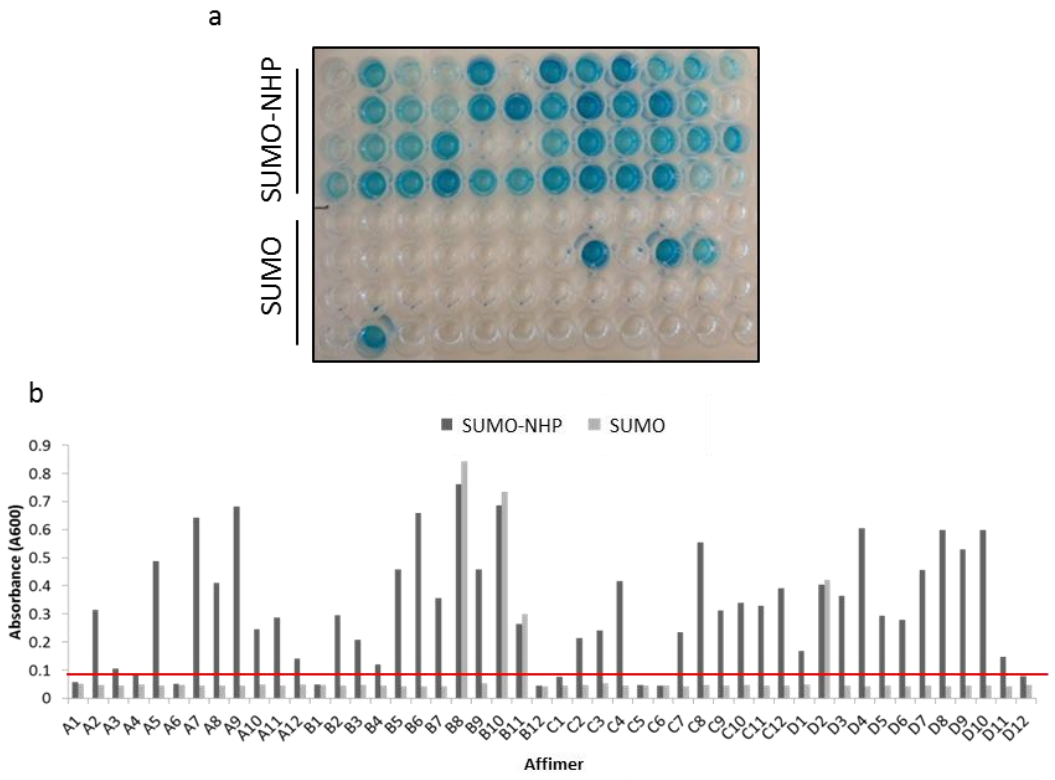

Figure 3.18 Affimer screen against SUMO-NHP. (a) Following three phage display panning rounds, 48 colonies were picked and a phage ELISA performed. Each colony represented one Affimer and these were screened against the target or against an empty control well. Phage binding was probed using anti-Fd bacteriophage-HRP antibody and visualisation with TMB. Four colonies picked for phage ELISA showed binding to the control SUMO wells and were discounted from further investigation. **(b)** Absorbance measurements were taken of the wells and show the phage binding to the target protein in preference to the blank control wells. An arbitrary cut off was used to determine which Affimers would undergo sequence analysis.

The ELISA assay identified a number of Affimers which could be eliminated from the study as well as the Affimers which required further investigation (31 were successfully sequenced). Affimers B8, B10, B11 and D2 were discounted as they appeared to bind to the SUMO-tag, Affimers A1, A3, A4, A6, B1, B4, B12, C1, C5, C6, D11 and D12 were also eliminated as they did not appear to bind to the target well in the phage ELISA. The remaining Affimers were analysed for loop sequence identity and to determine the number of unique binders which were identified as shown in table 2 (GATC Biotech AG).

Table 3.2 Loop sequences of unique binders to SUMO-NHP.

Affimer	Loop 1	Loop 2	Number of appearances
A2	L E V N M M W V D	P G P Y P Q E F S	1
A5	V E I E H M W E D	F A E N H S W P I	7
A7	I E E W D M W M D	D N R P F S R V E	8
A10	L E V N M M W D D	Q P D V E T L M Y	1
A11	I E I N E M W D D	H R S P T H A V K	2
B6	W E E Y Y M W F D	N D W F N N Q W Y	6
B7	F E M I Y M W N D	P E R D Y R S T W	2
C4	F E E T F M W F D	N G D S S Y E T F	1
C12	V E L D G M W D D	G T E T L T D K R	1
D7	V Q L V D L T W L	N H L L E N P F D	1
D9	I E L T N M W D D	R V W N S E N A N	1

Like the Affimers which were identified against the his_6-tagged NLP protein, there appears to be sequence similarity between the eight unique SUMO-NHP Affimers. This is especially evident in the first variable loop region where there is a conserved MWXD, where X is either a hydrophobic (valine, methionine) or negatively charged amino acid (glutamic acid, aspartic acid).

3.9. Affimer screening against SUMO-NLP

In order to increase the number of Affimers available for NLP, the SUMO fusion protein was screened using the second pan phage from the screen which was

carried out against the his_6-tagged NLP protein. This allowed for an already enriched library to be screened with the intention of eliminating any Affimers which bound to the SUMO-tag. One panning round was performed and 48 binders were chosen for further investigation. These were entered into a phage ELISA and presented to either SUMO-NLP or SUMO immobilised onto a plate. The phage ELISA identified 47 binders which appeared to bind to the target and not the SUMO-tag (figure 3.19). The ELISA allowed binder B8 to be discounted as a non-binder to either the target protein or the SUMO-tag. The high number of binders identified as positive hits was expected due to the enriched nature of the initial library used in this screen.

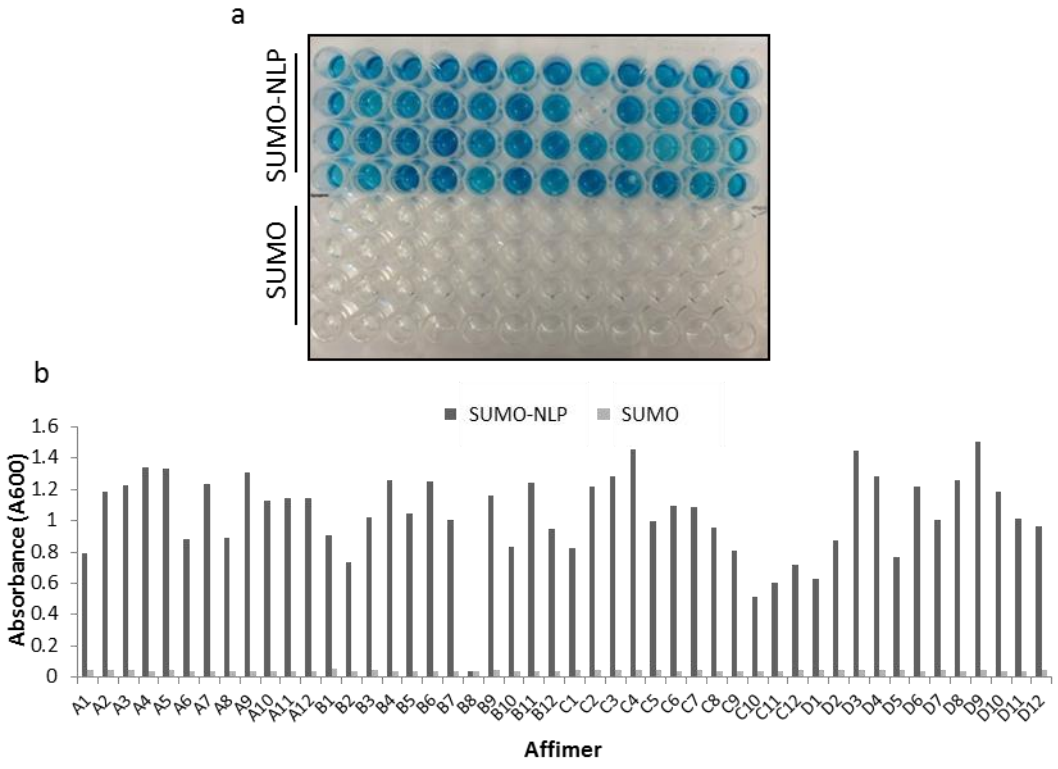

Figure 3.19 Affimer screen against SUMO-NLP. (a) Following three phage display panning rounds, 48 colonies were picked and a phage ELISA performed. Each colony represented one Affimer and these were screened against the target or against an empty control well. Phage binding was probed using anti-Fd bacteriophage-HRP antibody and visualisation with TMB. **(b)** Absorbance measurements showed the phage binding to the target protein in preference to the blank control wells.

As the phage ELISA suggested that the Affimers bound well to the target protein, due to the high absorbance readings it was not possible to determine the Affimers with increased specificity. Therefore, all 47 Affimers underwent sequence analysis

to identify any unique binders with five Affimers identified as unique, the remaining 36 Affimers sequenced had the same unique sequences as those identified in the original screen. The loop regions of these additional five binders are shown in table 3.3.

Table 3.3 Loop sequences of unique binders to SUMO-NLP

Affimer	Loop 1	Loop 2	Number of appearances
SUMO-NLP A8	P Y S Y L W H F D	G D L Y I L P L I	1
SUMO-NLP B3	A E W L P I Y E Q	D Y S K K P W M P	1
SUMO-NLP B7	H Y Y G Q F L Y H	R K N L L Q E F K	4
SUMO-NLP D9	V Q L V D L T W L	N H L L E N P F D	4
SUMO-NLP D12	F Y A D W L N H F	Q H E S G R F M N	1

3.10. Discussion

3.10.1. Protein expression and purification

In this chapter a number of expression and purification challenges were identified with both of the target N proteins used. Expression levels and solubility of the expressed proteins was investigated using recombinant tags as well as a range of expression systems and conditions.

Initially, five Affimers were identified as binding proteins against his-NLP. However, further analysis of this protein revealed that there was a 20 amino acid excess at the C terminus before the His tag, derived from the cloning method used although it was possible to determine if the Affimers were binding to this region by returning to the panning stages, it was not known if this additional sequence would cause a conformational change to the protein. If this was the case, the Affimers may have been identified due to conformational binding to a novel structure not found in the wild type protein. As a result of this, the NLP and NHP proteins were cloned using a number of epitope tags and promoter sequences.

The most successful expression system used for NHP was the Tac promoter in conjunction with a GST fusion tag from the pGEX6p1 vector. However, this resulted in a high level of insoluble protein expression using BL21(DE3)pLysS cells at 37°C for four hours. Protein production may have been too rapid and the resulting recombinant protein being incorrectly folded in the *E.coli*. Expression of this fusion protein was undertaken in different *E.coli* strains, BL21-Gold(DE3), BL21-CodonPlus-RIL and BL21-CodonPlus-RP cells, to try to improve protein solubility. The properties of these bacterial strains combined with the highly soluble GST tag was hypothesised to increase the total recombinant protein levels, increasing the percentage of the total soluble recombinant protein (Esposito and Chatterjee, 2006). GST fusion has been used in the improvement of protein solubility since its introduction as an expression system in 1988 (Smith and Johnson, 1988) and has been used to improve solubility and expression of Hantavirus N protein (Mir and Panganiban, 2004).

BL21-Gold(DE3) cells are able to express recombinant proteins at high levels, and were chosen to attempt to improve the percentage of soluble N protein. However, the protein levels were lower than that observed using BL21(DE3)pLysS cells. BL21-CodonPlus-RIL cells contain extra genes encoding for the tRNAs of *argU* (AGA, AGG), *ileY* (AUA), *leuW* (CUA) which are often poorly expressed in alternative BL21 strains where they are a limiting factor in the translation of proteins. The use of this strain of bacteria showed protein expression of a similar level to BL21(DE3)pLysS cells. The NHP protein sequence is approximately 18% arginine/isoleucine/leucine and so it was expected that this approach may increase the protein expression compared to other BL21 strains. BL21-CodonPlus-RP cells encode additional genes for *argU* (AGA, AGG), *proL* (CCC), the protein sequence for NHP is approximately 15% arginine/proline residues and the expression of the recombinant protein in these cells was comparable to BL21(DE3)pLysS and BL21-CodonPlus-RIL cells and again, higher than the BL21-Gold(DE3) cells. The presence of GST-NHP in the soluble fractions of some of these *E.coli* strains may suggest that further optimisation of the conditions may improve the ratio of soluble to insoluble protein, however, upon purification the protein could not be obtained at high enough concentrations for requirements.

The addition of a SUMO-tag has shown to increase solubility and protein expression in a number of expression systems both in prokaryotic and eukaryotic systems (Lee *et al*. 2008; Panavas *et al*. 2009; Wang *et al*. 2010). SUMO fusion have also been used in the production of virus like particles, for example FMDV (Lee *et al*., 2009), outlining the versatility of this system. However, solubility challenges continued for both NHP and NLP when using the SUMO tag.

The relative expression levels of the SUMO-tagged recombinant protein was lower compared to the GST tagged recombinant protein, however, the expression of SUMO-NLP and SUMO-NHP resulted in the expression of a highly soluble protein. Unfortunately, following cleavage of the SUMO-tag under dialysis conditions, the viral proteins were no longer soluble. Optim®1000 analysis was performed investigate the solubility of the precipitated protein (data not shown) to determine dialysis conditions for cleavage of the SUMO-tag from the protein. A selection of the most favourable dialysis conditions were performed (data not shown) however the cleaved protein remained insoluble. Future experiments were performed without cleavage of the SUMO-tag. Whilst not ideal, numerous studies have shown that a SUMO-tag does not adversely affect protein function and can be used to dramatically improve the solubility, provide protection from proteolytic degradation and improve protein expression due to enhance mRNA stability and mRNA copy number (Butt *et al*. 2005; Malakhov *et al*. 2004). A number of viral N proteins have been successfully expressed with this modification for example, Rift valley fever virus N protein (Raymond *et al*., 2010), SARS coronavirus N protein (Zuo *et al*., 2005) and Crimean-Congo haemorrhagic fever virus N protein (Carter *et al*., 2012).

3.10.2. Affimer screening and analysis

The final pool of Affimers raised against the two SUMO-tagged recombinant proteins, as well as those raised against the his_6-tagged NLP protein, were analysed for sequence similarity. Interestingly, it is possible to begin to infer properties of these Affimers from this information combined with the ELISA data before any further experimental analysis by evaluating the number of times each Affimer appeared in the sequencing data and the absorption reading from the ELISA plate.

The appearance of Affimer 1 raised against NLP-his_6 19 times out of the 24 Affimers sequenced, suggests this may be the strongest binder to the target protein and that the remaining four Affimers against this target have a lower binding capacity than Affimer 1 although this requires further biophysical analysis in order to determine the Kd values for these interactions. It is also possible that Affimer 1 was expressed more efficiently by the phage than the other Affimers meaning that there was a higher concentration of this phage within the sample which correlates with a higher number of hits to the target protein. It is not possible to determine this, however, without performing phage titring. Affimer 17 does not seem to bind as strongly to the target as the other Affimers which have much higher absorbance readings although this could be investigated in further experiments as it may also be due poor expression of Affimer 17 bateriophage in comparison to the other Affimers. The binding of the Affimers in the context of a bacteriophage may result in a skewed result for binding due to steric hindrance provided by the bulky bacteriophage. Therefore, future experiments used purified Affimers expressed recombinantly in *E.coli* in order to eliminate the presence of the large bacteriophage complex.

The Affimers raised against SUMO-NHP show a similarity in the first variable loop region where there is a conserved MWXD suggesting this is a vital interaction region with the target protein. The Affimers may bind at the same epitope, although this is not confirmed by epitope mapping. The Affimers appear to have variable binding abilities to each other in the phage ELISA despite this similarity in amino acid sequence, this may suggest that the binding may also be conformation dependent. However, the binding kinetics have not been investigated for these Affimers.

Chapter 4

Determining the specificity of the Affimer reagents to the target proteins

4. Determining the specificity of the Affimer reagents to the target proteins

4.1. Introduction

Lateral flow devices (LFDs) provide a reliable and specific test result in a short time scale and can be easily used in the field, removing the requirement for extensive laboratory testing of clinical samples. The most important feature of reagents used in a LFD is therefore their specificity to the target to be detected. High specificity is essential to prevent cross-reactivity to other proteins within a clinical sample, for example, components of blood, plasma, urine or saliva; this can be overcome with the use of filter membranes onto which the sample can be loaded within the LFD. Such filters are commercially available (GE Healthcare Life Sciences) and are designed to filter out undesirable components of the clinical sample and are specific to sample type; blood, plasma, saliva, urine. Examples of these filters include GF/DVA, used in devices to analyse saliva samples which has been applied to HIV diagnostics (Rohrman and Richards-Kortum, 2012) and LF1, MF1 and VF2 glass fibre filters used for serum and whole blood samples (Songjaroen *et al*., 2012; Biagini *et al*., 2006; Choi *et al*., 2015). Fusion 5 is new to the market and replaces the need for modular filters by combining the filter into a single layer matrix membrane (Aller Pellitero *et al*., 2016). Replacement of these different filter components allows for multiple devices to be produced which can detect the same target protein in different clinical samples. It is also important that specificity is provided against homologous proteins from other pathogens. In the case of this study, the nucleocapsid (N) proteins from other strains of PRRSV or other related arteriviruses. Moreover, it is important to be able to distinguish between viruses which can cause clinically similar diseases but are less economically relevant and have lower morbidity levels. For example a LFD capable of differentiating between the clinically indistinguishable vesicular stomatitis (VS) and swine vesicular disease (SVD) from foot and mouth disease virus (FMDV) would be of value (Yang *et al*., 2015a). FMDV is one of the most economically devastating viral infections of cloven-hoofed animals, it is highly contagious and has a high mortality rate (Salguero *et al*., 2005). In the case of PRRSV, it is essential for detection to be rapid

and reliable in order to contain any outbreaks of this highly contagious porcine virus. This is particularly useful when the test is performed before the movement or introduction of new animals into the herd to prevent the introduction of the virus to naïve animals. Other porcine diseases can be similar in clinical symptoms such as porcine parvovirus (Mengeling *et al*., 2000), leptospirosis (Ramos *et al*., 2006) and erysipelas (Hoffmann and Bilkei, 2002). However, it is possible to vaccinate naïve herds against these infections before the introduction of new animals.

For the production of a LFD which can distinguish between two strains of a virus, as proposed in this study, it is essential that the detection reagent is able to recognise multiple strains of a viral protein (serotyping). In order to perform a test to this effect, two labelled reagents are required, one which is able to detect all viral strains and a second which can recognise a specific strain. As a result, there is a requirement for the Affimers used in the LFD to function as pairs. Moreover, they must recognise different epitopes on the target proteins to prevent competing with each other for binding. LFDs have been developed for the use of serotyping, again with FMDV being used as a proof of principle, using antibodies as detection reagents (Morioka *et al*., 2015; M. Yang *et al*., 2015a). A multiplex assay using monoclonal antibodies has also been developed for the detection of the enteropathogenic bacteria *Yersinia* species *Y. enterocolitica* and *Y. pseudotuberculosis* which allows the appropriate administration of antibiotics (Laporte *et al*., 2015).

The identification of pairs of reagents which recognise the same target protein at a different epitope can be carried out in a number of ways, the simplest and quickest being the enzyme-linked immunosorbent assay (ELISA) (Avrameas and Gulibert, 1972). The sandwich ELISA technique is commonly used in molecular biology laboratories in a wide variety of applications, particularly for diagnostic purposes in both human and animal clinical samples (Ferris and Dawson, 1988; Laviada *et al*., 1992; Gonzalez *et al*., 2008; Saliki *et al*., 2006; Vashist *et al*., 2014; Shukla *et al*., 2009). ELISAs involving the detection of viral N proteins have been developed over the last decade (Singh *et al*., 2004; Jansen van Vuren and Paweska, 2009; Xu *et al*.,

2007; Lau *et al*., 2004; Yadav *et al*., 2009; He *et al*., 2005) and so the use of this technique as a basis for the identification of pairs of Affimer reagents against the N protein of PRRSV is well grounded.

This chapter discusses the cross-reactivity of the Affimers identified in Chapter 3 between the two viral strains of the PRRSV N protein, as well as methods employed to identify pairs of reagents based upon ELISA techniques. Firstly cross-reactivity of the Affimers with the SUMO tagged N proteins was investigated using phage ELISA based assays to reduce the number of reagents taken forward for pair identification. Once a reduced number of Affimers had been identified for each target N protein, the reagents were prioritised using further ELISA and pulldown assays to discriminate between two viral N proteins which are similar in both structure and sequence to be used in the development of a novel Affimer based point of care (POC) biosensor.

4.2. Cross-reactivity between Affimers raised against PRRSV strains

To investigate the cross-reactivity of Affimers raised against each strain of the PRRSV N protein, phage ELISAs were performed, as described in sections 3.3 and 3.7, where the phage expressed Affimers were incubated with either strain of the SUMO-N protein, as well as the SUMO-tag (figure 4.1). This determined the preference of the Affimers to the specific SUMO-N protein shown using the absorbance readings taken from the phage ELISA (figure 4.1b). The Affimers used in this ELISA were taken from a pool enriched for NLP-his_8. Pan 2 phage from the original NLP-his_8 screen was used to screen SUMO-NLP (section 3.3) and so it was expected that they would show a preference for SUMO-NLP over SUMO-NHP. Not surprisingly the results show that the Affimers did indeed bind more strongly to SUMO-NLP compared to SUMO-NHP (figure 4.1a). No Affimer binding was observed to the SUMO-tag as expected. The phage ELISA data was analysed in combination with the sequencing data previously gathered for this set of Affimers (data not shown) and three binders were taken forward (B3, B7, D12) as strong binders to SUMO-NLP but weak binders to SUMO-NHP as indicated (figure 4.1b*). Their unique loop sequences are listed in table 4.1, combined with the Affimers

previously raised against NLP-his_8 (Affimers 1, 15, 16, 17 and 23) for further characterisation. Affimer A12 (Figure 4.1b*) was also taken forward from as a binder able to recognise both PRRSV SUMO-N proteins, its unique loop sequences are shown in table 4.2. The remaining Affimers were not taken forward due to lack of unique loop sequences or inability to sufficiently discriminate between the two PRRSV N proteins.

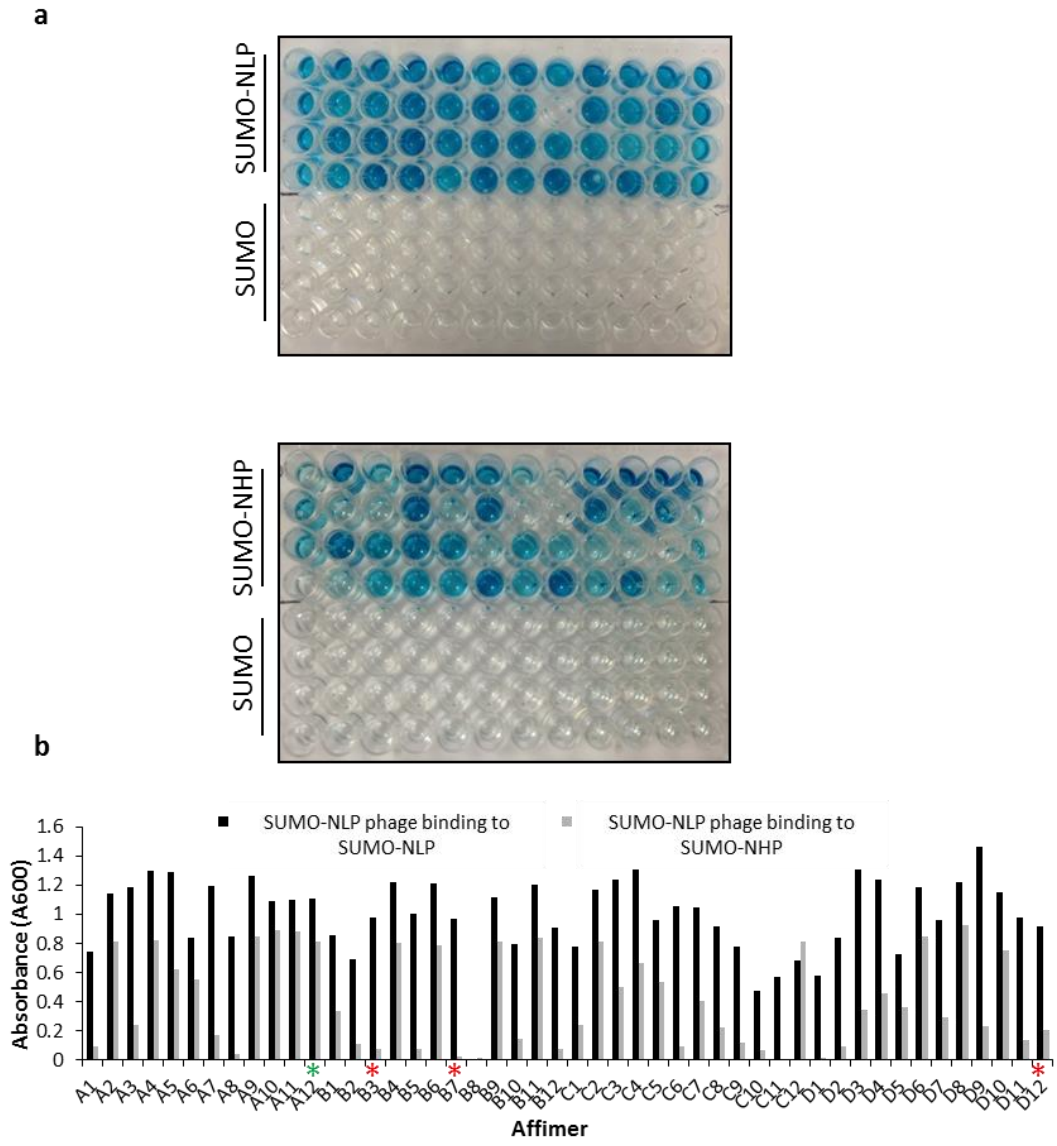

Figure 4.1 Cross-reactivity of Affimers between PRRSV viral strains. The phage expressed Affimers raised against SUMO-NLP were incubated with either SUMO-NLP or SUMO-NHP and a phage ELISA performed. Phage binding to the target protein was confirmed by detection with an anti-bacteriophage antibody labelled with HRP and visualisation with TMB. **(a)** The Affimers showed a preference for SUMO-NLP in this assay, although cross-reactivity was seen between the PRRSV viral strains. There was no binding of Affimers to the SUMO tag. **(b)** Absorbance readings confirmed a preference for SUMO-NLP. Three Affimers were taken forward for further analysis as binders against SUMO-NLP, B3, B7 and D12 (*). A12 was taken forward as a binder which was able to recognise both strains of the viral N protein (*).

Table 4.1 Final list of Affimers raised againt SUMO-NLP

Adhiron (NLP)	Loop 1	Loop 2
A8	P Y S Y L W H F D	G D L Y I L P L I
B3	A E W L P I Y E Q	D Y S K K P W M P
D12	F Y A D W L N H F	Q H E S G R F M N
1	V Q L V D L T W L	N H L L E N P F D
15	W E P L E Q Q H R	L T V I N Y N I L
16	W I A E E P G V V	R Y L M G H W M W
17	H Y Y G Q F L Y H	R K N L L Q E F K
23	H D P F E M P V Q	L F I Y G R H M L

The same phage ELISA as described in section 3.3 was then performed using the 48 Affimers raised against SUMO-NHP to determine the specificity of this pool of binders to SUMO-NHP over SUMO-NLP (figure 4.2). There were fewer Affimers identified as binders from this ELISA (figure 4.2a) compared to the enriched Affimer library used in the SUMO-NLP screen (figure 4.1) and the same four Affimers were identified as binders to the SUMO-tag in both SUMO-N protein plates (figure 4.2a), these were eliminated from further investigation. Again, as expected, there is a preference for the PRRSV N protein to which the Affimers were raised, in this case SUMO-NHP, although to a lesser extent than in the equivalent SUMO-NLP ELISA. The Affimers identified as binders which bound preferentially to SUMO-NHP over SUMO-NLP (figure 4.2b*) (A2, B7, C11, C12, D9) were taken forward for further investigation and their unique loop sequences are listed in table 4.2. These Affimers did show less specificity to the PRRSV viral strains than those identified in table 4.1 and so some cross reaction maybe expected in future assays. Based on sequence identification, A5 and A7 (figure 4.2b*) were also taken forward because they showed a preference for both PRRSV viral strains. A7 in particular was a strong binder to both target proteins. For the purposes of the LFD it is necessary to also have non discriminate reagents which are able to detect the presence of the PRRSV viral N proteins from multiple strains.

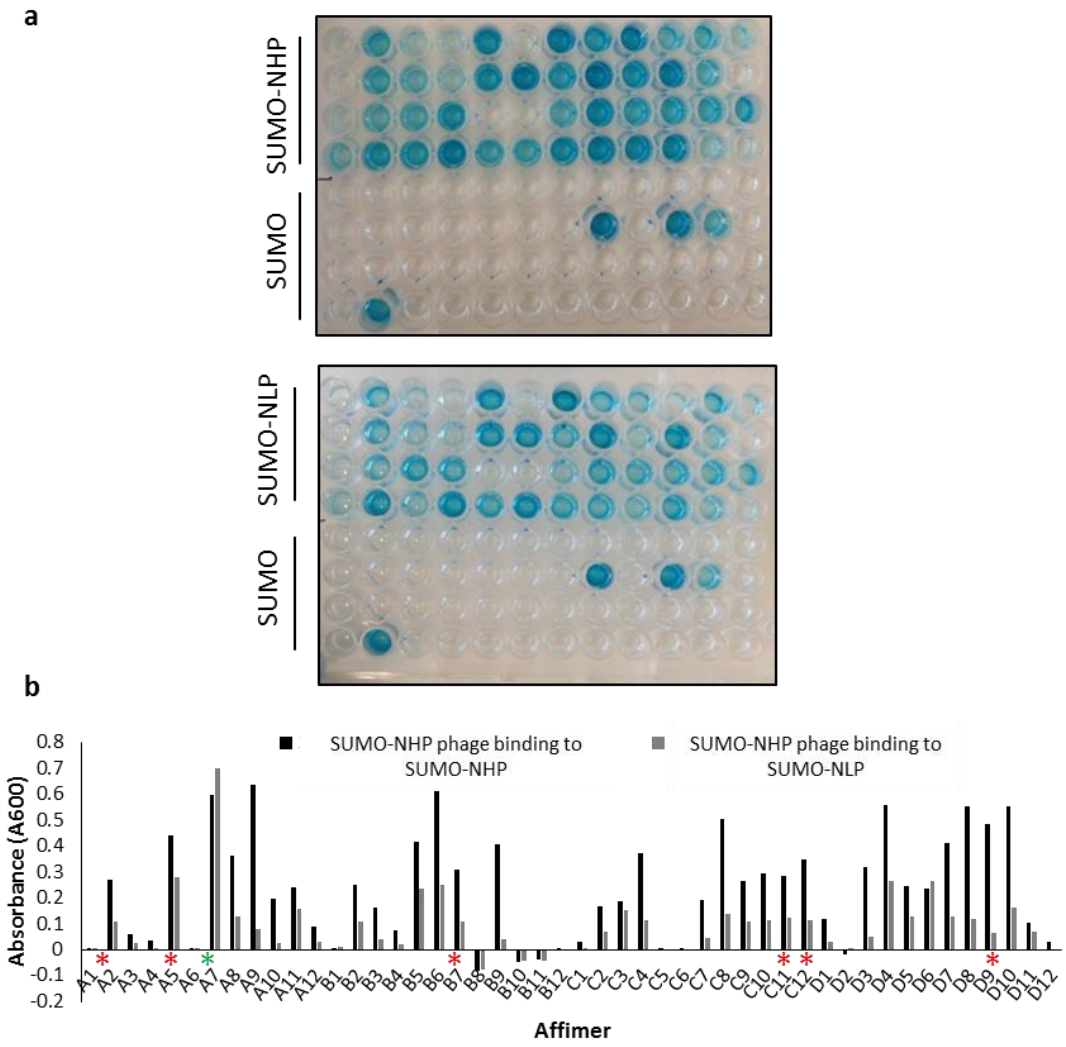

Figure 4.2 Cross-reactivity of Affimers between viral strains. The phage expressed Affimers raised against SUMO-NHP were incubated with either SUMO-NHP or SUMO-NLP and a phage ELISA performed. Phage binding to the target protein was confirmed by detection with an anti-bacteriophage antibody labelled with HRP and visualisation with TMB. **(a)** The Affimers showed a preference for SUMO-NHP although cross-reactivity was seen between the PRRSV viral strains. **(b)** Absorbance readings confirmed a preference for SUMO-NHP. Six Affimers were taken forward for further analysis as binders against SUMO-NHP, A2, A5, B7, C11 and D12(*). A7 (*) was taken forward as an Affimer which did not show preference for either SUMO-NLP or SUMO-NHP.

Table 4.2 Final list of Affimers raised against SUMO-NHP

Adhiron (NHP)	Loop 1	Loop 2
A2	L E V N M M W V D	P G P Y P Q E F S
A5	V E I E H M W E D	F A E N H S W P I
A7	I E E W D M W M D	D N R P F S R V E
A12 *	H E I I N N T L W	W W G Y P Y T G I
B7	F E M I Y M W N D	P E R D Y R S T W
C11	I E I N E M W D D	H R S P T H A V K
C12	V E L D G M W D D	G T E T L T D K R
D9	I E L T N M W D D	R V W N S E N A N

4.3. Cloning of Affimers into expression vectors and bacterial expression

The Affimers listed in tables 4.1 and 4.2 were then PCR amplified using primers containing *Nhe*I and *Not*I restriction sites (table 2.5) and cloned into a pET11a expression vector (data not shown). The cloning protocol was performed in parallel using primers which inserted a C-terminal cysteine (the only cysteine in the protein) or primers lacking this modification. Successful insertion of the Affimers into pET11a was confirmed by sequence analysis using a T7 primer (GATC Biotech AG, data not shown).

Affimer expression constructs, containing the additional cysteine were then transformed into BL21(DE3)pLysS cells and expression carried out at 30°C, with IPTG induction, overnight. Affimers were purified by nickel ion affinity chromatography using the C-terminal his_6-tag with a representative SDS-PAGE and Coomassie stain shown in figure 4.3 (Affimer 17) alongside the elution fractions of all of the Affimers. Only elutions from Affimers which remained soluble are shown, as those that were insoluble upon purification were discounted from further analysis. Affimer reagents were purified in concentrations ranging from 1 mg/ml to 5 mg/ml and protein concentration was determined using a BSA standard (data not shown) before diluting the Affimers to 1 mg/ml for use in future assays.

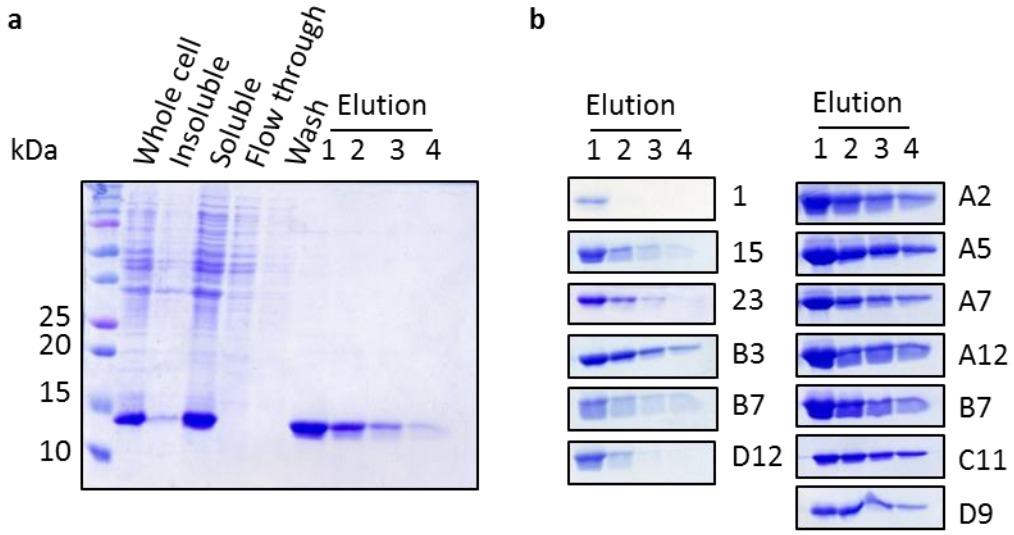

Figure 4.3 Purification of Affimers from bacterial cell lysates. (a) Affimers were expressed and purified from bacterial cell lysate using nickel ion affinity chromatography and elution with 300 mM imidazole. Purification fractions of the proteins which remained soluble were analysed by SDS-PAGE and Coomassie blue staining (representative figure, Affimer 17) with the highest concentration fraction taken forward. **(b)** Elution fractions of Affimers to determine the highest concentration fraction.

4.4. Identification of pairs of Affimer reagents to the PRRSV N proteins

Pairs of reagents are required for the production of a LFD, encompassing a capture and detection Affimer. In order to identify potential pairs of Affimers against the PRRSV N proteins, ELISA and pulldown assays were used where the detection Affimers were analysed using different tags and expression methods.

The bacterially expressed and purified Affimers were initially biotinylated using biotin-maleimide following the reduction of the single cysteine residue using TCEP resin, resulting in the addition of a single biotin molecule on the free cysteine residue. Following the removal of excess biotin, the addition of the biotin molecule was confirmed using an ELISA-based method, detected with streptavidin-HRP as described in section 3.7 (data not shown).

Firstly, the detection Affimer was presented to the target protein as a phage expressed molecule using the biotinylated Affimers as capture molecules. The purified and biotinylated capture Affimers were immobilised onto a streptavidin coated 96 well plate and incubated with the relevant PRRSV SUMO-N protein

before the addition of the detection Affimer expressed on the surface of the phage, with detection using anti-bacteriophage-HRP and TMB as illustrated (figure 4.4a). Biotinylated Affimers were immobilised vertically down the columns of the 96 well plate, with the bacteriophage expressed Affimers being added across the rows of the plate. This allowed for each Affimer to be tested as both a capture and a detection reagent, as the Affimers may display different sensitivities depending on whether they are immobilised or available in solution. From the ELISA plate (figure 4.4b), all chosen Affimers appear to work well as pairs. However, results suggest that this method of identification of pairs was not ideal, due to poor reproducibility, perhaps due to the quality and quantity of phage expressed Affimers used in each replicate.

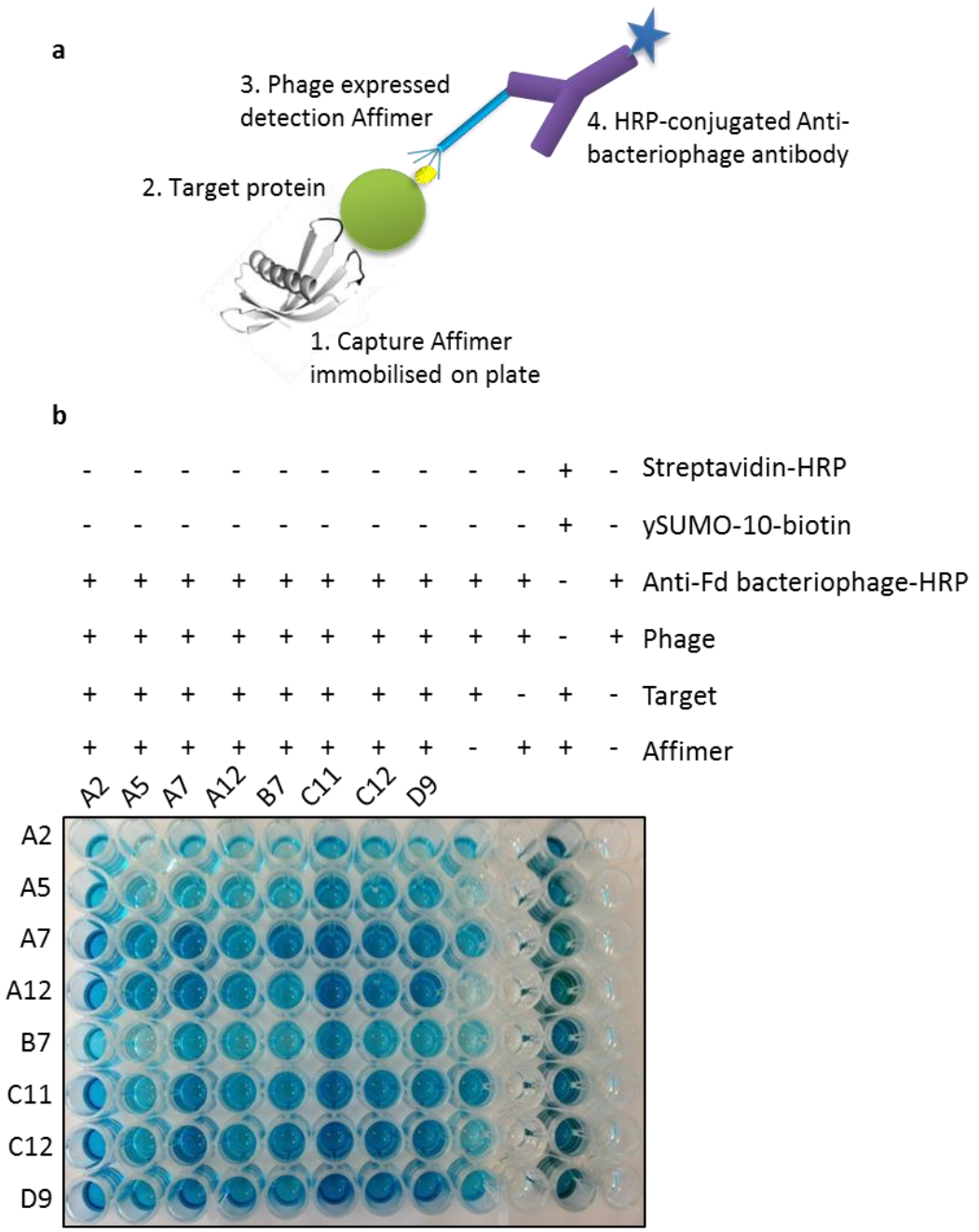

Figure 4.4 Phage ELISA to show Affimer pairs with SUMO-NHP Affimers (representative figure). (a) Schematic representation of ELISA, biotinylated Affimers were immobilised on a streptavidin coated plate. The target protein was captured by the immobilised Affimer and the captured target was detected by an Affimer expressed on a phage. Binding of pairs was confirmed by detection of bound phage using an anti-bacteriophage antibody. **(b)** A representative ELISA plate: pair binding was confirmed by the addition of TMB and measuring the absorbance. Positive pairs were identified with the blue colour change to the wells. Replicates of this assay were not analysed due to variability between ELISA plates and so average absorbance readings and pairs could not be identified.

In order to overcome the variability between batches of phage, Affimers expressed and purified from bacteria were used as both capture and detection reagents, to

provide standard concentrations of protein in an attempt to enhance reproducibility of the assay. The detection method of the following ELISAs were varied by the addition of labels to the single cysteine residue engineered into the Affimer protein sequence, HRP for direct detection with TMB and Alexa Fluor®-488 or Alexa Fluor®-546 for detection with a fluorescence plate reader. The detection of the PRRSV SUMO-N proteins using purified and directly labelled protein was preferred to the secondary detection of phage expressing Affimers as direct detection will be used in the LFD and the bulky phage may have masked binding of Affimers due to steric hindrance, resulting in the variable ELISA results.

Figure 4.5a shows the detection method using HRP-labelled Affimers with the addition of TMB for detection of target binding. Here, the biotinylated Affimers were immobilised onto the streptavidin coated plates and incubated with target PRRSV SUMO-NHP protein before the addition of HRP-labelled Affimers. As with the phage ELISA (figure 4.4), the biotinylated Affimers were immobilised vertically down the columns and the HRP-labelled Affimers were added across the rows of the plate. The representative image of a HRP ELISA shown in figure 4.5b indicates a number of positive hits for pairs of Affimers against the SUMO-NHP protein. In this case, Affimer B7 as a capture Affimer with Affimer A12 as a detection Affimer, Affimer D9 as a capture Affimer with Affimer C11 as a detection Affimer and Affimer A7 as a capture Affimer with Affimer A2 as a detection Affimer being the strongest pairs indicated in this assay. Interestingly, the use of these Affimers in reverse (swapping the detection and capture Affimer) resulted in a greatly reduced reaction upon the addition of TMB, suggesting that the reagents were less sensitive in this orientation. However, as with the previously described phage ELISA (figure 4.4), the reproducibility of this assay was not reliable. The control wells in this assay (Affimer binding to an immobilised target protein) were highly variable between experiments, suggesting that the HRP-Affimer binding was not optimal when presented to the immobilised target protein.

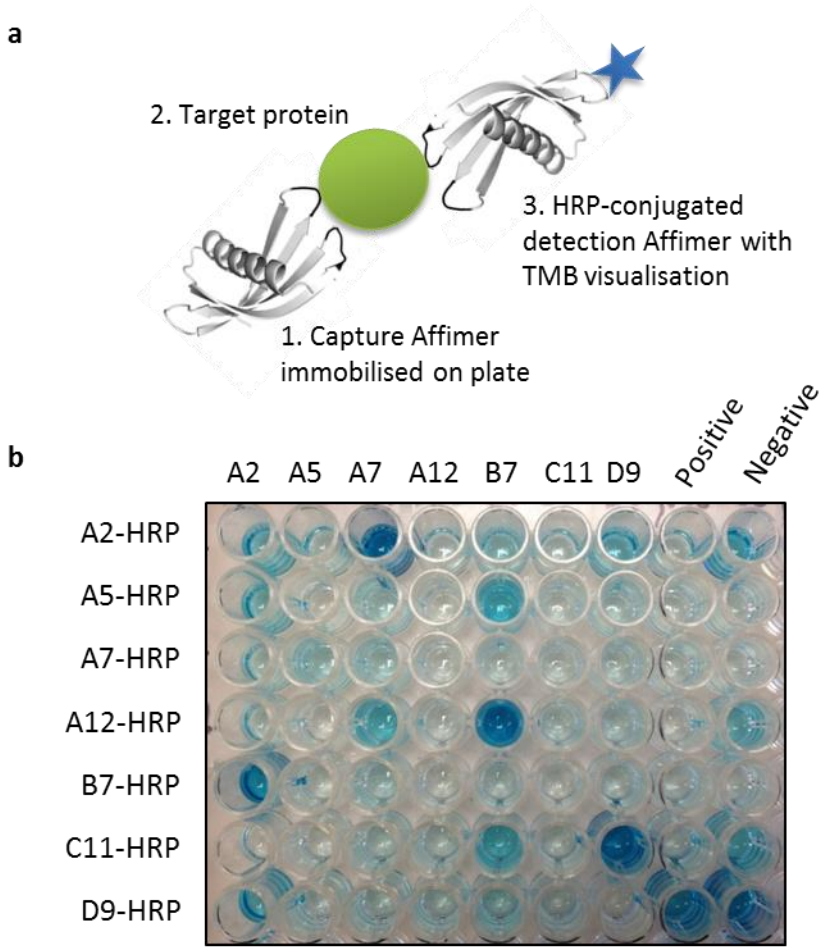

Figure 4.5 ELISA to identify Affimer pairs with SUMO-NHP Affimers labelled with HRP (representative figure). (a) Schematic representation of ELISA, biotinylated Affimers were immobilised on a streptavidin coated plate. The target protein was captured by the immobilised Affimer and the captured target was detected by an Affimer labelled with HRP. **(b)** Pair binding was confirmed by the addition of TMB and measuring the absorbance of the wells. As with figure 4.4, variability between replicates of this assay did not allow for pairs to be identified and therefore average absorbance readings are not shown.

Figure 4.6a illustrates the use of Affimers as pairs with the detection reagents when labelled with a fluorescent tag, in this case, Alexa Fluor®-488 or 546. The binding of the Affimers in a pairwise manner in the presence of target protein was confirmed by reading the fluorescence intensity on a plate reader. Initially, two fluorescent tags were used to determine the optimum labelling and detection method with regards to assay sensitivity. Here, an Affimer was chosen as a detection reagent, in this case SUMO-NHP B7, to be labelled with either Alexa Fluor®-488 or 546. SUMO-NHP B7-488 was incubated as a detection reagent and following wash steps, to remove any unbound Affimer, the fluorescence intensity of the ELISA plate was measured (figure 4.6b). The fluorescence intensities showed no variability

throughout the assay and the positive and negative controls (plus or minus immobilised target protein incubated with fluorescently labelled Affimer) did not appear to have been successful with this detection method. Moreover, the fluorescence intensity values are very high for this ELISA, which may indicate that the wash steps were not sufficient to remove the unbound Affimer. The same experiment was performed using SUMO-NHP B7-546 (figure 4.6c) with more promising results, the positive and negative controls appear to have been successful and a number of pairs were possibly identified, B7 with A5, B7 with A7 and B7 with D9. Alexa Fluor®-546 was chosen as the label to be taken forward for the labelling of further Affimer reagents. Figure 4.6d shows Affimer SUMO-NLP 15-546 incubated with capture Affimers and target proteins. Again, a number of pairs may be indicated for example, Affimer 15 as a detection Affimer with Affimers 17, B3 and D12 as capture Affimers. However, as with the other ELISA methods described in this chapter, the variability between the assay results meant there was little confidence in the ability of the chosen Affimers to function as pairs of reagents in a LFD.

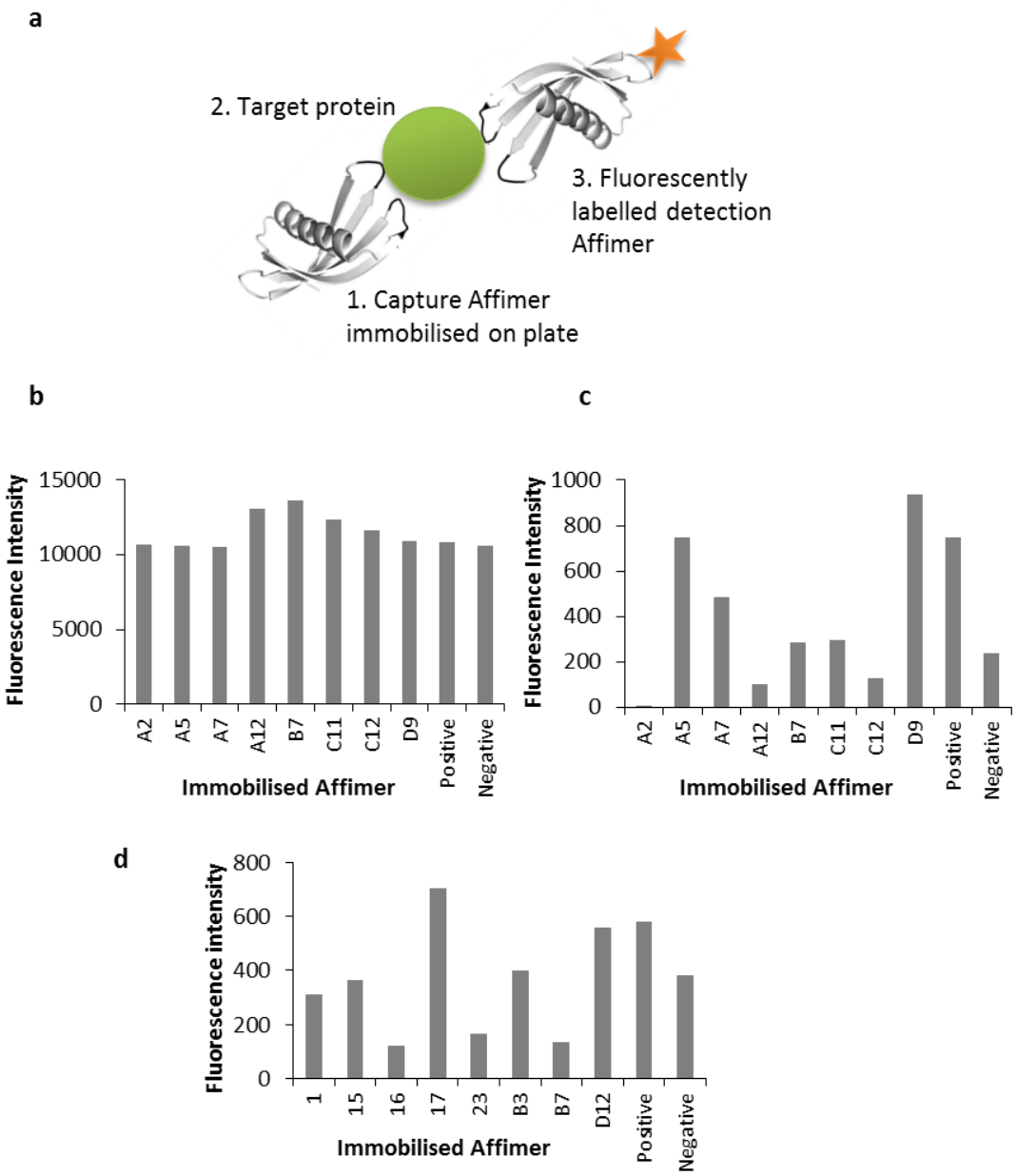

Figure 4.6 ELISA using fluorescently labelled Affimers. (a) Schematic representation of ELISA, biotinylated Affimers were immobilised on a streptavidin coated plate. The target protein was captured by the immobilised Affimer and the captured target was detected by an Affimer labelled with a fluorescent label. **(b)** Biotinylated Affimers against SUMO-NHP were immobilised on the streptavidin plate and target binding was confirmed using Affimer B7 labelled with Alexa Fluor®-488 (c) Biotinylated Affimers against SUMO-NHP were immobilised on the streptavidin plate and target binding was confirmed using Affimer B7 labelled with Alexa Fluor®-546 (d) Biotinylated Affimers against SUMO-NLP were immobilised on streptavidin coated plates and target binding was confirmed using Affimer 15 labelled with Alexa Fluor®-546.

As a result of the variable data collected from a number of different ELISA assays, pulldown assays were performed using Affimers immobilised on magnetic beads and incubated with target proteins presented in a clinically relevant sample (pig

serum) as shown in figure 4.7a. Experiments were performed using both SUMO-N proteins in order to determine the cross-reactivity of the Affimers in the presence of other proteins present in the pig serum. Moreover, it also compared the cross-reactivity highlighted in the earlier ELISA experiments (figures 4.1 and 4.2). Pulldown assays proved to be far more reproducible than the previously described ELISAs. Figure 4.7b shows the results of the pulldown assay performed in pig serum spiked with SUMO-NLP, using Affimers raised against this target protein. None of the Affimers showed any binding to the SUMO protein used as a control, ensuring the Affimers recognised the untagged region of NLP. These results confirm the findings of the ELISA shown in figure 4.1, highlighting the specificity of the Affimers to NLP. The Affimers which showed specificity to the target protein via pulldown assays were 1, 15, B3, B7 and D12 and when compared to the previous ELISA data (figures 3.3, 4.1), the binding to the target protein was confirmed. Affimers 1 and 15 in particular showed a strong reaction in the ELISA assay using the his-NLP protein as a target. Affimer 17 showed reduced affinity in the same ELISA and again this was confirmed in pulldown assays, in fact showing no binding capability. However, Affimer 23 was a surprising result as it initially displayed good binding to his-NLP (figure 3.3). Upon the addition of the SUMO-tag, binding ability is lost in pulldown assays. The poor binding of Affimers 17 and 23 could be attributed to the addition of the SUMO tag which when immobilised onto magnetic beads (1 μm) may block the binding sites for these two Affimers, although this requires further investigation. Combining all the data from the multiple assays, Affimers B3, B7 and D12 bind the target NLP protein efficiently and were taken forward.

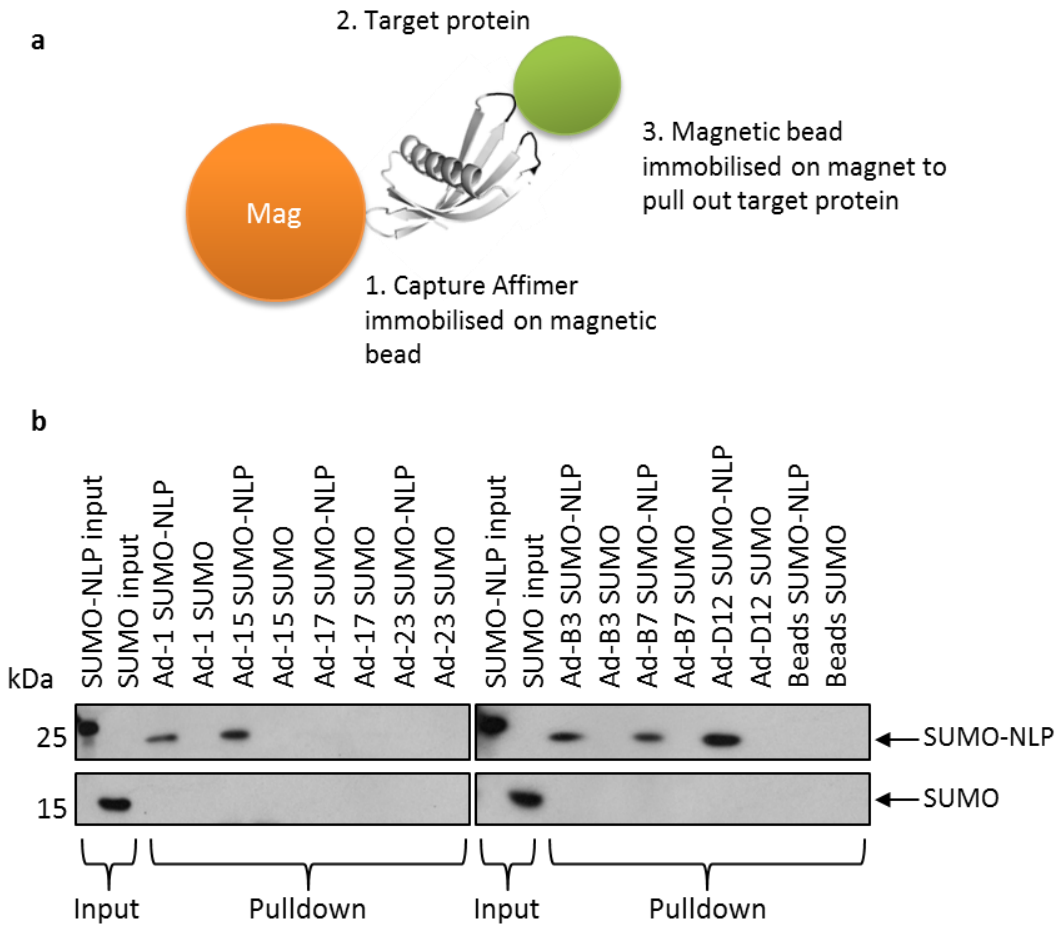

Figure 4.7 Pulldown analysis of Affimer binding to SUMO-NLP. (a) Schematic representation of pulldown assay. Affimers raised against SUMO-NLP were biotinylated and bound to streptavidin coated magnetic beads and incubated with SUMO-NLP in the presence of pig serum. **(b)** Binding of the target protein was analysed using SDS-PAGE and western blot analysis. No Affimers showed any binding to the SUMO tag, Affimers 1, 15, B3, B7 and D12 were able to pulldown SUMO-NLP.

As previously mentioned, the ability of the Affimer reagents to discriminate between the two viral strains is desirable for the production of a LFD allowing the sensor to determine which viral strain an animal is infected with. Therefore, the same pulldown assay was performed using the Affimers raised against SUMO-NLP incubated with SUMO-NHP (figure 4.8). The Affimers that bound in this assay are 1, 15, 23 and D12, showing some cross-reactivity of the Affimers between the two viral strains. The Affimers which were originally raised against his-NLP (1, 15, 17 and 23) had not previously been investigated for their ability to bind to SUMO-NHP by ELISA and so were included in the pulldown assays, to ensure they were able to bind to both of the SUMO-tagged proteins. D12 was the only other Affimer in the assay pulldown which showed cross-reactivity. The ELISA data (figure 4.1)

suggested that this Affimer was more specific for SUMO-NLP than SUMO-NHP. The ability of the Affimer to detect both target proteins is, however, desirable as a non-discriminate Affimer is also required for the assembly of a LFD.

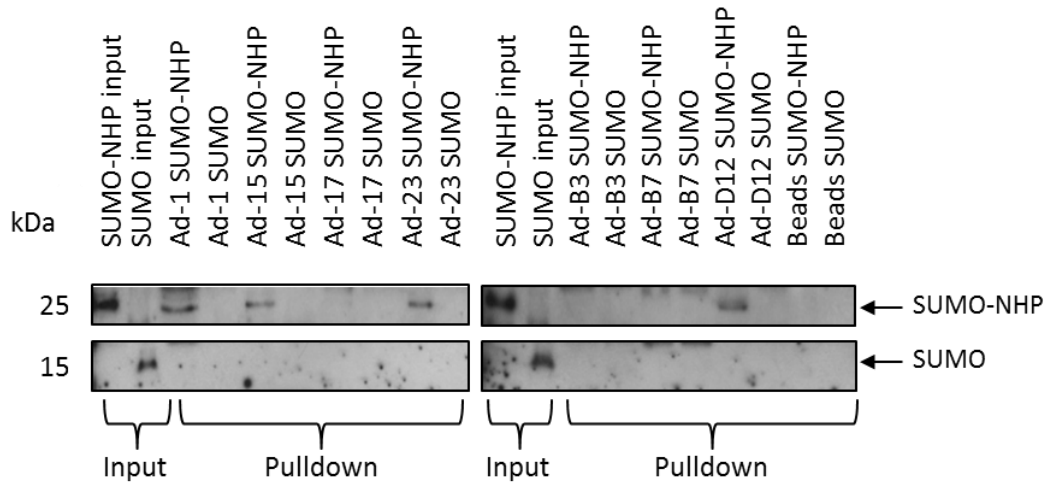

Figure 4.8 Pulldown analysis of Affimer cross-reactivity between viral strains. Affimers raised against SUMO-NLP were biotinylated and bound to streptavidin coated magnetic beads and incubated with SUMO-NHP in the presence of pig serum. Binding of the target protein was analysed using SDS-PAGE and western blot analysis. Affimers 1, 15, 23 and D12 were able to bind to SUMO-NHP.

The same pulldown assays were also performed for the SUMO-NHP Affimers where they were incubated with either SUMO-NHP (figure 4.9) or SUMO-NLP (figure 4.10). As with the previous pulldown experiments, these pulldowns were performed in pig serum, in order to provide a clinically relevant buffer. The Affimers which were able to identify SUMO-NHP were Affimers A2, A5, A7, B7, C11 and D9 (figure 4.9). Results also concluded that the Affimers only bound the target N protein, as they showed no binding affinity to the SUMO tag, further confirming the data collected from initial phage ELISAs (figure 4.2).

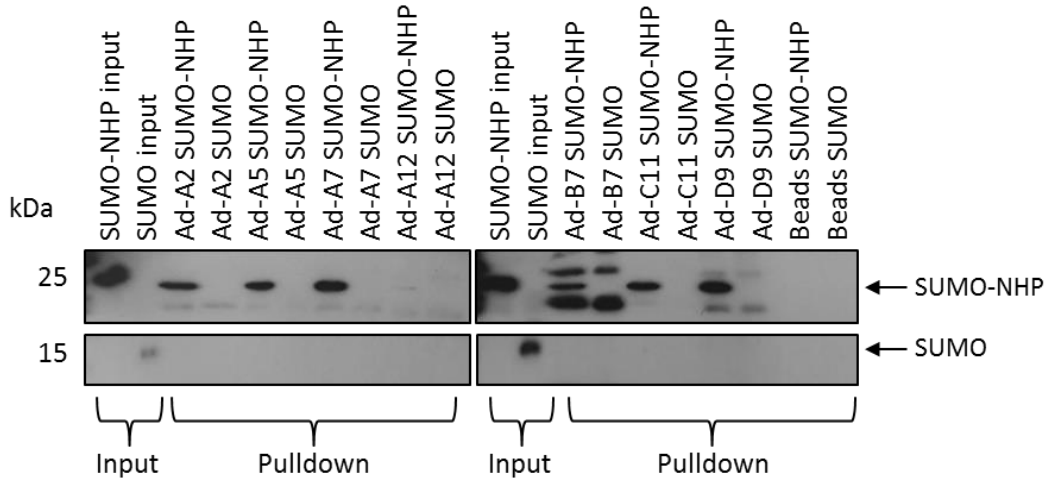

Figure 4.9 Pulldown analysis of Affimer binding to SUMO-NHP. Affimers raised against SUMO-NHP were biotinylated and bound to streptavidin coated magnetic beads and incubated with SUMO-NHP in the presence of pig serum. Binding of the target protein was analysed using SDS-PAGE and western blot analysis. Affimers A2, A5, A7, B7, C11 and D9 were able to bind SUMO-NHP and none of the Affimers were shown to bind to the SUMO tag. The non-specific bands are thought to be proteins from the pig serum which interact with the Affimers.

Pulldown assays were also performed using SUMO-NLP target protein as a test for cross-reactivity (figure 4.10). A number of Affimers displayed the ability to recognise both strains of the viral N proteins, A2, A5, A7, C11 and D9. However, B7 was not able to recognise the low pathogenic strain of the viral protein and A12 was able to recognise only the low pathogenic strain of the protein, which is contrary to the ELISA data shown in figure 4.1 where this Affimer had shown preference for both of the viral N proteins. A summary of the binding of the target N proteins to the Affimers in pulldown assays is show in table 4.3. The three Affimers chosen to be taken forward are highlighted in purple text.

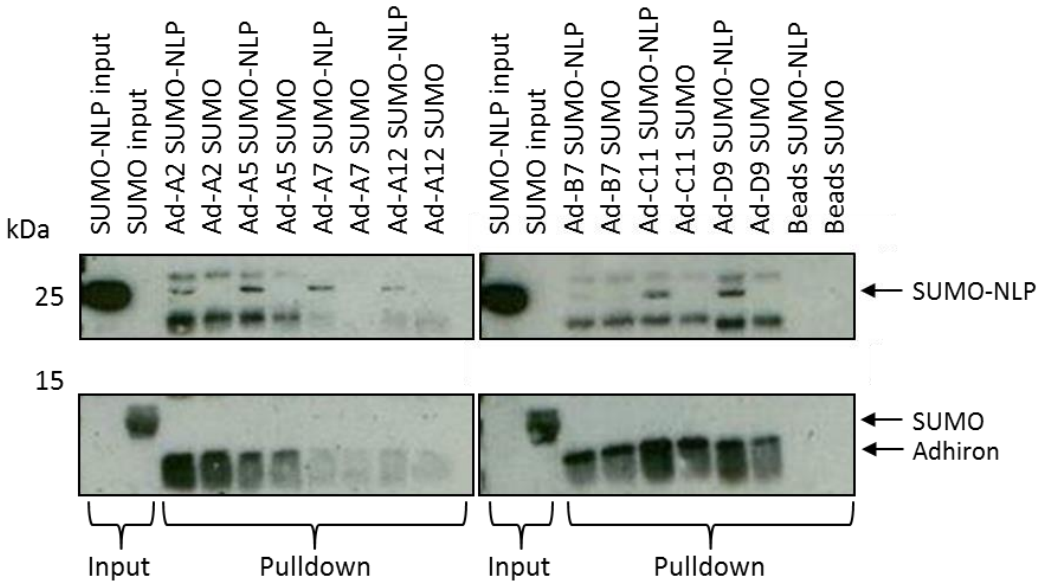

Figure 4.10 Pulldown analysis of Affimer binding to SUMO-NLP. Affimers raised against SUMO-NHP were biotinylated and bound to streptavidin coated magnetic beads and incubated with SUMO-NLP in the presence of pig serum. Binding of the target protein was analysed using SDS-PAGE and western blot analysis. Affimers A2, A5, A7, A12, C11 and D9 were able to bind SUMO-NLP but none of the Affimers showed binding to the SUMO tag. The non-specific bands are highlighted as Affimers eluted from the streptavidin beads or are thought to be proteins from the pig serum which interact with the Affimers.

Table 4.3 Summary of Affimer binding to target proteins in pulldown assays

	Target protein			Target protein	
Affimer	**SUMO-NLP**	**SUMO-NHP**	**Affimer**	**SUMO-NLP**	**SUMO-NHP**
SUMO-NLP 1	Yes	Yes	**SUMO-NHP A2**	Yes	Yes
SUMO-NLP 15	Yes	Yes	**SUMO-NHP A5**	Yes	Yes
SUMO-NLP 17	No	No	**SUMO-NHP A7**	Yes	Yes
SUMO-NLP 23	No	Yes	**SUMO-NHP A12**	Yes	No
SUMO-NLP B3	Yes	No	**SUMO-NHP B7**	No	Yes
SUMO-NLP B7	Yes	No	**SUMO-NHP C11**	Yes	Yes
SUMO-NLP D12	Yes	Yes	**SUMO-NHP D9**	Yes	Yes

4.5. Discussion

This chapter describes the analysis of the Affimers raised against the two viral N proteins to investigate the cross-reactivity of the Affimers when challenged with recognising the two strains of the proteins and to identify Affimers able to discriminate between the two strains.

Initially, the phage ELISA method was used as a preliminary investigation into the specificity of Affimers to the two viral strains of the N protein in order to identify the Affimers to be cloned into bacterial expression vectors for further analysis. The binding of the Affimers to each of the target proteins in these ELISAs was used in conjunction with the unique loop regions of the Affimers identified in table 3.2 and 3.3 to further reduce the number of Affimers taken forward for investigation based upon specificity to the target.

The ELISA data showed that there was cross-reactivity between the viral proteins. This is not unexpected due to the amino acid sequence similarity between the two N proteins. Moreover, it is highly likely that the Affimers are also recognising structural conformations likely to be conserved between the two viral strains. Although the entire crystal structure of the PRRSV N protein is yet to be solved, a truncated structure of the 65 C-terminal amino acids of the North American strain VR-2332 is available (Doan and Dokland, 2003). The amino acid similarity in this region between the two viral N proteins in this study is high, with only 5 amino acid differences within the region (figure 1.18), suggesting that the overall structural similarity will be high.

When considering the unique loop regions of the Affimers taken forward in tables 4.1 and 4.2, it is important to observe that there is sequence similarity between the Affimers raised against each N protein. However, within each of the tables, we can observe amino acid sequences which are more common as previously discussed in Chapter 3 (section 3.8). It may therefore be hypothesised that the interactions between the Affimers target proteins are at a small number of regions on the protein and not spread at multiple locations. This is especially likely when considering SUMO-NHP Affimers which show less sequence diversity.

Expression constructs allowed the expression of the chosen Affimers (tables 4.1 and 4.2) in bacterial systems. Cloning was performed in parallel to produce two expression constructs for each Affimer, one engineered to express Affimers containing a C-terminal cysteine and one without (Tiede *et al*., 2014). This is the only cysteine residue in the Affimers allowing for targeted modification for labelling purposes exploited in this chapter. Affimers expressed and containing this C-terminal cysteine appeared to be less stable than those without, readily forming disulphide bonds with other Affimers and precipitating out of solution at high concentrations. This was overcome by the dilution of the purified proteins and addition of any modifications promptly following purification to protect the reactive amino acid. Disulphide bonds are ordinarily a stabilising feature when found within proteins, providing thermodynamic stability, loss of conformational entropy of the unfolded state and restriction of motion of unstructured regions (Dombkowski *et al*., 2014). This has been exploited with additional cysteine residues being engineered into a protein sequence to introduce a stabilising disulphide bond (Wetzel *et al*., 1988; Kim *et al*., 2012; Wedemeyer *et al*., 2000). A number of Affimers were excluded from further investigation as they were particularly unstable following purification; SUMO-NLP 16 and A8 and SUMO-NHP C12. In addition to time restraints preventing investigation into stability, it was also observed from sequence analysis of the loop regions that these three Affimers contain a high proportion of hydrophobic residues which could promote protein aggregation (Fink, 1998). However, hydrophobic residues are also present in Affimers which do not show severe aggregation upon storage, this may be due to differential folding of the main structure and variable loops. If the Affimers are forming disulphide bonds via their free cysteines then this may be exasperated by the presence of hydrophobic regions (Fink, 1998).

The modifications added to the C-terminal cysteine of the purified Affimers in the assays in this chapter are maleimide additions where the label was HRP (Thermo Fisher Scientific), Alexa Fluor®-488 or 546 (Invitrogen) or biotin (Sigma Aldrich). The label of choice is conjugated to a maleimide compound which is highly electrophilic and has a high selectivity for reduced thiol residues, in this case the single cysteine residues (Kim *et al*., 2008; Chalker *et al*., 2009). Following desalting

to remove excess maleimide label, the proteins can be used in ELISA and pulldown assays as described.

Three sandwich ELISA methods were used to identify pairs of Affimers able to recognise the two viral N proteins; phage ELISA, ELISA using HRP-labelled Affimers and a fluorescence ELISA. The phage ELISA method used purified biotinylated Affimers immobilised on a streptavidin coated plate then incubated with target protein and detection of pairs determined using a phage expressed Affimer detected with anti-bacteriophage antibody-HRP and TMB. The variability observed between replicates of this assay was large and possibly attributed to the production of phage expressed Affimers. Without knowing the phage titre, it was not possible to quantify the number of phage used in each replicate causing variability in results. Although the calculation of phage titre is itself straightforward (Swanstrom and Adams, 1951), using plaque assays, it was not possible to perform this assay as the phage used in these experiments was packaging deficient and would therefore not form plaques. It was also hypothesised that the variability of the assay was due the capture of the target protein in an unfavourable position obscuring the binding sight for the bulky phage expressed detection Affimer. This was further investigated using a solution based assay, by immobilising the capture Affimers onto a streptavidin coated bead before being incubated with the target protein and then the phage expressed detection Affimer, allowing more flexible binding conditions.

In order to improve the reliability of these assays, the use of a known concentration of both capture and detection Affimer was needed. ELISAs were performed with purified and HRP or fluorescently-labelled Affimers of known concentrations. Input protein concentrations for each replicate were the same when compared to the variability of the phage ELISA, as well as providing a direct read out of detection Affimer binding rather than indirect detection of the phage expressed Affimer with an antibody. The protocol was also significantly faster allowing for rapid optimisation and identification of pairs more quickly. However, the reliably of these assays was not significantly improved upon compared to the phage ELISA previously discussed. As with the phage ELISA, the binding of the

target protein to the immobilised capture protein could be a contributing factor to the variability of binding, this is addressed in chapter 5.

The pulldown assay experiments discussed in this chapter eliminated Affimers likely to detect both of the target PRRSV N proteins and identified those taken forward specific to one N protein or another. Three Affimers were taken forward, B3 detecting SUMO-NLP, B7 detecting SUMO-NHP and D12 able to detect both of the viral N proteins. Simplifying the assay to determine the best binders against the target proteins, further reduced the pool of Affimers investigated for pairs of reagents and allowed for more optimisation of future assays. These Affimers were investigated as functioning pairs in the final chapter of the project.

Chapter 5

Determining pairs of Affimers and development of a novel Affimer based lateral flow device

5. Determining pairs of Affimers and development of a novel Affimer based lateral flow device

5.1. Introduction

Modifications of lateral flow devices (LFDs) using alternatives to antibodies have been developed over the last decade with the application of various reagents such as DNA or RNA aptamers (Chen and Yang, 2015b; Gopinath *et al*., 2016; Xu *et al*., 2009; Liu *et al*., 2009; Shim *et al*., 2014). Additional modifications also involve the replacement of antibody components with other reagents, for example Affimers® (Affimers) (Avacta® Life Sciences), Affibodies® (Löfblom *et al*., 2010), DARPins (Stumpp and Amstutz, 2007), other peptide aptamers (Reverdatto *et al*., 2015) or Avimers (Jeong *et al*., 2005). These antibody alternatives have already been utilised in multiple molecular medicine applications; as tissue targeting vehicles (Tolmachev *et al*., 2007), enzyme inhibitors (Attucci *et al*., 2006), as alternatives to small molecule inhibitors (Silverman *et al*., 2005) or in cancer treatment (Mamluk *et al*., 2010; Stahl *et al*., 2013). They have also shown promising results in *in vivo* imaging and diagnostics (Yang *et al*. 2015; Gong *et al*. 2010; Nordberg *et al*. 2007; Tiede *et al*. 2017), and as antibody alternatives in molecular biology for example ELISAs (Miranda, *et al*., 2011), immunofluorescence (Lyakhov *et al*., 2010), immunohistochemistry (Lundberg *et al*., 2007) and as reagents to investigate protein structures (Flütsch *et al*., 2014; Scholz *et al*., 2014).

Despite the wide ranging uses of these non-antibody binding proteins within scientific research, they have not been exploited to their full potential in the development of point of care (POC) diagnostics. The success of these reagents as replacements for antibodies in such wide ranging applications provides confidence that Affimers would be suitable to replace antibodies within a LFD. The basis of this study is to investigate whether Affimers are suitable reagents to use in LFDs as direct replacements of antibodies, in order to provide a diagnostic which shows improved sensitivity and selectivity, compared to the antibody containing alternative.

As previously described, commercially available LFDs are based upon a high protein binding nitrocellulose membrane which has a control line antibody and a test line

antibody immobilised, as well as a low protein binding cellulose based membrane, where a third antibody is immobilised (Posthuma-Trumpie *et al*., 2009). These component parts are shown in figure 1.19. It is proposed that the Affimers would be used in the same manner as antibodies in these devices. This chapter therefore examines the ability of the previously identified Affimers to function as a pair of reagents to identify the target recombinant N protein. As such the Affimer pairs are required to recognise the targets at different epitopes on the protein surface. The identification of pairs of reagents was carried out using a gold nanoparticle/magnetic bead assay, adapted from Zhou *et al*. 2015. Upon identification, the pairs of Affimers were then assessed for their applicability within a basic LFD, comprising a simple dipstick assay.

5.2. Gold nanoparticle and magnetic bead pulldown assay for identification of Affimer pairs

The previous chapter identified Affimers that were able to distinguish between the two viral N proteins (B3 and B7) as well as an Affimer which was able to bind to both N proteins, (D12). To determine the best combination for pairs of Affimers, a sandwich assay was performed using magnetic beads and gold nanoparticles (GNPs), based on an assay by Zhou *et al*. (2015). Here the capture Affimer (B3/B7) was immobilised onto magnetic beads and the detection Affimer (D12) was immobilised on GNPs. Successful pairs of Affimers would be confirmed when a complex was formed as illustrated in figure 5.1a and the gold was 'pulled out' of solution onto a magnet via the magnetic beads. Figure 5.1b shows the ultraviolet-visible absorption spectra of the supernatant from the sandwich assay, following the incubation of the magnetic bead/gold nanoparticles functionalised with B7/D12 with either SUMO-NLP, SUMO-NHP, SUMO or no target and immobilisation of any formed complex onto a magnet.

Initially as a proof of principle for this assay, B7 was utilised. Affimer B7 shows a preference to SUMO-NHP compared to SUMO-NLP in previous pulldown assays (figure 4.9). Therefore, the sandwich assay should show a reduction in the amount of gold in the supernatant following the addition of SUMO-NHP target protein, as opposed to the addition of SUMO-NLP or SUMO. Results confirm this theory,

(figure 5.1b) as illustrated by the representative absorption spectra, where a decrease in the peak at 520 nm (peak absorption value) upon the addition of SUMO-NHP was observed. Figure 5.1c shows the quantification of three replicates of the sandwich assay as a percentage of the control (no added target). Here results show that upon the addition of SUMO-NHP there is a significant decrease in the peak at 520 nm ($p=0.03$), which confirms the formation of the Mag-Affimer-Target-Affimer-Au complex and the successful pair interaction of B7 and D12, with detection of SUMO-NHP within a sample.

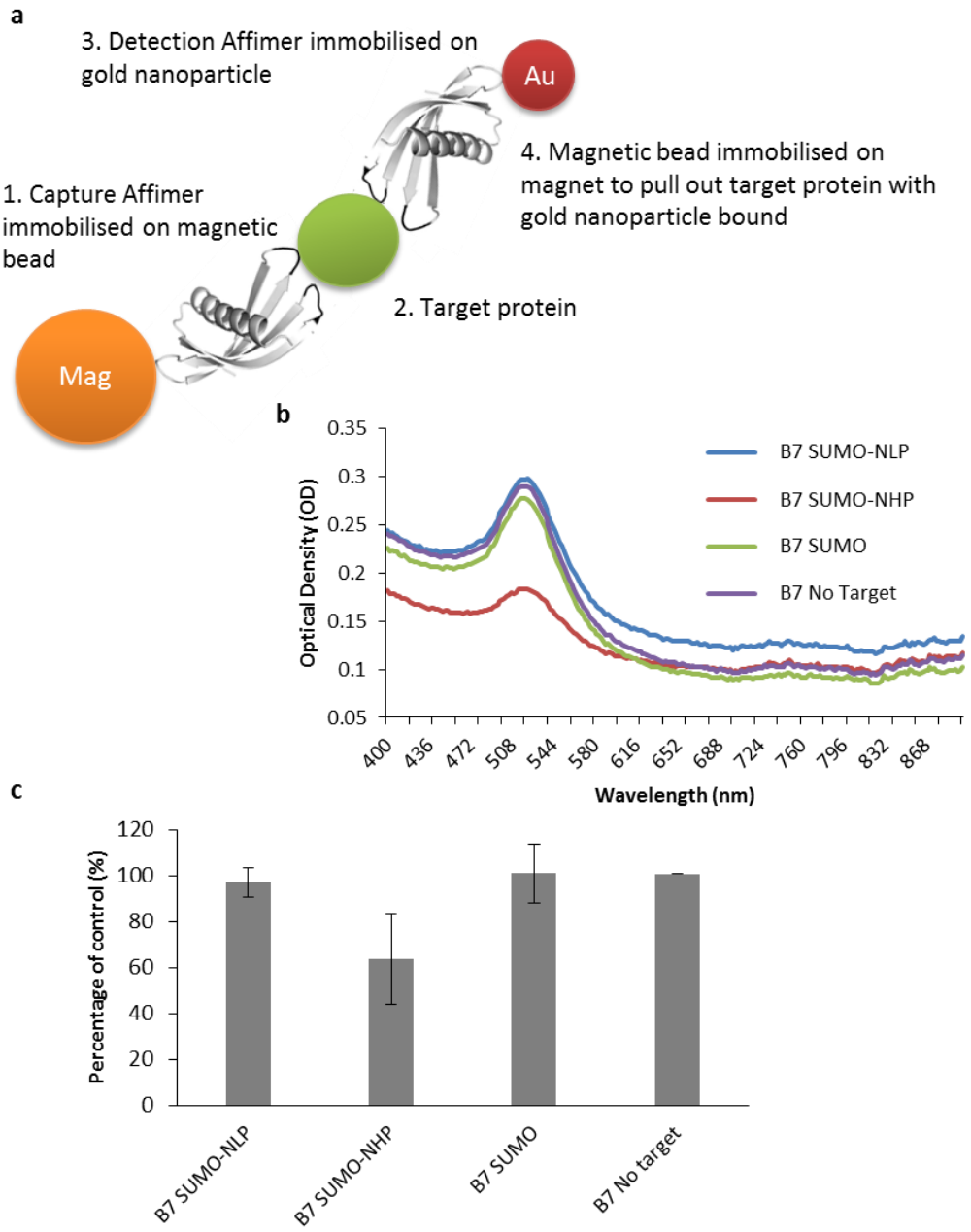

Figure 5.1 Gold nanoparticle-magnetic bead based assay to determine pairs of Affimers against PRRSV N proteins (B7/D12). (a) Schematic representation of Affimer binding to target N protein in a pair wise manner. If the Mag-Affimer-Target-Affimer-Au complex is formed, upon immobilisation on a magnet, the gold will be removed from the supernatant. Removal of GNPs from solution can be confirmed by measuring the absorption spectrum of the supernatant. **(b)** Ultraviolet-visible absorption spectrum of supernatant containing GNPs. The removal of the gold from the supernatant is observed by the reduction of the peak at 520 nm, indicating a successful pair, B7 and D12 were a successful pair to detect the presence of SUMO-NHP. **(c)** The reduction in peak was quantified as a percentage of the control (no target), with a significant decrease in the peak upon the addition of SUMO-NHP when Affimer D12 is bound to the GNP and B7 to the magnetic bead ($p=0.03$).

The same sandwich assay was performed using B3 conjugated to magnetic beads and D12 conjugated to GNPs (figure 5.2). Again, the two Affimers appear to be

able to detect SUMO-NHP in this sandwich assay, with a reduction in the peak value at 520 nm upon the addition of this target into the assay (figure 5.2a). This was quantified from three replicates with a significant decrease in the peak value compared to the control (p=0.005) (figure 5.2b). However, this result was not expected, as it was hypothesised that this pair of Affimers should only recognise SUMO-NLP, as the target NLP was consistently detected in the pulldowns with the magnetic bead bound Affimers, in contrast to SUMO-NHP. However, as a result of these two sandwich assays, it was concluded that both of the combinations of these Affimers would be suitable to detect SUMO-NHP in solution and were therefore taken forward for incorporation into the LFD.

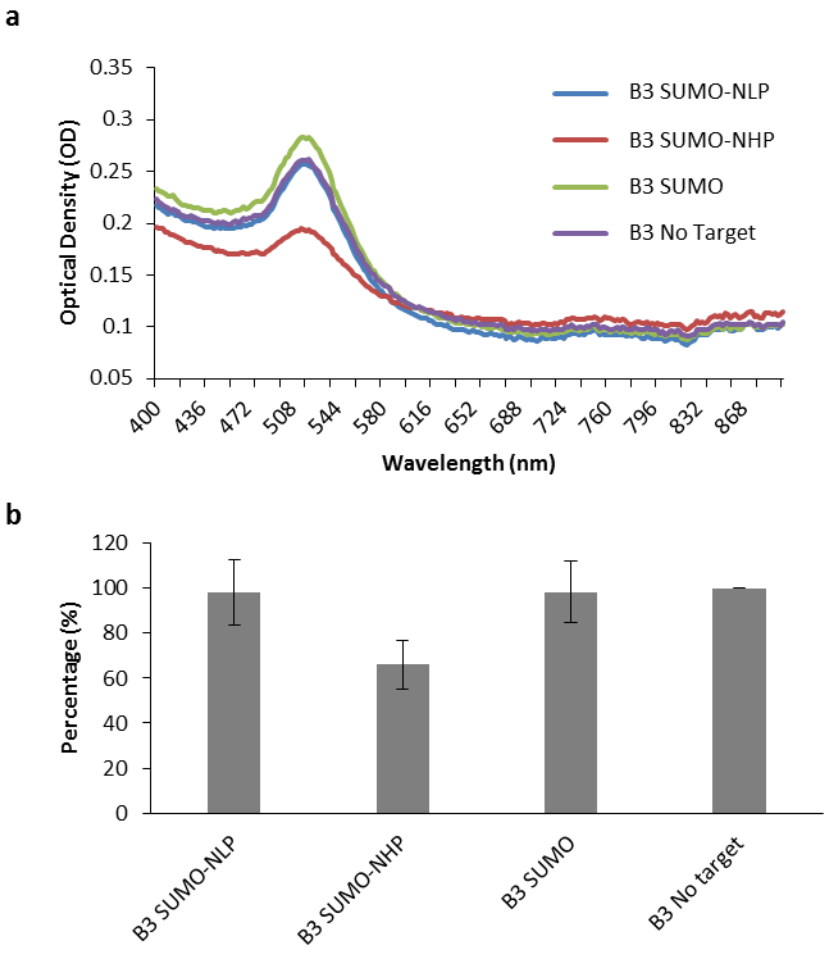

Figure 5.2 Gold nanoparticle-magnetic bead based assay to determine pairs of Affimers against PRRSV N proteins (B3/D12). (a) Ultraviolet-visible absorption spectrum of supernatant containing GNPs. The removal of the gold from the supernatant is observed by the reduction of the peak at 520 nm, indicating a successful pair, B3 and D12 were a successful pair to detect the presence of SUMO-NHP. **(b)** The reduction in peak was quantified as a percentage of the control (no target), with a significant decrease in the peak upon the addition of SUMO-NHP when Affimer D12 is bound to the GNP and B3 to the magnetic bead (p=0.005).

5.3. Development of a control line on nitrocellulose dipsticks

In order for a LFD to be developed for the detection of PRRSV N proteins, it is important to incorporate an internal control line into the device. This confirms the success of the assay and is independent of the appearance of the test line within the assay. This control line is able to identify the detection reagent within the assay (in this case, D12 bound to the GNP) and confirms to the user that this reagent has migrated sufficiently up the nitrocellulose membrane. In the case of this assay, an anti-his antibody was chosen for the control line component, as the Affimer bound to the GNP was labelled with a his_6-tag for purification. The use of an antibody is not ideal, as the purpose of the study was to eliminate antibodies from the device, replacing them with Affimers, however, it is not possible to raise an anti-Affimer Affimer. Therefore, due to time constraints, which did not allow for additional cloning of the Affimers, a his-specific antibody was used to detect the his_6 tagged affimers bound to the gold nanoparticles. Figure 5.3 illustrates the first optimisation steps of the control line using an anti-his antibody. Figure 5.3a is a schematic representation of the production of a dipstick strip containing a control line. Strips were prepared by diluting the anti-his antibody to the dilution shown (1:1000 or 1:250) and striping the antibody onto the membrane using a sequencing tip. The membrane was dried overnight and dipsticks prepared by cutting the membrane into 0.5 cm strips. The streptavidin coated GNPs were prepared with Affimer D12 immobilisation using biotin labelling of the single cysteine present on the sub-cloned Affimer and diluted to OD 1 or OD 0.5 before incubating the GNP with the dipsticks. Figure 5.3b shows the results of the incubation of the dipsticks with the GNPs functionalised with Affimer D12, with no control line appearing at the indicated position for either the 1:1000 or 1:250 dilution of antibody regardless of the concentration of GNPs. It was hypothesised that the concentration of antibody used on the membrane was too dilute for the GNPs to be detected.

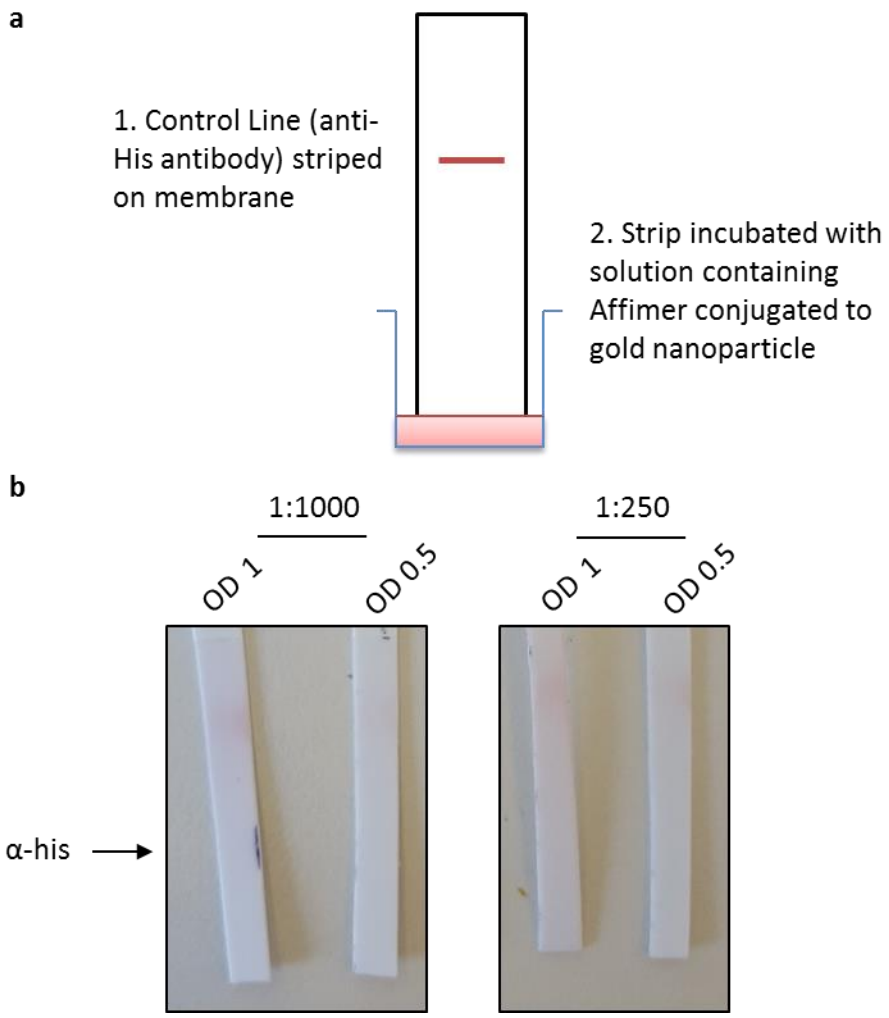

Figure 5.3 Optimisation of the control line for lateral flow device. (a) Schematic representation of lateral flow device using a control line. An anti-his antibody was striped onto the nitrocellulose membrane which detects the C-terminal his_6-tag of the Affimer bound to the GNP. **(b)** The anti-his antibody was striped at a dilution of 1:1000 or 1:250. The Affimer bound to the gold nanoparticle was diluted to OD 1 or OD 0.5. The strips were incubated with the GNPs for 30 mins.

Figure 5.4 shows further optimisation of the control line on the LFD, using 1 mg/ml of the anti-his antibody, which was undiluted from the original stock. Following the incubation of the Affimer functionalised GNPs with the indicated target protein (SUMO-NHP, SUMO-NLP, SUMO or no target), or a dipstick which did not contain striped antibody, a positive control line appeared at the position of the anti-his antibody on the SUMO-NHP and no target dipsticks. It was expected the line would appear on the dipsticks incubated with SUMO-NHP, SUMO-NLP, SUMO and no target protein, however, this was not observed. The detection in this case was of the his_6-tagged Affimers which accounts for the line appearing on the no target strip.

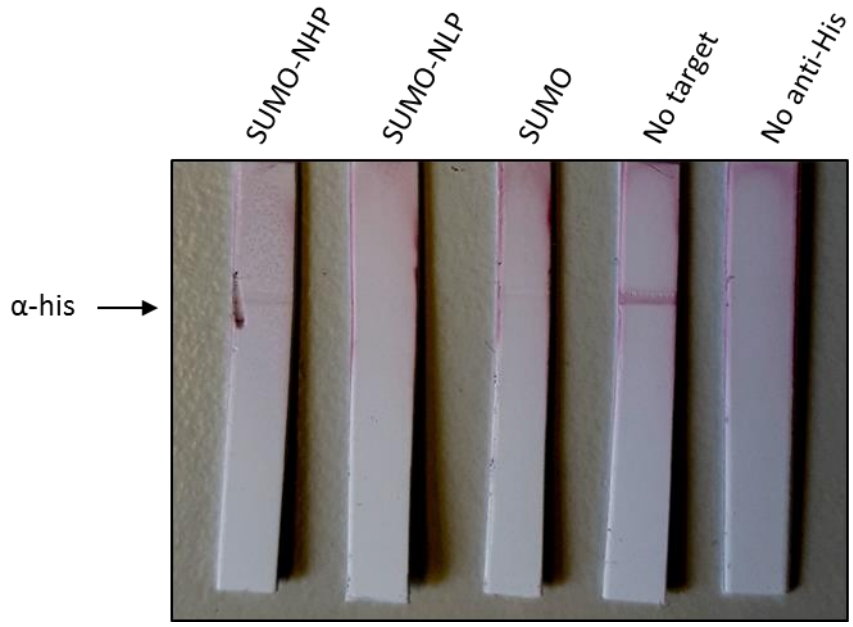

Figure 5.4 Further optimisation of control lines on lateral flow device. Undiluted anti-his antibody (1 mg/ml) was striped and dried onto the nitrocellulose membrane and D12 bound to GNPs was incubated with the target proteins as indicated. GNPs were incubated with the nitrocellulose strips and detection of the bound Affimer confirmed by the appearance of a pink line at the site of the antibody.

As there was no control line on the dipsticks which had been incubated with GNP-D12 in the presence of target proteins, an ELISA was performed to determine if the antibody was able to gain access to the his_6-tag on the immobilised Affimer in solution in the presence of the target protein (figure 5.5.). GNP-D12 was incubated with the target protein and a 1:10000 dilution of anti-his-HRP antibody was added to the solution. Following washing, the binding of the antibody was visualised using TMB and quantified using a microplate reader (figure 5.5). The ELISA confirmed the previous result (figure 5.4) on the dipsticks, that in the presence of the target proteins, there was little binding of the antibody to the Affimer immobilised on the GNP. The lack of wash steps between the addition of the target protein and the antibody was hypothesised to be the cause of the poor detection by the antibody. It is likely the antibody was binding to the excess his_6-tagged target and removed during subsequent wash steps.

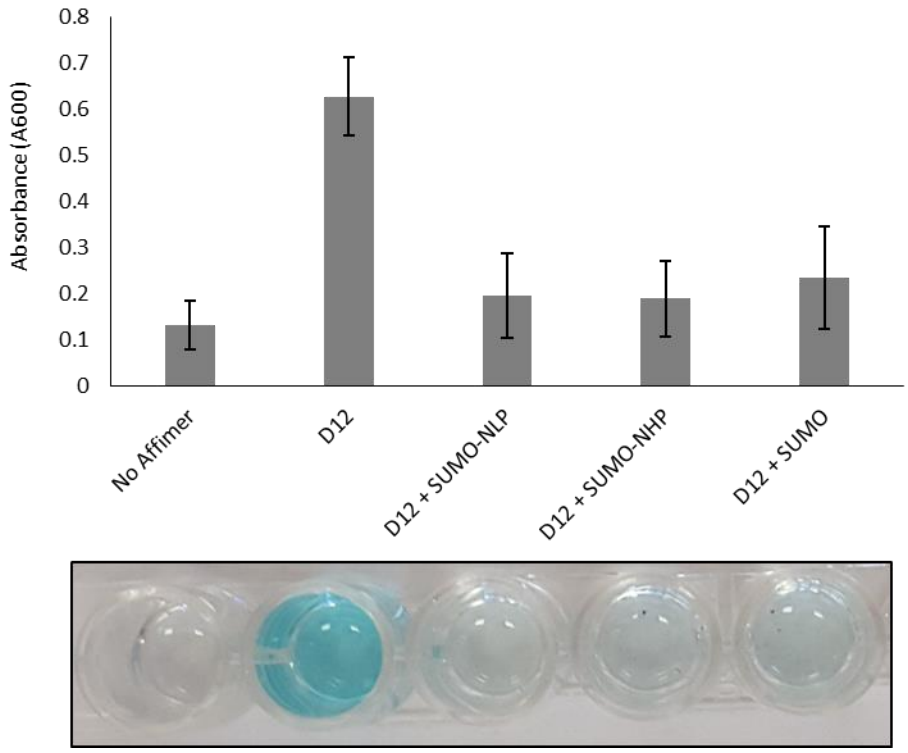

Figure 5.5 Solution based ELISA to confirm the detection of the Affimer C-terminal his_6-tag by the anti-his antibody. D12 was bound to the GNPs and incubated with the target proteins as indicated. Anti-his-HRP antibody was added to the solution and binding was detected with the addition of TMB to give a blue colour reaction and quantified using a plate reader.

In order to overcome this issue, an additional wash step was performed to remove the excess target protein before the addition of the anti-his-HRP antibody. Figure 5.6 shows the ELISA plate following the additional wash steps in the protocol and quantification using the microplate reader. The removal of the excess target protein results in an increase in antibody binding to the immobilised Affimer (or the His_6-tagged protein bound to the immobilised Affimer), and the visualisation of this binding using TMB when GNP-D12 is incubated with the target protein.

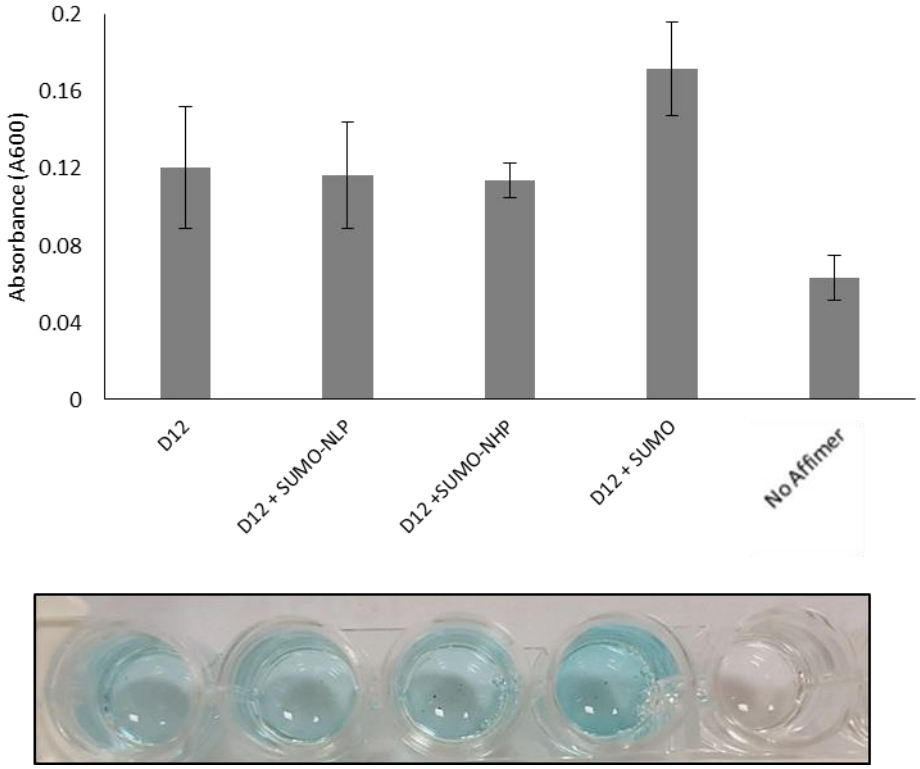

Figure 5.6 Optimisation of solution based ELISA to confirm the detection of the Affimer C-terminal his_6-tag by the anti-His antibody. D12 was bound to the GNPs and incubated with the target proteins as indicated. GNPs were washed three times before the addition of the anti-His-HRP antibody was added to the solution and binding was detected with the addition of TMB to give a blue colour reaction and quantified using a plate reader.

The additional wash step protocol was then incorporated into the assay using the anti-his antibody immobilised on the dispstick (figure 5.7). Removal of the excess target resulted in the formation of control lines as expected on the dipsticks where anti-his was present. The no target control shows that it is the Affimer which is bound to the GNP which can be detected and not the his_6-tagged recombinant protein. However, it is expected that the target proteins contribute to the binding when they are present in complex with the Affimer and it is not possible to distinguish which his-tag is recognised.

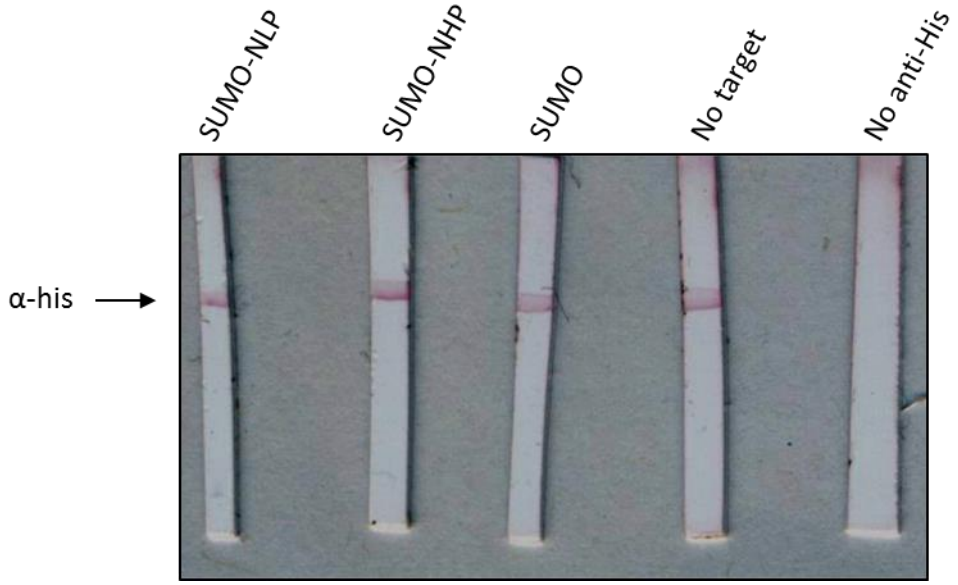

Figure 5.7 Control lines with optimised wash steps for detection of the Affimer C-terminal his_6-tag by the anti-his antibody. Undiluted anti-his antibody was striped and dried onto the nitrocellulose membrane and D12 bound to GNPs incubated with the target proteins as indicated. GNPs were incubated with the nitrocellulose strips and detection of the bound Affimer confirmed by the appearance of a pink line at the site of the antibody.

5.4. Addition of Affimer test line on nitrocellulose dipsticks

At present, it was unknown if the Affimers could be successfully adsorbed onto the nitrocellulose membrane and remain functional. Therefore, they were immobilised onto the membrane using the same protocol for immobilising the antibody control line, before being detected using an anti-his-HRP antibody. The membrane was then developed using a similar technique to western blotting in order to determine if the Affimers could be successfully immobilised on the membrane by drying, before being rehydrated (figure 5.8). The chosen Affimers were successfully adsorbed onto the membrane, and importantly, remained on the membrane upon the addition of buffer and rehydration. Importantly, they could be detected via the his-tag specific antibody.

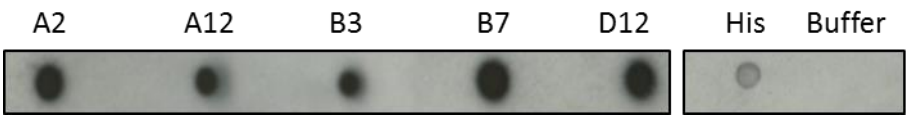

Figure 5.8 Immobilisation of Affimers onto nitrocellulose membrane. Purified Affimer was immobilised to nitrocellulose membrane and dried for 1 hour at 37°C. The successful immobilisation was confirmed with detection of the C terminal his_6-tag of the Affimer using an anti-his antibody. A his_6-tagged protein (SUMO-NLP) and buffer control were used.

Following the successful immobilisation of the Affimer onto the membrane, dipsticks were prepared containing both an Affimer test line (B3 or B7) and an anti-his control line (figure 5.9). These dipsticks were then incubated with GNPs functionalised with D12 and the indicated target proteins. Faint control lines were visible on the dipsticks as indicated (*) for the dipsticks prepared with B3, however, no control lines were visible on the dipsticks prepared with B7. It was hypothesised that the dilution of the GNPs was too dilute in the presence of the target protein and so the dipsticks were saturated with buffer before the GNPs could migrate up the membrane. It is also possible that the presence of excess free target protein (with the his_8-tag) was again interfering with the binding of the captured Affimer and GNPs at the site of the anti-his-antibody as previously discussed (figure 5.4.). Results showed a very faint line at the B7 test line for SUMO-NLP and SUMO-NHP. This could also be attributed to the distribution of the GNPs over both the control lines and the test line being too low, where as in the previous control line only dipsticks (figure 5.7) the GNPs were concentrated only at the anti-his-antibody line giving an enhanced signal.

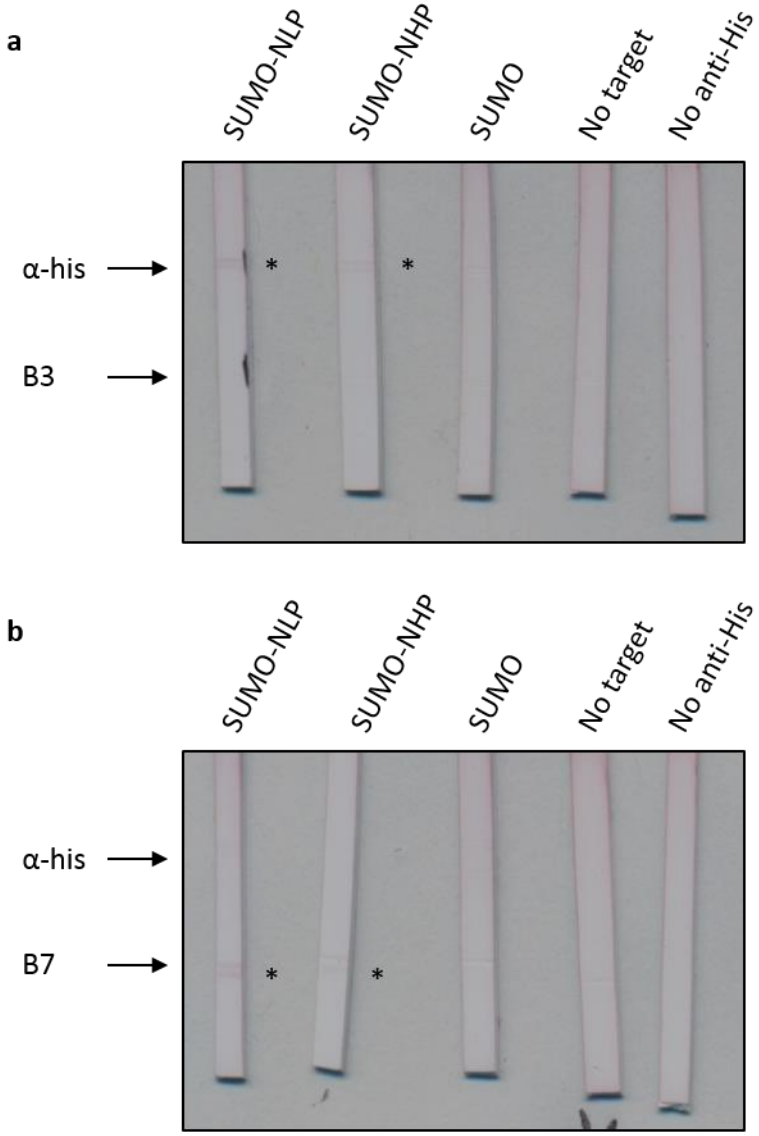

Figure 5.9 Addition of Affimer test line. D12 bound to GNPs was incubated with the target proteins as indicated. GNPs were washed three times before being incubated with the nitrocellulose strips striped with B3 (a) or B7 (b) and detection of the bound Affimer confirmed by the appearance of a pink line at the indicated position. A faint line can be seen at the positions (*).

Due to the reduced signal at the control line seen in figure 5.9 upon the addition of an Affimer control line, further optimisation of the test protocol was carried out. Here, the excess target was removed using further wash steps, as with the ELISA (figure 5.6) and an increase in the concentration of the labelled GNPs was used (20 µl of OD1 instead of 10 µl OD1). The addition of the solution containing the target, bound to GNP-D12, to the dipsticks with immobilised anti-his-antibody and Affimer B3 resulted in the appearance of the control lines as expected on all dipsticks with the exception of the dipstick which contained no antibody (figure 4.10). This

suggests that in the dipstick format, the Affimers B3 and D12 are not able to function as pairs of reagents for the detection of SUMO-NLP or SUMO-NHP, which is contradictory to the GNP/magnetic bead assay (figure 5.2), which had initially shown that this pair of Affimers were able to detect SUMO-NHP.

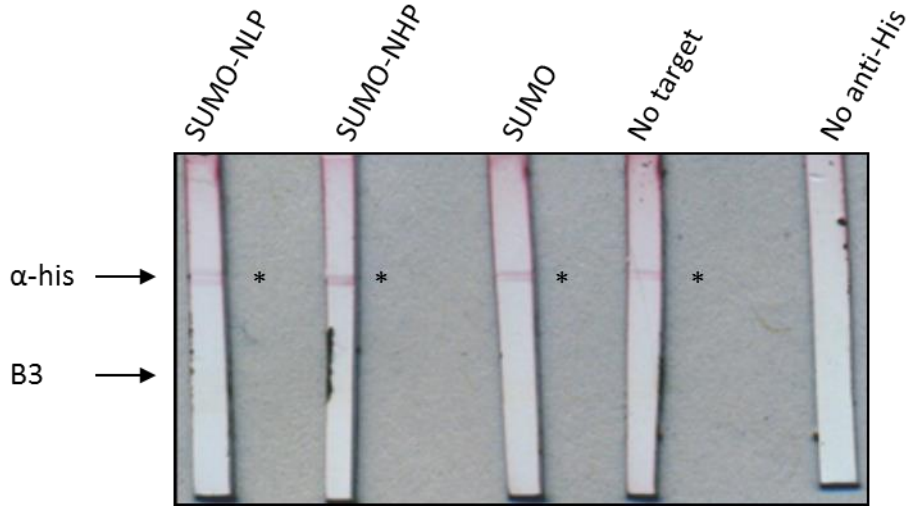

Figure 5.10 Optimisation of Affimer capture line using B3. D12 bound to gold nanoparticles was incubated with the target proteins as indicated. The GNPs were washed three times to remove excess target protein before being incubated with the nitrocellulose strips striped with B3. D12 bound to GNPs was detected at the control lines on all strips (*) except where there was no anti-his present.

Figure 5.11 shows further optimisation of the Affimer test line using Affimers B7 and D12; again the concentration of the GNPs and the number of washes were increased to remove the excess target and to increase the signal. The dipsticks are representative of three replicates and show that these Affimers are able to detect the presence of SUMO-NLP and SUMO-NHP within the sample, with the confirmation of a successful test by the appearance of the control antibody line. This test has confirmed that it is possible to use Affimers as replacements for antibodies within a lateral flow device and thereby proving the hypothesis of the study.

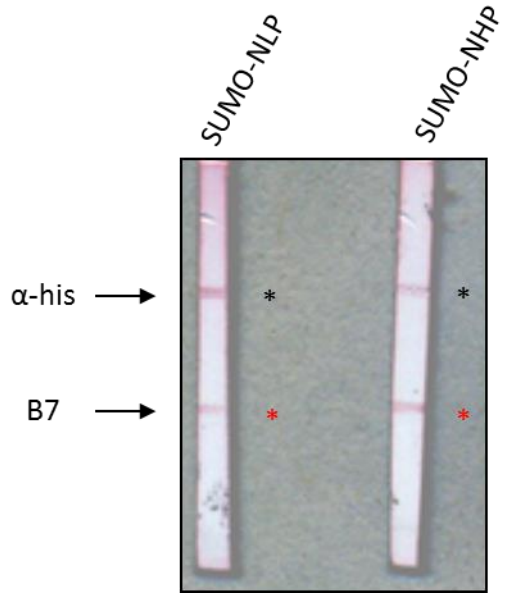

Figure 5.11 Optimisation of Affimer capture line using B7. D12 bound to GNPs was incubated with the target proteins as indicated. The GNPs were washed three times to remove excess target protein before being incubated with the nitrocellulose strips striped with B7. D12 bound to GNPs was detected as indicated (*). The presence of the lower line on the SUMO-NLP and SUMO-NHP strips indicates the detection of these target proteins within the sample (*).

5.5. Discussion

The use of a GNP/magnetic bead assay (Zhou *et al*., 2015) to determine the ability of the identified Affimers to function as pairs of reagents was significantly more reliable than the previously discussed ELISA methods (Chapter 4). It was confirmed that D12 was able to function as a pair with both B3 and B7 able to detect SUMO-NHP within a sample. Although this was a solution based assay, it was assumed that the functionality of the Affimers would remain upon their immobilisation onto a solid state platform. Despite this, a number of challenges were presented with the development of the LFD. As the Affimer reagents had never been used in this application before, optimisation of the required protein concentrations was required as well as the required concentration of the GNPs and target protein.

The most important component of a LFD is the internal control line which confirms that the test has been performed successfully, independent of the appearance of the test line. It is important that this line appears on every LFD used as a test and if it is absent, the test must be discounted. Unfortunately it is not possible to raise an Affimer against an Affimer due to the similarity in structure and sequence despite

the changes in loop sequences. Therefore, an alternative test line was required for the control line in this test. The ideal method for producing a reagent for the test line in this case would be to clone a large tag onto the detection Affimer (D12) for example, maltose binding protein (MBP), GST or SUMO and raising an Affimer against the tag which would then be used as a control line. Affimers have been raised against the yeast SUMO proteins, confirming that this would be an example of a suitable tag to use in the development of a suitable control line in the future (Tiede *et al*., 2014). However, for the purpose of this LFD and as a proof of principle, an antibody control line was chosen, in this case an anti-his-antibody to detect the his_6-tag on the detection Affimer. This was chosen as it is already well documented that antibodies can be used in LFDs following the patent of the immobilisation of antibodies in this manner (Grubb & Glad., 1979). However, this control line was not ideal due to the his_6-tag present on the target proteins for purification, N-terminal to the SUMO-tag. This presented a challenge with the use of an anti-his-antibody as the control line. The target protein that is not captured by the Affimer-GNP is able to migrate up the nitrocellulose membrane faster than the target protein captured by the Affimer on the GNP due to the size discrepancy. Therefore, if there is excess target present in the sample, the control line is saturated with uncaptured target protein by the time that the captured target reaches the antibody and the colourimetric change cannot be detected (Verma *et al*., 2015). Although this poses a problem in the development of the biosensor in this study, it is overcome with the detection of native, untagged viral proteins within a clinical sample.

The results presented in this chapter demonstrate for the first time the use of novel non-antibody binding proteins in a LFD for the detection of a viral protein within a sample. Although preliminary experiments do not conclusively demonstrate the ability of the Affimers chosen in this study to discriminate between the two PRRSV viral strains, they do provide exciting data as to the scope for the use of these reagents within a LFD. The Affimers were successfully immobilised onto a solid state platform and they remained at the immobilisation site upon rehydration as well as remaining functional in their ability to detect the target proteins. These key features of reagents used in LFDs lead us to believe that

further optimisation of the Affimers on a LFD platform will provide scope for the production of a wealth of these POC devices against a wide variety of pathogens in the future.

Chapter 6

Discussion

6. Discussion and future perspectives

This thesis investigated the suitability of novel Affimer reagents for use in point of care (POC) lateral flow devices (LFDs) for the direct detection of PRRSV N protein in clinical samples. PRRSV was chosen as the proof of principle viral infection as it is a hugely economically damaging infection of swine and is under reported and poorly controlled in many regions of the world (Lunney *et al*., 2010). This is partly due to the poor identification by animal producers but also as a result of poor biosecurity and lack of viable preventative and treatment measures, such as vaccines and anti-viral reagents (Arruda *et al*., 2016). The situation is further worsened by the lack of affordable, reliable and fast diagnostic tests available in the worst affected areas, allowing the virus to spread undetected between large numbers of animals (Chand *et al*., 2012). Therefore, in addition to assessing the suitability of Affimers in LFDs, the thesis demonstrated the feasibility of developing a cheap POC device for PRRSV, which is not currently available. This proof of concept study has shown Affimers can be used as replacements for antibodies in basic LFDs, for the direct detection of a viral protein, in this case the swine virus PRRSV N protein as the detection antigen. Compared to antibodies, Affimers are cheaper and easier to produce and remove the requirement of animals in the production process, making them a desirable alternative reagent for this purpose. The findings suggest that Affimers are indeed strong candidates for antibody alternatives in LFDs.

This is the first study to investigate the application of non-antibody binding proteins in a LFD. To this point the LFD has been developed to the stage of a functional dipstick device. In order to progress to a fully integrated LFD, further components are required. These include the addition of a conjugate pad containing the detection reagent as well as the assembly of the device into the plastic casing to produce the final POC device. The detection reagent also requires further development, in this thesis an antibody detection reagent was used. For the elimination of antibodies from the device entirely, it would be possible to use a detection Affimer tagged with a protein, for example Sumo or GFP and raise an Affimer against the protein tag to use as the control line reagent in replacement of the antibody.

6.1. PRRSV Affimers - application in LFDs

The production of the Affimer reagents against PRRSV N proteins was relatively straightforward with two pools of reagents produced, one for each of the two viral strains of N protein, collected from three successive screening rounds. It was anticipated that the screening of these proteins to identify Affimer reagents would result in a level of cross reactivity of Affimers between the two strains due to high sequence homology (the two strains chosen in this study have a sequence homology of 93.5%). As expected, some cross-reactivity was observed within the pools of Affimers, likely because the Affimers were binding in a structure or sequence specific manner, conserved between the proteins. Although the aim was to produce Affimers to discriminate between the two proteins, this cross-reactivity was useful as the LFD required a reagent that could detect both of the target proteins. Despite the cross-reactivity, a total of 5 Affimers were able to differentiate between strains, identifying one specific strain of the viral N protein. This highlights a significant advantage of the Affimer technology. Although this pool of Affimers was able to detect the N proteins in solution, it was unknown if they would remain functional following dehydration prior to immobilisation onto a nitrocellulose membrane. To add further complexity, it was proposed that the device would detect the N protein from both PRRSV strains on one strip. A further problem to address was the ability of the Affimers to detect the target protein in the context of swine serum to ensure the device was clinically relevant. The study has shown that these issues have been addressed and successfully overcome, with the Affimers functioning as detection reagents once immobilised and dehydrated, as well as in the presence of a clinically relevant sample containing 'contaminating proteins' which may have interfered with Affimer-N protein interactions.

Since first documented in 2014 (Tiede *et al*., 2014), Affimers have been raised against over 300 target proteins/molecules and their suitability for a number of uses has been quickly established (Tiede *et al*., 2017). It can be argued that Affimer reagents are not only competitors against antibodies, but also other non-antibody binding proteins discussed in this study. These other binding proteins have predominantly been shown to function as potential replacements for therapeutic antibodies, however, AdNectins™, Affibodies, DARPins and nanobodies have also

been used in a number of molecular biology techniques (Kim *et al*., 2017; Gilbreth *et al*., 2011; Binz *et al*., 2004; Moon *et al*., 2016; de Bruin *et al*., 2016; Platonova *et al*., 2015; Ries *et al*., 2012). Affimers, however, have shown great potential for use as direct antibody replacements in a number of molecular biology techniques, whilst also being candidates for therapeutic reagents for example targeted delivery of drugs, pending further investigation (Tiede *et al*., 2017; Xie *et al*., 2017; Bedford *et al*., 2017; Johnson *et al*., 2012).

When considering the commercial value of these reagents, it is important to appreciate their clinical relevance; Affimers have already been raised against Zika virus. There was recently a much discussed and unprecedented Zika virus outbreak affecting the South Pacific region, with a strong correlation observed between infection during pregnancy and birth defects (Sarno *et al*., 2016). Due to the locality of the infection, which closely aligns with the regions affected by dengue fever virus, it was nearly impossible to diagnose infection beyond the acute phase as they share common symptoms, however, the added complication of asymptomatic Zika infection also hampers diagnostic testing (Weaver *et al*., 2016). With this in mind, Affimer reagents were raised against a Zika virus target protein. Three Affimer binders were identified 13 weeks after receiving the viral target. Like the Affimers identified in this study, the binders were raised against a viral protein, in this case NS1. The reagents were tested for specificity and cross-reactivity between closely related viruses (dengue virus, yellow fever virus, West Nile virus and Japanese encephalitis virus) and were shown to be specific for Zika virus (Avacta, 2016). The ability of the Affimers to distinguish reliably between closely related viruses and those that share similar symptoms is an important step forward in the case of Zika virus diagnosis. The incorporation of these reagents into a suitable diagnostic platform, such as LFDs as used in this study, would allow for rapid and accurate diagnosis, particularly useful for couples in, and travellers returning from, affected regions when planning pregnancies.

Although this study investigates the implementation of Affimers into a LFD, it is not the first time these reagents have been incorporated into diagnostic platforms. Affimers have been shown in label free biosensors where electric impedance is

measured. The binding of IL-8 was detected without the requirement for labelled reagents, upon binding of IL-8 to the immobilised Affimer the change in electrical impedance was measured. This was performed using spiked serum as the clinical sample, similar to the approach taken with the clinical sample used in this study. This supports the results shown in this study and illustrates that the Affimers are sensitive enough to detect antigen concentrations in the pM region when immobilised (Raina *et al*., 2015; Sharma *et al*., 2016). The LFD designed in this study did not eliminate the use of antibodies entirely due to time constraints and the aim of illustrating Affimers can function in this platform. However, the production of a combinational chemiluminescence assay using Affimers and antibodies has been shown for the detection of a hepatocellular carcinoma biomarker (GPC3). The Affimer was used as a capture reagent and the antibody as the detection reagent, comparing the results of the combination assay with the dual antibody assay. The nature of the Affimer reagents, specificity for the target protein, meant that the Affimer-antibody assay was able to distinguish between the carcinoma it had been produced to detect whilst eliminating other liver diseases from the diagnosis. The improvement of sensitivity was increased by 36-65% in the dual antibody assay to 62.5% in the combination assay while specificity was shown to be improved to 92.3% from a range of between 55-100% in the dual assay (Xie *et al*., 2017). The increase in specificity and sensitivity is likely due to the greater sensitivity of the Affimers to the target antigen compared to the antibody counterpart as a result of the initial screening process carried out to identify suitable Affimer reagents. This combination approach has shown that Affimers can at least compete and perhaps outperform antibodies in commonly used assays. It would be interesting to explore any further improvement to specificity using a dual Affimer assay.

Until now, the preferred application of non-antibody binding proteins in diagnostic techniques has been their incorporation into ELISA assays, due to their sensitivity (Hausammann *et al*., 2013). As such it has previously been more common to find DNA or RNA aptamers as replacements for antibodies in LFDs and other diagnostics (Chen and Yang, 2015a; van den Kieboom *et al*., 2015).

Ordinarily, LFDs detecting any viral infection use antibodies directed against the host antibody response to an infection as this is usually easier to detect than the pathogen itself. Due to the intracellular nature of viral lifecycles it is likely that in the context of infection there is a much higher concentration of these antibodies within the clinical samples than the viral antigens themselves. However, in the case of PRRSV, antibody response to an infection can take more than a week and commonly longer for detectable N protein antibodies (Ferrin *et al*., 2004). Considering the N protein is the major immunogenic protein, it is therefore likely that early detection of this virus would be impossible at the pen-side by detecting the antibody response alone. Conversely, it is possible to detect very small viral loads in clinical samples using techniques such as PCR, where viremia can be detected as early as 12 hours post infection (Rossow *et al*., 1995). However this cannot be performed pen-side and is invariably more costly due to staff and reagent costs. Detection of viremia at such early time points post infection would suggest that viral antigens may be detectable by a device targeted at them at similarly early time points. With this in mind, the PRRSV N protein was chosen as the candidate for early and direct viral detection. The protein is the ideal candidate, as well as comprising a large proportion of the virion (40%), it is also produced in excess of its structural requirements, due to its additional roles in virus biology (Meulenberg *et al*., 1995). As high levels of antibodies are produced against the N protein during infection it was likely that it could be detected at sufficient levels in clinical samples, as was shown with a number of other virus N proteins (Singh *et al*., 2004; Xu *et al*., 2007; Jansen van Vuren and Paweska, 2009; Lau *et al*., 2004).

The novel nature of Affimer reagents meant that it was unknown how they would perform in many aspects of the LFD development process. As well as being immobilised, they also were required to migrate along a membrane whilst maintaining their ability to recognise their target protein. A key feature of the device is the immobilisation and dehydration of the Affimer reagents at the test line site. It was not known if this would result in the proteins becoming denatured or if they would be able to maintain functionality once rehydrated. Importantly, the Affimers were indeed shown to maintain their binding ability to the target

sample upon rehydration, suggesting that they retained their structural integrity during the dehydration and rehydration processes. Due to time constraints of the study, the Affimers dehydrated on the membranes were not stored for longer than 24 hours before rehydration and so it is not possible to comment on the long term storage stability of these reagents. It is likely that the Affimers will be stable once immobilised onto the nitrocellulose membrane for a number of weeks if not months if they are kept at an ambient temperature and not exposed to moisture. Their small size lends itself to compact packing onto the membrane and along with their beta-barrel structured nature we can infer that unfolding is not likely to occur if stored correctly. Antibody based tests have been shown to be stable for 2 years post manufacture if stored according to the manufacturer's instructions (Life Assay Diagnostics. 2010). Affimers have been shown to be stable in solution up to approximately 100 °C (Tiede *et al*., 2014), suggesting they would be suitable for use in both temperate and tropical temperatures, vital for the incorporation into a diagnostic against PRRSV which is a global disease. This is also important regarding their use in this format for tropical diseases, where diagnostics containing antibodies, are often less stable at high temperatures, compared to the Affimer.

The detection Affimer conjugated to GNPs was not evaluated for its response to dehydration onto a conjugate pad in this study, although it is likely that this would not be a disadvantage to the Affimer functionality, considering the results of the non-conjugated counterparts. The LFDs were tested as LF dipsticks with the conjugate Affimer provided in solution. This allowed the samples to be tested more quickly and removed the variables associated with the conjugate Affimer also be immobilised during early testing, when the basic functioning of the Affimer reagents was not known in this format. Despite this, LF dipstick tests would also be a suitable user-friendly pen-side test. It would be possible to provide a sample of the detection reagent in solution to be added to the clinical sample before incubation with the test dip-stick. This present work has shown that Affimers have strong potential for use in the development of LFDs for the detection of viral proteins in clinical samples which can be easily and quickly expanded to multiple economically and clinically relevant diseases.

The most important feature of these tests, next to antigen recognition, is device sensitivity. It is important that the maximum sensitivity is achieved in order to provide early and conclusive diagnosis. The sensitivity of Affimers in LFD was not evaluated in this study and so the lower detection limit is currently unknown for the PRRSV N protein in a clinical sample, although this has previously been mentioned to be in the pM region for other Affimers (Raina *et al*., 2015). Of course, as there is currently no alternative antibody based detection device for this infection, it is not possible to draw a comparison of the sensitivity and specificity of the LFD. It would therefore be interesting to produce an Affimer LFD that could be used to provide a direct comparison, for example, human pregnancy tests detecting hCG. Alongside sensitivity, it is also important that the LFD is able to accurately diagnose the correct infection. Although this is straightforward for the host specific arterivirus PRRSV, it may not be so simple for viruses that infect multiple hosts or share common symptoms, for example FMDV and swine vesicular disease (SVD), which are often clinically indistinguishable. Both of these diseases are notifiable in the UK, but it is vital when considering the response to correctly diagnose the infection (Gov.uk. 2015).

The sample used in this study was swine serum spiked with recombinant protein and therefore it is necessary to test this diagnostic approach using a virus-infected sample. A range of samples (urine, semen, faeces and blood) also needs to be investigated, as well as the requirement for simple sample processing for example the incorporation of filters into the device. A number of patented filtration devices are available, particularly for the filtration of whole blood samples, which could be employed in the LFD (Patent Numbers: (US)5240862 (Koenhen and Scharstuhl, 1989), (WO)9610177 (Scharstuhl and Shaikh, 1995), (WO)9603194 (Pall and Manteuffel, 1995)).

Although this study was performed using two viral strains of PRRSV, the results will be vast and far reaching. This proof of concept study has shown that Affimers can be raised against an economically important target in order to improve upon the diagnosis of a damaging disease. Perhaps more excitingly, these devices and technology have multiple clinical applications for the detection of not only

veterinary illnesses, but also human diseases. Affimers have already been identified against a number of cancer biomarkers and viral proteins (Xie *et al*., 2017; Tiede *et al*., 2017). The simplicity of the LFD construction compliments the relatively rapid screening process required to isolate a pool of Affimer reagents against a target protein. The combination of the two lends itself to the production of diagnostic devices against diseases which could ordinarily only be detected in the laboratory. An example of this could be the production of a LFD which can detect the presence of Ebola virus. The location and nature outbreaks of this virus means that there are often very few laboratory resources for the analysis of samples using PCR, ELISA or virus isolation (Broadhurst *et al*., 2016).

6.2. Use of Affimers to overcome antibody limitations

The production process of Affimers can also overcome the difficulty of mutagenic viruses and viruses with homologous proteins. RNA viruses like PRRSV are highly mutagenic and so it is not guaranteed that the reagents (Affimers or antibodies or DNA or RNA aptamers) used in diagnostic tests will always identify the proteins of interest during a prolonged outbreak. If a mutation occurs during an outbreak at the epitope of the protein where the reagent binds the test becomes redundant. Phage display production of Affimers offers a clear advantage over antibody production in this case. A number of proteins (strains of proteins or individual viral proteins) can be screened at the same time reducing the time to produce reagents. The Affimer production process can also be exploited in this instance, screening of target proteins often produces an excess of binders and Affimers from each screening round is stored. These stores can be revisited if a mutation occurs, without beginning the process from scratch, to identify Affimers which recognise a different protein sequence or structural region of the mutated/homologous target antigen. If using antibodies in this way, depending on the method of antibody production, it is feasible that each mutated protein would have to be used to inoculate individual animals, making the process lengthy and ethically controversial. This is also a consideration for targets screened as peptides rather than proteins as mutations may not occur in the screened peptide sequence for further screening post mutation. The production of Affimer based LFDs can also be

easily modified to detect a number of viral antigens giving increased sensitivity and the reduction in false positive or false negative results. A multiplex system can also be employed to include a number of Affimers binding to different epitopes of one protein as it is unlikely that a mutation would occur at the covered epitopes at the same time, hence prolonging the life of the device during an outbreak. Multiplex devices using antibodies have been produced to detect mycotoxins (Song *et al*., 2014), antibiotic detection (Chen *et al*., 2016) and multiple FMDV strains (M. Yang *et al*., 2015b) and DNA aptamers used in papillomavirus detection (Xu *et al*., 2014).

The screening process of Affimers can also incorporate the addition of negative screening, if a protein is known to have homologues of a similar structure or sequence, these homologous proteins can be used within the screening rounds to eliminate Affimers in the pool of reagents which bind to both the target and homologous proteins, further raising specificity and reducing false positive results on the final test. It is also difficult to obtain this kind of specificity within the antibody production process as only one antigen can be use in the inoculation in order to prevent cross-reactivity.

In addition to the improved specificity of Affimer reagents compared to antibodies, there is also the consideration of the impact of Affimers on the reduction of the use of animals in the production process of detection reagents. Antibody production for research and development processes uses a large number of animals, ordinarily 1-3 per target (of which not all immunisations are successful and repetition is required using higher numbers). Commercial development of Affimers is underway at Avacta for Affimer use as therapeutics and reagents for research and diagnostic applications and it is predicted that current use of these Affimer reagents could reduce the number of procedures carried out on animals by between 360 and 960 per year. This would increase dramatically with widespread uptake of the technology with the potential to remove the need for animal procedures entirely (CRACKIT, 2015).

6.3. Affimers and clinical diagnostic applications

Affimer based LFDs have huge potential for use in a clinical setting for the diagnosis of cancer, a prominent disease which is increasing in prevalence. Although the

treatments for this disease are improving, the prognosis of this disease in a lot of cases would be dramatically improved with early diagnosis (Miller *et al*., 2016). Often cancer diagnosis is made following the biopsy of a solid tumour and this can be associated with late diagnosis. However, it is known that there are a huge numbers of endogenous proteins that are upregulated in cancerous cells, many more than can be discussed (Hanahan and Weinberg, 2000; Singh *et al*., 2017; Hanahan and Weinberg, 2011). It is possible to detect some of these hallmarks of cancer in the blood (Werner *et al*., 2016; Xie *et al*., 2017). Therefore the identification of Affimers against these proteins provides ideal candidates for the production of a LFD that could detect the presence of cancerous cells rapidly and in a non-invasive manner. Again, as with viral infections, such tests can be made multiplex to detect a number of upregulated proteins on one device to provide improved accuracy of diagnosis. Previously this analysis would have been performed in the laboratory using techniques such as PCR, flow cytometry and mass spectrometry. The production of reliable point-of-care diagnostics for such important diseases would not only improve prognosis of patients from early diagnosis but also reduce the cost of laboratory testing and potentially reduce treatment costs.

Prostate cancer has been diagnosed with the assistance of a blood test for a number of years using the levels of prostate-specific antigen (PSA). PSA is found in the serum of most men, however, it is upregulated in many patients suffering prostate cancer (above 4 ng/ml). Although a quantitative analysis of the PSA levels is required in the diagnosis of prostate cancer, the vast research into this protein and its relation to prostate cancer provides a basis for the development of a multiplex test which, when used in combination with other techniques, would enhance the diagnostic process. In the case of prostate cancer, it may be advantageous to combine the detection of PSA with another prostate cancer biomarker such as α-Methylacyl coenzyme A racemase (AMACR) or thymosin β15. It is possible to detect these proteins in a urine sample, a suitable sample for LFDs (Bolduc *et al*., 2007; Ploussard and de la Taille, 2010; Hutchinson *et al*., 2005). Affimers raised against these proteins and incorporated into a LFD would provide a more conclusive test for the presence of prostate cancer before more invasive

approaches are taken. Critically, the relatively low cost of the production of Affimer-based LFDs means that they are highly suitable as diagnostics in the developing world where more expensive diagnostics are not currently available.

Ultimately, the restriction of Affimer use in LFD is the ability to raise reagents against the protein of interest and the availability of relevant proteins within clinical samples. Therefore, the potential of these reagents is vast; it is possible to modify the production process for difficult target proteins, for example using small exposed peptide regions of membrane bound proteins which are difficult to purify (Tiede *et al*., 2017).

6.4. Additional uses of N protein Affimer reagents

As well as the use of these Affimer reagents in the development of diagnostic devices for PRRSV, they are also potential candidates for the detailed study of the molecular biology of PRRSV. There is currently no suitable structural information of the entire PRRSV N protein (Doan and Dokland, 2003). However, it is possible that the Affimers could be used to aid in the crystallisation process of the complete N protein as chaperones of folding. Binding of these reagents could constrain less structured regions of the protein, promoting crystal packing whilst in addition also identifying the binding sites of the Affimers. Using protein scaffolds as chaperones in the crystallisation process, has been previously successful using other non-antibody binding proteins (nanobodies, AdNectins™ and DARPins) (Rasmussen *et al*., 2011; Staus *et al*., 2016; Gilbreth *et al*., 2011; Bukowska and Grütter, 2013; Schilling *et al*., 2014). Epitope binding of the Affimers to the N proteins in this study is not known and so it is yet to be determined if the reagents are binding in a conformation specific or sequence specific manner. It may be possible to perform *in silico* docking of these Affimers using the truncated structure of the N protein available. In addition to structural investigation, it would be interesting to employ these reagents in the study of virus biology. Affimers have been expressed in cells in tissue culture to investigate intracellular signalling pathways (Tiede *et al*., 2017), and it would be interesting to probe their function in disrupting the viral life cycle of PRRSV. It is likely that the expression of Affimers targeting the N protein in cell culture would result in the attenuation of the virus as a result of the disruption of

virus assembly, as the N protein is a major structural protein. It may also provide further insights into the role of the N protein in the host cell response to infection, attenuating the activity of the N protein using Affimer binding, it may be possible to determine the role the N protein has on immune evasion and response. Expression of recombinant N protein alongside the Affimers and analysis of protein-protein interactions would also be interesting to investigate. As previously mentioned, in 2012 a proteomic study was performed using the PRRSV N protein to investigate N protein-host cell interactions (Jourdan *et al*., 2012). Using the generated Affimers to try to disrupt of the N protein-host cell interactions may provide further clues as to the function of the N protein in addition to its structural role. It may also be possible to further probe the trafficking of the N protein in and out of the nucleus and nucleolus using Affimers if they are able to block the NLS regions of the protein (Rowland and Yoo, 2003). This would be exciting in the context of viral lifecycle as it is currently unknown why the N protein traffics through these sub-cellular regions. To date, NLS null PRRSV N proteins have been utilised to probe the role of the N protein in the nucleus and nucleolus. Results showed that virus replication was attenuated, however, there was a high rate of reversion to wild type nucleolar localised protein, suggesting an essential role of the nuclear/nucleolus on PRRSV biology (Lee *et al*., 2006). Using the Affimer reagents would overcome the problem of reversion to wild type and perhaps provide a greater insight into the requirement of this trafficking.

Affimers also hold the potential for use as therapeutic reagents for PRRSV, for which there are no available anti-viral drugs. Affimers have been shown to function as tools for *in vivo* imaging, following injection into the body (Tiede *et al*., 2017). The successful delivery of Affimers to the location of the tumour to be imaged, suggests that it would be possible to target Affimers against essential proteins of PRRSV. As viral replication occurs intracellularly, it is unlikely that Affimers targeting the N protein would not be relevant for this approach unless an efficient method of Affimer delivery into cells can be developed. Currently is it possible to transfect plasmids encoding Affimers into cells *in vitro*, however, delivery of these scaffolds through the cell membrane is more difficult. A number of approaches have been taken for the delivery of proteins into the cell for

therapeutic means, for example, the use of biodegradeable polymersomes, liposomes and cell-penetrating oligopeptides and these could be investigated for the delivery of Affimers intracellularly (Liu *et al*., 2010; Aryasomayajula *et al*., 2017; Tashima, 2017). The simplest method by which the Affimers could be delivered to cells would be by the addition of a cell-penetrating peptide (CPP), the most widely studied being the *trans*-activator of transcription factor (TAT) from HIV-1 (Frankel and Pabo, 1988). Since the discovery of TAT, the delivery of target molecules into cells has been further developed and small molecule mimics have been used for efficient transport of proteins into the cell (Okuyama *et al*., 2007). Recently a patent was filed (US 9657064 B2) using the ZEBRA CPP from Epstein-Barr virus to deliver protein cargo to cells. Whilst the delivery method would have to take into consideration the targeting of Affimers to affected cells, the specificity shown by these molecules to their target proteins is very high, reducing the likeliness of off target effects if the Affimers encountered non affected cells. The reduction of off target effects is highly desirable for the treatment of diseases such as cancer, where current chemotherapy drugs are non-specific for cancer cells. The successful delivery of an Affimer targeted against cancer cells could revolutionise the treatment of these diseases.

In addition to the intracellular delivery of Affimers targeting PRRSV, during acute infection, Affimers that bind to the envelope glycoproteins of PRRSV may be functional in the prevention of virus entry into cells, reducing viremia, virus shedding, clinical symptoms and length of infection. In the case of veterinary diseases like PRRSV, Affimers are likely to be suitable 'drugs' as they are very small and it is predicted that the clearance of these proteins from the body swift, important for animals entering the food chain (Tiede *et al*., 2017). If Affimers were shown to possess anti-viral properties, this would not only be an advantage to PRRSV but also other viruses previously discussed such as, Zika and Ebola as well as influenza. Targeting a virus using multiple Affimers covering a broad spectrum of viral proteins or against a number of epitopes of fewer proteins has the potential to be more successful than using small molecule inhibitors that can often become redundant quickly during infection due to mutation rates of viruses.

Perhaps the most exciting find of this study is the confirmation of a new application of Affimers as molecular biology tools. As the uses of these reagents are more widely explored, it is becoming evident that they are able to match or outcompete antibodies in the majority of applications; they are user friendly, can be easily validated and above all are renewable, ethical resources.

7. References

A Hicks, J., Yoo, D. and Liu, H.-C. 2013. Characterization of the microRNAome in porcine reproductive and respiratory syndrome virus infected macrophages. F. C. C. Leung, ed. *PloS one*. **8**(12),p.e82054.

Ahlquist, P. 2006. Parallels among positive-strand RNA viruses, reverse-transcribing viruses and double-stranded RNA viruses. *Nature Reviews Microbiology*. **4**(5),pp.371–382.

van Aken, D., Zevenhoven-Dobbe, J., Gorbalenya, A.E. and Snijder, E.J. 2006. Proteolytic maturation of replicase polyprotein pp1a by the nsp4 main proteinase is essential for equine arteritis virus replication and includes internal cleavage of nsp7. *The Journal of general virology*. **87**(Pt 12),pp.3473–82.

Alagaili, A.N., Briese, T., Mishra, N., Kapoor, V., Sameroff, S.C., de Wit, E., Munster, V.J., Hensley, L.E., Zalmout, I.S., Kapoor, A., Epstein, J.H., Karesh, W.B., Daszak, P., Mohammed, O.B. and Lipkin, W.I. 2014. Middle East Respiratory Syndrome Coronavirus Infection in Dromedary Camels in Saudi Arabia. *mBio*. **5**(2),pp.e00884-14-e00884-14.

Alavizadeh, S.H., Akhtari, J., Badiee, A., Golmohammadzadeh, S. and Jaafari, M.R. 2016. Improved therapeutic activity of HER2 Affibody-targeted cisplatin liposomes in HER2-expressing breast tumor models. *Expert Opinion on Drug Delivery*. **13**(3),pp.325–336.

Alexis, F., Basto, P., Levy-Nissenbaum, E., Radovic-Moreno, A.F., Zhang, L., Pridgen, E., Wang, A.Z., Marein, S.L., Westerhof, K., Molnar, L.K. and Farokhzad, O.C. 2008. HER-2-targeted nanoparticle-affibody bioconjugates for cancer therapy. *ChemMedChem*. **3**(12),pp.1839–43.

Ali, M.A., Solanki, P.R., Patel, M.K., Dhayani, H., Agrawal, V.V., John, R., Malhotra, B.D., Malhotra, B.D. and Tornow, M. 2013. A highly efficient microfluidic nano biochip based on nanostructured nickel oxide. *Nanoscale*. **5**(7),p.2883.

Aller Pellitero, M., Kitsara, M., Eibensteiner, F. and del Campo, F.J. 2016. Rapid prototyping of electrochemical lateral flow devices: stencilled electrodes. *The Analyst*. **141**(8),pp.2515–2522.

Amarilla, S.P., Gómez-Laguna, J., Carrasco, L., Rodríguez-Gómez, I.M., Caridad y Ocerín, J.M., Graham, S.P., Frossard, J.-P., Steinbach, F. and Salguero, F.J. 2016. Thymic depletion of lymphocytes is associated with the virulence of PRRSV-1 strains. *Veterinary Microbiology*. **188**,pp.47–58.

Ansari, I.H., Kwon, B., Osorio, F.A. and Pattnaik, A.K. 2006. Influence of N-linked glycosylation of porcine reproductive and respiratory syndrome virus GP5 on virus infectivity, antigenicity, and ability to induce neutralizing antibodies. *Journal of virology*. **80**(8),pp.3994–4004.

Arechaga, I., Miroux, B., Runswick, M.J. and Walker, J.E. 2003. Over-expression of Escherichia coli F 1 F o -ATPase subunit a is inhibited by instability of the uncB gene transcript. *FEBS Letters*. **547**(1–3),pp.97–100.

Ariza, A., Tanner, S.J., Walter, C.T., Dent, K.C., Shepherd, D.A., Wu, W., Matthews, S. V, Hiscox, J.A., Green, T.J., Luo, M., Elliott, R.M., Fooks, A.R., Ashcroft, A.E., Stonehouse, N.J., Ranson, N.A., Barr, J.N. and Edwards, T.A. 2013.

Nucleocapsid protein structures from orthobunyaviruses reveal insight into ribonucleoprotein architecture and RNA polymerization. *Nucleic acids research*. **41**(11),pp.5912–26.

Arrata, I., Barnard, A., Tomlinson, D.C. and Wilson, A.J. 2017. Interfacing native and non-native peptides: using Affimers to recognise α-helix mimicking foldamers. *Chemical communications (Cambridge, England)*. **53**(19),pp.2834–2837.

Arruda, A.G., Friendship, R., Carpenter, J., Greer, A., Poljak, Z., Thoren, P. and Goss-Cutard, J. 2016. Evaluation of Control Strategies for Porcine Reproductive and Respiratory Syndrome (PRRS) in Swine Breeding Herds Using a Discrete Event Agent-Based Model J. Sanchez, ed. *PLOS ONE*. **11**(11),p.e0166596.

Aryasomayajula, B., Salzano, G. and Torchilin, V.P. 2017. Multifunctional Liposomes *In*: *Methods in molecular biology (Clifton, N.J.)* [Online]., pp. 41–61.

Attucci, S., Gauthier, A., Korkmaz, B., Delépine, P., Martino, M.F.-D., Saudubray, F., Diot, P. and Gauthier, F. 2006. EPI-hNE4, a proteolysis-resistant inhibitor of human neutrophil elastase and potential anti-inflammatory drug for treating cystic fibrosis. *The Journal of pharmacology and experimental therapeutics*. **318**(2),pp.803–9.

Avacta 2016. Avacta rapidly generates Affimer binders - Zika virus diagnostics.

Avrameas, S. and Gulibert, B. 1972. Enzyme-immunoassay for the measurement of antigens using peroxidase conjugates. *Biochimie*. **54**(7),pp.837–842.

Bailey, A.L., Lauck, M., Weiler, A., Sibley, S.D., Dinis, J.M., Bergman, Z., Nelson, C.W., Correll, M., Gleicher, M., Hyeroba, D., Tumukunde, A., Weny, G., Chapman, C., Kuhn, J.H., Hughes, A.L., Friedrich, T.C., Goldberg, T.L. and O'Connor, D.H. 2014. High genetic diversity and adaptive potential of two simian hemorrhagic fever viruses in a wild primate population. *PloS one*. **9**(3),p.e90714.

Baltimore, D. 1971. Expression of animal virus genomes. *Bacteriological reviews*. **35**(3),pp.235–41.

Bao, D., Wang, R., Qiao, S., Wan, B., Wang, Y., Liu, M., Shi, X., Guo, J. and Zhang, G. 2013. Antibody-dependent enhancement of PRRSV infection down-modulates TNF-α and IFN-β transcription in macrophages. *Veterinary Immunology and Immunopathology*. **156**(1),pp.128–134.

Bautista, E.M., Faaberg, K.S., Mickelson, D. and McGruder, E.D. 2002. Functional properties of the predicted helicase of porcine reproductive and respiratory syndrome virus. *Virology*. **298**(2),pp.258–70.

Bedford, R., Tiede, C., Hughes, R., Curd, A., McPherson, M.J., Peckham, M. and Tomlinson, D.C. 2017. Alternative reagents to antibodies in imaging applications. *Biophysical reviews*. **9**(4),pp.299–308.

Beerens, N., Selisko, B., Ricagno, S., Imbert, I., van der Zanden, L., Snijder, E.J. and Canard, B. 2007. De Novo Initiation of RNA Synthesis by the Arterivirus RNA-Dependent RNA Polymerase. *Journal of Virology*. **81**(16),pp.8384–8395.

Beghein, E. and Gettemans, J. 2017. Nanobody Technology: A Versatile Toolkit for Microscopic Imaging, Protein–Protein Interaction Analysis, and Protein Function Exploration. *Frontiers in Immunology*. **8**,p.771.

Bekir, K., Barhoumi, H., Braiek, M., Chrouda, A., Zine, N., Abid, N., Maaref, A., Bakhrouf, A., Ouada, H. Ben, Jaffrezic-Renault, N. and Mansour, H. Ben 2015. Electrochemical impedance immunosensor for rapid detection of stressed pathogenic Staphylococcus aureus bacteria. *Environmental Science and*

Pollution Research. **22**(20),pp.15796–15803.

Berglund, L., Björling, E., Oksvold, P., Fagerberg, L., Asplund, A., Szigyarto, C.A.-K., Persson, A., Ottosson, J., Wernérus, H., Nilsson, P., Lundberg, E., Sivertsson, A., Navani, S., Wester, K., Kampf, C., Hober, S., Pontén, F. and Uhlén, M. 2008. A genecentric Human Protein Atlas for expression profiles based on antibodies. *Molecular & cellular proteomics : MCP*. **7**(10),pp.2019–27.

Bertier, L., Boucherie, C., Zwaenepoel, O., Vanloo, B., Van Troys, M., Van Audenhove, I. and Gettemans, J. 2017. Inhibitory cortactin nanobodies delineate the role of NTA- and SH3-domain–specific functions during invadopodium formation and cancer cell invasion. *The FASEB Journal*. **31**(6),pp.2460–2476.

Beura, L.K., Sarkar, S.N., Kwon, B., Subramaniam, S., Jones, C., Pattnaik, A.K. and Osorio, F.A. 2010. Porcine Reproductive and Respiratory Syndrome Virus Nonstructural Protein 1 Modulates Host Innate Immune Response by Antagonizing IRF3 Activation. *Journal of Virology*. **84**(3),pp.1574–1584.

Beuttler, J., Rothdiener, M., Müller, D., Frejd, F.Y. and Kontermann, R.E. 2009. Targeting of epidermal growth factor receptor (EGFR)-expressing tumor cells with sterically stabilized affibody liposomes (SAL). *Bioconjugate chemistry*. **20**(6),pp.1201–8.

Biagini, R.E., Sammons, D.L., Smith, J.P., MacKenzie, B.A., Striley, C.A.F., Snawder, J.E., Robertson, S.A. and Quinn, C.P. 2006. Rapid, sensitive, and specific lateral-flow immunochromatographic device to measure anti-anthrax protective antigen immunoglobulin g in serum and whole blood. *Clinical and vaccine immunology : CVI*. **13**(5),pp.541–6.

Binjawadagi, B., Lakshmanappa, Y.S., Longchao, Z., Dhakal, S., Hiremath, J., Ouyang, K., Shyu, D.-L., Arcos, J., Pengcheng, S., Gilbertie, A., Zuckermann, F., Torrelles, J.B., Jackwood, D., Fang, Y. and Renukaradhya, G.J. 2016. Development of a porcine reproductive and respiratory syndrome virus-like-particle-based vaccine and evaluation of its immunogenicity in pigs. *Archives of Virology*. **161**(6),pp.1579–1589.

Binz, H.K., Amstutz, P., Kohl, A., Stumpp, M.T., Briand, C., Forrer, P., Grütter, M.G. and Plückthun, A. 2004. High-affinity binders selected from designed ankyrin repeat protein libraries. *Nature Biotechnology*. **22**(5),pp.575–582.

Boklund, A., Toft, N., Alban, L. and Uttenthal, Å. 2009. Comparing the epidemiological and economic effects of control strategies against classical swine fever in Denmark. *Preventive Veterinary Medicine*. **90**(3–4),pp.180–193.

Bolduc, S., Lacombe, L., Naud, A., Grégoire, M., Fradet, Y. and Tremblay, R.R. 2007. Urinary PSA: a potential useful marker when serum PSA is between 2.5 ng/mL and 10 ng/mL. *Canadian Urological Association journal = Journal de l'Association des urologues du Canada*. **1**(4),pp.377–81.

den Boon, J.A., Diaz, A. and Ahlquist, P. 2010. Cytoplasmic Viral Replication Complexes. *Cell Host & Microbe*. **8**(1),pp.77–85.

den Boon, J.A., Snijder, E.J., Chirnside, E.D., de Vries, A.A., Horzinek, M.C. and Spaan, W.J. 1991. Equine arteritis virus is not a togavirus but belongs to the coronaviruslike superfamily. *Journal of virology*. **65**(6),pp.2910–20.

Bordeaux, J., Welsh, A., Agarwal, S., Killiam, E., Baquero, M., Hanna, J., Anagnostou, V. and Rimm, D. 2010. Antibody validation. *BioTechniques*. **48**(3),pp.197–209.

Borisov, S.M. and Wolfbeis, O.S. 2008. Optical Biosensors. *Chem. Rev*.

(108),pp.423–461.
Boursnell, M.E.G., Brown, T.D.K., Foulds, I.J., Green, P.F., Tomley, F.M. and Binns, M.M. 1987. Completion of the Sequence of the Genome of the Coronavirus Avian Infectious Bronchitis Virus. *Journal of General Virology*. **68**(1),pp.57–77.
Bradbury, A. and Plückthun, A. 2015. Reproducibility: Standardize antibodies used in research. *Nature*. **518**(7537),pp.27–29.
Van Breedam, W., Delputte, P.L., Van Gorp, H., Misinzo, G., Vanderheijden, N., Duan, X. and Nauwynck, H.J. 2010. Porcine reproductive and respiratory syndrome virus entry into the porcine macrophage. *Journal of General Virology*. **91**(7),pp.1659–1667.
Van Breedam, W., Van Gorp, H., Zhang, J.Q., Crocker, P.R., Delputte, P.L. and Nauwynck, H.J. 2010. The M/GP(5) glycoprotein complex of porcine reproductive and respiratory syndrome virus binds the sialoadhesin receptor in a sialic acid-dependent manner. *PLoS pathogens*. **6**(1),p.e1000730.
Brian, D.A., Dennis, D.E. and Guy, J.S. 1980. Genome of porcine transmissible gastroenteritis virus. *Journal of virology*. **34**(2),pp.410–5.
Broadhurst, M.J., Brooks, T.J.G. and Pollock, N.R. 2016. Diagnosis of Ebola Virus Disease: Past, Present, and Future. *Clinical microbiology reviews*. **29**(4),pp.773–93.
de Bruin, R.C.G., Lougheed, S.M., van der Kruk, L., Stam, A.G., Hooijberg, E., Roovers, R.C., van Bergen en Henegouwen, P.M.P., Verheul, H.M.W., de Gruijl, T.D. and van der Vliet, H.J. 2016. Highly specific and potently activating Vγ9Vδ2-T cell specific nanobodies for diagnostic and therapeutic applications. *Clinical Immunology*. **169**,pp.128–138.
Bukowska, M.A. and Grütter, M.G. 2013. New concepts and aids to facilitate crystallization. *Current opinion in structural biology*. **23**(3),pp.409–16.
Bukrinsky, M. and Sviridov, D. 2006. Human immunodeficiency virus infection and macrophage cholesterol metabolism. *Journal of Leukocyte Biology*. **80**(5),pp.1044–1051.
Bunyakul, N. and Baeumner, A. 2014. Combining Electrochemical Sensors with Miniaturized Sample Preparation for Rapid Detection in Clinical Samples. *Sensors*. **15**(1),pp.547–564.
Bunyakul, N., Promptmas, C. and Baeumner, A.J. 2015. Microfluidic biosensor for cholera toxin detection in fecal samples. *Analytical and Bioanalytical Chemistry*. **407**(3),pp.727–736.
Burkard, C., Lillico, S.G., Reid, E., Jackson, B., Mileham, A.J., Ait-Ali, T., Whitelaw, C.B.A. and Archibald, A.L. 2017. Precision engineering for PRRSV resistance in pigs: Macrophages from genome edited pigs lacking CD163 SRCR5 domain are fully resistant to both PRRSV genotypes while maintaining biological function D. R. Perez, ed. *PLOS Pathogens*. **13**(2),p.e1006206.
Butt, T.R., Edavettal, S.C., Hall, J.P. and Mattern, M.R. 2005. SUMO fusion technology for difficult-to-express proteins. *Protein expression and purification*. **43**(1),pp.1–9.
Campo, M.S. and Roden, R.B.S. 2010. Papillomavirus prophylactic vaccines: established successes, new approaches. *Journal of virology*. **84**(3),pp.1214–20.
Cao, Q.M., Subramaniam, S., Ni, Y.-Y., Cao, D. and Meng, X.-J. 2016. The non-structural protein Nsp2TF of porcine reproductive and respiratory syndrome virus down-regulates the expression of Swine Leukocyte Antigen class I.

Virology. **491**,pp.115–124.

Carrara, S., Shumyantseva, V. V., Archakov, A.I. and Samorì, B. 2008. Screen-printed electrodes based on carbon nanotubes and cytochrome P450scc for highly sensitive cholesterol biosensors. *Biosensors and Bioelectronics*. **24**(1),pp.148–150.

Carter, S.D., Barr, J.N. and Edwards, T.A. 2012. Expression, purification and crystallization of the Crimean-Congo haemorrhagic fever virus nucleocapsid protein. *Acta crystallographica. Section F, Structural biology and crystallization communications*. **68**(Pt 5),pp.569–73.

Chalker, J.M., Bernardes, G.J.L., Lin, Y.A. and Davis, B.G. 2009. Chemical modification of proteins at cysteine: opportunities in chemistry and biology. *Chemistry, an Asian journal*. **4**(5),pp.630–40.

Chand, R.J., Trible, B.R. and Rowland, R.R. 2012. Pathogenesis of porcine reproductive and respiratory syndrome virus. *Current Opinion in Virology*. **2**(3),pp.256–263.

Charerntantanakul, W. 2012. Porcine reproductive and respiratory syndrome virus vaccines: Immunogenicity, efficacy and safety aspects. *World journal of virology*. **1**(1),pp.23–30.

Chavan, T., Maduke, M. and Swartz, K. 2017. Protein ligands for studying ion channel proteins. *The Journal of general physiology*. **149**(4),pp.407–411.

Chen, A. and Yang, S. 2015a. Replacing antibodies with aptamers in lateral flow immunoassay. *Biosensors and Bioelectronics*. **71**,pp.230–242.

Chen, A. and Yang, S. 2015b. Replacing antibodies with aptamers in lateral flow immunoassay. *Biosensors & bioelectronics*. **71**,pp.230–42.

Chen, H., Wang, J., Xiao, S., Fang, L., Wang, D., Xu, S., Jiang, Y., Dong, J. and Luo, R. 2015. Porcine reproductive and respiratory syndrome virus 3C protease cleaves the mitochondrial antiviral signalling complex to antagonize IFN-β expression. *Journal of General Virology*. **96**(10),pp.3049–3058.

Chen, J., Shi, X., Zhang, X., Wang, L., Luo, J., Xing, G., Deng, R., Yang, H., Li, J., Wang, A. and Zhang, G. 2015. Porcine Reproductive and Respiratory Syndrome Virus (PRRSV) Inhibits RNA-Mediated Gene Silencing by Targeting Ago-2. *Viruses*. **7**(10),pp.5539–5552.

Chen, X., Zhang, Q., Bai, J., Zhao, Y., Wang, X., Wang, H. and Jiang, P. 2017. The Nucleocapsid Protein and Nonstructural Protein 10 of Highly Pathogenic Porcine Reproductive and Respiratory Syndrome Virus Enhance CD83 Production via NF-κB and Sp1 Signaling Pathways J. K. Pfeiffer, ed. *Journal of Virology*. **91**(18),pp.e00986-17.

Chen, Y., Chen, Q., Han, M., Liu, J., Zhao, P., He, L., Zhang, Y., Niu, Y., Yang, W. and Zhang, L. 2016. Near-infrared fluorescence-based multiplex lateral flow immunoassay for the simultaneous detection of four antibiotic residue families in milk. *Biosensors & bioelectronics*. **79**,pp.430–4.

Chen, Z., Li, M., He, Q., Du, J., Zhou, L., Ge, X., Guo, X. and Yang, H. 2014. The amino acid at residue 155 in nonstructural protein 4 of porcine reproductive and respiratory syndrome virus contributes to its inhibitory effect for interferon-β transcription in vitro. *Virus Research*. **189**,pp.226–234.

Cheng, A., Zhang, W., Xie, Y., Jiang, W., Arnold, E., Sarafianos, S.G. and Ding, J. 2005. Expression, purification, and characterization of SARS coronavirus RNA polymerase. *Virology*. **335**(2),pp.165–176.

Choi, J.-W., Hong, S.T., Kang, D.E., Paik, K.C., Han, M.S., Lim, C.S. and Cho, B.R. 2016. Two-Photon Tracer for Human Epidermal Growth Factor Receptor-2: Detection of Breast Cancer in a Live Tissue. *Analytical chemistry*. **88**(19),pp.9412–9418.

Choi, J.R., Tang, R., Wang, S., Wan Abas, W.A.B., Pingguan-Murphy, B. and Xu, F. 2015. Paper-based sample-to-answer molecular diagnostic platform for point-of-care diagnostics. *Biosensors and Bioelectronics*. **74**,pp.427–439.

Chung, J., Kang, J.S., Jurng, J.S., Jung, J.H. and Kim, B.C. 2015. Fast and continuous microorganism detection using aptamer-conjugated fluorescent nanoparticles on an optofluidic platform. *Biosensors and Bioelectronics*. **67**,pp.303–308.

Collins, J., Benfield, D., Christianson, W., Harris, L., Hennings, J., Shaw, D., Goyal, S., McCullough, S., Morrison, R., Joo, H., Gorcyca, D. and Chladek, D. 1992. Isolation of swine infertility and respiratory syndrome virus (isolate ATCC VR-2332) in North America and experimental reproduction of the disease in gnotobiotic pigs. *Journal of veterinary diagnostic investigation*. **4**(2),pp.117–126.

Conde, J.P., Madaboosi, N., Soares, R.R.G., Fernandes, J.T.S., Novo, P., Moulas, G. and Chu, V. 2016. Lab-on-chip systems for integrated bioanalyses. *Essays in biochemistry*. **60**(1),pp.121–31.

Corstjens, P.L.A.M., Abrams, W.R. and Malamud, D. 2012. Detecting viruses by using salivary diagnostics. *Journal of the American Dental Association (1939)*. **143**(10 Suppl),p.12S–8S.

CRACKIT 2015. Affimers - Animal free alternatives to antibodies.

Daginakatte, G.C. and Kapil, S. 2001. Mapping of the RNA-binding domain of the porcine reproductive and respiratory syndrome virus nucleocapsid protein. *Advances in experimental medicine and biology*. **494**,pp.547–52.

Daprà, J., Lauridsen, L.H., Nielsen, A.T. and Rozlosnik, N. 2013. Comparative study on aptamers as recognition elements for antibiotics in a label-free all-polymer biosensor. *Biosensors and Bioelectronics*. **43**,pp.315–320.

Darwich, L., Díaz, I. and Mateu, E. 2010. Certainties, doubts and hypotheses in porcine reproductive and respiratory syndrome virus immunobiology. *Virus Research*. **154**(1–2),pp.123–132.

Dea, S., Bilodeau, R., Athanassious, R., Sauvageau, R. and Martineau, G.P. 1992. Swine reproductive and respiratory syndrome in Québec: Isolation of an enveloped virus serologically-related to Lelystad virus. *The Canadian veterinary journal. La revue vétérinaire canadienne*. **33**(12),pp.801–8.

Dea, S., Gagnon, C.A., Mardassi, H., Pirzadeh, B. and Rogan, D. 2000. Current knowledge on the structural proteins of porcine reproductive and respiratory syndrome (PRRS) virus: comparison of the North American and European isolates. *Archives of virology*. **145**(4),pp.659–88.

Delgado, J., Pollard, S., Pearn, K., Snary, E.L., Black, E., Prpich, G. and Longhurst, P. 2016. U.K. Foot and Mouth Disease: A Systemic Risk Assessment of Existing Controls. *Risk Analysis*. **37**(9),pp.1768–1782.

Delputte, P.L., Breedam, W. Van, Barbé, F., Reeth, K. Van and Nauwynck, H.J. 2007. IFN-α Treatment Enhances Porcine Arterivirus Infection of Monocytes via Upregulation of the Porcine Arterivirus Receptor Sialoadhesin. *Journal of Interferon and Cytokine Research*. **27**(9),pp.757–766.

Delrue, I., Delputte, P.L., Nauwynck, H.J., Doorsselaere, J. Van, Karniychuk, U.U.,

Nauwynck, H.J., Doorsselaere, J. Van, Gagnon, C., Nauwynck, H., Pujols, J. and Mateu, E. 2009. Assessing the functionality of viral entry-associated domains of porcine reproductive and respiratory syndrome virus during inactivation procedures, a potential tool to optimize inactivated vaccines. *Veterinary Research*. **40**(6),p.62.

Deshpande, A., Wang, S., Walsh, M.A. and Dokland, T. 2007. Structure of the equine arteritis virus nucleocapsid protein reveals a dimer–dimer arrangement. *Acta Crystallographica Section D Biological Crystallography*. **63**(5),pp.581–586.

van Dinten, L.C., Rensen, S., Gorbalenya, A.E. and Snijder, E.J. 1999. Proteolytic processing of the open reading frame 1b-encoded part of arterivirus replicase is mediated by nsp4 serine protease and Is essential for virus replication. *Journal of virology*. **73**(3),pp.2027–37.

Dmitriev, O.Y., Lutsenko, S. and Muyldermans, S. 2016. Nanobodies as Probes for Protein Dynamics in Vitro and in Cells. *The Journal of biological chemistry*. **291**(8),pp.3767–75.

Doan, D.N.. and Dokland, T. 2003. Structure of the Nucleocapsid Protein of Porcine Reproductive and Respiratory Syndrome Virus. *Structure*. **11**(11),pp.1445–1451.

Dombkowski, A.A., Sultana, K.Z. and Craig, D.B. 2014. Protein disulfide engineering. *FEBS Letters*. **588**(2),pp.206–212.

Drake, J.W. and Holland, J.J. 1999. Mutation rates among RNA viruses. *Proceedings of the National Academy of Sciences*. **96**(24),pp.13910–13913.

Drigo, M., Franzo, G., Belfanti, I., Martini, M., Mondin, A. and Ceglie, L. 2014. Validation and comparison of different end point and real time RT-PCR assays for detection and genotyping of porcine reproductive and respiratory syndrome virus. *Journal of Virological Methods*. **201**,pp.79–85.

Duan, X., Nauwynck, H.J., Favoreel, H.W. and Pensaert, M.B. 1998. Identification of a putative receptor for porcine reproductive and respiratory syndrome virus on porcine alveolar macrophages. *Journal of virology*. **72**(5),pp.4520–3.

Duan, X., Nauwynck, H.J. and Pensaert, M.B. 1997. Virus quantification and identification of cellular targets in the lungs and lymphoid tissues of pigs at different time intervals after inoculation with porcine reproductive and respiratory syndrome virus (PRRSV). *Veterinary Microbiology*. **56**(1–2),pp.9–19.

Dunowska, M., Biggs, P.J., Zheng, T. and Perrott, M.R. 2012. Identification of a novel nidovirus associated with a neurological disease of the Australian brushtail possum (Trichosurus vulpecula). *Veterinary microbiology*. **156**(3–4),pp.418–24.

Ebersbach, H., Fiedler, E., Scheuermann, T., Fiedler, M., Stubbs, M.T., Reimann, C., Proetzel, G., Rudolph, R. and Fiedler, U. 2007. Affilin–Novel Binding Molecules Based on Human γ-B-Crystallin, an All β-Sheet Protein. *Journal of Molecular Biology*. **372**(1),pp.172–185.

Esposito, D. and Chatterjee, D.K. 2006. Enhancement of soluble protein expression through the use of fusion tags. *Current opinion in biotechnology*. **17**(4),pp.353–8.

Fan, B., Li, Y., Wang, H., Jiang, P., Liu, X. and Bai, J. 2015. The N-N non-covalent domain of the nucleocapsid protein of type 2 porcine reproductive and

respiratory syndrome virus enhances induction of IL-10 expression. *Journal of General Virology*. **96**(6),pp.1276–1286.

Fan, B., Liu, X., Bai, J., Zhang, T., Zhang, Q. and Jiang, P. 2015. The amino acid residues at 102 and 104 in GP5 of porcine reproductive and respiratory syndrome virus regulate viral neutralization susceptibility to the porcine serum neutralizing antibody. *Virus research*. **204**,pp.21–30.

Fang, Y. and Snijder, E.J. 2010. The PRRSV replicase: Exploring the multifunctionality of an intriguing set of nonstructural proteins. *Virus Research*. **154**(1),pp.61–76.

Fang, Y., Treffers, E.E., Li, Y., Tas, A., Sun, Z., van der Meer, Y., de Ru, A.H., van Veelen, P.A., Atkins, J.F., Snijder, E.J. and Firth, A.E. 2012. Efficient -2 frameshifting by mammalian ribosomes to synthesize an additional arterivirus protein. *Proceedings of the National Academy of Sciences*. **109**(43),pp.E2920–E2928.

Ferguson, B.S., Hoggarth, D.A., Maliniak, D., Ploense, K., White, R.J., Woodward, N., Hsieh, K., Bonham, A.J., Eisenstein, M., Kippin, T.E., Plaxco, K.W. and Soh, H.T. 2013. Real-Time, Aptamer-Based Tracking of Circulating Therapeutic Agents in Living Animals. *Science Translational Medicine*. **5**(213),p.213ra165-213ra165.

Fernandes, A., Duarte, C., Cardoso, F., Bexiga, R., Cardoso, S. and Freitas, P. 2014. Lab-on-Chip Cytometry Based on Magnetoresistive Sensors for Bacteria Detection in Milk. *Sensors*. **14**(8),pp.15496–15524.

Ferrer-Orta, C., Arias, A., Escarmís, C. and Verdaguer, N. 2006. A comparison of viral RNA-dependent RNA polymerases. *Current Opinion in Structural Biology*. **16**(1),pp.27–34.

Ferrin, N.H., Fang, Y., Johnson, C.R., Murtaugh, M.P., Polson, D.D., Torremorell, M., Gramer, M.L. and Nelson, E.A. 2004. Validation of a blocking enzyme-linked immunosorbent assay for detection of antibodies against porcine reproductive and respiratory syndrome virus. *Clinical and diagnostic laboratory immunology*. **11**(3),pp.503–14.

Ferris, N.P. and Dawson, M. 1988. Routine application of enzyme-linked immunosorbent assay in comparison with complement fixation for the diagnosis of foot-and-mouth and swine vesicular diseases. *Veterinary Microbiology*. **16**(3),pp.201–209.

Fink, A.L. 1998. Protein aggregation: folding aggregates, inclusion bodies and amyloid. *Folding and Design*. **3**(1),pp.R9–R23.

Fisher, T. 2011. Thermo Scientific Pierce Antibody Production and Purification Technical Handbook Introduction to Antibody Production, Purification and Modification.

Flütsch, A., Schroeder, T., Barandun, J., Ackermann, R., Bühlmann, M. and Grütter, M.G. 2014. Specific targeting of human caspases using designed ankyrin repeat proteins. *Biological chemistry*. **395**(10),pp.1243–52.

Frankel, A. and Pabo, C. 1988. Cellular uptake of the tat protein from human immunodeficiency virus. *Cell*. **55**(6),pp.1189–1193.

Free, A.H., Adams, E.C., Kercher, M. Lou, Free, H.M. and Cook, M.H. 1957. Simple Specific Test for Urine Glucose. *Clin. Chem.* **3**(3),pp.163–168.

Garcia Duran, M., Costa, S., Sarraseca, J., de la Roja, N., Garc?a, J., Garc?a, I. and Rodr?guez, M.J. 2016. Generation of porcine reproductive and respiratory syndrome (PRRS) virus-like-particles (VLPs) with different protein composition.

Journal of Virological Methods. **236**,pp.77–86.

De Genst, E., Silence, K., Decanniere, K., Conrath, K., Loris, R., Kinne, J., Muyldermans, S. and Wyns, L. 2006. Molecular basis for the preferential cleft recognition by dromedary heavy-chain antibodies. *Proceedings of the National Academy of Sciences of the United States of America*. **103**(12),pp.4586–91.

Gilbreth, R.N., Truong, K., Madu, I., Koide, A., Wojcik, J.B., Li, N.-S., Piccirilli, J.A., Chen, Y. and Koide, S. 2011. Isoform-specific monobody inhibitors of small ubiquitin-related modifiers engineered using structure-guided library design. *Proceedings of the National Academy of Sciences of the United States of America*. **108**(19),pp.7751–6.

Gong, H., Kovar, J., Little, G., Chen, H. and Olive, D.M. 2010. In Vivo Imaging of Xenograft Tumors Using an Epidermal Growth Factor Receptor-Specific Affibody Molecule Labeled with a Near-infrared Fluorophore. *Neoplasia*. **12**(2),pp.139–149.

Gonzalez, R.M., Seurynck-Servoss, S.L., Crowley, S.A., Brown, M., Omenn, G.S., Hayes, D.F. and Zangar, R.C. 2008. Development and validation of sandwich ELISA microarrays with minimal assay interference. *Journal of proteome research*. **7**(6),pp.2406–14.

Gopinath, S.C.B., Lakshmipriya, T., Chen, Y., Phang, W.-M. and Hashim, U. 2016. Aptamer-based 'point-of-care testing'. *Biotechnology advances*. **34**(3),pp.198–208.

Gorbalenya, A.E., Enjuanes, L., Ziebuhr, J. and Snijder, E.J. 2006. Nidovirales: evolving the largest RNA virus genome. *Virus research*. **117**(1),pp.17–37.

Gorbalenya, A.E., Snijder, E.J. and Ziebuhr, J. 2000. Virus-encoded proteinases and proteolytic processing in the Nidovirales. *Journal of General Virology*. **81**(4),pp.853–879.

Gou, H., Deng, J., Pei, J., Wang, J., Liu, W., Zhao, M. and Chen, J. 2014. Rapid and sensitive detection of type II porcine reproductive and respiratory syndrome virus by reverse transcription loop-mediated isothermal amplification combined with a vertical flow visualization strip. *Journal of virological methods*. **209**,pp.86–94.

Gov.uk 2015. Notifiable diseases in animals - GOV.UK.

Graham, R.L., Donaldson, E.F. and Baric, R.S. 2013. A decade after SARS: strategies for controlling emerging coronaviruses. *Nature Reviews Microbiology*. **11**(12),pp.836–848.

Green, M.R., Hughes, H. and Sambrook, J. 2012. Molecular Cloning: A Laboratory Manual (Fourth Edition).

Grubb, A. and Glad, U. 1979. Immunoassay with test strip having antibodies bound thereto.

Grzyb, J., Latowski, D. and Strzałka, K. 2006. Lipocalins – a family portrait. *Journal of Plant Physiology*. **163**(9),pp.895–915.

Guiseppi-Elie, A., Lei, C. and Baughman, R.H. 2002. Direct electron transfer of glucose oxidase on carbon nanotubes. *Nanotechnology*. **13**(5),pp.559–564.

Guo, R., Katz, B.B., Tomich, J.M., Gallagher, T. and Fang, Y. 2016. Porcine Reproductive and Respiratory Syndrome Virus Utilizes Nanotubes for Intercellular Spread S. Perlman, ed. *Journal of Virology*. **90**(10),pp.5163–5175.

Gürtler, C. and Bowie, A.G. 2013. Innate immune detection of microbial nucleic acids. *Trends in Microbiology*. **21**(8),pp.413–420.

Halstead, S.B., O'Rourke, E.J. and Allison, A.C. 1977. Dengue viruses and mononuclear phagocytes. II. Identity of blood and tissue leukocytes supporting in vitro infection. *The Journal of experimental medicine*. **146**(1),pp.218–29.

Hamers-Casterman, C., Atarhouch, T., Muyldermans, S., Robinson, G., Hammers, C., Songa, E.B., Bendahman, N. and Hammers, R. 1993. Naturally occurring antibodies devoid of light chains. *Nature*. **363**(6428),pp.446–448.

Hammond, J.L., Formisano, N., Estrela, P., Carrara, S. and Tkac, J. 2016. Electrochemical biosensors and nanobiosensors. *Essays in biochemistry*. **60**(1),pp.69–80.

Han, L., Liu, P., Petrenko, V.A. and Liu, A. 2016. A Label-Free Electrochemical Impedance Cytosensor Based on Specific Peptide-Fused Phage Selected from Landscape Phage Library. *Scientific reports*. **6**(1),p.22199.

Hanahan, D. and Weinberg, R. 2011. Hallmarks of Cancer: The Next Generation. *Cell*. **144**(5),pp.646–674.

Hanahan, D. and Weinberg, R. 2000. The Hallmarks of Cancer. *Cell*. **100**(1),pp.57–70.

Harris, J.F., Micheva-Viteva, S., Li, N. and Hong-Geller, E. 2013. Small RNA-mediated regulation of host–pathogen interactions. *Virulence*. **4**(8),pp.785–795.

Hausammann, S., Vogel, M., Kremer Hovinga, J.A., Lacroix-Desmazes, S., Stadler, B.M. and Horn, M.P. 2013. Designed ankyrin repeat proteins: a new approach to mimic complex antigens for diagnostic purposes? *PloS one*. **8**(4),p.e60688.

Hay, I.D., Du, J., Burr, N. and Rehm, B.H.A. 2015. Bioengineering of bacteria to assemble custom-made polyester affinity resins. *Applied and environmental microbiology*. **81**(1),pp.282–91.

He, Q., Du, Q., Lau, S., Manopo, I., Lu, L., Chan, S.-W., Fenner, B.J. and Kwang, J. 2005. Characterization of monoclonal antibody against SARS coronavirus nucleocapsid antigen and development of an antigen capture ELISA. *Journal of virological methods*. **127**(1),pp.46–53.

He, Q., Li, Y., Zhou, L., Ge, X., Guo, X. and Yang, H. 2015. Both Nsp1β and Nsp11 are responsible for differential TNF-α production induced by porcine reproductive and respiratory syndrome virus strains with different pathogenicity in vitro. *Virus Research*. **201**,pp.32–40.

Herce, H.D., Schumacher, D., Schneider, A.F.L., Ludwig, A.K., Mann, F.A., Fillies, M., Kasper, M.-A., Reinke, S., Krause, E., Leonhardt, H., Cardoso, M.C. and Hackenberger, C.P.R. 2017. Cell-permeable nanobodies for targeted immunolabelling and antigen manipulation in living cells. *Nature Chemistry*. **9**(8),pp.762–771.

Higgins, I.. and Lowe, C.. 1987. Biosensors - Introduction to the principles and applications of biosensors. *Philosophical Transactions of the Royal Society of London B: Biological Sciences*. **316**(1176).

van der Hoeven, B., Oudshoorn, D., Koster, A.J., Snijder, E.J., Kikkert, M. and Bárcena, M. 2016. Biogenesis and architecture of arterivirus replication organelles. *Virus Research*. **220**,pp.70–90.

Hoffmann, C. and Bilkei, G. 2002. Case Study: Chronic Erysipelas of the Sow - a Subclinical Manifestation of Reproductive Problems. *Reproduction in Domestic Animals*. **37**(2),pp.119–120.

Hoogenboom, H.R., Griffiths, A.D., Johnson, K.S., Chiswell, D.J., Hudson, P. and

Winter, G. 1991. Multi-subunit proteins on the surface of filamentous phage: methodologies for displaying antibody (Fab) heavy and light chains. *Nucleic Acids Research*. **19**(15),pp.4133–4137.

Horak, J., Dincer, C., Bakirci, H. and Urban, G. 2014. A disposable dry film photoresist-based microcapillary immunosensor chip for rapid detection of Epstein–Barr virus infection. *Sensors and Actuators B: Chemical*. **191**,pp.813–820.

Hou, J., Wang, L., He, W., Zhang, H. and Feng, W. 2012. Highly pathogenic porcine reproductive and respiratory syndrome virus impairs LPS- and poly(I:C)-stimulated tumor necrosis factor-alpha release by inhibiting ERK signaling pathway. *Virus Research*. **167**(1),pp.106–111.

Huang, C., Du, Y., Yu, Z., Zhang, Q., Liu, Y., Tang, J., Shi, J. and Feng, W.-H. 2016. Highly Pathogenic Porcine Reproductive and Respiratory Syndrome Virus Nsp4 Cleaves VISA to Impair Antiviral Responses Mediated by RIG-I-like Receptors. *Scientific reports*. **6**,p.28497.

Huang, C., Zhang, Q. and Feng, W. 2015. Regulation and evasion of antiviral immune responses by porcine reproductive and respiratory syndrome virus. *Virus Research*. **202**,pp.101–111.

Huang, C., Zhang, Q., Guo, X., Yu, Z., Xu, A., Tang, J. and Feng, W. 2014. Porcine reproductive and respiratory syndrome virus nonstructural protein 4 antagonizes beta interferon expression by targeting the NF-κB essential modulator. *Journal of virology*. **88**(18),pp.10934–45.

Hushegyi, A., Pihíková, D., Bertok, T., Adam, V., Kizek, R. and Tkac, J. 2016. Ultrasensitive detection of influenza viruses with a glycan-based impedimetric biosensor. *Biosensors and Bioelectronics*. **79**,pp.644–649.

Hutchinson, L.M., Chang, E.L., Becker, C.M., Ushiyama, N., Behonick, D., Shih, M.-C., DeWolf, W.C., Gaston, S.M. and Zetter, B.R. 2005. Development of a sensitive and specific enzyme-linked immunosorbent assay for thymosin β15, a urinary biomarker of human prostate cancer. *Clinical Biochemistry*. **38**(6),pp.558–571.

Iseki, H., Kawashima, K., Tung, N., Inui, K., Ikezawa, M., Shibahara, T. and Yamakawa, M. 2017. Efficacy of Type 2 porcine reproductive and respiratory syndrome virus (PRRSV) vaccine against the 2010 isolate of Vietnamese highly pathogenic PRRSV challenge in pigs. *Journal of Veterinary Medical Science*. **79**(4),pp.765–773.

Ithete, N.L., Stoffberg, S., Corman, V.M., Cottontail, V.M., Richards, L.R., Schoeman, M.C., Drosten, C., Drexler, J.F. and Preiser, W. 2013. Close relative of human Middle East respiratory syndrome coronavirus in bat, South Africa. *Emerging infectious diseases*. **19**(10),pp.1697–9.

Jansen van Vuren, P. and Paweska, J.T. 2009. Laboratory safe detection of nucleocapsid protein of Rift Valley fever virus in human and animal specimens by a sandwich ELISA. *Journal of virological methods*. **157**(1),pp.15–24.

Jeffrey J. Zimmerman, Locke A. Karriker, Alejandro Ramirez, Kent J. Schwartz, G.W.S. 2012. *Diseases of Swine (10th Edition)*. Wiley-Blackwell Oxford.

Jeong, K.J., Mabry, R. and Georgiou, G. 2005. Avimers hold their own. *Nature biotechnology*. **23**(12),pp.1493–4.

Jiang, W., Jiang, P., Wang, X., Li, Y., Wang, X. and Du, Y. 2007. Influence of porcine reproductive and respiratory syndrome virus GP5 glycoprotein N-linked glycans on immune responses in mice. *Virus genes*. **35**(3),pp.663–71.

Johnson, A., Song, Q., Ko Ferrigno, P., Bueno, P.R. and Davis, J.J. 2012. Sensitive affimer and antibody based impedimetric label-free assays for C-reactive protein. *Analytical chemistry*. **84**(15),pp.6553–60.

Jourdan, S.S., Osorio, F. and Hiscox, J.A. 2012. An interactome map of the nucleocapsid protein from a highly pathogenic North American porcine reproductive and respiratory syndrome virus strain generated using SILAC-based quantitative proteomics. *PROTEOMICS*. **12**(7),pp.1015–1023.

Justino, C.I.L., Duarte, A.C. and Rocha-Santos, T.A.P. 2015. Analytical applications of affibodies. *TrAC Trends in Analytical Chemistry*. **65**,pp.73–82.

Kappes, M.A. and Faaberg, K.S. 2015. PRRSV structure, replication and recombination: Origin of phenotype and genotype diversity. *Virology*. **479**,pp.475–486.

Kappes, M.A. and Faaberg, K.S. 2015. PRRSV structure, replication and recombination: Origin of phenotype and genotype diversity. *Virology*. **479–480**,pp.475–86.

Karniychuk, U.U. and Nauwynck, H.J. 2013. Pathogenesis and prevention of placental and transplacental porcine reproductive and respiratory syndrome virus infection. *Veterinary research*. **44**,p.95.

van Kasteren, P.B., Bailey-Elkin, B.A., James, T.W., Ninaber, D.K., Beugeling, C., Khajehpour, M., Snijder, E.J., Mark, B.L. and Kikkert, M. 2013. Deubiquitinase function of arterivirus papain-like protease 2 suppresses the innate immune response in infected host cells. *Proceedings of the National Academy of Sciences of the United States of America*. **110**(9),pp.E838-47.

van den Kieboom, C.H., van der Beek, S.L., Mészáros, T., Gyurcsányi, R.E., Ferwerda, G. and de Jonge, M.I. 2015. Aptasensors for viral diagnostics. *TrAC Trends in Analytical Chemistry*. **74**,pp.58–67.

Kim, D.Y., Kandalaft, H., Ding, W., Ryan, S., van Faassen, H., Hirama, T., Foote, S.J., MacKenzie, R. and Tanha, J. 2012. Disulfide linkage engineering for improving biophysical properties of human VH domains. *Protein engineering, design & selection : PEDS*. **25**(10),pp.581–9.

Kim, H.S., Kwang, J., Yoon, I.J., Joo, H.S. and Frey, M.L. 1993. Enhanced replication of porcine reproductive and respiratory syndrome (PRRS) virus in a homogeneous subpopulation of MA-104 cell line. *Archives of virology*. **133**(3–4),pp.477–83.

Kim, M.-A., Yoon, H.S., Park, S.-H., Kim, D.-Y., Pyo, A., Kim, H.S., Min, J.-J. and Hong, Y. 2017. Engineering of monobody conjugates for human EphA2-specific optical imaging R. Zhou, ed. *PLOS ONE*. **12**(7),p.e0180786.

Kim, M. and Kim, T. 2014. Aptamer-functionalized microtubules for continuous and selective concentration of target analytes. *Sensors and Actuators B: Chemical*. **202**,pp.1229–1236.

Kim, Y., Ho, S.O., Gassman, N.R., Korlann, Y., Landorf, E. V, Collart, F.R. and Weiss, S. 2008. Efficient site-specific labeling of proteins via cysteines. *Bioconjugate chemistry*. **19**(3),pp.786–91.

King, A.A., Sands, J.J. and Porterfield, J.S. 1984. Antibody-mediated Enhancement of Rabies Virus Infection in a Mouse Macrophage Cell Line (P388D1). *Journal of General Virology*. **65**(6),pp.1091–1093.

Ko, S., Seo, S., Sunwoo, S., Yoo, S.J., Kim, M. and Lyoo, Y.S. 2016. Efficacy of commercial genotype 1 porcine reproductive and respiratory syndrome virus

(PRRSV) vaccine against field isolate of genotype 2 PRRSV. *Veterinary Immunology and Immunopathology*. **172**,pp.43–49.

Koenhen, D. and Scharstuhl, J. 1989. Process and device for the separation of a body fluid from particulate materials.

Koide, A. and Koide, S. 2007. Monobodies: Antibody Mimics Based on the Scaffold of the Fibronectin Type III Domain *In*: *Protein Engineering Protocols* [Online]. New Jersey: Humana Press, pp. 95–110.

Koonin, E. V. 1991. The phylogeny of RNA-dependent RNA polymerases of positive-strand RNA viruses. *Journal of General Virology*. **72**(9),pp.2197–2206.

Koutsoumpeli, E., Tiede, C., Murray, J., Tang, A., Bon, R.S., Tomlinson, D.C. and Johnson, S. 2017. Antibody Mimetics for the Detection of Small Organic Compounds Using a Quartz Crystal Microbalance. *Analytical Chemistry*. **89**(5),pp.3051–3058.

Kramer, L., Renko, M., Završnik, J., Turk, D., Seeger, M.A., Vasiljeva, O., Grütter, M.G., Turk, V. and Turk, B. 2017. Non-invasive *in vivo* imaging of tumour-associated cathepsin B by a highly selective inhibitory DARPin. *Theranostics*. **7**(11),pp.2806–2821.

Kreutz, L.C. and Ackermann, M.R. 1996. Porcine reproductive and respiratory syndrome virus enters cells through a low pH-dependent endocytic pathway. *Virus Research*. **42**(1–2),pp.137–147.

Kroese, M. V., Zevenhoven-Dobbe, J.C., Bos-de Ruijter, J.N.A., Peeters, B.P.H., Meulenberg, J.J.M., Cornelissen, L.A.H.M. and Snijder, E.J. 2008. The nsp1 and nsp1 papain-like autoproteinases are essential for porcine reproductive and respiratory syndrome virus RNA synthesis. *Journal of General Virology*. **89**(2),pp.494–499.

Kroneman, A., Cornelissen, L.A., Horzinek, M.C., de Groot, R.J. and Egberink, H.F. 1998. Identification and characterization of a porcine torovirus. *Journal of virology*. **72**(5),pp.3507–11.

Kuhn, J.H., Lauck, M., Bailey, A.L., Shchetinin, A.M., Vishnevskaya, T. V., Bào, Y., Ng, T.F.F., LeBreton, M., Schneider, B.S., Gillis, A., Tamoufe, U., Diffo, J.L.D., Takuo, J.M., Kondov, N.O., Coffey, L.L., Wolfe, N.D., Delwart, E., Clawson, A.N., Postnikova, E., Bollinger, L., Lackemeyer, M.G., Radoshitzky, S.R., Palacios, G., Wada, J., Shevtsova, Z. V., Jahrling, P.B., Lapin, B.A., Deriabin, P.G., Dunowska, M., Alkhovsky, S. V., Rogers, J., Friedrich, T.C., O'Connor, D.H. and Goldberg, T.L. 2016. Reorganization and expansion of the nidoviral family Arteriviridae. *Archives of Virology*. **161**(3),pp.755–768.

Kuhn, J.H., Lauck, M., Bailey, A.L., Shchetinin, A.M., Vishnevskaya, T. V, Bào, Y., Ng, T.F.F., LeBreton, M., Schneider, B.S., Gillis, A., Tamoufe, U., Diffo, J.L.D., Takuo, J.M., Kondov, N.O., Coffey, L.L., Wolfe, N.D., Delwart, E., Clawson, A.N., Postnikova, E., Bollinger, L., Lackemeyer, M.G., Radoshitzky, S.R., Palacios, G., Wada, J., Shevtsova, Z. V, Jahrling, P.B., Lapin, B.A., Deriabin, P.G., Dunowska, M., Alkhovsky, S. V, Rogers, J., Friedrich, T.C., O'Connor, D.H. and Goldberg, T.L. 2016. Reorganization and expansion of the nidoviral family Arteriviridae. *Archives of virology*. **161**(3),pp.755–68.

Kummer, L., Hsu, C.-W., Dagliyan, O., MacNevin, C., Kaufholz, M., Zimmermann, B., Dokholyan, N.V., Hahn, K.M. and Plückthun, A. 2013. Knowledge-Based Design of a Biosensor to Quantify Localized ERK Activation in Living Cells. *Chemistry & Biology*. **20**(6),pp.847–856.

Kunert, R. and Reinhart, D. 2016. Advances in recombinant antibody manufacturing. *Applied microbiology and biotechnology*. **100**(8),pp.3451–61.

Kyle, H.F., Wickson, K.F., Stott, J., Burslem, G.M., Breeze, A.L., Tiede, C., Tomlinson, D.C., Warriner, S.L., Nelson, A., Wilson, A.J. and Edwards, T.A. 2015. Exploration of the HIF-1α/p300 interface using peptide and Adhiron phage display technologies. *Mol. BioSyst.* **11**(10),pp.2738–2749.

Lafleur, J.P., Jönsson, A., Senkbeil, S. and Kutter, J.P. 2016. Recent advances in lab-on-a-chip for biosensing applications. *Biosensors and Bioelectronics*. **76**,pp.213–233.

Laporte, J., Savin, C., Lamourette, P., Devilliers, K., Volland, H., Carniel, E., Créminon, C. and Simon, S. 2015. Fast and sensitive detection of enteropathogenic Yersinia by immunoassays. *Journal of clinical microbiology*. **53**(1),pp.146–59.

Lau, S.K.P., Woo, P.C.Y., Li, K.S.M., Huang, Y., Tsoi, H.-W., Wong, B.H.L., Wong, S.S.Y., Leung, S.-Y., Chan, K.-H. and Yuen, K.-Y. 2005. Severe acute respiratory syndrome coronavirus-like virus in Chinese horseshoe bats. *Proceedings of the National Academy of Sciences of the United States of America*. **102**(39),pp.14040–5.

Lau, S.K.P., Woo, P.C.Y., Wong, B.H.L., Tsoi, H.-W., Woo, G.K.S., Poon, R.W.S., Chan, K.-H., Wei, W.I., Peiris, J.S.M. and Yuen, K.-Y. 2004. Detection of severe acute respiratory syndrome (SARS) coronavirus nucleocapsid protein in sars patients by enzyme-linked immunosorbent assay. *Journal of clinical microbiology*. **42**(7),pp.2884–9.

Lauber, C., Ziebuhr, J., Junglen, S., Drosten, C., Zirkel, F., Nga, P.T., Morita, K., Snijder, E.J. and Gorbalenya, A.E. 2012. Mesoniviridae: a proposed new family in the order Nidovirales formed by a single species of mosquito-borne viruses. *Archives of virology*. **157**(8),pp.1623–8.

Lauck, M., Sibley, S.D., Hyeroba, D., Tumukunde, A., Weny, G., Chapman, C.A., Ting, N., Switzer, W.M., Kuhn, J.H., Friedrich, T.C., O'Connor, D.H. and Goldberg, T.L. 2013. Exceptional Simian Hemorrhagic Fever Virus Diversity in a Wild African Primate Community. *Journal of Virology*. **87**(1),pp.688–691.

Laviada, M.D., Babín, M., Dominguez, J. and Sánchez-Vizcaíno, J.M. 1992. Detection of African horsesickness virus in infected spleens by a sandwich ELISA using two monoclonal antibodies specific for VP7. *Journal of Virological Methods*. **38**(2),pp.229–242.

Lecellier, C.-H., Dunoyer, P., Arar, K., Lehmann-Che, J., Eyquem, S., Himber, C., Saïb, A. and Voinnet, O. 2005. A cellular microRNA mediates antiviral defense in human cells. *Science (New York, N.Y.)*. **308**(5721),pp.557–60.

Lee, C.-D., Sun, H.-C., Hu, S.-M., Chiu, C.-F., Homhuan, A., Liang, S.-M., Leng, C.-H. and Wang, T.-F. 2008. An improved SUMO fusion protein system for effective production of native proteins. *Protein science : a publication of the Protein Society*. **17**(7),pp.1241–8.

Lee, C.-D., Yan, Y.-P., Liang, S.-M. and Wang, T.-F. 2009. Production of FMDV virus-like particles by a SUMO fusion protein approach in Escherichia coli. *Journal of biomedical science*. **16**(1),p.69.

Lee, C., Hodgins, D., Calvert, J.G., Welch, S.-K.W., Jolie, R. and Yoo, D. 2006. Mutations within the nuclear localization signal of the porcine reproductive and respiratory syndrome virus nucleocapsid protein attenuate virus

replication. *Virology*. **346**(1),pp.238–250.
Lee, C. and Yoo, D. 2006. The small envelope protein of porcine reproductive and respiratory syndrome virus possesses ion channel protein-like properties. *Virology*. **355**(1),pp.30–43.
Lee, L., Nordman, E., Johnson, M. and Oldham, M. 2013. A Low-Cost, High-Performance System for Fluorescence Lateral Flow Assays. *Biosensors*. **3**(4),pp.360–373.
Leenaars, M. and Hendriksen, C.F.M. 2005. Critical Steps in the Production of Polyclonal and Monoclonal Antibodies: Evaluation and Recommendations. *ILAR Journal*. **46**(3),pp.269–279.
Lehmann, K.C., Gorbalenya, A.E., Snijder, E.J. and Posthuma, C.C. 2016. Arterivirus RNA-dependent RNA polymerase: Vital enzymatic activity remains elusive. *Virology*. **487**,pp.68–74.
Leuvering, J.H.W., Thal, P.J.H.M., Waart, M. v. d. and Schuurs, A.H.W.M. 1980. Sol particle agglutination immunoassay for human chorionic gonadotrophin. *Fresenius' Zeitschrift f*[illegible]*r Analytische Chemie*. **301**(2),pp.132–132.
Li, H., Zheng, Z., Zhou, P., Zhang, B., Shi, Z., Hu, Q. and Wang, H. 2010. The cysteine protease domain of porcine reproductive and respiratory syndrome virus non-structural protein 2 antagonizes interferon regulatory factor 3 activation. *The Journal of general virology*. **91**(Pt 12),pp.2947–58.
Li, Y., Wang, X., Bo, K., Wang, X., Tang, B., Yang, B., Jiang, W. and Jiang, P. 2007. Emergence of a highly pathogenic porcine reproductive and respiratory syndrome virus in the Mid-Eastern region of China. *The Veterinary Journal*. **174**(3),pp.577–584.
Life Assay Diagnostics 2010. Test-it™ Brucella IgM / IgG Lateral Flow Assay.
Lipovsek, D. 2011. Adnectins: engineered target-binding protein therapeutics. *Protein Engineering Design and Selection*. **24**(1–2),pp.3–9.
Liu, G., Ma, S., Li, S., Cheng, R., Meng, F., Liu, H. and Zhong, Z. 2010. The highly efficient delivery of exogenous proteins into cells mediated by biodegradable chimaeric polymersomes. *Biomaterials*. **31**(29),pp.7575–7585.
Liu, G., Mao, X., Phillips, J.A., Xu, H., Tan, W. and Zeng, L. 2009. Aptamer-nanoparticle strip biosensor for sensitive detection of cancer cells. *Analytical chemistry*. **81**(24),pp.10013–8.
Liu, J. -k., Zhou, X., Zhai, J. -q., Li, B., Wei, C. -h., Dai, A. -l., Yang, X. -y. and Luo, M. -l. 2017. Emergence of a novel highly pathogenic porcine reproductive and respiratory syndrome virus in China. *Transboundary and Emerging Diseases*.
Liu, L., Lear, Z., Hughes, D.J., Wu, W., Zhou, E., Whitehouse, A., Chen, H. and Hiscox, J.A. 2015. Resolution of the cellular proteome of the nucleocapsid protein from a highly pathogenic isolate of porcine reproductive and respiratory syndrome virus identifies PARP-1 as a cellular target whose interaction is critical for virus biology. *Veterinary Microbiology*. **176**(1–2),pp.109–119.
Liu, L., Tian, J., Nan, H., Tian, M., Li, Y., Xu, X., Huang, B., Zhou, E., Hiscox, J.A. and Chen, H. 2016. Porcine Reproductive and Respiratory Syndrome Virus Nucleocapsid Protein Interacts with Nsp9 and Cellular DHX9 To Regulate Viral RNA Synthesis. *Journal of virology*. **90**(11),pp.5384–98.
Lo, A.W., Tang, N.L. and To, K.-F. 2006. How the SARS coronavirus causes disease: host or organism? *The Journal of Pathology*. **208**(2),pp.142–151.
Löfblom, J., Feldwisch, J., Tolmachev, V., Carlsson, J., Ståhl, S. and Frejd, F.Y. 2010.

Affibody molecules: engineered proteins for therapeutic, diagnostic and biotechnological applications. *FEBS letters*. **584**(12),pp.2670–80.

Lorey, S., Fiedler, E., Kunert, A., Nerkamp, J., Lange, C., Fiedler, M., Bosse-Doenecke, E., Meysing, M., Gloser, M., Rundfeldt, C., Rauchhaus, U., Hänssgen, I., Göttler, T., Steuernagel, A., Fiedler, U. and Haupts, U. 2014. Novel Ubiquitin-derived High Affinity Binding Proteins with Tumor Targeting Properties. *Journal of Biological Chemistry*. **289**(12),pp.8493–8507.

Lundberg, E., Höidén-Guthenberg, I., Larsson, B., Uhlén, M. and Gräslund, T. 2007. Site-specifically conjugated anti-HER2 Affibody molecules as one-step reagents for target expression analyses on cells and xenograft samples. *Journal of immunological methods*. **319**(1–2),pp.53–63.

Lunney, J.K., Benfield, D.A. and Rowland, R.R.R. 2010. Porcine reproductive and respiratory syndrome virus: An update on an emerging and re-emerging viral disease of swine. *Virus Research*. **154**(1–2),pp.1–6.

Luo, R., Fang, L., Jiang, Y., Jin, H., Wang, Y., Wang, D., Chen, H. and Xiao, S. 2011. Activation of NF-?B by nucleocapsid protein of the porcine reproductive and respiratory syndrome virus. *Virus Genes*. **42**(1),pp.76–81.

Lyakhov, I., Kuban, M., Zielinski, R., Kramer-Marek, G. and Capala, J. 2010. HER2- and EGFR-specific Affiprobes - Novel recombinant optical probes for cell imaging. *Proceedings of the American Association for Cancer Research Annual Meeting*. **51**,pp.278–279.

Maestre, A.M., Garzón, A. and Rodríguez, D. 2011. Equine torovirus (BEV) induces caspase-mediated apoptosis in infected cells. *PloS one*. **6**(6),p.e20972.

Magnusson, P., Hyllseth, B. and Marusyk, H. 1970. Morphological studies on equine arteritis virus. *Archiv f*  *ur die gesamte Virusforschung*. **30**(2–3),pp.105–112.

Malakhov, M.P., Mattern, M.R., Malakhova, O.A., Drinker, M., Weeks, S.D. and Butt, T.R. 2004. SUMO fusions and SUMO-specific protease for efficient expression and purification of proteins. *Journal of structural and functional genomics*. **5**(1–2),pp.75–86.

Mamluk, R., Carvajal, I.M., Morse, B.A., Wong, H., Abramowitz, J., Aslanian, S., Lim, A.-C., Gokemeijer, J., Storek, M.J., Lee, J., Gosselin, M., Wright, M.C., Camphausen, R.T., Wang, J., Chen, Y., Miller, K., Sanders, K., Short, S., Sperinde, J., Prasad, G., Williams, S., Kerbel, R., Ebos, J., Mutsaers, A., Mendlein, J.D., Harris, A.S. and Furfine, E.S. 2010. Anti-tumor effect of CT-322 as an adnectin inhibitor of vascular endothelial growth factor receptor-2. *MABS*. **2**(2),pp.199–208.

van Marle, G., Dobbe, J.C., Gultyaev, A.P., Luytjes, W., Spaan, W.J. and Snijder, E.J. 1999. Arterivirus discontinuous mRNA transcription is guided by base pairing between sense and antisense transcription-regulating sequences. *Proceedings of the National Academy of Sciences of the United States of America*. **96**(21),pp.12056–61.

Marquardt, M.T., Phalen, T. and Kielian, M. 1993. Cholesterol Is Required in the Exit Pathway of Semliki Forest Virus. *Journal of Cell Biology*. **123**(1),pp.57–65.

Martín-Acebes, M.A., González-Magaldi, M., Sandvig, K., Sobrino, F. and Armas-Portela, R. 2007. Productive entry of type C foot-and-mouth disease virus into susceptible cultured cells requires clathrin and is dependent on the presence of plasma membrane cholesterol. *Virology*. **369**(1),pp.105–18.

Matatagui, D., Fontecha, J., Fernández, M., Gràcia, I., Cané, C., Santos, J. and

Horrillo, M. 2014. Love-Wave Sensors Combined with Microfluidics for Fast Detection of Biological Warfare Agents. *Sensors*. **14**(7),pp.12658–12669.

Mebus, C., Stair, E., Rhodes, M. and Twiehaus, M. 1973. Neonatal calf diarrhea-propagation, attenuation, and characteristics of a coronavirus-like agent. *American Journal of Veterinary Research*. **34**(2),pp.145–150.

van der Meer, Y., van Tol, H., Locker, J.K. and Snijder, E.J. 1998. ORF1a-encoded replicase subunits are involved in the membrane association of the arterivirus replication complex. *Journal of virology*. **72**(8),pp.6689–98.

Mengeling, W.L., Lager, K.M., Vorwald, A.C., Benfield, D.A., Christopher-Hennings, J., Nelson, E.A., Rowland, R.R.R., Nelson, J.K., Chase, C.C.L., Rossow, K.D., Collins, J.E., Carman, S., Sanford, S.E., Dea, S., Cartwright, S.F., Huck, R.A., Choi, C.S., Molitor, T.W., Joo, H.S., Gunther, R., Christopher-Hennings, J., Nelson, E.A., Nelson, J.A., Hines, R.J., Swenson, S.L., Hill, H.T., Zimmerman, J.J., Katz, J.B., Yaeger, M.J., Chase, C.C.L., Benfield, D.A., Gorcyca, D., Schlesinger, K., Chladek, D., Behan, W., Polson, D., Roof, M., Doitchenoff, D., Joo, H.S., Donaldson-Wood, C.R., Johnson, R.H., Joo, H.S., Donaldson-Wood, C.R., Johnson, R.H., Kapur, V., Elam, M.R., Pawlovich, T.M., Murtaugh, M.P., Keffaber, K.K., Kim, H.S., Kwang, J., Yoon, I.J., Joo, H.S., Frey, M.L., Lager, K.M., Halbur, P.G., Mengeling, W.L., Mengeling, W.L., Cutlip, R.C., Mengeling, W.L., Paul, P.S., Mengeling, W.L., Brown, T.T., Paul, P.S., Gutekunst, D.E., Mengeling, W.L., Paul, P.S., Brown, T.T., Mengeling, W.L., Ridpath, J.F., Vorwald, A.C., Mengeling, W.L., Vorwald, A.C., Lager, K.M., Clouser, D.F., Wesley, R.D., Meulenberg, J.J.M., Hulst, M.M., Meijer, E.J. de, Moonen, P.L.J.M., Besten, A. den, Kluyver, E.P. de, Wensvoort, G., Moorman, R.J.M., Meulenberg, J.J.M., Besten, A.P., Kluyver, E.P. de, Moorman, R.J.M., Schaaper, W.M.M., Wensvoort, G., Narita, M., Inui, S., Kawakami, Y., Kitamura, K., Maeda, A., Paul, P.S., Mengeling, W.L., Brown, T.T., Paul, P.S., Mengeling, W.L., Pirtle, E.C., Umthun, A.R., Mengeling, W.L., Wensvoort, G., Terpstra, C., Pol, J.M.A., Laak, E.A. ter, Bloemraad, M., Kluyver, E.P. de, Kragten, C., Buiten, L. van, Besten, A. den, Wagenaar, F., Broekhuijsen, J.M., Moonen, P.L.J.M., Zestra, T., Boer, E.A. de, Tibben, H.J., Jong, M.F. de, Veld, P. van't, Groenland, G.J.R., Gennep, J.A. van, Voets, M.T., Verheijden, J.H.M., Braamskamp, J., Wensvoort, G., Kluyver, E.P. de, Luijtze, E.A., Besten, A. den, Harris, L., Collins, J.E., Christianson, W.T., Chaldek, D., Wesley, R.D., Mengeling, W.L., Andreyev, V., Lager, K.M., Wills, R.W., Zimmerman, J.J., Swenson, S.L., Yoon, K.-J., Hill, H.T., Bundy, D.S., McGinley, M.J., Zimmerman, J., Epperson, W., Wills, R.W. and McKean, J.D. 2000. The effect of porcine parvovirus and porcine reproductive and respiratory syndrome virus on porcine reproductive performance. *Animal reproduction science*. **60**–**61**,pp.199–210.

Meulenberg, J.J., Bende, R.J., Pol, J.M., Wensvoort, G. and Moormann, R.J. 1995. Nucleocapsid protein N of Lelystad virus: expression by recombinant baculovirus, immunological properties, and suitability for detection of serum antibodies. *Clinical and diagnostic laboratory immunology*. **2**(6),pp.652–6.

Meulenberg, J.J.M., Hulst, M.M., de Meijer, E.J., Moonen, P.L.J.M., den Besten, A., de Kluyver, E.P., Wensvoort, G. and Moormann, R.J.M. 1993. Lelystad Virus, the Causative Agent of Porcine Epidemic Abortion and Respiratory Syndrome (PEARS), Is Related to LDV and EAV. *Virology*. **192**(1),pp.62–72.

Miller, K.D., Siegel, R.L., Lin, C.C., Mariotto, A.B., Kramer, J.L., Rowland, J.H., Stein,

K.D., Alteri, R. and Jemal, A. 2016. Cancer treatment and survivorship statistics, 2016. *CA: A Cancer Journal for Clinicians*. **66**(4),pp.271–289.

Millet, J.K. and Whittaker, G.R. 2015. Host cell proteases: Critical determinants of coronavirus tropism and pathogenesis. *Virus research*. **202**,pp.120–34.

Mir, M.A. and Panganiban, A.T. 2004. Trimeric hantavirus nucleocapsid protein binds specifically to the viral RNA panhandle. *Journal of virology*. **78**(15),pp.8281–8.

Miranda, F.F., Brient-Litzler, E., Zidane, N., Pecorari, F. and Bedouelle, H. 2011. Reagentless fluorescent biosensors from artificial families of antigen binding proteins. *Biosensors & bioelectronics*. **26**(10),pp.4184–90.

Mocellin, S. and Nitti, D. 2013. CTLA-4 blockade and the renaissance of cancer immunotherapy. *Biochimica et Biophysica Acta (BBA) - Reviews on Cancer*. **1836**(2),pp.187–196.

Moon, H., Bae, Y., Kim, H., Kang, S., Hong, S.Y., Kang, S., Altman, R.B., Kaneko, T., Firestone, R.A., Hicks, D.G., Gandjbakhche, A. and Hassan, M. 2016. Plug-and-playable fluorescent cell imaging modular toolkits using the bacterial superglue, SpyTag/SpyCatcher. *Chem. Commun.* **52**(97),pp.14051–14054.

Morales-Narváez, E., Naghdi, T., Zor, E. and Merkoçi, A. 2015. Photoluminescent lateral-flow immunoassay revealed by graphene oxide: highly sensitive paper-based pathogen detection. *Analytical chemistry*. **87**(16),pp.8573–7.

Morioka, K., Fukai, K., Yoshida, K., Kitano, R., Yamazoe, R., Yamada, M., Nishi, T. and Kanno, T. 2015. Development and Evaluation of a Rapid Antigen Detection and Serotyping Lateral Flow Antigen Detection System for Foot-and-Mouth Disease Virus. *PloS one*. **10**(8),p.e0134931.

Mross, K., Fischer, R., Richly, H., Scharr, D., Buechert, M., Stern, A., Hoth, D., Gille, H., Audoly, L.P. and Scheulen, M.E. 2014. Abstract A212: First in human phase I study of PRS-050 (Angiocal), a VEGF-A targeting anticalin, in patients with advanced solid tumors: Results of a dose escalation study. *Molecular Cancer Therapeutics*. **10**(11 Supplement).

Murthy, A., Ni, Y., Meng, X. and Zhang, C. 2015. Production and Evaluation of Virus-Like Particles Displaying Immunogenic Epitopes of Porcine Reproductive and Respiratory Syndrome Virus (PRRSV). *International Journal of Molecular Sciences*. **16**(4),pp.8382–8396.

Murzin, A.G. 1993. OB(oligonucleotide/oligosaccharide binding)-fold: common structural and functional solution for non-homologous sequences. *The EMBO journal*. **12**(3),pp.861–7.

Music, N. and Gagnon, C.A. 2010. The role of porcine reproductive and respiratory syndrome (PRRS) virus structural and non-structural proteins in virus pathogenesis. *Animal Health Research Reviews*. **11**(2),pp.135–163.

Myers, J.K. and Oas, T.G. 2001. Preorganized secondary structure as an important determinant of fast protein folding. *Nature structural biology*. **8**(6),pp.552–8.

Nathues, H., Alarcon, P., Rushton, J., Jolie, R., Fiebig, K., Jimenez, M., Geurts, V. and Nathues, C. 2017. Cost of porcine reproductive and respiratory syndrome virus at individual farm level ? An economic disease model. *Preventive Veterinary Medicine*. **142**,pp.16–29.

Nebel, R.L., Whittier, W.D., Cassell, B.G. and Britt, J.H. 1987. Comparison of On-Farm and Laboratory Milk Progesterone Assays for Identifying Errors in Detection of Estrus and Diagnosis of Pregnancy. *Journal of Dairy Science*.

70(7),pp.1471–1476.

Neethirajan, S., Tuteja, S.K., Huang, S.-T. and Kelton, D. 2017. Recent advancement in biosensors technology for animal and livestock health management. *Biosensors and Bioelectronics*. **98**,pp.398–407.

Nestorova, G.G., Adapa, B.S., Kopparthy, V.L. and Guilbeau, E.J. 2016. Lab-on-a-chip thermoelectric DNA biosensor for label-free detection of nucleic acid sequences. *Sensors and Actuators B: Chemical*. **225**,pp.174–180.

Neumann, E.J., Kliebenstein, J.B., Johnson, C.D., Mabry, J.W., Bush, E.J., Seitzinger, A.H., Green, A.L. and Zimmerman, J.J. 2005. Assessment of the economic impact of porcine reproductive and respiratory syndrome on swine production in the United States. *Journal of the American Veterinary Medical Association*. **227**(3),pp.385–392.

Newman, J.D. and Turner, A.P.F. 2005. Home blood glucose biosensors: a commercial perspective. *Biosensors and Bioelectronics*. **20**(12),pp.2435–2453.

Newnham, L.E., Wright, M.J., Holdsworth, G., Kostarelos, K., Robinson, M.K., Rabbitts, T.H. and Lawson, A.D. 2015. Functional inhibition of β-catenin-mediatedWnt signaling by intracellular VHHantibodies. *mAbs*. **7**(1),pp.180–191.

Nga, P.T., Parquet, M. del C., Lauber, C., Parida, M., Nabeshima, T., Yu, F., Thuy, N.T., Inoue, S., Ito, T., Okamoto, K., Ichinose, A., Snijder, E.J., Morita, K. and Gorbalenya, A.E. 2011. Discovery of the first insect nidovirus, a missing evolutionary link in the emergence of the largest RNA virus genomes. *PLoS pathogens*. **7**(9),p.e1002215.

Ni, J., Yang, S., Bounlom, D., Yu, X., Zhou, Z., Song, J., Khamphouth, V., Vatthana, T. and Tian, K. 2012. Emergence and pathogenicity of highly pathogenic Porcine reproductive and respiratory syndrome virus in Vientiane, Lao People's Democratic Republic. *Journal of Veterinary Diagnostic Investigation*. **24**(2),pp.349–354.

Nieuwenhuis, N., Duinhof, T.F. and Van Nes, A. 2012. Economic analysis of outbreaks of porcine reproductive and respiratory syndrome virus in nine sow herds.

Noad, R. and Roy, P. 2003. Virus-like particles as immunogens. *Trends in microbiology*.

Van Noort, A., Nelsen, A., Pillatzki, A.E., Diel, D.G., Li, F., Nelson, E. and Wang, X. 2017. Intranasal immunization of pigs with porcine reproductive and respiratory syndrome virus-like particles plus 2', 3'-cGAMP VacciGrade™ adjuvant exacerbates viremia after virus challenge. *Virology Journal*. **14**(1),p.76.

Nordberg, E., Friedman, M., Göstring, L., Adams, G.P., Brismar, H., Nilsson, F.Y., Ståhl, S., Glimelius, B. and Carlsson, J. 2007. Cellular studies of binding, internalization and retention of a radiolabeled EGFR-binding affibody molecule. *Nuclear medicine and biology*. **34**(6),pp.609–18.

Novakovic, P., Harding, J.C.S., Al-Dissi, A.N., Ladinig, A., Detmer, S.E., Holtkamp, D., Kliebenstein, J., Neumann, E., Zimmerman, J., Rotto, H., Yoder, T., Done, S., Paton, D., White, M., Rossow, K., Plagemann, P., Zimmerman, J., Benfield, D., Murtaugh, M., Osorio, F., Stevenson, G., Torremorell, M., Zimmerman, J., Karriker, L., Ramirez, A., Schwartz, K., Stevenson, G., Boddicker, N., Garrick, D., Rowland, R., Lunney, J., Reecy, J., Dekkers, J., Karniychuk, U., Nauwynck, H.,

Lager, K., Halbur, P., Christianson, W., Choi, C., Collins, J., Molitor, T., Morrison, R., Joo, H., Rowland, R., Lawson, S., Rossow, K., Benfield, D., Lager, K., Mengeling, W., Karniychuk, U., Saha, D., Geldhof, M., Vanhee, M., Cornillie, P., Broeck, W. Van den, Rowland, R., Cano, J., Dee, S., Murtaugh, M., Rovira, A., Morrison, R., Cheon, D., Chae, C., Karniychuk, U., Saha, D., Vanhee, M., Geldhof, M., Cornillie, P., Caij, A., Han, K., Seo, H., Oh, Y., Kang, I., Park, C., Chae, C., Ladinig, A., Wilkinson, J., Ashley, C., Detmer, S., Lunney, J., Plastow, G., Allende, R., Kutish, G., Laegreid, W., Lu, Z., Lewis, T., Rock, D., Ladinig, A., Detmer, S., Clarke, K., Ashley, C., Rowland, R., Lunney, J., Rossow, K., Laube, K., Goyal, S., Collins, J., Rossow, K., Morrison, R., Goyal, S., Singh, G., Collins, J., Rossow, K., Bautista, E., Goyal, S., Molitor, T., Murtaugh, M., Morrison, R., Cribier, B., Couilliet, D., Meyer, P., Grosshans, E., Gross, W., Trabandt, A., Reinhold-Keller, E., Halbur, P., Miller, L., Paul, P., Meng, X.-J., Huffman, E., Andrews, J., Ladinig, A., Ashley, C., Detmer, S., Wilkinson, J., Lunney, J. and Plastow, G. 2016. Pathologic Evaluation of Type 2 Porcine Reproductive and Respiratory Syndrome Virus Infection at the Maternal-Fetal Interface of Late Gestation Pregnant Gilts F. C. Leung, ed. *PLOS ONE*. **11**(3),p.e0151198.

Okuyama, M., Laman, H., Kingsbury, S.R., Visintin, C., Leo, E., Eward, K.L., Stoeber, K., Boshoff, C., Williams, G.H. and Selwood, D.L. 2007. Small-molecule mimics of an α-helix for efficient transport of proteins into cells. *Nature Methods*. **4**(2),pp.153–159.

Olwill, S.A., Joffroy, C., Gille, H., Vigna, E., Matschiner, G., Allersdorfer, A., Lunde, B.M., Jaworski, J., Burrows, J.F., Chiriaco, C., Christian, H.J., Hulsmeyer, M., Trentmann, S., Jensen, K., Hohlbaum, A.M. and Audoly, L. 2013. A Highly Potent and Specific MET Therapeutic Protein Antagonist with Both Ligand-Dependent and Ligand-Independent Activity. *Molecular Cancer Therapeutics*. **12**(11),pp.2459–2471.

Orlova, A., Tran, T.A., Ekblad, T., Karlström, A.E. and Tolmachev, V. 2010. (186)Re-maSGS-Z (HER2:342), a potential Affibody conjugate for systemic therapy of HER2-expressing tumours. *European journal of nuclear medicine and molecular imaging*. **37**(2),pp.260–9.

Pall, D. and Manteuffel, R. 1995. Fibrous web and process of preparing same.

Palmer, G.A., Kuo, L., Chen, Z., Faaberg, K.S. and Plagemann, P.G. 1995. Sequence of the genome of lactate dehydrogenase-elevating virus: heterogenicity between strains P and C. *Virology*. **209**(2),pp.637–42.

Panavas, T., Sanders, C. and Butt, T.R. 2009. SUMO fusion technology for enhanced protein production in prokaryotic and eukaryotic expression systems. *Methods in molecular biology (Clifton, N.J.)*. **497**,pp.303–17.

Pasternak, A.O., Spaan, W.J.M. and Snijder, E.J. 2006. Nidovirus transcription: how to make sense...? *The Journal of general virology*. **87**(Pt 6),pp.1403–21.

Patel, S., Nanda, R., Sahoo, S. and Mohapatra, E. 2016. Biosensors in Health Care: The Milestones Achieved in Their Development towards Lab-on-Chip-Analysis. *Biochemistry Research International*. **2016**,pp.1–12.

Paul, D. and Bartenschlager, R. 2013. Architecture and biogenesis of plus-strand RNA virus replication factories. *World journal of virology*. **2**(2),pp.32–48.

Pei, Y., Hodgins, D.C., Lee, C., Calvert, J.G., Welch, S.-K.W., Jolie, R., Keith, M. and Yoo, D. 2008. Functional mapping of the porcine reproductive and respiratory syndrome virus capsid protein nuclear localization signal and its pathogenic

association. *Virus Research*. **135**(1),pp.107–114.

Peiris, J.S.M. and Porterfield, J.S. 1979. Antibody-mediated enhancement of Flavivirus replication in macrophage-like cell lines. *Nature*. **282**(5738),pp.509–511.

Pensaert, M.B., Duan, X., Nauwynck, H.J., Van Oostveldt, P. and Favoreel, H.W. 1999. Entry of porcine reproductive and respiratory syndrome virus into porcine alveolar macrophages via receptor-mediated endocytosis. *Journal of General Virology*. **80**(2),pp.297–305.

Plagemann, P.G.W. and Moennig, V. 1992. *Advances in Virus Research Volume 41* [Online]. Elsevier.

Platonova, E., Winterflood, C.M., Junemann, A., Albrecht, D., Faix, J. and Ewers, H. 2015. Single-molecule microscopy of molecules tagged with GFP or RFP derivatives in mammalian cells using nanobody binders. *Methods*. **88**,pp.89–97.

Ploussard, G. and de la Taille, A. 2010. Urine biomarkers in prostate cancer. *Nature Reviews Urology*. **7**(2),pp.101–109.

Pol, R., Céspedes, F., Gabriel, D. and Baeza, M. 2017. Microfluidic lab-on-a-chip platforms for environmental monitoring. *TrAC Trends in Analytical Chemistry*. **95**,pp.62–68.

Ponnuraj, E.M., Springer, J., Hayward, A.R., Wilson, H. and Simoes, E.A.F. 2003. Antibody-Dependent Enhancement, a Possible Mechanism in Augmented Pulmonary Disease of Respiratory Syncytial Virus in the Bonnet Monkey Model. *The Journal of Infectious Diseases*. **187**(8),pp.1257–1263.

Popescu, C.-I., Riva, L., Vlaicu, O., Farhat, R., Rouillé, Y. and Dubuisson, J. 2014. Hepatitis C virus life cycle and lipid metabolism. *Biology*. **3**(4),pp.892–921.

Posthuma-Trumpie, G.A., Korf, J. and van Amerongen, A. 2009. Lateral flow (immuno)assay: its strengths, weaknesses, opportunities and threats. A literature survey. *Analytical and bioanalytical chemistry*. **393**(2),pp.569–82.

Posthuma, C.C., Pedersen, K.W., Lu, Z., Joosten, R.G., Roos, N., Zevenhoven-Dobbe, J.C. and Snijder, E.J. 2008. Formation of the Arterivirus Replication/Transcription Complex: a Key Role for Nonstructural Protein 3 in the Remodeling of Intracellular Membranes. *Journal of Virology*. **82**(9),pp.4480–4491.

Prajapati, B.M., Gupta, J.P., Pandey, D.P., Parmar, G.A. and Chaudhari, J.D. 2017. Molecular markers for resistance against infectious diseases of economic importance. *Veterinary world*. **10**(1),pp.112–120.

Pratelli, A. and Correspondence, V.C. 2016. Role of the lipid rafts in the life cycle of canine coronavirus. . **96**,pp.331–337.

Qiu, W., Xu, H., Takalkar, S., Gurung, A.S., Liu, B., Zheng, Y., Guo, Z., Baloda, M., Baryeh, K. and Liu, G. 2015. Carbon nanotube-based lateral flow biosensor for sensitive and rapid detection of DNA sequence. *Biosensors and Bioelectronics*. **64**,pp.367–372.

Raina, M., Sharma, R., Deacon, S.E., Tiede, C., Tomlinson, D., Davies, A.G., McPherson, M.J. and Wälti, C. 2015. Antibody mimetic receptor proteins for label-free biosensors. *The Analyst*. **140**(3),pp.803–10.

Ramanathan, K. and Danielsson, B. 2001. Principles and applications of thermal biosensors. *Biosensors and Bioelectronics*. **16**(6),pp.417–423.

Ramos, A.C.F., Souza, G.N., Lilenbaum, W., Faine, S., Adler, B., Bolin, C., Perolat, P.,

Boqvist, S., Thu, H.T.V., Vagsholm, I., Magnusson, U., Kazami, A., Watanabe, H., Hayashi, T., Kobayashi, K., Ogawa, Y., Yamamoto, K., al., et, Girio, R.J.S., Dias, H.L.T., Mathias, L.A., Santana, A.E., Alessi, A.C., Favero, A.C.M., Pinheiro, S.R., Vasconcellos, S.A., Morais, Z.M., Ferreira, F., Neto, J.S.F., Ramos, A.C.F., Fraguas, S., Ristow, P., Cardoso, V., Braga, D.F., Lilenbaum, W., Ramos, A.C.F., Lilenbaum, W., Neto, J.S.F., Vasconcellos, S.A., Ito, F.H., Moretti, A.S., Camargo, C.A., Sakamoto, S.M., al., et, Dohoo, I., Martin, W., Stryhn, H., Souza, G.N., Brito, J.R.F., Bastos, R.R., Rubiale, L., Ellis, W.A., Thiermann, A.B., Rosa, C.A.S., Giorgi, W., Silva, A.S., Teruya, J.M., Til, L.D. Van, Dohoo, I.R., Bolin, C.A. and Cassells, J.A. 2006. Influence of leptospirosis on reproductive performance of sows in Brazil. *Theriogenology*. **66**(4),pp.1021–5.

Rasmussen, S.G.F., Choi, H.-J., Fung, J.J., Pardon, E., Casarosa, P., Chae, P.S., Devree, B.T., Rosenbaum, D.M., Thian, F.S., Kobilka, T.S., Schnapp, A., Konetzki, I., Sunahara, R.K., Gellman, S.H., Pautsch, A., Steyaert, J., Weis, W.I. and Kobilka, B.K. 2011. Structure of a nanobody-stabilized active state of the β(2) adrenoceptor. *Nature*. **469**(7329),pp.175–80.

Rawlings, A.E., Bramble, J.P., Tang, A.A.S., Somner, L.A., Monnington, A.E., Cooke, D.J., McPherson, M.J., Tomlinson, D.C. and Staniland, S.S. 2015. Phage display selected magnetite interacting Adhirons for shape controlled nanoparticle synthesis. *Chem. Sci.* **6**(10),pp.5586–5594.

Raymond, D.D., Piper, M.E., Gerrard, S.R. and Smith, J.L. 2010. Structure of the Rift Valley fever virus nucleocapsid protein reveals another architecture for RNA encapsidation. *Proceedings of the National Academy of Sciences of the United States of America*. **107**(26),pp.11769–74.

Reverdatto, S., Burz, D.S. and Shekhtman, A. 2015. Peptide aptamers: development and applications. *Current topics in medicinal chemistry*. **15**(12),pp.1082–101.

Richter, A., Eggenstein, E. and Skerra, A. 2014. Anticalins: Exploiting a non-Ig scaffold with hypervariable loops for the engineering of binding proteins. *FEBS Letters*. **588**(2),pp.213–218.

Ries, J., Kaplan, C., Platonova, E., Eghlidi, H. and Ewers, H. 2012. A simple, versatile method for GFP-based super-resolution microscopy via nanobodies. *Nature methods*. **9**(6),pp.582–4.

Robinson, W.E., Montefiori, D. and Mitchell, W. 1988. Antibody-dependent enhancement of human immunodeficiency virus type-1 infection. *The Lancet*. **331**(8589),pp.790–794.

Rocha-Santos, T.A.P. 2014. Sensors and biosensors based on magnetic nanoparticles. *TrAC Trends in Analytical Chemistry*. **62**,pp.28–36.

Rohrman, B.A. and Richards-Kortum, R.R. 2012. A paper and plastic device for performing recombinase polymerase amplification of HIV DNA. *Lab on a chip*. **12**(17),pp.3082–8.

Romero-Brey, I. and Bartenschlager, R. 2014. Membranous replication factories induced by plus-strand RNA viruses. *Viruses*. **6**(7),pp.2826–57.

Rossow, K.D., Collins, J.E., Goyal, S.M., Nelson, E.A., Christopher-Hennings, J. and Benfield, D.A. 1995. Pathogenesis of porcine reproductive and respiratory syndrome virus infection in gnotobiotic pigs. *Veterinary pathology*. **32**(4),pp.361–73.

Rowland, R.R.R. and Yoo, D. 2003. Nucleolar-cytoplasmic shuttling of PRRSV nucleocapsid protein: a simple case of molecular mimicry or the complex

regulation by nuclear import, nucleolar localization and nuclear export signal sequences. *Virus Research*. **95**(1–2),pp.23–33.

Sajid, M., Kawde, A.-N. and Daud, M. 2014. Designs, formats and applications of lateral flow assay: A literature review. *Journal of Saudi Chemical Society*. **19**(6),pp.689–705.

Salguero, F.J., Sánchez-Martín, M.A., Díaz-San Segundo, F., de Avila, A. and Sevilla, N. 2005. Foot-and-mouth disease virus (FMDV) causes an acute disease that can be lethal for adult laboratory mice. *Virology*. **332**(1),pp.384–96.

Saliki, J.T., Huchzermeier, R. and Dubovi, E.J. 2006. Evaluation of a New Sandwich ELISA Kit That Uses Serum for Detection of Cattle Persistently Infected with BVD Virus. *Annals of the New York Academy of Sciences*. **916**(1),pp.358–363.

Samsonova, J.V., Safronova, V.A. and Osipov, A.P. 2015. Pretreatment-free lateral flow enzyme immunoassay for progesterone detection in whole cows' milk. *Talanta*. **132**,pp.685–689.

Sarno, M., Sacramento, G.A., Khouri, R., do Rosário, M.S., Costa, F., Archanjo, G., Santos, L.A., Nery, N., Vasilakis, N., Ko, A.I. and de Almeida, A.R.P. 2016. Zika Virus Infection and Stillbirths: A Case of Hydrops Fetalis, Hydranencephaly and Fetal Demise P. J. Hotez, ed. *PLOS Neglected Tropical Diseases*. **10**(2),p.e0004517.

Scharstuhl, J. and Shaikh, N. 1995. Method and device for determination of proteins.

Schilling, J., Schöppe, J., Sauer, E. and Plückthun, A. 2014. Co-crystallization with conformation-specific designed ankyrin repeat proteins explains the conformational flexibility of BCL-W. *Journal of molecular biology*. **426**(12),pp.2346–62.

Scholz, O., Hansen, S. and Plückthun, A. 2014. G-quadruplexes are specifically recognized and distinguished by selected designed ankyrin repeat proteins. *Nucleic acids research*. **42**(14),pp.9182–94.

Schütz, M., Batyuk, A., Klenk, C., Kummer, L., de Picciotto, S., Gülbakan, B., Wu, Y., Newby, G.A., Zosel, F., Schöppe, J., Sedlák, E., Mittl, P.R.E., Zenobi, R., Wittrup, K.D. and Plückthun, A. 2016. Generation of Fluorogen-Activating Designed Ankyrin Repeat Proteins (FADAs) as Versatile Sensor Tools. *Journal of Molecular Biology*. **428**(6),pp.1272–1289.

Sharma, R., Deacon, S.E., Nowak, D., George, S.E., Szymonik, M.P., Tang, A.A.S., Tomlinson, D.C., Davies, A.G., McPherson, M.J. and Wälti, C. 2016. Label-free electrochemical impedance biosensor to detect human interleukin-8 in serum with sub-pg/ml sensitivity. *Biosensors and Bioelectronics*. **80**,pp.607–613.

Shi, M., Holmes, E.C., Brar, M.S. and Leung, F.C.-C. 2013. Recombination Is Associated with an Outbreak of Novel Highly Pathogenic Porcine Reproductive and Respiratory Syndrome Viruses in China. *Journal of Virology*. **87**(19),pp.10904–10907.

Shi, Y., Pellarin, R., Fridy, P.C., Fernandez-Martinez, J., Thompson, M.K., Li, Y., Wang, Q.J., Sali, A., Rout, M.P. and Chait, B.T. 2015. A strategy for dissecting the architectures of native macromolecular assemblies. *Nature methods*. **12**(12),pp.1135–8.

Shim, W.-B., Kim, M.J., Mun, H. and Kim, M.-G. 2014. An aptamer-based dipstick assay for the rapid and simple detection of aflatoxin B1. *Biosensors & bioelectronics*. **62**,pp.288–94.

Shukla, J., Khan, M., Tiwari, M., Sannarangaiah, S., Sharma, S., Rao, P.V.L. and Parida, M. 2009. Development and evaluation of antigen capture ELISA for early clinical diagnosis of chikungunya. *Diagnostic microbiology and infectious disease*. **65**(2),pp.142–9.

Silva-Campa, E., Cordoba, L., Fraile, L., Flores-Mendoza, L., Montoya, M. and Hernández, J. 2010. European genotype of porcine reproductive and respiratory syndrome (PRRSV) infects monocyte-derived dendritic cells but does not induce Treg cells. *Virology*. **396**(2),pp.264–271.

Silverman, J., Liu, Q., Lu, Q., Bakker, A., To, W., Duguay, A., Alba, B.M., Smith, R., Rivas, A., Li, P., Le, H., Whitehorn, E., Moore, K.W., Swimmer, C., Perlroth, V., Vogt, M., Kolkman, J. and Stemmer, W.P.C. 2005. Multivalent avimer proteins evolved by exon shuffling of a family of human receptor domains. *Nature biotechnology*. **23**(12),pp.1556–61.

Singh, D.K., Gholamalamdari, O., Jadaliha, M., Ling Li, X., Lin, Y.-C., Zhang, Y., Guang, S., Hashemikhabir, S., Tiwari, S., Zhu, Y.J., Khan, A., Thomas, A., Chakraborty, A., Macias, V., Balla, A.K., Bhargava, R., Janga, S.C., Ma, J., Prasanth, S.G., Lal, A. and Prasanth, K. V. 2017. PSIP1/p75 promotes tumorigenicity in breast cancer cells by promoting the transcription of cell cycle genes. *Carcinogenesis*.,pp.1–10.

Singh, R.P., Sreenivasa, B.P., Dhar, P. and Bandyopadhyay, S.K. 2004. A sandwich-ELISA for the diagnosis of Peste des petits ruminants (PPR) infection in small ruminants using anti-nucleocapsid protein monoclonal antibody. *Archives of virology*. **149**(11),pp.2155–70.

Skerra, A. 2007. Alternative non-antibody scaffolds for molecular recognition. *Current opinion in biotechnology*. **18**(4),pp.295–304.

Skládal, P. 2016. Piezoelectric biosensors. *TrAC Trends in Analytical Chemistry*. **79**,pp.127–133.

Skottrup, P.D., Leonard, P., Kaczmarek, J.Z., Veillard, F., Enghild, J.J., O'Kennedy, R., Sroka, A., Clausen, R.P., Potempa, J. and Riise, E. 2011. Diagnostic evaluation of a nanobody with picomolar affinity toward the protease RgpB from Porphyromonas gingivalis. *Analytical Biochemistry*. **415**(2),pp.158–167.

Smith, C.A., Farrah, T., Goodwin, R.G., Alderson, M., Armitage, R., Maraskovsky, E., Tough, T., Roux, E., Schooley, K., Ramsdell, F., Lynch, D., Allen, R., Marshall, J., Roths, R., Sidman, C., Baens, M., Chaffanet, M., Cassiman, H.J., Berghe, H. van den, Maryen, P., Banner, D., D'Arcy, A., Janes, W., Gentz, R., Schoenfeld, H.-J., Broger, C., Loetscher, H., Lesslauer, W., Beutler, B., Browning, J., Ngam-ek, A., Lawton, P., DeMarinis, J., Tizard, R., Chow, E., Hession, C., O'Brine-Greco, B., Foley, S., Ware, C., Callard, R., Armitage, R., Fanslow, W., Spriggs, K., Vos, A. de, Ultsch, M., Kossiakoff, A., Eck, M., Ultsch, M., Rinderknecht, E., Vos, A. de, Spring, S., Farrah, T., Smith, C., Goebel, S., Johnson, G., Perkus, M., Davis, S., Winslow, J., Paoletti, E., Goodwin, R., Din, W., Davis-Smith, T., Anderson, D., Gimpel, S., Sato, T., Maliszewski, C., Brannan, C., Copeland, N., Jenkins, N., Farrah, T., Armitage, R., Fanslow, W., Smith, C.A., Jones, E., Stuart, D., Walker, N., Mapara, M., Bargou, R., Zugck, C., Doehner, H., Ustaoglu, F., Jonker, R., Krammer, P., Dorken, B., Pfeffer, K., Matsuyama, T., Kundig, T., Wakeham, A., Kishihara, K., Shahinian, A., Wiegmann, K., Ohashi, P., Kronke, M., Mak, T., Russel, J., Wang, R., Schoenfeld, H., Poeschl, B., Frey, J., Loetscher, W., Hunziker, W., Lustig, A., Zulauf, M., Shchelkunov, S., Blinov, V., Sandakhchiev,

L., Sidman, C., Marshall, J., Boehmer, H., Smith, C., Davis, T., Wignall, J., Din, W., Farrah, T., Upton, C., McFadden, G., Goodwin, R., Smith, C., Gruss, H., Davis, T., Anderson, M.D., Farah, T., Baker, E., Sutherland, R., Brannan, C., Copeland, N., Jenkins, N., Grabstein, K., Gliniac, B., McAllister, I., Fanslow, W., Alderson, M., Falk, B., Gimpel, S., Gillis, S., Din, W., Goodwin, R., Armitage, R., Suda, T., Takahashi, T., Golstein, P., Nagata, S., Takahashi, T., Tanaka, M., Brannan, C.I., Jenkins, N.A., Copeland, N.G., Suda, T., Nagata, S., Tartaglia, L., Ayres, T., Wong, G., Goeddel, D., Upton, C., Macen, J., Schreiber, M., McFadden, G., Watanabe-Fukunaga, R., Brannan, C., Copeland, N., Jenkins, N. and Nagta, S. 1994. The TNF receptor superfamily of cellular and viral proteins: Activation, costimulation, and death. *Cell*. **76**(6),pp.959–962.

Smith, D.B. and Johnson, K.S. 1988. Single-step purification of polypeptides expressed in Escherichia coli as fusions with glutathione S-transferase. *Gene*. **67**(1),pp.31–40.

Snijder, E.J., Dobbe, J.C. and Spaan, W.J.M. 2003. Heterodimerization of the Two Major Envelope Proteins Is Essential for Arterivirus Infectivity. *Journal of Virology*. **77**(1),pp.97–104.

Snijder, E.J. and Horzinek, M.C. 1993. Toroviruses: replication, evolution and comparison with other members of the coronavirus-like superfamily. *The Journal of general virology*. **74 (Pt 11**(11),pp.2305–16.

Snijder, E.J., Kikkert, M. and Fang, Y. 2013. Arterivirus molecular biology and pathogenesis. *The Journal of general virology*. **94**(Pt 10),pp.2141–63.

Snijder, E.J. and Meulenberg, J.J. 1998. The molecular biology of arteriviruses. *The Journal of general virology*. **79 (Pt 5)**,pp.961–79.

Snijder, E.J., van Tol, H., Pedersen, K.W., Raamsman, M.J. and de Vries, A.A. 1999. Identification of a novel structural protein of arteriviruses. *Journal of virology*. **73**(8),pp.6335–45.

Snijder, E.J., van Tol, H., Roos, N. and Pedersen, K.W. 2001. Non-structural proteins 2 and 3 interact to modify host cell membranes during the formation of the arterivirus replication complex. *The Journal of general virology*. **82**(Pt 5),pp.985–94.

Snowder, G.D., Van Vleck, L.D., Cundiff, L. V. and Bennett, G.L. 2006. Bovine respiratory disease in feedlot cattle: Environmental, genetic, and economic factors. *Journal of Animal Science*. **84**(8),p.1999.

Song, C., Krell, P. and Yoo, D. 2010. Nonstructural protein 1α subunit-based inhibition of NF-κB activation and suppression of interferon-β production by porcine reproductive and respiratory syndrome virus. *Virology*. **407**(2),pp.268–280.

Song, S., Liu, N., Zhao, Z., Njumbe Ediage, E., Wu, S., Sun, C., De Saeger, S. and Wu, A. 2014. Multiplex lateral flow immunoassay for mycotoxin determination. *Analytical chemistry*. **86**(10),pp.4995–5001.

Songjaroen, T., Dungchai, W., Chailapakul, O., Henry, C.S., Laiwattanapaisal, W., Shen, W., Amerongen, A. van and Doekes, G. 2012. Blood separation on microfluidic paper-based analytical devices. *Lab on a Chip*. **12**(18),p.3392.

Sörensen, J., Sandberg, D., Sandström, M., Wennborg, A., Feldwisch, J., Tolmachev, V., Åström, G., Lubberink, M., Garske-Román, U., Carlsson, J. and Lindman, H. 2014. First-in-human molecular imaging of HER2 expression in breast cancer metastases using the 111In-ABY-025 affibody molecule. *Journal of nuclear*

medicine : official publication, Society of Nuclear Medicine. **55**(5),pp.730–5.

Sörensen, J., Velikyan, I., Sandberg, D., Wennborg, A., Feldwisch, J., Tolmachev, V., Orlova, A., Sandström, M., Lubberink, M., Olofsson, H., Carlsson, J. and Lindman, H. 2016. Measuring HER2-Receptor Expression In Metastatic Breast Cancer Using [68Ga]ABY-025 Affibody PET/CT. *Theranostics*. **6**(2),pp.262–71.

Spear, A. and Faaberg, K.S. 2015. Development of a genome copy specific RT-qPCR assay for divergent strains of type 2 porcine reproductive and respiratory syndrome virus. *Journal of Virological Methods*. **218**,pp.1–6.

Spilman, M.S., Welbon, C., Nelson, E. and Dokland, T. 2009. Cryo-electron tomography of porcine reproductive and respiratory syndrome virus: organization of the nucleocapsid. *The Journal of general virology*. **90**(Pt 3),pp.527–35.

Stadler, L.K.J., Tomlinson, D.C., Lee, T., Knowles, M.A. and Ko Ferrigno, P. 2014. The use of a neutral peptide aptamer scaffold to anchor BH3 peptides constitutes a viable approach to studying their function. *Cell Death and Disease*. **5**(1),p.e1037.

Stahl, A., Stumpp, M.T., Schlegel, A., Ekawardhani, S., Lehrling, C., Martin, G., Gulotti-Georgieva, M., Villemagne, D., Forrer, P., Agostini, H.T. and Binz, H.K. 2013. Highly potent VEGF-A-antagonistic DARPins as anti-angiogenic agents for topical and intravitreal applications. *Angiogenesis*. **16**(1),pp.101–11.

Ståhl, S., Gräslund, T., Eriksson Karlström, A., Frejd, F.Y., Nygren, P.-Å. and Löfblom, J. 2017. Affibody Molecules in Biotechnological and Medical Applications. *Trends in Biotechnology*. **35**(8),pp.691–712.

Staus, D.P., Strachan, R.T., Manglik, A., Pani, B., Kahsai, A.W., Kim, T.H., Wingler, L.M., Ahn, S., Chatterjee, A., Masoudi, A., Kruse, A.C., Pardon, E., Steyaert, J., Weis, W.I., Prosser, R.S., Kobilka, B.K., Costa, T. and Lefkowitz, R.J. 2016. Allosteric nanobodies reveal the dynamic range and diverse mechanisms of G-protein-coupled receptor activation. *Nature*. **535**(7612),pp.448–452.

Steemson, J.D., Baake, M., Rakonjac, J., Arcus, V.L. and Liddament, M.T. 2014. Tracking Molecular Recognition at the Atomic Level with a New Protein Scaffold Based on the OB-Fold S. Dübel, ed. *PLoS ONE*. **9**(1),p.e86050.

Storz, J., Purdy, C.W., Lin, X., Burrell, M., Truax, R.E., Briggs, R.E., Frank, G.H. and Loan, R.W. 2000. Isolation of respiratory bovine coronavirus, other cytocidal viruses, and Pasteurella spp from cattle involved in two natural outbreaks of shipping fever. *Journal of the American Veterinary Medical Association*. **216**(10),pp.1599–1604.

Stumpp, M.T. and Amstutz, P. 2007. DARPins: a true alternative to antibodies. *Current opinion in drug discovery & development*. **10**(2),pp.153–9.

Suarez, P., Zardoya, R., Prieto, C., Solana, A., Tabares, E., Bautista, J.M. and Castro, J.M. 1994. Direct detection of the porcine reproductive and respiratory syndrome (PRRS) virus by reverse polymerase chain reaction (RT-PCR). *Archives of Virology*. **135**(1–2),pp.89–99.

Sun, Y., Han, M., Kim, C., Calvert, J.G. and Yoo, D. 2012. Interplay between Interferon-Mediated Innate Immunity and Porcine Reproductive and Respiratory Syndrome Virus. *Viruses*. **4**(12),pp.424–446.

Sun, Y., Xiao, S., Wang, D., Luo, R., Li, B., Chen, H. and Fang, L. 2011. Cellular membrane cholesterol is required for porcine reproductive and respiratory syndrome virus entry and release in MARC-145 cells. *Science China Life*

Sciences. **54**(11),pp.1011–1018.

Swanstrom, M. and Adams, M. 1951. Agar layer method for production of high titre phage stocks. *Proceedings of the Society for Experimental Biology and Medicine*. **78**(2),pp.372–375.

Syedmoradi, L., Daneshpour, M., Alvandipour, M., Gomez, F.A., Hajghassem, H. and Omidfar, K. 2017. Point of care testing: The impact of nanotechnology. *Biosensors and Bioelectronics*. **87**,pp.373–387.

Takada, A., Feldmann, H., Ksiazek, T.G. and Kawaoka, Y. 2003. Antibody-Dependent Enhancement of Ebola Virus Infection. *Journal of Virology*. **77**(13),pp.7539–7544.

Takada, A. and Kawaoka, Y. 2003. Antibody-dependent enhancement of viral infection: molecular mechanisms andin vivo implications. *Reviews in Medical Virology*. **13**(6),pp.387–398.

Tanaka, S.-I., Takahashi, T., Koide, A., Ishihara, S., Koikeda, S. and Koide, S. 2015. Monobody-mediated alteration of enzyme specificity. *Nature chemical biology*. **11**(10),pp.762–4.

Tang, M.W., Clemons, K. V, Katzenstein, D.A. and Stevens, D.A. 2015. The cryptococcal antigen lateral flow assay: A point-of-care diagnostic at an opportune time. *Critical reviews in microbiology*.,pp.1–9.

Tashima, T. 2017. Intelligent substance delivery into cells using cell-penetrating peptides. *Bioorganic & medicinal chemistry letters*. **27**(2),pp.121–130.

Temiz, Y., Lovchik, R.D., Kaigala, G. V. and Delamarche, E. 2015. Lab-on-a-chip devices: How to close and plug the lab? *Microelectronic Engineering*. **132**,pp.156–175.

Terpstra, C., Wensvoort, G. and Pol, J.M. 1991. Experimental reproduction of porcine epidemic abortion and respiratory syndrome (mystery swine disease) by infection with Lelystad virus: Koch's postulates fulfilled. *The Veterinary quarterly*. **13**(3),pp.131–6.

Thaa, B., Kabatek, A., Zevenhoven-Dobbe, J.C., Snijder, E.J., Herrmann, A. and Veit, M. 2009. Myristoylation of the arterivirus E protein: the fatty acid modification is not essential for membrane association but contributes significantly to virus infectivity. *Journal of General Virology*. **90**(11),pp.2704–2712.

Thaa, B., Sinhadri, B.C., Tielesch, C., Krause, E. and Veit, M. 2013. Signal peptide cleavage from GP5 of PRRSV: a minor fraction of molecules retains the decoy epitope, a presumed molecular cause for viral persistence. *PloS one*. **8**(6),p.e65548.

Thakur, M.S. and Ragavan, K. V 2013. Biosensors in food processing. *Journal of food science and technology*. **50**(4),pp.625–41.

Thanawongnuwech, R., Thacker, E.L. and Halbur, P.G. 1997. Effect of porcine reproductive and respiratory syndrome virus (PRRSV) (isolate ATCC VR-2385) infection on bactericidal activity of porcine pulmonary intravascular macrophages (PIMs): in vitro comparisons with pulmonary alveolar macrophages (PAMs). *Veterinary Immunology and Immunopathology*. **59**(3–4),pp.323–335.

Theofilopoulos, A.N., Baccala, R., Beutler, B. and Kono, D.H. 2004. Type I interferons (α/β) in immunity and autoimmunity. *Annu. Rev*. (23),pp.307–336.

Theurillat, J.-P., Dreier, B., Nagy-Davidescu, G., Seifert, B., Behnke, S., Zürrer-Härdi, U., Ingold, F., Plückthun, A. and Moch, H. 2010. Designed ankyrin repeat

proteins: a novel tool for testing epidermal growth factor receptor 2 expression in breast cancer. *Modern pathology : an official journal of the United States and Canadian Academy of Pathology, Inc*. **23**(9),pp.1289–97.

Tian, D., Wei, Z., Zevenhoven-Dobbe, J.C., Liu, R., Tong, G., Snijder, E.J. and Yuan, S. 2012. Arterivirus minor envelope proteins are a major determinant of viral tropism in cell culture. *Journal of virology*. **86**(7),pp.3701–12.

Tiede, C., Bedford, R., Heseltine, S.J., Smith, G., Wijetunga, I., Ross, R., AlQallaf, D., Roberts, A.P., Balls, A., Curd, A., Hughes, R.E., Martin, H., Needham, S.R., Zanetti-Domingues, L.C., Sadigh, Y., Peacock, T.P., Tang, A.A., Gibson, N., Kyle, H., Platt, G.W., Ingram, N., Taylor, T., Coletta, L.P., Manfield, I., Knowles, M., Bell, S., Esteves, F., Maqbool, A., Prasad, R.K., Drinkhill, M., Bon, R.S., Patel, V., Goodchild, S.A., Martin-Fernandez, M., Owens, R.J., Nettleship, J.E., Webb, M.E., Harrison, M., Lippiat, J.D., Ponnambalam, S., Peckham, M., Smith, A., Ferrigno, P.K., Johnson, M., McPherson, M.J. and Tomlinson, D.C. 2017. Affimer proteins are versatile and renewable affinity reagents. *eLife*. **6**,p.e24903.

Tiede, C., Tang, A.A.S., Deacon, S.E., Mandal, U., Nettleship, J.E., Owen, R.L., George, S.E., Harrison, D.J., Owens, R.J., Tomlinson, D.C. and McPherson, M.J. 2014. Adhiron: a stable and versatile peptide display scaffold for molecular recognition applications. *Protein engineering, design & selection : PEDS*. **27**(5),pp.145–55.

Tildesley, M.J., Bessell, P.R., Keeling, M.J. and Woolhouse, M.E.J. 2009. The role of pre-emptive culling in the control of foot-and-mouth disease. *Proceedings of the Royal Society of London B: Biological Sciences*. **276**(1671).

Tolcher, A.W., Sweeney, C.J., Papadopoulos, K., Patnaik, A., Chiorean, E.G., Mita, A.C., Sankhala, K., Furfine, E., Gokemeijer, J., Iacono, L., Eaton, C., Silver, B.A. and Mita, M. 2011. Phase I and Pharmacokinetic Study of CT-322 (BMS-844203), a Targeted Adnectin Inhibitor of VEGFR-2 Based on a Domain of Human Fibronectin. *Clinical Cancer Research*. **17**(2),pp.363–371.

Tolmachev, V., Orlova, A., Pehrson, R., Galli, J., Baastrup, B., Andersson, K., Sandström, M., Rosik, D., Carlsson, J., Lundqvist, H., Wennborg, A. and Nilsson, F.Y. 2007. Radionuclide therapy of HER2-positive microxenografts using a 177Lu-labeled HER2-specific Affibody molecule. *Cancer research*. **67**(6),pp.2773–82.

Tong, G.-Z., Zhou, Y.-J., Hao, X.-F., Tian, Z.-J., An, T.-Q. and Qiu, H.-J. 2007. Highly Pathogenic Porcine Reproductive and Respiratory Syndrome, China. *Emerging Infectious Diseases*. **13**(9),pp.1434–1436.

Tong, J., Yu, Y., He, X., Wang, S., Li, Y., Zhang, C., Cai, X., Wang, G., Zhou, E.-M., Han, Z., Liu, Y., Tu, Y., Li, L. and Jiang, C. 2016. Highly pathogenic porcine reproductive and respiratory syndrome virus infection and induction of apoptosis in bone marrow cells of infected piglets. *Journal of General Virology*. **97**(6),pp.1356–1361.

Uribe-Campero, L., Monroy-García, A., Durán-Meza, A.L., Villagrana-Escareño, M. V., Ruíz-García, J., Hernández, J., Núñez-Palenius, H.G. and Gómez-Lim, M.A. 2015. Plant-based porcine reproductive and respiratory syndrome virus VLPs induce an immune response in mice. *Research in Veterinary Science*. **102**,pp.59–66.

Vanderheijden, N., Delputte, P.L., Favoreel, H.W., Vandekerckhove, J., Van Damme,

J., van Woensel, P.A. and Nauwynck, H.J. 2003. Involvement of Sialoadhesin in Entry of Porcine Reproductive and Respiratory Syndrome Virus into Porcine Alveolar Macrophages. *Journal of Virology*. **77**(15),pp.8207–8215.

Vashist, S.K., Marion Schneider, E., Lam, E., Hrapovic, S. and Luong, J.H.T. 2014. One-step antibody immobilization-based rapid and highly-sensitive sandwich ELISA procedure for potential in vitro diagnostics. *Scientific reports*. **4**,p.4407.

Vazquez-Lombardi, R., Phan, T.G., Zimmermann, C., Lowe, D., Jermutus, L. and Christ, D. 2015. Challenges and opportunities for non-antibody scaffold drugs. *Drug Discovery Today*. **20**(10),pp.1271–1283.

Veit, M., Matczuk, A.K., Sinhadri, B.C., Krause, E. and Thaa, B. 2014. Membrane proteins of arterivirus particles: Structure, topology, processing and function. *Virus Research*. **194**,pp.16–36.

Verma, M.S., Rogowski, J.L., Jones, L. and Gu, F.X. 2015. Colorimetric biosensing of pathogens using gold nanoparticles. *Biotechnology advances*. **33**(6 Pt 1),pp.666–80.

Verma, R., Boleti, E. and George, A.J.. 1998. Antibody engineering: Comparison of bacterial, yeast, insect and mammalian expression systems. *Journal of Immunological Methods*. **216**(1–2),pp.165–181.

de Vries, A.A., Chirnside, E.D., Bredenbeek, P.J., Gravestein, L.A., Horzinek, M.C. and Spaan, W.J. 1990. All subgenomic mRNAs of equine arteritis virus contain a common leader sequence. *Nucleic acids research*. **18**(11),pp.3241–7.

de Vries, A.A., Post, S.M., Raamsman, M.J., Horzinek, M.C. and Rottier, P.J. 1995. The two major envelope proteins of equine arteritis virus associate into disulfide-linked heterodimers. *Journal of virology*. **69**(8),pp.4668–74.

Wang, C., Zhang, Y., Luo, J., Ding, H., Liu, S., Amer, S., Xie, L., Lyv, W., Su, W., Li, M., Sun, Q., Dai, J., He, H., Bartel, D.P., Ambros, V., Gottwein, E., Cullen, B.R., Skalsky, R.L., Cullen, B.R., Tian, K., Rossow, K.D., Mateu, E., Diaz, I., Wang, D., Xiao, S., Gao, L., Guo, X.K., Lee, S.M., Kleiboeker, S.B., Brown, B.D., Sarasin-Filipowicz, M., Krol, J., Markiewicz, I., Heim, M.H., Filipowicz, W., Jangra, R.K., Yi, M., Lemon, S.M., Jopling, C.L., Yi, M., Lancaster, A.M., Lemon, S.M., Sarnow, P., Murakami, Y., Aly, H.H., Tajima, A., Inoue, I., Shimotohno, K., Pedersen, I.M., Lecellier, C.H., Song, L., Liu, H., Gao, S., Jiang, W., Huang, W., Huang, J., Zhang, G.L., Otsuka, M., Wang, P., Hayden, M.S., Ghosh, S., Asamitsu, K., Ludwig, S., Planz, O., Nimmerjahn, F., Wurzer, W.J., Williams, S.A., Kwon, H., Chen, L.F., Greene, W.C., Luo, R., Luo, R., Sun, Z., Chen, Z., Lawson, S.R., Fang, Y., Song, C., Krell, P., Yoo, D., Song, S., Wang, C.M., Xiao, Y.Q., Bøtner, A., Nielsen, J., Bille-Hansen, V., Jung, K., Chen, X., Li, R., Li, Y., Kristiansen, K., Wang, J., An, H., Hou, J., Wang, C., Li, H., Lang, J.D. and Han, D.P. 2016. Identification of miRNomes reveals ssc-miR-30d-R_1 as a potential therapeutic target for PRRS viral infection. *Scientific Reports*. **6**,p.24854.

Wang, D., Fan, J., Fang, L., Luo, R., Ouyang, H., Ouyang, C., Zhang, H., Chen, H., Li, K. and Xiao, S. 2015. The nonstructural protein 11 of porcine reproductive and respiratory syndrome virus inhibits NF-κB signaling by means of its deubiquitinating activity. *Molecular Immunology*. **68**(2),pp.357–366.

Wang, G., Yu, Y., Tu, Y., Tong, J., Liu, Y., Zhang, C., Chang, Y., Wang, S., Jiang, C., Zhou, E.-M. and Cai, X. 2015. Highly Pathogenic Porcine Reproductive and Respiratory Syndrome Virus Infection Induced Apoptosis and Autophagy in Thymi of Infected Piglets F. C. Leung, ed. *PLOS ONE*. **10**(6),p.e0128292.

Wang, R. and Zhang, Y.-J. 2014. Wang, R. & Zhang, Y.-J., 2014. Antagonizing Interferon-Mediated Immune Response by Porcine Reproductive and Respiratory Syndrome Virus. BioMed Research International, 2014, pp.1–9. Available at: http://www.hindawi.com/journals/bmri/2014/315470/ [Accessed. *BioMed Research International*. **2014**,pp.1–9.

Wang, W., Guo, Y., Tiede, C., Chen, S., Kopytynski, M., Kong, Y., Kulak, A., Tomlinson, D., Chen, R., McPherson, M. and Zhou, D. 2017. Ultraefficient Cap-Exchange Protocol To Compact Biofunctional Quantum Dots for Sensitive Ratiometric Biosensing and Cell Imaging. *ACS Applied Materials & Interfaces*. **9**(18),pp.15232–15244.

Wang, X., Marthaler, D., Rovira, A., Rossow, S. and Murtaugh, M.P. 2015. Emergence of a virulent porcine reproductive and respiratory syndrome virus in vaccinated herds in the United States. *Virus research*. (210),pp.34–41.

Wang, Y., Guo, J., Qiao, S., Li, Q., Yang, J., Jin, Q. and Zhang, G. 2016. GP5 Protein-based ELISA for the Detection of PRRSV Antibodies. *Polish Journal of Veterinary Sciences*. **19**(3),pp.495–501.

Wang, Y., Telmer, C.A., Schmidt, B.F., Franke, J.D., Ort, S., Arndt-Jovin, D.J. and Bruchez, M.P. 2015. Fluorogen Activating Protein–Affibody Probes: Modular, No-Wash Measurement of Epidermal Growth Factor Receptors. *Bioconjugate Chemistry*. **26**(1),pp.137–144.

Wang, Z., Li, H., Guan, W., Ling, H., Wang, Z., Mu, T., Shuler, F.D. and Fang, X. 2010. Human SUMO fusion systems enhance protein expression and solubility. *Protein expression and purification*. **73**(2),pp.203–8.

Wang, Z., Zhi, D., Zhao, Y., Zhang, H., Wang, X., Ru, Y. and Li, H. 2014. Lateral flow test strip based on colloidal selenium immunoassay for rapid detection of melamine in milk, milk powder, and animal feed. *International Journal of Nanomedicine*. **9**(1),p.1699.

Weaver, S.C., Costa, F., Garcia-Blanco, M.A., Ko, A.I., Ribeiro, G.S., Saade, G., Shi, P.-Y. and Vasilakis, N. 2016. Zika virus: History, emergence, biology, and prospects for control. *Antiviral research*. **130**,pp.69–80.

Wedemeyer, W.J., Welker, E., Narayan, M. and Scheraga, H.A. 2000. Disulfide Bonds and Protein Folding †. *Biochemistry*. **39**(15),pp.4207–4216.

Weidle, U.H., Auer, J., Brinkmann, U., Georges, G. and Tiefenthaler, G. 2013. The emerging role of new protein scaffold-based agents for treatment of cancer. *Cancer genomics & proteomics*. **10**(4),pp.155–68.

Wensvoort, G., Terpstra, C., Pol, J.M., ter Laak, E.A., Bloemraad, M., de Kluyver, E.P., Kragten, C., van Buiten, L., den Besten, A. and Wagenaar, F. 1991. Mystery swine disease in The Netherlands: the isolation of Lelystad virus. *The Veterinary quarterly*. **13**(3),pp.121–30.

Werner, S., Krause, F., Rolny, V., Strobl, M., Morgenstern, D., Datz, C., Chen, H. and Brenner, H. 2016. Evaluation of a 5-Marker Blood Test for Colorectal Cancer Early Detection in a Colorectal Cancer Screening Setting. *Clinical cancer research : an official journal of the American Association for Cancer Research*. **22**(7),pp.1725–33.

Wetzel, R., Perry, L.J., Baase, W.A. and Becktel, W.J. 1988. Disulfide bonds and thermal stability in T4 lysozyme. *Proceedings of the National Academy of Sciences of the United States of America*. **85**(2),pp.401–5.

Whitworth, K.M., Rowland, R.R.R., Ewen, C.L., Trible, B.R., Kerrigan, M.A., Cino-

Ozuna, A.G., Samuel, M.S., Lightner, J.E., McLaren, D.G., Mileham, A.J., Wells, K.D. and Prather, R.S. 2015. Gene-edited pigs are protected from porcine reproductive and respiratory syndrome virus. *Nature biotechnology*. **34**(1),pp.20–22.

Wieringa, R., de Vries, A.A.F., van der Meulen, J., Godeke, G.-J., Onderwater, J.J.M., van Tol, H., Koerten, H.K., Mommaas, A.M., Snijder, E.J. and Rottier, P.J.M. 2004. Structural Protein Requirements in Equine Arteritis Virus Assembly. *Journal of Virology*. **78**(23),pp.13019–13027.

Wieringa, R., de Vries, A.A.F. and Rottier, P.J.M. 2003. Formation of disulfide-linked complexes between the three minor envelope glycoproteins (GP2b, GP3, and GP4) of equine arteritis virus. *Journal of virology*. **77**(11),pp.6216–26.

Wijegoonawardane, P.K.M., Cowley, J.A., Phan, T., Hodgson, R.A.J., Nielsen, L., Kiatpathomchai, W. and Walker, P.J. 2008. Genetic diversity in the yellow head nidovirus complex. *Virology*. **380**(2),pp.213–25.

Wills, R.W., Zimmerman, J.J., Yoon, K.-J., Swenson, S.L., McGinley, M.J., Hill, H.T., Platt, K.B., Christopher-Hennings, J. and Nelson, E.A. 1997. Porcine reproductive and respiratory syndrome virus: a persistent infection. *Veterinary Microbiology*. **55**(1–4),pp.231–240.

Wissink, E.H.J., Kroese, M. V, Maneschijn-Bonsing, J.G., Meulenberg, J.J.M., van Rijn, P.A., Rijsewijk, F.A.M. and Rottier, P.J.M. 2004. Significance of the oligosaccharides of the porcine reproductive and respiratory syndrome virus glycoproteins GP2a and GP5 for infectious virus production. *The Journal of general virology*. **85**(Pt 12),pp.3715–23.

Wissink, E.H.J., Kroese, M. V, van Wijk, H.A.R., Rijsewijk, F.A.M., Meulenberg, J.J.M. and Rottier, P.J.M. 2005. Envelope protein requirements for the assembly of infectious virions of porcine reproductive and respiratory syndrome virus. *Journal of virology*. **79**(19),pp.12495–506.

Wongyanin, P., Buranapraditkul, S., Yoo, D., Thanawongnuwech, R., Roth, J.A. and Suradhat, S. 2012. Role of porcine reproductive and respiratory syndrome virus nucleocapsid protein in induction of interleukin-10 and regulatory T-lymphocytes (Treg). *Journal of General Virology*. **93**(Pt_6),pp.1236–1246.

Wood, E. 1977. An apparently new syndrome of porcine epidemic diarrhoea. *Veterinary Record*. **100**(12),pp.243–244.

Wood, O., Tauraso$, N. and Liebhaber, H. 1970. Electron Microscopic Study of Tissue Cultures Infected with Simian Haemorrhagic Fever Virus. *gen. Virol. (I97O)*. **7**,pp.29–36.

Wootton, S.K. and Yoo, D. 2003. Homo-Oligomerization of the Porcine Reproductive and Respiratory Syndrome Virus Nucleocapsid Protein and the Role of Disulfide Linkages. *Journal of Virology*. **77**(8),pp.4546–4557.

Workman, S., Wells, S.K., Pau, C.-P., Owen, S.M., Dong, X.F., LaBorde, R. and Granade, T.C. 2009. Rapid detection of HIV-1 p24 antigen using magnetic immuno-chromatography (MICT). *Journal of Virological Methods*. **160**(1–2),pp.14–21.

Wudiri, G.A., Pritchard, S.M., Li, H., Liu, J., Aguilar, H.C., Gilk, S.D. and Nicola, A. V. 2014. Molecular Requirement for Sterols in Herpes Simplex Virus Entry and Infectivity. *Journal of Virology*. **88**(23),pp.13918–13922.

Xiao, S., Chen, Y., Wang, L., Gao, J., Mo, D., He, Z. and Liu, X. 2014. Simultaneous Detection and Differentiation of Highly Virulent and Classical Chinese-Type

Isolation of PRRSV by Real-Time RT-PCR. *Journal of Immunology Research*. **2014**,pp.1–7.

Xiao, Y.H., Wang, T.T., Zhao, Q., Wang, C.B., Lv, J.H., Nie, L., Gao, J.M., Ma, X.C., Hsu, W.H. and Zhou, E.M. 2014. Development of Indirect ELISAs for Differential Serodiagnosis of Classical and Highly Pathogenic Porcine Reproductive and Respiratory Syndrome Virus. *Transboundary and Emerging Diseases*. **61**(4),pp.341–349.

Xie, C., Tiede, C., Zhang, X., Wang, C., Li, Z., Xu, X., McPherson, M.J., Tomlinson, D.C. and Xu, W. 2017. Development of an Affimer-antibody combined immunological diagnosis kit for glypican-3. *Scientific reports*. **7**(1),p.9608.

Xu, G., Weber, P., Hu, Q., Xue, H., Audry, L., Li, C., Wu, J. and Bourhy, H. 2007. A simple sandwich ELISA (WELYSSA) for the detection of lyssavirus nucleocapsid in rabies suspected specimens using mouse monoclonal antibodies. *Biologicals : journal of the International Association of Biological Standardization*. **35**(4),pp.297–302.

Xu, H., Mao, X., Zeng, Q., Wang, S., Kawde, A.-N. and Liu, G. 2009. Aptamer-functionalized gold nanoparticles as probes in a dry-reagent strip biosensor for protein analysis. *Analytical chemistry*. **81**(2),pp.669–75.

Xu, Y., Liu, Y., Wu, Y., Xia, X., Liao, Y. and Li, Q. 2014. Fluorescent Probe-Based Lateral Flow Assay for Multiplex Nucleic Acid Detection. *Analytical Chemistry*. **86**(12),pp.5611–5614.

Yadav, V., Balamurugan, V., Bhanuprakash, V., Sen, A., Bhanot, V., Venkatesan, G., Riyesh, T. and Singh, R.K. 2009. Expression of Peste des petits ruminants virus nucleocapsid protein in prokaryotic system and its potential use as a diagnostic antigen or immunogen. *Journal of virological methods*. **162**(1–2),pp.56–63.

Yang, H., Cai, W., Xu, L., Lv, X., Qiao, Y., Li, P., Wu, H., Yang, Y., Zhang, L. and Duan, Y. 2015. Nanobubble-Affibody: Novel ultrasound contrast agents for targeted molecular ultrasound imaging of tumor. *Biomaterials*. **37**,pp.279–88.

Yang, M., Caterer, N.R., Xu, W. and Goolia, M. 2015a. Development of a multiplex lateral flow strip test for foot-and-mouth disease virus detection using monoclonal antibodies. *Journal of virological methods*. **221**,pp.119–26.

Yang, M., Caterer, N.R., Xu, W. and Goolia, M. 2015b. Development of a multiplex lateral flow strip test for foot-and-mouth disease virus detection using monoclonal antibodies. *Journal of virological methods*. **221**,pp.119–26.

Yang, Q., Zhang, Q., Tang, J. and Feng, W. 2015. Lipid rafts both in cellular membrane and viral envelope are critical for PRRSV efficient infection. *Virology*. **484**,pp.170–180.

Yoon, K.-J., Wu, L.-L., Zimmerman, J.J. and Platt, K.B. 1997. Field isolates of porcine reproductive and respiratory syndrome virus (PRRSV) vary in their susceptibility to antibody dependent enhancement (ADE) of infection. *Veterinary Microbiology*. **55**(1–4),pp.277–287.

You, J.-H., Howell, G., Pattnaik, A.K., Osorio, F.A. and Hiscox, J.A. 2008. A model for the dynamic nuclear/nucleolar/cytoplasmic trafficking of the porcine reproductive and respiratory syndrome virus (PRRSV) nucleocapsid protein based on live cell imaging. *Virology*. **378**(1),pp.34–47.

Yu, J., Liu, Y., Zhang, Y., Zhu, X., Ren, S., Guo, L., Liu, X., Sun, W., Chen, Z., Cong, X., Chen, L., Shi, J., Du, Y., Li, J., Wu, J. and Wang, J. 2017. The integrity of PRRSV

nucleocapsid protein is necessary for up-regulation of optimal interleukin-10 through NF-κB and p38 MAPK pathways in porcine alveolar macrophages. *Microbial Pathogenesis*. **109**,pp.319–324.

Zeman, D., Neiger, R., Yaeger, M., Nelson, E., Benfield, D., Leslie-Steen, P., Thomson, J., Miskimins, D., Daly, R. and Minehart, M. 1993. Laboratory Investigation of PRRS Virus Infection in Three Swine Herds. *Journal of Veterinary Diagnostic Investigation*. **5**(4),pp.522–528.

Zhang, J., Timoney, P.J., MacLachlan, N.J. and Balasuriya, U.B.R. 2008. Identification of an additional neutralization determinant of equine arteritis virus. *Virus Research*. **138**(1),pp.150–153.

Zhang, L., Zhou, L., Ge, X., Guo, X., Han, J. and Yang, H. 2016. The Chinese highly pathogenic porcine reproductive and respiratory syndrome virus infection suppresses Th17 cells response in vivo. *Veterinary Microbiology*. **189**,pp.75–85.

Zhang, Q., Huang, C., Yang, Q., Gao, L., Liu, H.-C., Tang, J. and Feng, W. -h. 2016. MicroRNA-30c Modulates Type I IFN Responses To Facilitate Porcine Reproductive and Respiratory Syndrome Virus Infection by Targeting JAK1. *The Journal of Immunology*. **196**(5),pp.2272–2282.

Zhao, W., Brook, M.A. and Li, Y. 2008. Design of Gold Nanoparticle-Based Colorimetric Biosensing Assays. *ChemBioChem*. **9**(15),pp.2363–2371.

Zhao, Y., Wang, H., Zhang, P., Sun, C., Wang, X., Wang, X., Yang, R., Wang, C. and Zhou, L. 2016. Rapid multiplex detection of 10 foodborne pathogens with an up-converting phosphor technology-based 10-channel lateral flow assay. *Scientific reports*. **6**,p.21342.

Zhi, X., Deng, M., Yang, H., Gao, G., Wang, K., Fu, H., Zhang, Y., Chen, D. and Cui, D. 2014. A novel HBV genotypes detecting system combined with microfluidic chip, loop-mediated isothermal amplification and GMR sensors. *Biosensors and Bioelectronics*. **54**,pp.372–377.

Zhou, X., Cao, P., Zhu, Y., Lu, W., Gu, N. and Mao, C. 2015. Phage-mediated counting by the naked eye of miRNA molecules at attomolar concentrations in a Petri dish. *Nature materials*. **14**(10),pp.1058–64.

Zhou, Y., Bai, J., Li, Y., Wang, X. and Wang, X. 2012. Suppression of immune responses in pigs by nonstructural protein 1 of porcine reproductive and respiratory syndrome virus. *Canadian journal of veterinary research*. **76**(4),pp.255–260.

Zhou, Z., Ni, J., Cao, Z., Han, X., Xia, Y., Zi, Z., Ning, K., Liu, Q., Cai, L., Qiu, P., Deng, X., Hu, D., Zhang, Q., Fan, Y., Wu, J., Wang, L., Zhang, M., Yu, X., Zhai, X. and Tian, K. 2011. The epidemic status and genetic diversity of 14 highly pathogenic porcine reproductive and respiratory syndrome virus (HP-PRRSV) isolates from China in 2009. *Veterinary Microbiology*. **150**(3),pp.257–269.

Ziebuhr, J. and Siddell, S. 2003. *Nidoviruses*.

Zirkel, F., Kurth, A., Quan, P.-L., Briese, T., Ellerbrok, H., Pauli, G., Leendertz, F.H., Lipkin, W.I., Ziebuhr, J., Drosten, C. and Junglen, S. 2011. An insect nidovirus emerging from a primary tropical rainforest. *mBio*. **2**(3),pp.e00077-11.

Zuo, X., Mattern, M.R., Tan, R., Li, S., Hall, J., Sterner, D.E., Shoo, J., Tran, H., Lim, P., Sarafianos, S.G., Kazi, L., Navas-Martin, S., Weiss, S.R. and Butt, T.R. 2005. Expression and purification of SARS coronavirus proteins using SUMO-fusions. *Protein expression and purification*. **42**(1),pp.100–10.